



University
of Glasgow

Charalambous, Chrystalla (2005) The role of LMP1 in the epithelium carcinogenesis in vivo. PhD thesis.

<http://theses.gla.ac.uk/4844/>

Copyright and moral rights for this thesis are retained by the author

A copy can be downloaded for personal non-commercial research or study, without prior permission or charge

This thesis cannot be reproduced or quoted extensively from without first obtaining permission in writing from the Author

The content must not be changed in any way or sold commercially in any format or medium without the formal permission of the Author

When referring to this work, full bibliographic details including the author, title, awarding institution and date of the thesis must be given.

The role of LMP1 in the epithelium carcinogenesis
in vivo

By

Chrystalla Charalambous

Thesis submitted to IBLs, University of Glasgow for the degree of
Doctor of Philosophy

*This thesis is dedicated to my parents
Laki and Androulla.*

Αφιερωμένο στους γονείς μου.

Acknowledgments

I would like to thank my supervisor, Joanna Wilson, for having faith in me from the first time we spoke on the phone and for giving me the opportunity to pursue a PhD. It would have been impossible otherwise. Thank you for supporting me throughout my PhD in any way, whether that was (your much needed!) patience, advise or pushing me to perform my best.

Thank you to everyone in the JBW lab, past and present, Adele, Claire, David, Donald, Jenny, Liz, Mark, Monica, Nooshin, Yazeed and all the summer and project students not only for their help but also the fun times we shared. A special thank you goes to Monica for all her help throughout the years.

This work would have been impossible (or very very dull) without the help from the CRF staff, especially Colin Chapman, who has made the lesion counts much more fun with his stories.

I would like to thank Prof. Marian Scott for her advise on statistic analysis and my accessors Dr Joe Gray and Dr David Evans.

A big thank you goes to my friends, Eileen, Mel and Patricia. They were there whenever I needed them to offer me support and lots of laughter... Thank you girls!!!

Last but certainly not least a big thank you goes to my family for always loving me, always supporting me and always having faith in me. My dad, Lakis, for his love of adventure that he instilled in me and for always accepting my decisions, good or bad. My mum, Androulla, who is always there when I am in pieces to help put me back together, who tells me the truth even when I do not want to listen to it and for the love that has so generously given. My brother, Giorgos, who I am using as a lab rat for every new recipe that I try and whose careless fun nature always lifts me up!!! I could have never done any of these without you!

Finally I would like to thank the Institute of Biological and Life Sciences and the Overseas Research Awards for funding my work.

Declaration

The research reported in this thesis is my original work except where otherwise stated, and has not been submitted for any other degree.



Chrystalla Charalambous

ITHAKA

As you set out for Ithaka
hope the voyage is a long one,
full of adventure, full of discovery.
Laistrygonians and Cyclops,
angry Poseidon-don't be afraid of them;
you'll never find things like that on your way
as long as you keep your thoughts raised high,
as long as a rare excitement
stirs your spirit and your body.
Laistrygonians and Cyclops,
wild Poseidon-you won't encounter them
unless you bring them along inside your soul,
unless your soul sets them up in front of you.

Hope the voyage is a long one.
May there be many a summer morning when,
with what pleasure, what joy,
you come into harbors seen for the first time;
may you stop at Phoenician trading stations
to buy fine things,
mother of pearl and coral, amber and ebony,
sensual perfume of every kind-
as many sensual perfumes as you can;
and may you visit many Egyptian cities
to gather stores of knowledge from their scholars.

Keep Ithaka always in your mind.
Arriving there is what you are destined for.
But do not hurry the journey at all.
Better if it lasts for years,
so you are old by the time you reach the island,
wealthy with all you have gained on the way,
not expecting Ithaka to make you rich.

Ithaka gave you the marvellous journey.
Without her you would not have set out.
She has nothing left to give you now.

And if you find her poor, Ithaka won't have fooled you.
Wise as you will have become, so full of experience,
you will have understood by then what these Ithakas mean.

The poem Ithaka by C.P.Cavafy, *Collected Poems*; translated by Edmund Keely and Philip Sherrard; edited by George Savidis, Rev. Ed. 1992, Princeton Press, pp.36-37.
One of my favourite poems and one that I often recited to keep me going during these three years.

Table of contents

LIST OF TABLES	9
LIST OF FIGURES	10
ABSTRACT	13
ABBREVIATIONS	15
CHAPTER 1: INTRODUCTION	21
1.1 Epstein Barr Virus (EBV)	21
Viral structure and genome	21
EBV types	22
1.2 Natural History of EBV	23
Lytic Cycle	23
Latent Cycle	24
EBNA1	27
EBNA2	28
EBNA 3A,B,C	29
EBNALP	29
LMP2A and B	30
Epstein Barr Virus small RNAs (EBERS) 1 and 2	31
<i>Bam</i> HI A RNA transcripts (BARTs)	32
BARF0	32
BARF1	32
1.3 LMP1	33
Structure of LMP1	33
LMP1 signalling	38
LMP1 Function	42
1.4 EBV related diseases	43
EBV Associated Diseases	44
Infectious Mononucleosis (IM)	44
Oral Hairy Leukoplakia (OHL)	44
X-Linked lymphoproliferative syndrome (XPLS)	44
Lymphoid Tumours:	45
Burkitt's Lymphoma (BL)	45
Hodgkin's Disease (HD)	46
T/NK cell lymphoma	46
Post-transplant Lymphoproliferative Disorder (PTLD)	46
AIDS-associated immunoblastic and primary central nervous system lymphomas	47
Epithelial tumours:	47
Gastric Adenocarcinoma	47
Breast Cancer	47
Nasopharyngeal Carcinoma (NPC)	48
LMP1 strains	52

1.5 RAS	55
RAS transgenic mouse models	59
Ras and chemical carcinogenesis	60
Relationship between Ras, LMP1 and NPC	61
Ras, apoptosis and senescence	62
1.6 Ras Association Domain Family (RASSF)	62
1.7 TGFα and EGFR signalling	63
Epidermal Growth Factor Receptor (EGFR)	63
The Shc, Grb2, Ras/MAPK pathway	67
The Src pathway	67
The JAK/STAT pathway	70
PLD, PLC γ and PI3-K	70
EGFR and Cancer	71
EGFR animal models	71
EGFR and LMP1	72
Regulators of EGFR ligand shedding	72
TGF α	73
EGFR ligands animal models	74
1.8 INK4a Locus	76
The INK4 family	76
The p16 ^{INK4a} /CDK4/CyclinD1/Rb pathway	79
The p19^{ARF} protein	81
The p19 ^{ARF} /MDM2/p53 pathway	81
Transgenic Mouse Models of INK4a locus	84
LMP1 , NPC and p16 ^{INK4a}	85
1.9 Mouse models of LMP1 expression in the epithelium	86
The Structure of the Skin	86
LMP1 transgenic models	90
1.10 Aims	97
CHAPTER 2: MATERIALS AND METHODS	98
2.1 Materials	98
2.1.1 Antisera	98
2.1.2 Oligonucleotides	100
2.1.3 Cell Lines	101
2.1.4 Frequently used solutions	102
2.1.5 Frequently used growth media	105
2.2 Methods	105
2.2.1 Animal procedures	105
A) Breeding and record keeping of transgenic mice	106
B) Animal Health	106
C) Mouse lines	107
D) Sample collection from mice	107
D.I Disperse epidermis separation	107
D.II Removal of papillomas and carcinomas	108
D.III Removal of internal tissues	108
E) Chemical Carcinogen Treatment of mice	108
F) Papilloma monitoring of mice	109
G) Ear Monitoring of mice	109
2.2.2 Bacterial cell culture techniques	109
A) Bacterial cell culture	109
B) Transformation	110

2.2.3 DNA techniques	110
A) Small scale extraction of plasmid DNA	110
B) Large scale extraction of plasmid DNA	111
C) Purification of plasmid DNA by caesium chloride (CsCl) gradient	111
D) Extraction of genomic DNA	112
E) Quantification of DNA	113
F) Restriction Digestion of Genomic DNA for Southern blotting	113
G) Agarose Gel Electrophoresis of DNA	113
H) Southern blotting of DNA	114
I) Generation of specific probe fragments	114
J) ³² P radioactive Labelling of probe fragment and hybridisation	115
K) Washing of Southern blots	115
L) Stripping of Southern blots	115
M) Amplification of DNA fragments using PCR	116
N) Purification of DNA for PCR	118
2.2.4 Protein techniques	119
A) Protein sample preparation from tissue	119
B) Protein sample preparation from cultured mammalian cells	119
C) Protein Immunoprecipitation (IP)	120
D) Quantification of protein concentration	120
E) SDS Polyacrylamide Gel Electrophoresis of protein samples	121
F) Western blotting of protein gel	121
G) Stripping and reprobing of western blots	122
H) Electrophoretic Mobility Shift Assay (EMSA)	122
H.I Protein sample preparation from tissues	122
H.II Labeling Oligonucleotide and probe purification	123
H.III Polyacrylamide Gel preparation for EMSAs	123
H.IV Sample Preparation for EMSAs	124
2.2.5 RNA techniques	124
RNA extraction	124
A) Total RNA Extraction	124
B) Quantification of RNA	126
C) Formaldehyde gel electrophoresis of RNA	126
D) Electrophoresis and Northern blotting of RNA gels	126
2.2.6 Cell culture techniques	127
A) Explantation of papillomas and carcinomas	127
B) Sub-culturing of mammalian cells	127
C) Freezing viable cells in liquid nitrogen	128
D) Revival of frozen stocks	128
E) Transfection of cells with plasmid and selection	128
F) Viable Cell Counting with Trypan Blue	129
2.2.7 Immunohistochemistry	129

CHAPTER 3: CHARACTERISATION OF LMP1 TRANSGENIC MOUSE LINES 131

3.1 Outline of approach	131
3.2 Histopathology Analysis	132
3.3 LMP1 expression patterns in transgenic lines 117, 105A and 105B mice	136
3.3A RNA Expression	136
3.3B Protein expression	142
3.4 Spontaneous papilloma formation on lines 117, 117/113 and 117/113/1205	156
3.5 Does L2LMP1 ^{CAO} act as a chemical initiator?	167
3.6 Conclusions and Discussion	171

CHAPTER 4: SIGNALLING PATHWAYS ACTIVATED BY LMP1	175
4.1 Outline of Approach	175
4.2 LMP1 ^{CAO} and the TGF α /EGFR/Ras/MAPK Signalling Pathway	176
4.3 LMP1 ^{CAO} and PI3K/Akt pathway	197
4.4 LMP1 ^{CAO} and the p38 MAPK pathway	208
4.5 LMP1 ^{CAO} and the AP1 family	210
4.6 LMP1 ^{CAO} and NF- κ B	218
4.7 Conclusion and Discussion (summary in table 4.4)	221
CHAPTER 5: DOES LMP1 INDUCE HYPERPLASIA BY UPREGULATING TGFα?	225
5.1 Outline of approach	225
5.2 Phenotypic examination of LMP1/TGF α null mice	226
5.3 Analysis of signalling pathways activation in LMP1 ^{CAO} /TGF α null mice	237
A. TGF α /EGFR/Ras/MAPK pathway	237
B. Apoptotic and Progression proteins	255
C. Proliferation and Cell cycle suppression	271
5.4 Conclusions and Discussion (summary in table 5.11)	286
CHAPTER 6: FINAL DISCUSSION	293
6.1 LMP1 ^{CAO} as a tumour promoter or initiator?	293
6.2 LMP1 ^{CAO} and INK4a locus	294
6.3 LMP1 ^{CAO} and the Ras/MAPK pathway	295
6.4 LMP1 ^{CAO} and Other Signalling pathways	296
6.5 Future Directions	301
REFERENCES	304
APPENDICES	344

List of Tables

Chapter 1

Table 1.1	ORF, gene product, alternative nomenclature and cellular localisation of the product of EBV latent genes	26
Table 1.2	The latency patterns of EBV	26
Table 1.3	Latency programs and tumour association	43

Chapter 2

Table 2.1	Primary antibodies used	98
Table 2.2	Secondary antibodies used	99
Table 2.3	Factor binding sites	100
Table 2.4	PCR oligos	101
Table 2.5	Cell lines and their transgenic status	102
Table 2.6	Mouse lines used	107
Table 2.7	Lesion size	109
Table 2.8	Genomic digests and probe fragments	114
Table 2.9	RT-PCR programs	117
Table 2.10	PCR programs	118
Table 2.11	Standard protein curve reactions	121
Table 2.12	The composition of running and stack gels for Western blotting	121

Chapter 3

Table 3.1	Table showing presence of the LMP1 ^{CAO} 66kDa product in tissues from lines 117, 105A and 105B	155
Table 3.2	Categorisation of lesions by size	156

Chapter 4

Table 4.1	Densitometric analysis of phospho-MEK1/2 to total MEK1/2	181
Table 4.2	Densitometric analysis of phospho-ERK1/2 to total ERK1/2	187
Table 4.3	Densitometric analysis of phospho-Akt to total Akt	202
Table 4.4	Summary of the proteins examined in line 117 (L2LMP1 ^{CAO}) ears	224

Chapter 5

Table 5.1	53/125 litter genotyping and Mendelian inheritance	231
Table 5.2	Correlation of genotype and observed phenotype of cross 53/125 pups	232
Table 5.3	Densitometric analysis on total EGFR levels	239
Table 5.4	Densitometric analysis on phosphorylated EGFR (tyr845) levels	243
Table 5.5	Densitometric analysis on BRAF levels	247
Table 5.6	Densitometric analysis on MEK1/2 levels	251
Table 5.7	Densitometric analysis on ERK1/2 levels	254
Table 5.8	Densitometric analysis on total caspase-3 levels	260
Table 5.9	Densitometric analysis on Akt (thr) levels	270
Table 5.10	Densitometric analysis on Rassf1 levels	281
Table 5.11	Summary of the proteins examined in lines 117 and 117/125 mice	292

List of Figures

Chapter 1

Figure 1.1	The EBV Genome	25
Figure 1.2	The structure of LMP1	34
Figure 1.3	Signalling pathways activated by LMP1	36
Figure 1.4	Ras activation	57
Figure 1.5	Signalling pathways activated by Ras	58
Figure 1.6	Ligands of the EGFR family	65
Figure 1.7	EGFR signalling pathways	68
Figure 1.8	The INK4A locus	78
Figure 1.9	The p16 ^{INK4a} role in inhibiting S phase entry	80
Figure 1.10	p19 ^{ARF} signalling and p16 ^{INK4a}	83
Figure 1.11	Structure of the skin	87
Figure 1.12a	Construct used to generate line 53	91
Figure 1.12b	Phenotype of line 53 pups	91
Figure 1.13	Construct used to generate line 117, 105A and 105B	93
Figure 1.14	Ear phenotype of line 117 mice	94
Figure 1.15	Phenotype of a 117 mouse bred into FVB background	96

Chapter 3

Figure 3.1	A Haematoxylin and Eosin staining of an ear of a transgenic mouse of line 117	133
Figure 3.2	A Haematoxylin and Eosin staining of an enlarged cervical lymph node of a transgenic mouse of line 117	135
Figure 3.3	Diagram depicting the three exons of LMP1 and where the primer pairs used for RT-PCR correspond	137
Figure 3.4	A nested RT-PCR of tissues from line 117	138
Figure 3.5	A nested RT-PCR of tissues from line 105A	139
Figure 3.6	A nested RT-PCR of tissues from line 105B	140
Figure 3.7	A Northern on tissues from a 117 transgenic mouse	143
Figure 3.8	Western blots of trial extraction buffers probed with anti-LMP1 antibodies S12 (A) and 1G6 (B)	144
Figure 3.9	Western blot of line 117 tissues using S12 (A) and CAO cocktail (B) antibodies	147
Figure 3.10	Western blot of line 117 tissues using anti-LMP1 S12 antibody	150
Figure 3.11	A Western blot for LMP1 on ear extracts of line 117 mice of different phenotypic stages	152
Figure 3.12	Western blot of line 105B tissues using S12 antibody	153
Figure 3.13	Western blot of line 105A tissues using S12 antibody	154
Figure 3.14	Development of spontaneous cutaneous lesions in mice of line 117	157
Figure 3.15	Genotyping of line 117/113 mice using PCR	160
Figure 3.16	Southern blot genotyping of line 117/113	161
Figure 3.17	Development of spontaneous cutaneous lesions in mice of line 117/113 and line 117	163
Figure 3.18	Development of spontaneous cutaneous lesions in mice of line 117/113 according to size	165
Figure 3.19	Development of cutaneous lesions in mice of line 117 that have been TPA treated	169

Chapter 4

Figure 4.1	TGF α expression in the skin of line 53 mice	177
Figure 4.2	TGF α expression in LMP1 transgenic and control carcinoma derived cell lines	178
Figure 4.3	EGFR expression in the ears of line 117 mice	179
Figure 4.4	Total EGFR and phospho-EGFR (Tyr845) expression in the epidermis of 5 day old pups of line 53	180
Figure 4.5	EGFR and phospho-EGFR expression in cell pellets derived from line 53, 117 and 105B carcinomas	182
Figure 4.6	EGFR activates the Ras/MAPK cascade	184
Figure 4.7	Total MEK1/2 and phospho-MEK1/2 of ears of line 117 mice	185
Figure 4.8	Total MEK1/2 expression in LMP1 and control carcinoma derived cell lines	188
Figure 4.9	Total and phospho-ERK1/2 expression in the ears of line 117 mice	189
Figure 4.10	An EMSA showing specific binding of ear extracts of line 117 to SRE binding oligo	192
Figure 4.11	An EMSA showing specific binding of ear extracts of line 117 to Sp1 binding oligo	194
Figure 4.12	An EMSA showing specific binding of ear extracts of line 117 to ETS1 binding oligo	196
Figure 4.13	Phospho-Akt (ser) expression in the ears of line 117 mice	198
Figure 4.14	Phospho-Akt (thr) and total Akt expression in ears of line 117 mice	199
Figure 4.15	Total Akt expression in the skin or ears of lines 53, 105A, 105B, 104, 106 and 117 mice	201
Figure 4.16	Phospho-Akt (ser and thr) expression in the ears of lines 105A, 105B and line 117 mice	204
Figure 4.17	PTEN and phospho-GSK3 β expression in skin and ears of lines 53, 105A, 105B, 113 and 117 mice	205
Figure 4.18	Phospho-GSK3 β expression in LMP1 and control carcinoma derived cell lines	207
Figure 4.19	p38 expression in ears of line 117 mice	209
Figure 4.20	Pan Fos and c-Jun expression in the skin and ears of lines 53 and 117 mice	211
Figure 4.21	Fra-1 and -2 expression in ears of line 117 mice	213
Figure 4.22	JunB expression in ears of line 117 mice	215
Figure 4.23	An EMSA showing specific binding of ear extracts of line 117 to TRE binding oligo	217
Figure 4.24	An EMSA showing specific binding of ear extracts of line 117 to NF- κ B binding oligo	219
Figure 4.25	An EMSA showing supershifting in ear extracts of line 117 to NF- κ B binding oligo	220

Chapter 5

Figure 5.1	Genotyping of line 125 by PCR	227
Figure 5.2	Whisker phenotype of 53/125 pups and 117/125 adult mice	228
Figure 5.3	Skin and tail phenotype of 53/125 pups	230
Figure 5.4	Graphs showing the phenotypic progression of ears of mice from line 117/125	235
Figure 5.5	Western blot of protein extracts from ears of line 117 and 117/125 probed with total EGFR	238

Figure 5.6	Phosphorylated EGFR (Tyr 845) western blot of protein extracts from ears of mice of lines 117 and 117/125	240
Figure 5.7	Phosphorylated EGFR (Tyr 1068) western blot of protein extracts from ears of mice of lines 117 and 117/	242
Figure 5.8	Phosphorylated HER2/ErbB2 western blot of protein extracts from ears of mice of lines 117 and 117/125	245
Figure 5.9	Braf western blot of protein extracts from ears of mice of lines 117 and 117/125	246
Figure 5.10	Phosphorylated MEK1/2 and total MEK1/2 western blot of protein extracts from ears of mice of lines 117 and 117/125	249
Figure 5.11	Phosphorylated ERK1/2 and total ERK1/2 western blot of protein extracts from ears of mice of lines 117 and 117/125	252
Figure 5.12	Phosphorylated SEK/MKK4 western blot of protein extracts from ears of mice of lines 117 and 117/125	256
Figure 5.13	SAPK/JNK western blot of protein extracts from ears of mice of lines 117 and 117/125	257
Figure 5.14	Total and activated caspase-3 western blot of protein extracts from ears of mice of lines 117 and 117/125	258
Figure 5.15	PCNA staining on ears from lines 117 and 117/125	262
Figure 5.16	Caspase-3 staining on ears from lines 117 and 117/125	265
Figure 5.17	Phosphorylated Akt (thr) and total Akt western blot of protein extracts from ears of mice of lines 117 and 117/125	268
Figure 5.18	MMP9 western blot of protein extracts from ears of mice of lines 117 and 117/125	272
Figure 5.19	JunB western blot of protein extracts from ears of mice of lines 117 and 117/125	273
Figure 5.20	p16 western blot of protein extracts from ears of mice of lines 117 and 117/125	274
Figure 5.21	p53 western blot of protein extracts from ears of mice of lines 117 and 117/125	277
Figure 5.22	Total Rb western blot of protein extracts from ears of mice of lines 117 and 117/125	278
Figure 5.23	Phosphorylated Rb western blot of protein extracts from ears of mice of lines 117 and 117/125	279
Figure 5.24	Rassf1 western blot of protein extracts from ears of mice of lines 117 and 117/125	280
Figure 5.25	Cyclin A western blot of extracts from mice of lines 117 and 117/125	283
Figure 5.26	Cyclin B western blot of extracts from mice of lines 117 and 117/125	284
Figure 5.27	Cyclin D1 western blot of extracts from mice of lines 117 and 117/125	285

Chapter 6

Figure 6.1	Signalling pathways activated by LMP1 ^{CAO}	299
------------	--	-----

Abstract

Epstein-Barr virus (EBV) is a human herpesvirus that has been associated over the past forty years with a number of malignancies both of lymphoid and epithelial origin. These include Burkitt's lymphoma (BL), Hodgkin's disease (HD) and nasopharyngeal carcinoma (NPC) to name only a few. One of the latent proteins of the virus, latent membrane protein 1 (LMP1) has been frequently detected in NPC biopsies and it plays a role in the initiation and development of the disease. Various strains of LMP1 have been detected, but the LMP1^{CAO} strain is the one most often encountered in endemic NPC cases. NPC tumours also show a deletion across chromosome 9p21 which leads to loss of the tumour suppressor locus INK4a as well as deletion or hypermethylation of 3p21.3 that leads to loss of another tumour suppressor the *Rassf1*. The aim of the work presented in this thesis is to investigate the exact role LMP1 plays both in the genesis and the development of epithelial malignancies such as NPC.

In order to investigate this, transgenic mouse models expressing two different strains of LMP1 at their epithelium were used. Use of other transgenic and knock out mice was also involved, in order to investigate cooperative relationships that LMP1 may have with other oncogenes or tumour suppressor genes. Minimal skin chemical carcinogenesis was employed in order to determine the role of LMP1 in initiation or progression of the tumourigenic process.

LMP1^{CAO} was found to be expressed in a wide variety of tissues in the transgenic mice, including both tissues of the epithelium as well as lymphoid tissues. LMP1^{CAO} is a weak initiator as LMP1^{CAO} transgenic mice develop lesions spontaneously and in some cases the ears of these mice progress from benign keratoacanthomas to malignant squamous cell carcinomas. LMP1^{CAO} cooperates with loss of INK4a locus to give an increased lesion load.

Signalling pathways that were found to be activated by LMP1 in lymphoid, epithelial cells or fibroblasts in previous studies, were investigated by Western blotting in order to determine whether they are activated by LMP1^{CAO} in the epithelium *in vivo*. LMP1^{CAO} in the epithelium *in vivo*, leads to activation of the p38, NF- κ B, AP-1 and MAPK pathways. Other proteins were shown to be upregulated or stabilised by LMP1 including p53, p16^{INK4a}, caspase-3 and MMP9. Whether this is a direct effect of LMP1^{CAO} or it is a secondary event due to the phenotype that LMP1 causes is still unclear.

The similarity between the LMP1 transgenic mice and TGF α transgenic mice, as well as increased levels of the epidermal growth factor receptor (EGFR) in NPC biopsies and NPC cells *in vitro*, led us to investigate the possibility that LMP1 may be acting via the TGF α /EGFR pathway. Indeed, TGF α levels were found to be upregulated in transgenic affected tissues when compared to wild type sibling tissues. EGFR activates many signalling pathways including MAPK. Investigation of the MAPK pathway showed that LMP1 does lead to its activation. In order to determine whether LMP1 acts via upregulation of TGF α , LMP1 transgenic mice were cross bred with TGF α null mice to create LMP1 transgenic / TGF α null mice. The phenotype of these mice was observed and it was discovered that paradoxically, loss of TGF α - a known oncogene- leads to a worsening of the phenotype.

Further studies into the signalling pathways that may be affected by loss of TGF α showed that TGF α in this system may be acting as a tumour suppressor by upregulating *Rassf1* and also may be acting as a control of some of the signalling pathways activated by LMP1.

The results show that LMP1^{CAO} is a weak initiator of proliferation but other cooperative events such as loss of tumour suppressors *INK4a* and/or *Rassf1* are needed for progression. This is consistent with previous studies performed in this laboratory as well as the facts that are currently known for NPC.

Abbreviations

aa	Amino acid
ACV	Acyclovir
ADAM	Metalloprotease with a disintegrin domain
AIDS	Acquired immunodeficiency syndrome
Akt	Protein Kinase B
APS	Ammonium-persulfate
API	Activator Protein 1
AR	Amphiregulin
ARF	Alternative reading frame
BARTs	<i>Bam</i> HI A RNA transcripts
BCR	B cell receptor
BL	Burkitt's lymphoma
BRAM	Bone morphogenic protein receptor associated molecule
BrdU	Bromodeoxyuridine
BSA	Bovine Serum Albumin
cDNA	Complementary DNA
CDK	Cyclin dependent kinase
CMV	Cytomegalovirus
CNS	Central nervous system
cpm	Counts per minute
CR	Complement receptor
CREB	Cyclic AMP-binding protein
CsCl	Caesium chloride
CSF	Colony stimulating factor
CTAR	C-terminal activating region
CTL	Cytotoxic T lymphocytes
CYP2E1	Cytochrome P450 2E1 enzyme
DAG	Diacylglycerol
DAPK	Death associated protein kinase
DEAE	Diethylaminoethanol
DEPC	Diethyl-polycarbonate
dH ₂ O	Distilled Water
DMBA	7,12- dimethyl-benz[a]anthracene

DMEM	Dulbecco's modified eagle medium
DMSO	Dimethyl sulfoxide
DNA	Deoxyribonucleic acid
ds	Double stranded
DS	Dyad of symmetry
EA	Early antigen
eBL	Endemic BL
<i>E.coli</i>	Escherichia coli
EBER	EBV encoded RNA
EBNA	Epstein Barr nuclear antigen
EBP2	EBNA1 binding protein 2
EBV	Epstein Barr virus
EDTA	Ethylenediaminetetraacetic acid
EGF	Epidermal growth factor
EGFR	Epidermal growth factor receptor
eIF2a	Eukaryotic translation initiation factor 2
ELISA	Enzyme Linked Immunosorbent Assay
EMSA	Electrophoretic mobility shift assay
eNOS	Endothelial nitric oxide synthase
ERK	Extracellular signal regulated kinase
EtBr	Ethidium Bromide
EtOH	Ethanol
FBS	Fetal bovine serum
FC	Phenol/chloroform
FCS	Fetal calf serum
Fig.	Figure
FR	Family of repeats
GAP	GTPase activating protein
GEF	Guanine nucleotide exchange factor
GI	Gastrointestinal
GSK3 β	Glycogen synthase kinase 3 β
gp	Glycoprotein
HB-EGF	Heparin-binding EGF
HD	Hodgkin's disease
HDAC	Histone deacetylase

HER	Heuregulin
hGH	Human growth hormone
HIF-1 α	Hypoxia factor -1 α
HIV	Human immunodeficiency virus
HK	Human keratin
HLA	Human leukocyte antigen
HPV	Human papilloma virus
H-ras	Harvey ras
hsp	Heat shock protein
ICAM	Intracellular adhesion molecule
Id	Inhibitor of differentiation
Ig	Immunoglobulin
IHC	Immunohistochemistry
I κ B	Inhibitory protein
IKK	I κ B regulatory Kinases
IL	Interleukin
IM	Infectious mononucleosis
INK4	Inhibitors of CDK4
IP	Immunoprecipitation
IR	Internal repeats
IRF	Interferon regulatory factor
JAK	Janus kinase
JNK	c-Jun N-terminal kinase
K	Keratin
Kb	Kilobase
kDa	Kilodalton
K-ras	Kirsten ras
LB	Luria-Bertani broth
LCL	Lymphoblastoid cell line
LGT	Low gelling temperature
LMP	Latent membrane protein
LOH	Loss of heterozygosity
LP	Leader protein
LPL	Lysophospholipids
LRS	LMP1 regulatory sequence

MAPK	Mitogen activated protein kinase
MAPKK	MAPK kinase
MEF	Mouse embryo fibroblast
MEK	MAPK kinase
μg	Microgram
min	Minute
μl	Microliter
μM	Micromolar
MMP	Matrixmetalloproteinase
mRNA	Messenger RNA
MST	Mammalian sterile20-like
MT-	Metallotheionin promoter
NK	Natural killer
NF-κB	Nuclear factor kappa B
ng	Nanogram
NIK	NF-κB inducing kinase
Nm23-H1	Nonmetastatic protein 23-homologue 1
NPC	Nasopharungeal carcinoma
NK	Natural killer
OD	Optical density
OHL	Oral hairy leukoplakia
ORF	Open reading frame
Ori	Origin of Replication
PAGE	Polyacrylamide gel electrophoresis
PBS	Phosphate buffered saline
PCNA	Proliferating nuclear cell antigen
PCR	Polymerase chain reaction
PDK1	Phosphoinositide-dependent kinase 1
PI3K	Phosphatidylinositol 3-kinase
PIP3	Phosphatidylinositol-3, 4, 5-triphosphate
PKC	Protein kinase C
PKR	Double stranded RNA activated protein kinase R
PLC	Phospholipase C
PMA	4 beta-phorbol 12-myristate 13-acetate
pmol	Picomoles

PNK	Polynucleotide kinase
PP2A	Protein phosphatase type 2A
PTEN	Protein Phosphatase and Tensin homologue deleted on chromosome 10
PTLD	Post-transplantation Lymphoproliferative Disease
Py	Polyoma
RA	Ras association domain
RASSF	Ras association domain family
Rb	Retinoblastoma
RBP-J κ	Recombination binding protein J
RIP	Receptor Interacting Protein
RNA	Ribonucleic acid
rpm	Revolutions per minute
RT	Reverse transcriptase
RT-PCR	Reversed transcribed PCR
RVC	Ribonucleoside vanadyl complexes
sBL	Sporadic BL
SCC	Squamous cell carcinoma
SDS	Sodium docecyl sulfate
SDS-PAGE	SDS polyacrylamide gel electrophoresis
sec	Seconds
SEK	Stress enhanced kinase
SH	Src homology domain
siRNA	Small interfering RNA
SOS	Son of sevenless
SRE	Serum response element
SRF	Serum Response Factor
STAT	Signal transducer and activation of transcription
TACE	TNF α Converting Enzyme
TBST	Tris buffered saline with Tween 20
TCF	Ternary Complex Factor
TEMED	N,N,N',N'-tetramethyldiamine
TES	Transformation effector site
TGF	Tumour growth factor
TNF	Tumour necrosis factor
TNFR	TNF receptor

TPA	12-O-tetradecanoyl phorbol-1,3-acetate
TR	Terminal repeats
TRADD	TNFR associated death domain
TRAF	TNFR associated factor
TRE	TPA response element
UV	Ultraviolet
VCA	Viral capsid antigen
VEGF	Vascular endothelial growth factor
WHO	World Health Organisation
wt	wild type

Chapter 1: Introduction

1.1 Epstein Barr Virus (EBV)

EBV is a human gammaherpesvirus that is associated with several lymphoid and epithelial malignancies. It was first discovered in 1964 by Epstein, Achong and Barr when an endemic Burkitt's lymphoma (eBL) biopsy viewed under an electron microscope showed what looked like herpesvirus particles present in those cells. EBV was subsequently shown to transform resting B cells and induce tumours in non human primates thus providing evidence for the role of EBV in tumourigenesis (Henle and Henle, 1967; Miller and Heston, 1974; Pope et al., 1968).

EBV is a very successful virus as more than 90% of the world population is seropositive. Primary infection with EBV takes place early in life, especially in developing countries, and infection is usually asymptomatic. In developed countries with higher hygiene standards, infection in a proportion of individuals is delayed to puberty or early adulthood. Delayed infection can lead to manifestation of infectious mononucleosis (IM).

Malignancies associated with EBV include BL, nasopharyngeal carcinoma (NPC), Hodgkin's disease (HD), Acquired Immunodeficiency Syndrome (AIDS) associated and post transplant lymphomas and others that will be discussed later.

Viral structure and genome

Within the viral particle, the linear EBV genome is complexed with various DNA binding proteins and is enclosed within an icosahedral nucleocapsid made up of 162 capsomeres. Surrounding the viral capsid is a protein tegument that is enclosed in the outer viral envelope. The viral envelope is made up of glycoproteins (gp) that mediate entry of the virus into the host cell. Initially viral encoded gp350/220 in the envelope can attach to the host cell via the cellular complement receptor (CR) CD21/CR2 present on B cells. Other viral envelope glycoproteins such as gp25(gL) and gp42/38 are complexed with gp85(gH) and can associate with the major histocompatibility complex class II molecules of the host cell, HLA-DR, DP and DQ for viral entry into the host cell (Knox and Young, 1995). After entry into the cell via a cytoplasmic vesicle, the virus envelope fuses with the vesicle membrane and the nucleocapsid along with the tegument is released into the cytoplasm.

The EBV genome consists of double stranded (ds) DNA of approximately 172kb, comprising 0.5kb terminal direct repeats (TR) and 3kb internal direct repeats (IR) that divide the genome

into short and long unique regions. Once infection takes place, the TR fuse, to form a circular DNA. Cleavage occurs randomly in the TR to produce linear genomes that will have a different number of TR unique to each genome. When those linear genomes circularise each will have a unique number of TR. Thus TR are a useful tool in determining whether latent infection is clonal or not.

EBV was the first herpesvirus to be cloned in *E.coli* and sequenced in 1984 (Arrand et al., 1981; Baer et al., 1984; Hatfull et al., 1988; Parker et al., 1990). Since a DNA *Bam*HI fragment library was used in the first genome analysis, each gene is given a name according to where transcription of its open reading frame (ORF) maps. For example, BZLF1 refers to *Bam*HI Z fragment left (direction according to linear map) open reading frame number 1. As such all the EBV genes have a *Bam*HI map name, but several are also named according to function or protein localisation as described below. EBV can encode 87 genes, 10 of which are latent genes and are described later.

EBV types

There are two main strain types of EBV, EBV1 (or A, prototypes are: B95-8 and W91) and EBV2 (or B, prototypes are: Jijoye and AG876). The main differences between these two viral strain types lie in the sequence differences of the Epstein Barr Nuclear Antigen (EBNA) 2, EBNA3s and EBNA leader protein (LP) genes (Dambaugh et al., 1984; Rowe et al., 1989; Sample et al., 1990). The two variants of EBNA2 show 50% homology at the amino acid (aa) sequence level, and the two EBNA3 variants show 70-80% homology (Addinger et al., 1985).

EBV1 is more prevalent in developed countries whereas EBV2 is more prevalent in Africa and Caucasian male homosexual AIDS patients (Yao et al., 1998).

Initial experiments where B cells were transformed *in vitro* with either EBV1 or 2, showed that EBV2 transformed cells had a lower growth rate than B cells transformed with EBV1 implying that EBV2 is not as potent in transformation as EBV1 (Rickinson et al., 1987). However, the finding that Caucasian male homosexual AIDS patients show a 30% increase in the EBV2 infection as compared to the healthy Caucasian population, as well as the fact that the Caucasian AIDS patients are coinfecting with EBV1, implies that EBV2 may be prevalent in the Caucasian population but not be readily detected in non immunocompromised individuals. Despite the fact that there are only two main EBV types, sequence variation between EBV strains of individual proteins such as LMP1 is quite common with as many as 9 different LMP1 strains (Miller et al., 1994b).

A further EBV type has been identified called the “f variant”. This type of EBV is mostly isolated from Southern Chinese NPCs. This strain has an extra *Bam*HI restriction site in the F region. This “f variant” has affinity for epithelial cells and is very rarely detected in lymphoblastoid cell lines (LCLs) from South Chinese healthy individuals, thus implying that it may be more potent in NPC formation (Lung and Chang, 1992; Lung et al., 1994).

1.2 Natural History of EBV

EBV is an orally transmitted virus. It is still unclear how it infects humans but the currently favoured hypothesis is that the primary site of infection is the circulating B cells that are found in the oral epithelia (Anagnostopoulos et al., 1995; Niedobitek et al., 1997). The virus enters the B cell via the glycoproteins as described before. Once in the B cell the viral presence leads to an initial T cell response. After this response, the number of B cells carrying EBV drops to about one in every 10^5 or 10^6 cells. In most B cells the virus exists in the latent state but in some it can be reactivated and enter the lytic phase. This leads to the apoptosis of the B cell and the release of new virions that are constantly shed into the saliva of infected individuals. Epithelial cells can also be infected with EBV and it is believed that this could happen independently of CD21 (Yoshiyama et al., 1997), via another receptor unique to the epithelial cells (Molesworth et al., 2000; Sixbey and Yao, 1992), or via very low CD21 expression (Fingerroth et al., 1999; Li et al., 1992) or simply via cell to cell contact with B cells that have a high viral load (Imai et al., 1998; Speck et al., 2000).

There is extensive evidence that the infection is maintained in B cells. This has been shown in patients that have received bone marrow transplants. Their own bone marrow was destroyed, and after transplant the EBV virus they harboured was that of the donor. Also patients suffering from the condition X-linked agammaglobulinemia leading to the absence of mature B cells, show no EBV infection whatsoever, while throat washings of healthy individuals showed that 94% were infected with EBV (Faulkner et al., 1999).

Lytic Cycle

The lytic cycle has been studied primarily in latently infected B cells that have been induced by chemicals such as phorbol esters to enter the lytic cycle. The first genes to be expressed are the immediate early genes BZLF1 and BRLF1. Initially the promoter of BZLF1 is activated by a physiologic change in the cell, BZLF1 is transcribed and translated. The Z protein then goes into the nucleus where it binds to activating protein 1 (AP1) DNA sites upstream of both BZLF1 and BRLF1, increasing BZLF1 transcription and activating BRLF1. These immediate early genes transactivate the early lytic genes. About 30 mRNAs are

transcribed from early lytic genes and these include genes that are responsible for structural viral proteins or proteins that allow the virus envelopment and viral exit from the host cell. These include genes that encode for viral DNA polymerase (BALF5), the major DNA binding protein (BALF2), ribonucleotide reductase (BORF2 and BaRF1), thymidine kinase (BXLF1), BHRF1 (homologous to the anti-apoptotic *bcl-2*), BXRf1 (the EBV basic core protein) and among others the BCRF1 which is homologous to human interleukin (IL) 10 and is believed to attenuate macrophage and natural killer (NK) cell function so as to prevent the host cell interferon response and allow for successful viral production and also genes needed for the viral replication. Some of the latent genes such as EBNA1 and latent membrane protein (LMP) 1 and LMP2A/B are present in the lytic cycle as the FQp promoter and the LMP promoters are active (Rickinson and Kieff, 1996).

Latent Cycle

EBV persists in human B cells in the latent state, as an episome, expressing only a limited subset of its genes, the latent genes. Latent genes were first identified in LCLs that are resting B cells that have been transformed by EBV and are permanently infected. These latent genes include EBNA1, 2, 3A, 3B, 3C, LP, LMP1, 2A and 2B as well as some *Bam* HI RNA transcripts which may encode proteins of important biological function. Note that an alternative nomenclature exists for some of the latent genes, for example EBNALP can also be called EBNA5. I will use the former nomenclature in this thesis. The ORF name, gene product, alternative nomenclature and cellular localisation are summarised on table 1.1 and the position of the latent genes is shown on fig.1.1.

After 12-16hrs post infection, EBV circularises in the infected cell nucleus and the Wp promoter initiates rightwards transcription. The first latent proteins to be expressed are EBNALP and EBNA2. EBNA2 can transactivate cellular genes and viral genes (eg. Latent membrane (LMP) 1 and LMP2) and also leads to promoter switching from Wp to Cp. The Cp promoter is upstream of Wp and leads to transcription of the longer EBNA mRNA thus leading to transcription of the other EBNA proteins. LMP1 and LMP2A and B are transcribed in opposite directions (LMP1 is leftforward) from two different unique to them promoters. 32hrs post infection all the latent proteins are made and EBNA1 can bind to the origin of replication (Ori) P and facilitate the episomal replication at S phase.

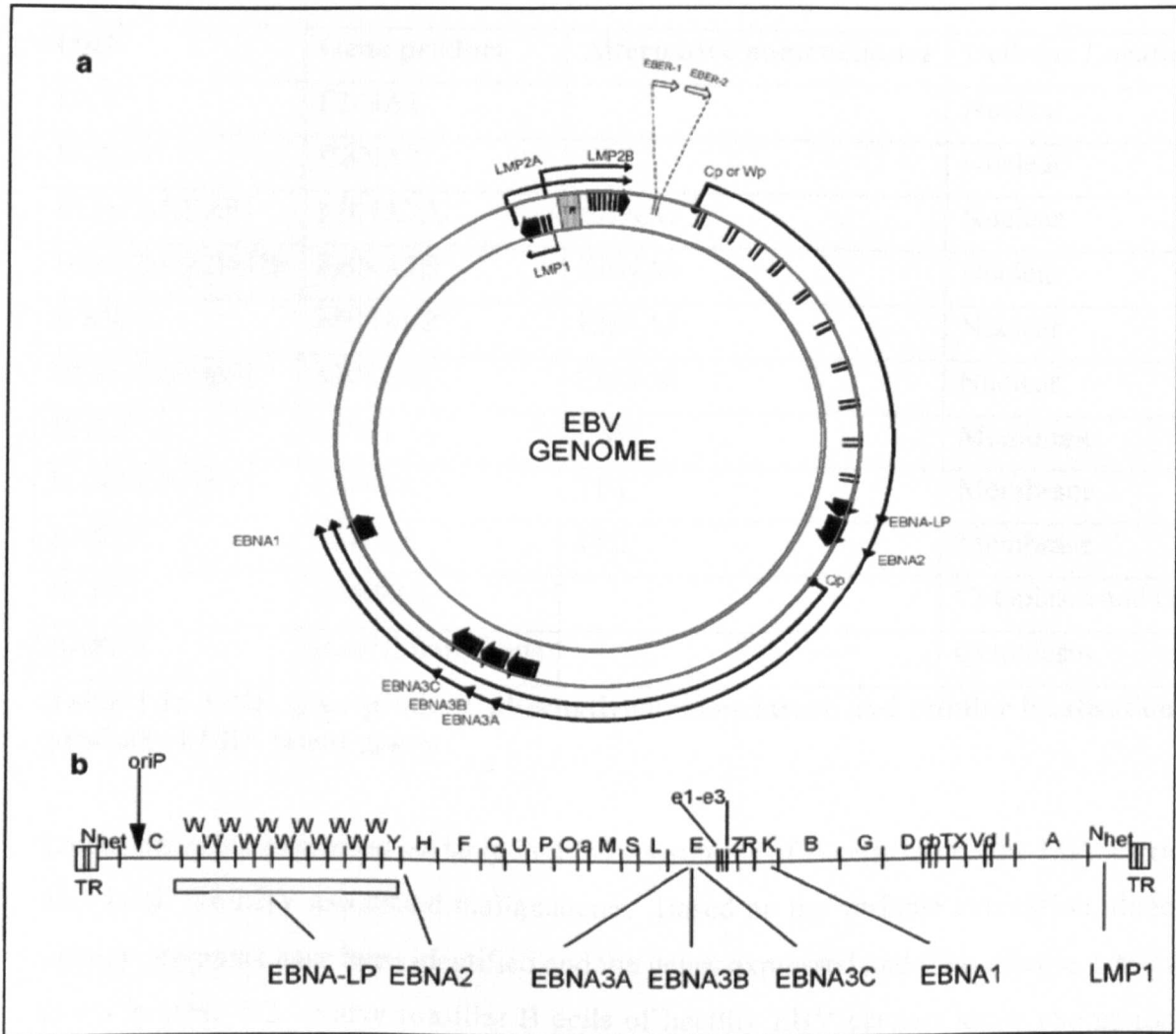


Figure 1.1: The EBV Genome

Figure from Young and Murray, 2003, *Oncogene* (22):5108-5121.

(a) is a diagrammatic representation showing the position and the transcriptional direction of the latent genes of EBV on the circular viral genome. The arrows show the direction in which the latent genes are transcribed. The latent genes represented are the EBNA1, 2, 3A, 3B, 3C, LP, LMP 1, 2A and B and the EBERs. LMP2A and B are transcribed from different promoters and their transcripts are positioned across the terminal repeats (TR). LMP1 is transcribed in the opposite direction to the rest of the latent genes. EBNA-LP is transcribed from several W repeat exons the number of which is variable.

(b) is a linear representation of the *Bam*HI map of EBV and the location of the ORFs of the latent genes. The fragments are named according to their size, with A being the largest. The Nhet represents the area over which the LMP2s are transcribed. Since they are transcribed over the terminal repeats which differ in number from one EBV strain to another the fragment is called Nhet to represent the heterogeneity that can occur.

ORF	Gene product	Alternative nomenclature	Cellular Location
BKRF1	EBNA1		Nuclear
BYRF1	EBNA2		Nuclear
BLRF3-BERF1	EBNA3A	EBNA3	Nuclear
BERF2a-BERF2b	EBNA3B	EBNA4	Nuclear
BWRF1	EBNALP	EBNA5	Nuclear
BERF3-BERF4	EBNA3C	EBNA6	Nuclear
BNLF1	LMP1	LMP	Membrane
BARF1/BNRF1	LMP2A	TP1	Membrane
BNRF2	LMP2B	TP2	Membrane
BCRF1	EBER1,2		Cytoplasm and nucleus
BARF0	<i>Bam</i> HI transcripts		Cytoplasm

Table 1.1: ORF, gene product, alternative nomenclature and cellular localisation of the product of EBV latent genes.

Latent genes are expressed variably in different subsets of B cells in healthy EBV carriers and also in all the EBV associated malignancies. Based on the variable expression, three major latency programs have been identified and the genes expressed and their disease association is given in table 1.2. Naïve tonsillar B cells of healthy EBV carriers show expression of all latent genes corresponding to latency III, whereas memory tonsillar B cells of healthy carriers show latency II pattern. Peripheral B cells express a very restricted pattern of latent genes possibly expressing only LMP2 (Babcock et al., 2000; Babcock and Thorley-Lawson, 2000; Joseph et al., 2000).

Latency pattern	Latent genes expressed
Latency I	EBNA1, EBERs, <i>Bam</i> A RNAs
Latency II	EBNA1, LMP1, 2A, 2B, EBERs, <i>Bam</i> A RNAs
Latency III	EBNA1, 2, 3A, 3B, 3C, LP, LMP1, 2A, 2B, EBERs, <i>Bam</i> A RNAs

Table 1.2: The latency patterns of EBV

The focus of my thesis is LMP1, however a brief description of the other latent genes is given below.

EBNA1

EBNA1 is 641 aa long and encodes a 65-94kDa protein. EBNA1 is expressed in all the EBV associated diseases and is one of the few latent proteins expressed in the lytic cycle of the virus. EBNA1 is made up of three distinct domains with further subdomains; the basic amino terminus (1-89aa), the glycine-alanine (Gly-Ala) repeats region (90-328aa), and the carboxy terminus (328-641aa). The Gly-Ala repeats give the virus the ability to evade the host immune response by preventing protein processing by ubiquitination, proteasomal degradation and presentation and also limit self expression (Levitskaya et al., 1995; Levitskaya et al., 1997). Flanking the Gly-Ala repeats are Arg-Gly motifs that resemble RGG motifs and allow EBNA1 to bind RNA (Snudden et al., 1994). The first region within the carboxy terminus is a Pro-Arg rich region (327-377aa) that mediates interactions between EBNA1 molecules bound to distant DNA binding sites mediating linking and looping (Goldsmith et al., 1993; Mackey et al., 1995; Su et al., 1991). Between residues 379-387 lies the nuclear localisation signal, followed by a serine rich region (375-400aa) which becomes phosphorylated but the importance of this phosphorylation is still unknown (Hearing and Levine, 1985; Polvino-Bodnar et al., 1988). Between residues 459-607 is the DNA binding and homodimerisation region of EBNA1 (Ambinder et al., 1990). At the carboxy terminus is an acidic rich region that plays a role in the episomal segregation into daughter cells during cell division.

The primary role of EBNA1 is the maintenance of the viral episome during cell division (Lee et al., 1999; Yates et al., 1984). To perform this function, EBNA1 binds as a dimer to two regions in the OriP of EBV. OriP has a region of 20 tandem direct 30bp repeats called the family of repeats (FR), each capable of binding an EBNA 1 dimer. An EBNA1 dimer can also bind at 4 sites in the dyad symmetry element (DS) 1kb downstream of FR. Binding of EBNA1 to FR allows FR to function as a transcriptional enhancer for RNA polymerase II transcribed genes thus allowing for EBNA1 autoregulation and regulation of the other latent EBV genes (Reisman and Sugden, 1986). The DS is essential for episomal replication but without the FR, DS is inefficient in maintaining transcription, plasmid replication or maintenance. EBNA1 can also bind the nuclear matrix attachment region in the host chromosomes (Jankelevich et al., 1992).

EBNA1 is the only viral protein that can associate with cellular chromosomes during mitosis and this is thought to be essential for the maintenance of the viral episome. EBNA1 also binds cellular proteins, EBP2 (EBNA1 binding protein 2) and P32/TAP. EBP2 binds to both mitotic chromosomes and EBNA1 thus mediating the interaction of EBNA1 with chromosomes and

facilitating the segregation of the viral episome into daughter cells (Kapoor and Frappier, 2003).

EBNA1 may also play a role in the oncogenicity of the virus, since transgenic animals that express EBNA1 in B cells succumb to malignant B cell lymphomas (Wilson et al., 1996; Wilson and Levine, 1992). Further, EBNA1 is essential in the survival of BL cells as its inhibition leads to apoptosis and it is necessary for efficient LCL formation, supporting an EBNA1 role in cell survival (Humme et al., 2003; Kennedy et al., 2003). Consistent with these, are the results obtained from transgenic EBNA1 mice premalignant B cells that show increased Bcl-x_L (an anti-apoptotic protein), RAG1 and RAG2 levels (Tsimbouri et al., 2002). Recent data from these mice also show that there is a dependency for survival on IL-2 signalling that is induced via EBNA1 (Tsimbouri *et al.*, in preparation).

EBNA2

EBNA2 is a 487 aa nuclear protein that along with EBNA1 are the first to be expressed after B cell infection with the virus *in vitro* (Allday et al., 1989; Rooney et al., 1989). EBNA2 cooperates with EBNA1 to induce transition of the infected cells from G0 to G1 (Sinclair et al., 1994). EBNA2 is essential for the initiation and maintenance of EBV transformation of B cells *in vitro* (Cohen and Kieff, 1991; Cohen et al., 1991; Hammerschmidt and Sugden, 1989; Kempkes et al., 1995). EBNA2 acts as a transcriptional regulator by binding to the cellular transcriptional repressor RBP-Jκ (involved in the Notch signalling pathway), which binds to DNA. By binding to RBP-Jκ, the repression function is alleviated and transcription of viral and cellular genes can take place. By binding to recombination binding protein Jκ (RBP-Jκ), EBNA2 can transactivate the LMP2A promoter, the Cp promoter, the LMP1 promoter and the CD23 promoter (Abbot et al., 1990; Fåhraeus et al., 1990; Laux et al., 1994; Ling et al., 1994; Ling et al., 1993; Sung et al., 1991; Wang et al., 1990; Zimmer-Strobl et al., 1993; Zimmer-Strobl et al., 1991). EBNA2 regulates expression of some cellular genes such as CD21, CD23, *c-myc*, *c-fgr*, EBI1/BLR2 and the immunoglobulin heavy chain gene (Burgstahler et al., 1995; Calender et al., 1987; Cordier et al., 1990; Jochner et al., 1996; Kaiser et al., 1999; Knutson, 1990; Wang et al., 1987). Binding of EBNA2 to RBP-Jκ is necessary but not sufficient for gene expression induction. EBNA2 requires binding of other cellular proteins such as PU.1 and AUF1.

EBNA2 competes with EBNA3A and 3C for RBP-Jκ binding (Johannsen et al., 1996; Robertson et al., 1995; Waltzer et al., 1996; Zhao et al., 1996).

EBNA 3A,B,C

The three EBNA3 genes are tandemly located in the EBV genome. They encode nuclear, hydrophilic proteins with heptad repeats of leucine, isoleucine or valine. EBNA3A and 3C are essential for B cell transformation in culture whereas EBNA3B is not (Tomkinson et al., 1993). The EBNA3s can bind to RBP-J κ and compete with EBNA2 for binding to it and also transcriptionally regulate genes with RBP-J κ binding sites (Allday and Farrell, 1994; Robertson et al., 1995; Robertson et al., 1996; Wang et al., 1990). EBNA3s can block the EBNA2 activation of the LMP2 promoter (Le Roux et al., 1994). EBNA3C can block EBNA2 mediated LMP1 promoter activation via repression of the Cp promoter or cooperate with EBNA2 and activate the LMP1 promoter under different conditions (Allday et al., 1993; Lin et al., 2002; Marshall and Sample, 1995). It is thought that since LMP1 levels are important for viral survival, EBNA3C activation or repression of the LMP1 promoter is essential in maintaining proper LMP1 levels and inhibiting uncontrolled expression. EBNA3C has been shown to cooperate with Ras and transform rodent fibroblasts in culture, to weakly interact with retinoblastoma (Rb) and remove the block induced by p16^{INK4a} in cycle progression (Parker et al., 1996; Parker et al., 2000). EBNA3C can also interact with cellular proteins including SUMO1/3, nonmetastatic protein 23- homologue 1(Nm23-H1) (Subramanian and Robertson, 2002), histone deacetylase (HDAC1) (Radkov et al., 1999) that are controlling transcription and also associate with CyclinA (Knight and Robertson, 2004) thus mediating progression through S phase and entry into mitosis. Despite the above role of EBNA3C in transformation and cell cycle progression, EBNA3s are not expressed in any of the EBV associated malignancies or in memory B cells from healthy carriers therefore their role in malignant disease is not clear. EBNA3s are the latent proteins for which the host cytotoxic T lymphocytes (CTL) elicit the strongest reaction to, both in healthy virus carriers and upon primary B cell viral infection and thus their downregulation permits viral persistence (reviewed in (Khanna and Burrows, 2000; Rickinson and Moss, 1997).

EBNALP

EBNALP is encoded by the leader of each of the bicistronic EBNA mRNAs and its size varies between the various EBV isolates. It is made up of repeating 22 or 44 aa exons called W1 and W2, two unique exons Y1 and Y2 and a 45 amino acid carboxy terminus. EBNALP and EBNA2 are the first proteins to be expressed in the latent infection of primary B cells in culture and even though EBNALP is not essential for B cell transformation it is required for

efficient transformation (Allan et al., 1992) mediated by the Y1 and Y2 exons (Mannick et al., 1991). EBNA1P and EBNA2 show cooperating effects in stimulating the increase in the expression of LMP1 and this is mapped to the W1 and W2 repeats of EBNA1P (Harada and Kieff, 1997; Nitsche et al., 1997). EBNA1P and EBNA2 also cooperate in activating cellular genes such as CD23 and CyclinD2 in resting B cells (Sinclair et al., 1994). EBNA1P has been shown to have a weak interaction with p53 and Rb in *in vitro* biochemical studies but these results have not been confirmed *in vivo* (Jiang et al., 1991; Szekely et al., 1993). More recently other cellular proteins that interact with EBNA1P have been identified. These include the heat shock protein 70 family (hsp72/hsc73) (Mannick et al., 1995), DNA-PK, HA95, hsp27, α -tubulin and β -tubulin (Han et al., 2001). The exact role played by these interactions is still unclear. EBNA1P transgenic mice were created showing a phenotype of premature death due to heart failure (Huen et al., 1993). However, expression of the transgene was directed to cardiac and other tissue by using the cytomegalovirus (CMV) promoter and as such the relevance to EBV associated disease is difficult to determine.

LMP2A and B

The LMP2 gene is transcribed only from the circular EBV genome as the transcription unit crosses the TR. Two different promoters (3kb apart) are used which give rise to transcripts differing in length at the 5' end. The translation product of the longer 9 exon transcript is LMP2A and the shorter 8 exon product (effectively 119aa N-terminal deletion of LMP2A) is termed LMP2B. Both LMP2 proteins are transmembrane, consisting of twelve transmembrane spanning domains (Sample et al., 1989). LMP2A and B have been detected in LCLs, and in NPC biopsies. In epithelial cells LMP2A may be involved in transformation by activating the PI3K/Akt pathway (Fukuda and Longnecker, 2004; Scholle et al., 2000). It is thought that LMP2A plays a role in the survival and persistence of infected B cells *in vivo*. LMP2 forms patches at the cell membrane and LMP2A is thought to act like a constitutively active B cell receptor (BCR) to promote B cell survival *in vivo*, demonstrated in transgenic mice (Caldwell et al., 1998). Phosphorylation of its amino terminal domain recruits members of the *src* family of tyrosine kinases, specifically *fyn* and *lyn* (Longnecker, 2000; Longnecker et al., 1991). By this recruitment LMP2A activates BCR signal transduction such as calcium mobilisation and may thus act to block the switch from the latent to the lytic cycle (Fruehling and Longnecker, 1997; Fruehling et al., 1998; Miller et al., 1994a; Miller et al., 1993). Due to its lack of the amino terminus LMP2B does not mimic or block BCR signalling but may act to control the effects of LMP2A (Longnecker, 2000). Therefore, LMP2s play a role in

maintaining the virus in its latent form, inhibiting reactivation and thus possible recognition by the host immune system.

Epstein Barr Virus small RNAs (EBERS) 1 and 2

EBERs 1 and 2 are non polyadenylated, untranslated RNAs that are expressed in all latency types apart from a new latency type discovered in liver tumour cells (Sugawara et al., 1999). EBERs are highly expressed in all other EBV associated tumours and thus used in *in situ* hybridisations as a marker for the presence of the EBV genome (Khan et al., 1992; Wu et al., 1991).

EBER genes can be deleted from the EBV genome without affecting the viral ability to infect, transform B cells in culture, remain latent or switch to the lytic cycle. However, they may play an important role in maintaining the immortalised phenotype of EBV infected cells (Greifenegger et al., 1998; Swaminathan et al., 1991).

The two EBERs are expressed from the *Eco* RI J fragment of the EBV genome, separated by 160 bp and they are transcribed by RNA polymerase III. Expression of the EBERs varies as in some BL cells EBER1 is detected at a 10 fold higher level than EBER2 (Lerner et al., 1981). Studies have suggested that the difference seen is because EBER1 has a longer half life than EBER 2 (Clarke et al., 1992).

EBER1 is 167 nucleotides, EBER2 is 172 nucleotides and they are 54% homologous at the primary sequence. Their primary sequence is highly conserved among different EBV strains (Arrand et al., 1989). Both show an extensive and similar predicted secondary structure (Glickman et al., 1988). Studies in which the predicted secondary structure was disrupted by replacement of inosine residues for guanosine resulted in complete inhibition of binding of EBER1 to one of the protein targets of EBERs, interferon inducible double stranded RNA activated protein kinase R (PKR) (Clarke et al., 1991). Thus the secondary structure is important for the EBER function. In the cell, EBERs are associated with the rough endoplasmic reticulum and can also associate with chromosomes during metaphase (Schwemmler et al., 1992).

EBERs can associate with three cellular proteins; the La antigen, the ribosomal protein L22 (or EAP) and PKR.

EBERs compete with viral generated dsRNA in binding to PKR. Usually, PKR is activated by viral dsRNA thus activating the interferon response leading to apoptosis and growth

inhibition, protecting the host from viral agents (Nanbo et al., 2002). Binding of EBERs to PKR thus prevents PKR activation therefore allowing survival of the virus infected cell (Katze et al., 1991).

An oncogenic property of EBERs has been suggested by transfection of EBERs into Akata (EBV negative) cells which induced cell growth in soft agar, tumour formation in SCID mice, conferred apoptosis resistance to the cells and upregulated levels of bcl-2 (Komano et al., 1999; Komano et al., 1998; Ruf et al., 2000). Similar effects were shown when EBERs were transfected into Bjab cells (EBV negative BL cell line), NIH3T3 cells and cord blood lymphocytes (Laing et al., 1995; Zeuthen, 1983). Recently, a binding site in the EBER1 promoter for c-myc was discovered (Niller et al., 2003). This opens up a new scenario for the involvement of EBERs in the development of BL. Translocation of *c-myc* in BL could lead to activation of the anti-apoptotic effect of EBERs in an EBV positive cell, thereby contributing to the transformation process.

Bam HI A RNA transcripts (BARTs)

BARTs have been identified in NPC, HD, BL, nasal T/ natural killer (T/NK) cell lymphoma, post-transplant lymphoproliferative disorders (PTLDs), and the peripheral blood of healthy individuals (Chen et al., 1999; Deacon et al., 1993; Hitt et al., 1989) but the protein products have been poorly characterised. RPMS1 ORF product binds to nuclear CBF1 (a component of the Notch signalling), preventing transcriptional activation and thus inhibiting Notch/EBNA2 action. Another ORF encodes the A73 protein that interacts with the cellular RACK1 that controls PKC and Src signalling, thus implying that A73 may play a role in growth regulation (Smith et al., 2000). BARF0 was one of the first products identified and is described below.

BARF0

BARF0 transcripts have been implicated in NPC but the BARF0 protein which is 16-20kDa has not yet been detected. Experiments using EBV virus deleted for 58kb including BARF0, transfected into B lymphocytes, led to B cell transformation showing that BARF0 does not play a role in this process (Robertson et al., 1994).

BARF1

BARF1 is a 31kDa protein that is secreted from infected B cells and has been detected in EBV associated NPC. Its gene transcript has been detected in EBV associated gastric carcinoma

(Decaussin et al., 2000; zur Hausen et al., 2000). It has an immortalising effect when expressed in primary simian epithelial cells and can transform rodent fibroblasts or human B cells and can act as a growth factor when added in culture (Sall et al., 2004; Sheng et al., 2003; Wei et al., 1997). BARF1 has been identified to be a receptor of human colony-stimulating factor 1 (CSF-1) and share homology with the CSF-1 receptor, the protooncogene *c-fms*. Since CSF-1 is a cytokine involved in macrophage differentiation it is possible that BARF1 plays a role in attenuating the host immune response to viral infection (Strockbine et al., 1998). It has also been discovered that BARF1 can activate Bcl-2 (an anti-apoptotic protein) via its N-terminal region.

1.3 LMP1

Structure of LMP1

The LMP1 gene consists of three exons and is read from the right end (as usually depicted) of the linear virus genome in the reverse orientation to the EBNA5s. LMP1 is a 63kDa protein of 386 aa. LMP1 is a transmembrane protein that is located in cellular membranes including the plasma membrane where it associates with vimentin in B cells and the cytoskeleton. It has been recently shown to be located in intracellular lipid rafts and primarily signal from there (Lam and Sugden, 2003). Once in the membrane LMP1 can undergo several post-translational modifications including cleavage at the carboxy terminus (at Leu 242) to release a 25kDa C-terminal fragment and phosphorylation on serine (Ser313) and threonine (Thr324) (Baichwal and Sugden, 1987; Moorthy and Thorley-Lawson, 1993). The half life of LMP1 varies from 2-15hrs depending on whether it is associated with the cytoskeleton or not and depending on LMP1 strain and cell type.

LMP1 comprises three distinct regions; a positively charged short amino terminus (1-24aa) followed by six transmembrane domains (25-186aa) and a long effector carboxy terminus (187-386aa) (Fennewald et al., 1984). The carboxy terminus can be further divided into three domains, termed carboxy terminus activating regions (CTAR) 1-3 that mediate binding of several cellular proteins and activate downstream signalling pathways. Within the carboxy terminus is an 11aa repeat motif, the number of repeats varies among the different LMP1 strain variants (fig.1.2).

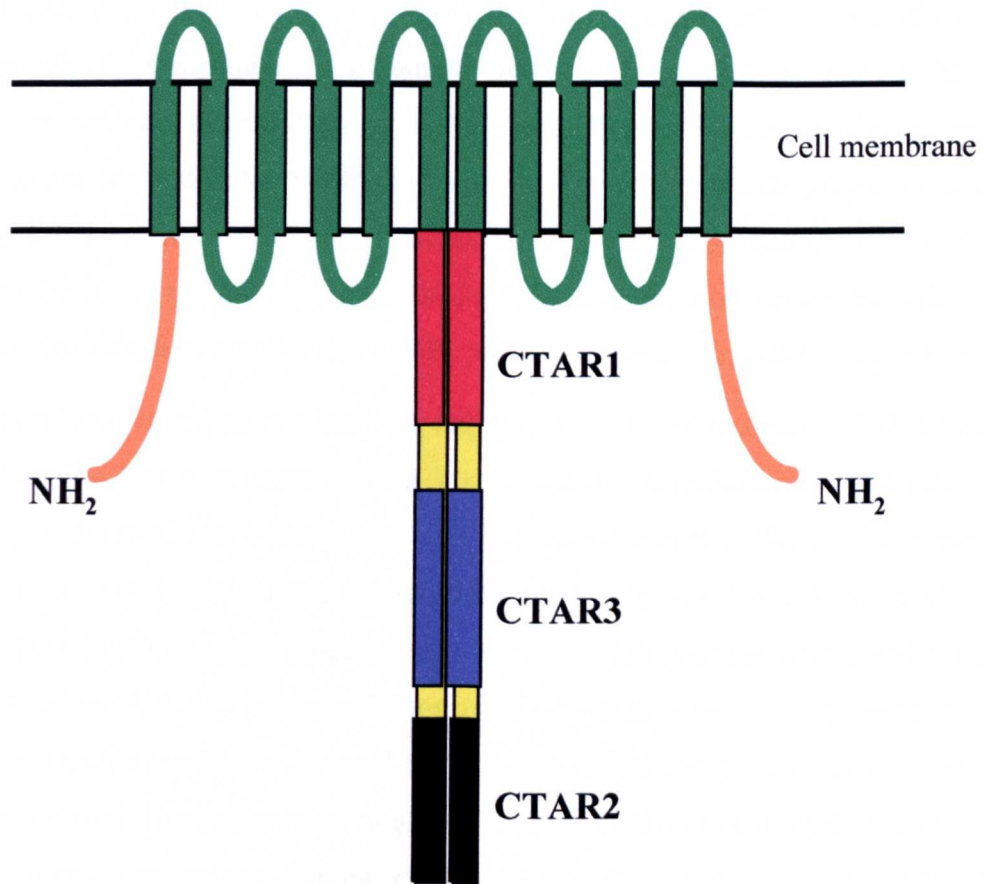


Figure 1.2: The structure of LMP1 (Not to scale)

LMP1 oligomerises at the membrane. LMP1 comprises a short amino terminus (orange), six transmembrane domains (green), and a long carboxy terminus. There are three regions within the carboxy terminus; CTAR1 (red), CTAR3 (blue) and CTAR2 (black) which associate with cellular proteins to mediate the signalling activity of LMP1.

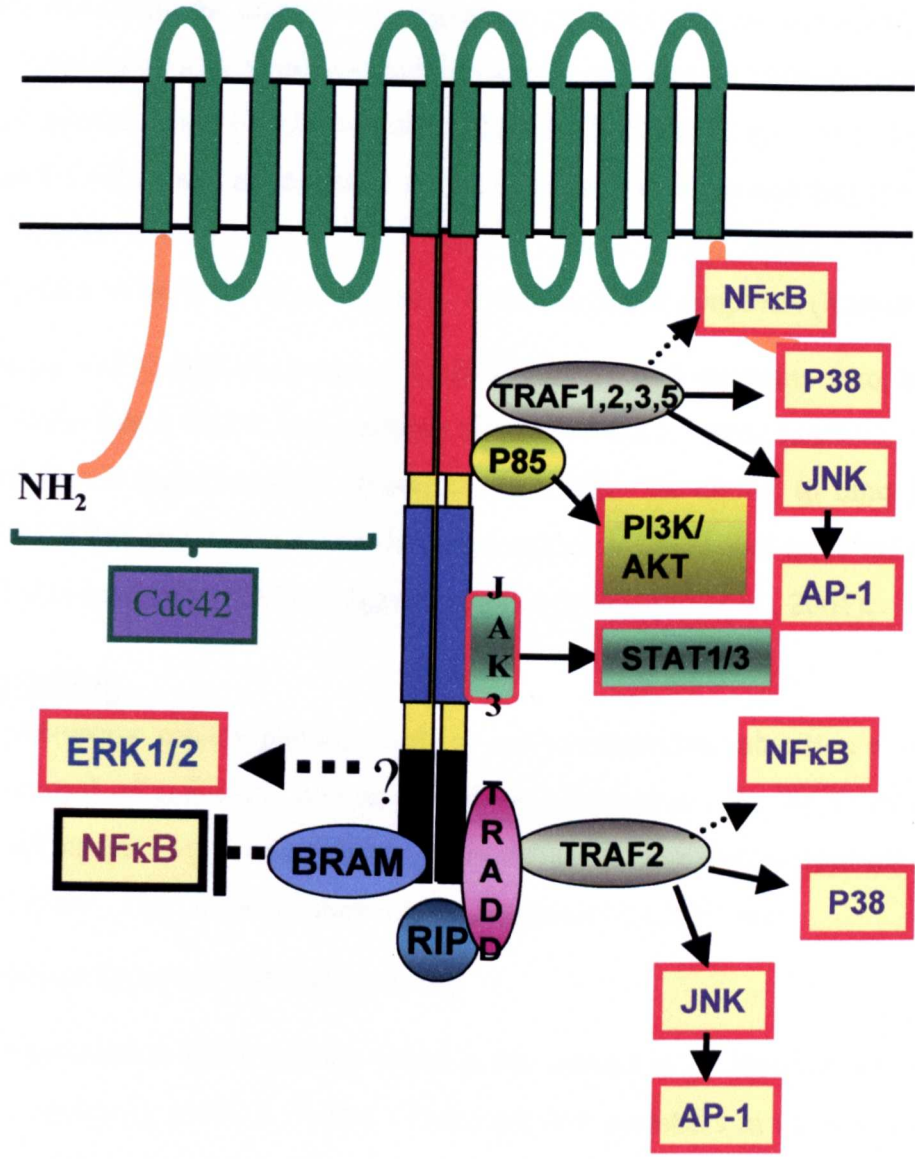
Deletion studies have been used as a means to determine the function of the various domains of LMP1. It was shown that the amino terminus of LMP1 is essential for efficient transformation, orienting LMP1 within the cell membrane (Coffin et al., 2001) and ubiquitin targeted degradation of LMP1. Deletion of the first 44aa of LMP1 - including the amino terminus and the first transmembrane domain - led to accumulation of LMP1 at the membrane but failed to induce aggregation of LMP1 and B cell transformation, showing that oligomerisation is needed for LMP1 to exert its function and that proper orientation and anchoring in the plasma membrane is essential for LMP1 aggregation (Izumi et al., 1994; Kaye et al., 1993). A mutant LMP1 that had a 12aa acid deletion within the amino terminus, failed to bind to ubiquitin and thus the LMP1 molecule was not degraded (Aviel et al., 2000).

The transmembrane domains of LMP1 are required for oligomerisation of LMP1 (Kaykas and Sugden, 2000; Kaykas et al., 2001) which is essential for its transforming and other functions (Baichwal and Sugden, 1989; Kaye et al., 1993; Liebowitz et al., 1992). The transmembrane domains are required for activating caspase-3 and inducing cell death (Nitta et al., 2004), are needed for protein stabilisation (Blake et al., 2001), for efficient signalling and for activating the small GTPase Cdc42, inducing cytoskeletal reorganisation and phosphorylating the eukaryotic translation initiation factor 2 (eIF2a) thus inhibiting gene expression (Lam et al., 2004). Expression of a dominant negative Cdc42 in fibroblasts and B cells, inhibited cytoskeletal reorganisation and deletion studies mapped the Cdc42 activation site in the LMP1 transmembrane domains (Puls et al., 1999; Wang et al., 1988). The first and second transmembrane domains are required for the cytostatic effects observed as a result of LMP1 overexpression and for LMP1 association with lipid rafts as demonstrated by deletion studies in epithelial, BL and T cells (Coffin et al., 2003; Kaykas and Sugden, 2000; Sandberg et al., 2000).

The carboxy terminus is responsible for mediating activation of several signalling pathways via interaction with cellular proteins and is essential for B cell transformation (Kaye et al., 1995; Peng-Pilon et al., 1995) (fig1.3). CTAR1 spans aa 194-232 and contains a PXQXXD motif that allows binding of tumour necrosis factor receptor-associated factors (TRAFs) 1,2,3,5 (Devergne et al., 1997; Devergne et al., 1996; Devergne et al., 1998; Kaye et al., 1996; Mosialos et al., 1995; Sandberg et al., 1997). The TRAF binding domain in CTAR1 is essential for B cell transformation as shown by a deletion mutant that lacks aa 185-211 (Izumi et al., 1997). CTAR2 spans aa 351-386 and contains a YYD motif that allows tumour necrosis factor associated death domain (TRADD) and bone morphogenic protein receptor associated

Figure 1.3: Signalling pathways activated by LMP1

The diagram shows the signalling pathways activated by LMP1. The amino terminus and the transmembrane domains of LMP1 can lead to Cdc42 activation which leads to cytoskeletal reorganisation. CTAR1 recruits the p85 subunit of PI3K leading to activation of the PI3K/Akt pathway. CTAR1 also recruits a TRAF complex consisting of TRAFs 1/2/3/5. This complex leads to p38 and JNK/AP1 activation directly and via TRAF6 to NF- κ B activation. Similarly, CTAR2 leads via recruitment of RIP and TRADD and their association with TRAF2 to activation of the same pathways. CTAR2 can also lead via an as yet unidentified molecule to ERK1/2 activation. CTAR2 associates with BRAM which plays a role in negatively regulating NF- κ B activation. CTAR3 associates with JAK3 leading to activation of STAT1/3. Note that activation is indicated by a red outline, whilst inhibition is indicated by a thick black outline. Pathways which involve other unknown molecules are shown as dotted arrows.



molecule (BRAM) binding. The CTAR2 region is essential for maintaining the outgrowth of LCLs as a mutant lacking the last 155 residues can initiate B cell proliferation but cannot maintain the growth of LCLs. It is believed that CTAR2 enables this by its ability to bind TRADD and activating the downstream signalling pathways (Izumi and Kieff, 1997; Kaye et al., 1995). It was shown by yeast-two-hybrid experiments that the carboxy terminus of LMP1 can directly interact with TRAFs 1-4 and TRADD (Brodeur et al., 1997; Devergne et al., 1996). Both CTAR1 and 2 are essential for B cell immortalisation and they are also known as the transformation effector sites (TES) 1 and 2 (Izumi et al., 1999). In epithelial cells, presence of either of these domains enhances TNF α mediated apoptosis (Kawanishi, 2000).

CTAR3 spans aa275-330 (between CTARs1 and 2) and contains two box 1 regions (PXXPXP) and a box 2 region that mediates binding of Janus kinase (JAK) 3. CTAR3 is not essential for B cell transformation (Izumi et al., 1999). Its ability to bind JAK3 may be affected by CTARs1 and 2 as use of a dominant negative LMP1 that inhibited CTAR1 and 2 signalling, led to inhibition of STAT signalling as well (Brennan et al., 2001).

LMP1 signalling

LMP1 is a pleiotropic protein playing a role in cell proliferation, inhibition of apoptosis, cell cytoostasis, control of cell cycle and angiogenesis. It mediates its functions by activating several signalling pathways and this has very different, sometimes opposite outcomes in different cell types. The pathways shown to be impacted by LMP1 are:

(1) the nuclear factor κ B (NF- κ B) pathway

NF- κ B is a transcription factor usually found in the cytosol as an inactive homo/heterodimer bound to the inhibitory proteins (I κ Bs). There are five members in the mammalian NF- κ B family; p65, c-Rel, RelB, p50/p105 (when unprocessed) and p52/p100 (when unprocessed). Binding of ligands to IL-1 receptors, TNF receptors, lysophospholipid (LPL) receptors and other extracellular signals activate the I κ B regulatory kinases (IKK) activating kinases (NIK or MEKK1) that can phosphorylate and activate IKKs. Activated IKKs, phosphorylate I κ Bs. I κ B phosphorylation leads to the release of the bound NF- κ B that can now translocate to the nucleus and activate various genes by binding to NF- κ B sites in their promoters (reviewed in (May and Ghosh, 1998).

The NF- κ B pathway is activated by both CTAR 1 and CTAR2 of LMP1. CTAR1 is responsible for about 20-30% of the total NF- κ B LMP1 mediated activation whilst CTAR2 is responsible for the rest (Floettmann and Rowe, 1997; Huen et al., 1995; Mitchell and Sugden,

1995; Paine et al., 1995). CTAR1 associates with the TRAF1,2,3,5 complex recruiting NIK, phosphorylating I κ B and releasing NF- κ B (Luftig et al., 2003; Luftig et al., 2004; Sylla et al., 1998). CTAR2 associates with TRADD, recruiting TRAF2 or associates with receptor interacting protein (RIP), both routes activating NF- κ B. Overexpression of LMP1 CTAR2 domain and either TRADD or RIP in 293 cells led to the conclusion that TRADD cooperates with CTAR2 in activating NF- κ B but RIP has only an additive effect on this activation (Izumi et al., 1999).

NF- κ B signalling is essential for the transforming properties of LMP1 both in B and Rat-1 cells (Cahir et al., 1999, He et al., 2000). Anti-apoptotic genes (*bcl-2*, *A20*, *Mcl-1*, *c-IAP2*), genes involved in angiogenesis, invasion and metastasis (*MMP9*, *COX-2*, *VEGF*, *IL-8*, *Id-1*) are activated by binding of NF- κ B to binding sites in their promoters (D'Souza et al., 2004; Li et al., 2004; Murono et al., 2001; Yoshizaki, 2002; Yoshizaki et al., 1998). EGFR is upregulated by NF- κ B in HNE2 cells in a similar way (Tao et al., 2004b). In a C33A (a cervical carcinoma line) cell line NF- κ B activity was not sufficient for EGFR upregulation (Miller et al., 1995; Miller et al., 1997) but both studies concluded that CTAR1 was essential for this activation.

NF- κ B activity can be modulated by binding of BRAM1 to CTAR2. This interaction, inhibits I κ B α phosphorylation leading to inhibition of NF- κ B activation (Chung et al., 2002). BRAM1 is therefore acting as a negative regulator of the LMP1 mediated functions. LMP1 also modulates NF- κ B activity via the A20 protein which is upregulated by activated NF- κ B. Upregulation of A20 leads to A20 interacting with LMP1 and competing with TRADD and TRAF1 for binding to the LMP1/TRAF1/2/TRADD complex. Displacement of TRADD and TRAF1 from LMP1 binding complexes leads to inhibition of CTAR2 mediated NF- κ B activation and CTAR1 mediated JNK activation. Decreased NF- κ B activity, leads to decreased A20 levels and so TRADD and TRAF1 can bind CTAR2 and CTAR1 respectively, activating NF- κ B and JNK signalling (Fries et al., 1999). In this way LMP1 negatively regulates its own biological functions.

(2) the c-Jun N-terminal kinase (JNK pathway)

CTAR2 mediates the activation of the JNK pathway. It has been revealed with mutational studies that the last 8aa of CTAR2 are important for this activation. However, a recent study using mouse embryo fibroblasts (MEFs) from knock out mice (RIP, TRAF6, TRAF2, IRAK4, TAB2 null) and small interfering RNA (siRNA), challenges the belief that JNK activation was

dependent on recruitment of TRADD and TRAF2 to CTAR2 and stress enhanced kinase (SEK) activation. The latter suggests that an unidentified linker leads to TRAF6 association with CTAR2 linking it to a TAB1/TAK1 complex that then activates JNKK1/2 that will then lead to JNK activation (Eliopoulos et al., 1999; Eliopoulos and Young, 1998; Kieser et al., 1997; Wan et al., 2004). Active JNK phosphorylates c-Jun leading to homo/heterodimer formation with other members of the Jun or Fos family thus producing an active AP1 complex. The TRAF 2,3,5 complex associates with CTAR1 and recruits TRAF1 which also leads to JNK/AP1 activation. A new heterodimer formation between c-Jun and JunB mediated by LMP1 in the HNE2 cell line, can expand the signalling pathways affected by LMP1 (Song et al., 2004b).

(3) the p38MAPK pathway

The p38MAPK pathway is activated in epithelial cells via the same regions and cellular effector proteins as for NF- κ B but the two pathways separate downstream of TRAF2 as chemical inhibitors and dominant negative TRAF2 expression studies have shown (Eliopoulos et al., 1999). Activation of p38MAPK leads to IL-6 and IL-8 upregulation that play a role in cell survival.

(4) the JAK/STAT pathway

The CTAR3 region contains 2 box1 elements and a box 2 that contain binding elements for JAK3. Binding of JAK3 to CTAR3 leads to its auto/transphosphorylation leading to activation of signal transducer and activation of transcription (STAT) 1 and 3, transcription factors in B and epithelial cells (Gires et al., 1999). Further, LMP1 expression in CNE-2 cells led to activation of STAT3 and 5 and STAT3 activation was shown to lead to the upregulation of the *c-myc* gene (Chen et al., 2003). A dominant negative form of LMP1 in which the PXQXXD motif was substituted for alanine (AXAXXA), and the first tyrosine of the YYD motif in CTAR2 region was replaced by glycine inhibited NF- κ B and AP1 signalling by preventing binding of TRAF2 to LMP1. Surprisingly, even though the CTAR3 region was intact, STAT signalling was inhibited, implying that intact CTAR1 and 2 domains play a role in CTAR3 mediated signalling (Brennan et al., 2001).

(5) the PI3K/Akt pathway

The CTAR1 region of LMP1 can lead to activation of the PI3K/Akt cascade in epithelial cells by recruiting the p85 subunit of the PI3K either directly or via a linker (Dawson et al., 2003).

Activation of Akt can lead to growth proliferation, decreased apoptosis and actin cytoskeleton reorganisation.

(6) the ERK1/2 pathway.

In rat fibroblasts LMP1 has been shown to increase ERK1/2 phosphorylation and this is Ras dependent. Where this activity maps on the LMP1 protein is not known. However, this study shows that LMP1 can possibly transform cells via activation of the Ras pathway (Roberts and Cooper, 1998). Activation of ERK1/2 can lead to transcription of genes involved in proliferation, angiogenesis and metastasis. One such factor that is upregulated by LMP1 via the ERK1/2 activation in human epithelial nasopharyngeal cells, is HIF-1 α which upregulates the vascular endothelial growth factor (VEGF), and RECK, a metastasis suppressor gene (Wakisaka et al., 2004). Transfection of an LMP1 expressing vector into an EBV negative NPC cell line (TW04) led to decrease of RECK protein and inhibition of its promoter (Liu et al., 2003). LMP1 transformed MDCK cells show increased levels of Ets1 – an ERK1/2 target - that contributes to metastatic invasion by upregulating c-Met (Horikawa et al., 2001). LMP1 mediated activation of ERK1/2 not only plays a role in proliferation but also in metastasis. Constitutive LMP1 mediated, ERK1/2 activation in gastric epithelial cells leads to TGF β inhibition thus releasing the cells from the TGF β mediated growth arrest (Fukuda et al., 2002). The TGF β /Smad pathway can also be inhibited in an NF- κ B mediated way in HEK293 cells and COS-7 fibroblasts (Prokova et al., 2002).

The role of LMP1 in cell cycle control has been investigated in murine and human fibroblasts where LMP1 expression led to their proliferation, downregulation of p16^{INK4a} and inhibition of Ras induced senescence (Yang et al., 2000a; Yang et al., 2000b). This LMP1 induced p16^{INK4a} inhibition, was found to be due to LMP1 promoting the nuclear export of Ets2 (transcriptional activator of p16) and E2F4/5 (downstream mediators of p16)(Ohtani et al., 2003). Even though LMP1 alone did not lead to transformation, its cooperation with an oncogene (mutant CDK4, that cannot be p16^{INK4a} inhibited) did.

LMP1 via CTAR1 leads to increased epithelial cell sensitivity to DNA damaging factors leading to micronucleus formation. Accumulation of unrepaired DNA can cause genomic instability (Liu et al., 2004). LMP1 also inhibits p53-mediated apoptosis in both BL and epithelial cells (Fries et al., 1996). LMP1 can also activate DNA methyltransferases via CTAR1, leading to hypermethylation of the E-cadherin promoter, enhancing invasiveness in epithelial cells .

LMP1 exerts different effects in different cell types but collectively all point to a very complex molecule that activates pathways associated with tumorigenesis.

LMP1 Function

Even though LMP1 has no primary sequence homology with any known proteins it shares functional similarities and core motifs to the TNFR family of receptors especially CD40. LMP1 has been shown to be constitutively active and be independent of ligand dependency (Gires et al., 1997; Hatzivassiliou et al., 1998). Expression of LMP1 independent of ligand allows for continual proliferation of human B cells infected with EBV. This proliferation is also possible with CD40 signalling. However, both LMP1 and CD40 induced proliferation was found to be EBNA2 dependent. In experiments where EBNA2 expression was inhibited, B cells did not maintain proliferation either in the presence of LMP1 or in the presence of CD40 (Kilger et al., 1998; Zimmer-Strobl et al., 1996). Even though LMP1 signals in the absence of a ligand, it can regulate its activity. Increased levels of LMP1 can lead to cytostasis thus protecting the host cell from excessive signalling and can lead to inhibition of gene products transcribed from the Cp and LMP1 promoters thus regulating its own expression as well as inhibiting cellular protein synthesis (Hammerschmidt et al., 1989; Sandberg et al., 2000).

Another role that LMP1 may have in the viral context is that it activates interferon regulatory factor (IRF) 7 that regulates latency via preferred promoter usage and also activates the cytotoxic T cells, enabling the host's immune system to kill cells that are undergoing uncontrolled proliferation induced by EBV. This agrees with the role LMP1 has in inducing cytostasis and inhibition of gene expression as described above and with the role it plays in inhibiting viral lytic cycle induction. Inhibition of lytic cycle prevents massive amounts of new virus being presented to the host immune system and also prevents extensive cell damage to the host (Adler et al., 2002). In B cells LMP1 expression can upregulate cell activation and cell adhesion factors such as CD23, CD39, CD40, CD44, CD83, MLH II, IL-10(Nakagomi et al., 1994), LFA-1, ICAM-1, LFA3 and can downregulate CD10 leading to cell growth and also elimination of transformed B cells to protect the host. It can also protect B cells from apoptosis via upregulation of bcl-2 and A20 , both anti-apoptotic proteins (D'Souza et al., 2000; Henderson et al., 1991; Rowe et al., 1994).

LMP1 has been classified as a classical oncogene since it can transform rodent fibroblasts and Balb/3T3 cells in culture (Baichwal and Sugden, 1988; Wang et al., 1985) and is essential for B cell immortalisation by EBV as shown by recombinant virus genetics (Kaye et al., 1993).

When LMP1 expression is directed under a polyoma virus (Py) early promoter to the skin epithelium of mice it causes skin hyperplasia (Wilson et al., 1990) and sensitises mice to chemical carcinogens (Curran et al., 2001). When LMP1 expression is directed to the B cell compartment of transgenic mice it predisposes the mice to B cell lymphomas (Kulwichit et al., 1998)(Wilson JB unpublished data).

In some epithelial cell lines (SCC12F, RHEK-1) LMP1 inhibits differentiation and alters keratinocyte morphology and keratins expression patterns (Dawson et al., 1990; Fåhraeus et al., 1990) whereas in others (HaCat) LMP1 expression led to tumour formation in SCID mice and (in HaCat, SCC12F and murine epithelial cells of transgenic mice) no inhibition of differentiation was observed (Nicholson et al., 1997; Wilson et al., 1990) showing that the genetic background of the cell used and LMP1 levels are important in determining function. LMP1 can also upregulate levels of EGFR protein and mRNA in C33A epithelial cells (Miller et al., 1995).

1.4 EBV related diseases

EBV was first postulated to play a role in disease in the 1960s when its presence was discovered in a BL cell line. Since then it has been associated with many other malignancies and has been classified as a class I carcinogen by the World Health Organisation (WHO). EBV infection is usually asymptomatic if the individual is infected early in life. However, immunocompromise due to genetic, iatrogenic or other reasons as well as environmental agents lead to EBV acting as a tumour promoting agent. Usually when EBV acts in tumourigenesis it is in its latent phase and there are several latency programs expressed with each type of malignancy.

Latency Program	Tumour
Latency I	BL, Gastric Carcinoma
Latency II	NPC, HD, T/NK cell lymphomas
Latency III	PTDL

Table 1.3: Latency programs and tumour association.

A brief description of the main diseases associated with EBV are given below:

EBV Associated Diseases

Infectious Mononucleosis (IM)

About 50% of people who contract EBV between the ages of 17 and 25 will develop IM. It is more common in developed countries where higher sanitary conditions and a decreased tendency to breastfeed lead to late EBV infection (reviewed in (Papesch and Watkins, 2001). The connection between IM and EBV came in the 1960s when a known EBV negative worker in the Henle lab developed IM. After recovering EBV was detected in her serum.

Primary infection occurs via the saliva and sexual contact as EBV virions have been detected in the sperm and the squamous epithelial uterine cells. IM shows a variety of symptoms including mild fever, headache, pharyngitis, lymphadenopathy, malaise and fatigue. EBV is detectable at high levels in the oropharynx of IM individuals. It is usually a self limiting disease. The prevalence of IM in adolescence compared to childhood may not be due to the age but due to the dose of the virus. It is more likely that an individual receives larger amounts of virus in adolescence through the more expanded social and sexual interactions and this can increase the initial pool of infected B cells. Once a threshold level of infected B cells is exceeded the immune system starts work and the T cells respond, producing the symptoms described above. The course of the disease follows the level of activated T cells in the blood. Acyclovir (ACV), a nucleoside analog that inhibits lytic EBV infection by inhibiting viral DNA polymerase, was shown to decrease the EBV shedding but did not alleviate any of the disease symptoms. This therefore indicates that the symptoms follow the nonproductive EBV infection in lymphocytes.

In acute IM B cells resemble EBV infected LCLs *in vitro* and show a latency III type expression pattern. Eventually, the disease resolves naturally (Papesch and Watkins, 2001).

Oral Hairy Leukoplakia (OHL)

OHL is almost exclusively found in AIDS patients. Raised white lesions develop in the tongue epithelium of these patients and EBV particles are found in those cells undergoing lytic infection. No latent EBV infection is detected (Webster-Cyriaque et al., 2000).

X-Linked lymphoproliferative syndrome (XPLS)

XLPS affects males who inherit the mutated XLPS gene. The gene is located on the X chromosome and it normally encodes for a protein (SLAM associated protein) that limits B and T cell proliferation. The mutated gene cannot produce such a protein so upon primary infection with EBV, a massive tissue destruction probably due to uncontrolled T cell

proliferation is seen and the patient dies within 2-3 weeks of fatal IM. Those who survive are likely to later develop other EBV associated lymphomas in 2 or 3 years (Hsu and Glaser, 2000).

Lymphoid Tumours: **Burkitt's Lymphoma (BL)**

BL was the first tumour to be associated with EBV and from which the virus was first isolated.

All BLs are characterised pathologically, by a mass of small noncleaved malignant B cells interfused with non-neoplastic macrophages giving rise to a "starry sky" appearance. There are three types of BL. eBL is predominantly a childhood cancer of the jaw that is most common in Africa and Papua New Guinea, areas that coincide with the *Plasmodium Falciparum* malarial zone. Incidence rates are about 6-15/100,000/year and occur in young children of 5-7years old. Males are more likely to be affected than females in a 3:1 ratio. The EBV episome has been detected in more than 95% of eBL cases and is monoclonal (Magrath, 1991). Increased IgA antibody titers to viral capsid antigen (VCA) were linked to a 30 fold increased risk in 42,000 African children (de-The et al., 1978). There is a possible genetic component to the disease in that certain carriers of HLA locus (DR7) are found to be more susceptible to developing the disease (Jones et al., 1985).

Sporadic BL (sBL), which occurs worldwide, is at least 50 times rarer than eBL. Only about 15-88% of sBL are associated with EBV. The tumour in sBL is localised in the abdomen and affects Caucasian children and older adults. The incidence rate is about 0.3/100 000/year and males are more susceptible than females in a rate of 3-4:1.

The third category, AIDS-related BL, occurs in non endemic regions and is an abdomen tumour affecting people of all ages. Latent EBV infection occurs in about 30-40% of the tumours and the EBV episome is monoclonal (Ballerini et al., 1993).

In all three classes of BL, there are common chromosomal translocations. These occur at the long arm of chromosome 8 (where the *c-myc* locus lies) and either chromosome 14 (the immunoglobulin heavy chain region) or with less frequency chromosomes 2 or 22 (in the region of the immunoglobulin light chain loci). The effect is deregulation of the *c-myc* protooncogene (Gutierrez et al., 1992). Along with these translocations EBV acts to stimulate B-cell proliferation. In eBL patients the immunosuppressive action of malaria is thought to make it easier for EBV to escape immune surveillance and infect B cells.

Despite the fact that EBV is not so common in sBL, one study showed that in a few sBL tumours, the EBNA1 gene may be absent but they still contain a defective EBV genome (Razzouk et al., 1996). This could imply that the virus was essential for the tumorigenesis but during malignant progression its presence became non essential and the genome was rearranged or lost in what is known as a “hit and run” scenario. If this is the case maybe EBV is associated with sBL at a much higher rate than that detected in presented tumours.

Viral expression in BL shows a latency I pattern.

Hodgkin's Disease (HD)

HD is a lymphoma that morphologically is presented as Reed-Sternberg cells among other inflammatory cells. HD has at least five pathological subtypes, all composed of different proportions of different cell types. It is a tumour of the lymph nodes and even though seen worldwide, is particularly common in the Western World where it comprises 20% of the lymphomas. HD affects mostly young adults. The EBV association with HD is strongest in HDs from developing countries compared to HDs from developed countries. For example, only 40-50% of the tumours in the Western World are EBV positive but 90% of the tumours in Honduras and Peru are EBV positive. Some of the first evidence that EBV was associated with HD came from the fact that individuals who had suffered from IM were 3-5 times more likely to subsequently develop HD. Also serological studies showed that there was an increase of IgA titers to VCA and EA years before the development of the disease and those individuals had 3-4 times higher risk to develop HD. The EBV episome in the EBV positive tumours is monoclonal. All Reed-Sternberg cells of EBV positive tumors express latency II (Dolcetti and Boiocchi, 1998).

T/NK cell lymphoma

T/NK cell lymphoma is a midline facial necrotic disease. More than 90% of the NK cell lymphoma cases present with monoclonal EBV episome in the tumour cells. This disease is rarely seen in the Western World but is more common in Asia and Peru where it constitutes 8% of the lymphomas of those regions.

Post-transplant Lymphoproliferative Disorder (PTLD)

PTLD occurs in about 10% of iatrogenically immunosuppressed individuals. The dose of the immunosuppressive agent and a primary EBV infection are risk factors. Seronegative

individuals who contract EBV after transplant have higher risks of developing PTLD. The tumour is more often presented in the central nervous system (CNS) or the brain. More than 95% of the cases show EBV episome in the tumour cells exhibiting latency III (Hopwood and Crawford, 2000).

AIDS-associated immunoblastic and primary central nervous system lymphomas

These AIDS-associated lymphomas occur at the later stages of the disease. About 90% of the primary CNS lymphomas and 70% of the immunoblastic lymphomas contain monoclonal EBV sequences. These lack HIV sequences implying that EBV and not HIV is the causal factor although HIV induced lack of T cell response must play a major role. The tumours express latency I or III, depending on the kind of tumour (Hsu and Glaser, 2000).

Epithelial tumours:

Gastric Adenocarcinoma

Gastric carcinoma is common worldwide. About 4-18% of gastric carcinomas are EBV positive, the percentage depending on geographic location. For example in Japan, 7% of gastric carcinoma tumours are EBV positive whilst only 4% is reported in the UK and 16% in the USA. Increased IgA antibody titers to VCA are seen years before the manifestation of the disease. Salted and certain preserved food consumption along with the infection of the *Helicobacter pylori* are potential cofactors for the development of the disease.

The *Bam* HI A RNAs and the EBERs are always expressed whilst LMP1 and LMP2B are not expressed. Of the latent proteins, EBNA1 and LMP2A or only EBNA1 are expressed. EBV positive gastric adenocarcinomas have a better prognosis and they all share genetic characteristics such as the loss of p16^{INK4a}. Premalignant gastric adenocarcinomas do not show EBV infection suggesting that EBV infection is a late event in the process of carcinogenesis in this tissue (Fukayama et al., 1994; Luo et al., 2005).

Breast Cancer

There is great controversy as to whether EBV plays any role in breast cancer (reviewed in (Magrath and Bhatia, 1999). Initial studies on medullary breast carcinoma that is morphologically similar to NPC showed that some cells within a subset of aggressive breast tumours were positive for expression of the EBNA1 gene (Bonnet et al., 1999) but only 50%

of the tumours examined showed presence of EBERs (Labrecque et al., 1995) and in the EBV positive cases, the viral DNA was only detected in a subset of the tumour cells suggesting that either infection took place after tumour initiation or that the virus was no longer required for cell growth and was lost. The whole story was confounded with several reports showing no detection of EBV DNA in breast cancer cells (Chu et al., 1998; Dadmanesh et al., 2001; Glaser et al., 1998; Herrmann and Niedobitek, 2003; Horiuchi et al., 1994; Lespagnard et al., 1995). This could be due to the methods used. For example, EBER *in situ* are used as a standard method for indicating the presence of EBV virus in a tumour. However there have been EBV positive tumour cases that do not show EBER expression (Sugawara et al., 1999). Furthermore, the way the tissue is fixed can affect detection of viral proteins. It is also important to be able to show presence of EBV in tumour cells only. Further doubt arose when the anti-EBNA1 antibody used in the positive breast cancer study was found to cross react with a tumour specific cellular protein (Murray et al., 2003). Based on these technical restrictions, weight of evidence is currently against EBV having a role in breast cancer, but this is not conclusive.

Nasopharyngeal Carcinoma (NPC)

Nasopharyngeal carcinoma is a tumour of the epithelium of the nasopharynx arising from the Rosenmuller fossa. The WHO has classified NPCs into three distinct categories depending on their histopathology. Type I NPCs are keratinising, well differentiated squamous cell carcinomas (SCC), type II are non-keratinising SCC and type III are undifferentiated carcinomas of the nasopharyngeal type. Type III carcinoma was also described as lymphoepithelioma due to the infiltration of the primary tumour with T cells.

One of the characteristics of NPC, is its significant geographical variation in incidence. The highest incidence of NPC is seen in S. China and South East Asia with intermediate incidence levels in Arctic and North African populations. Characteristically 80% of all new NPC cases in year 2000 were in S.China. Even in the high incidence areas there is variation. For example, in S.China the Kwangtung, Kwangsi, Hunan and Fukin regions have a much higher incidence than other areas of S.China. The incidence in high risk areas is about 30-50/100,000 cases per year, in intermediate risk areas the incidence is between 8-12/100,000 cases per year and in the Western world where NPC is a rare malignancy the incidence rate is about 0.5-2/100,000 cases per year. More males are affected than females independent of geographic location. The ratio of male to female is between 2.5-3:1. The age of onset is between 55-65

years for Caucasians but it drops to 40-45 for Chinese. In North African populations there is a bimodal age distribution of NPC with cases seen between 10-20 and at 55-65.

Symptoms of NPC include blood tinged sputum, a neck mass, nasal obstruction and aural symptoms such as hearing loss, frequent headaches and neurological symptoms. However, most often the only clinical manifestation of NPC is cervical lymph node metastasis.

The aetiology of NPC is multifactorial including environmental, genetic and viral (EBV) factors. Studies on high risk individuals who emigrated to low risk areas show clearly the genetic and environmental connection. Studies on Cantonese Chinese who emigrated to California showed that they had an increased incidence of NPC compared to Caucasians and that the risk was much higher if they were born outside the US. However their risk was lower compared to Chinese in S.China. Also second and third generation Cantonese Chinese living in low risk areas still developed NPC at a higher incidence than the local population suggesting that NPC has a genetic association or that the environmental factor is diet and maintained in the subsequent populations (Buell, 1974; Hildesheim and Levine, 1993). A recent study in Hong Kong showed that there was a 30% decrease in NPC cases over a period of 20 years (1980-1999) implying environmental changes are responsible for NPC (Lee AW, 2003). Sib-pair analysis of affected siblings showed that in high risk populations HLA.A2 , B46 and B14 alleles confer susceptibility to NPC whereas in US Caucasians the HLA.A2 allele (which is more common in Caucasians) confers protection (Burt et al., 1994). Similarly, the HLA-A*0207 allele was associated with NPC in Chinese but not Caucasians. It is thought that a gene linked to the HLA loci could be responsible for the NPC susceptibility. Such a gene could be the cytochrome P450 2E1 enzyme (CYP2E1) that can metabolise nitrosamines and it was shown that CYP2E1 c2 allele and NPC show a strong association in Chinese (Hildesheim et al., 1997). Polymorphisms at other genes such as GSTM1 (involved in detoxification) and XRCC1 and hOGG1 (involved in DNA repair) are also associated with increased risk of NPC (Nazar-Stewart et al., 1999).

The strongest environmental factor associated with NPC is the traditional foods of the high risk areas (eg. traditional Cantonese style salted fish and spiced meat) that contain volatile nitrosamines which are known carcinogens. Rats and mice fed with Cantonese style salted fish developed tumours (Huang et al., 1978). The nitrosamines could be acting as chemical carcinogens, predisposing the nasopharyngeal epithelium to genetic damage and latent infection with EBV.

EBV has been detected in 100% of NPC lesions . All the type II and III NPCs show increased IgG and IgA titers to VCA and EA. All tumour cells contain clonal EBV DNA implying that infection of the cell with EBV took place before the cell acquired its proliferative capacity and that EBV plays a role in tumour progression (Raab-Traub, 2002; Raab-Traub and Flynn, 1986). There is a controversy as to whether type I NPC is EBV associated or not (Krueger et al., 1981; Pearson et al., 1983; Sam et al., 1989). Several studies have shown by *in situ* hybridisation of EBERs or by EBV expression that there is EBV in all NPC types (Pathmanathan et al., 1995; Raab-Traub et al., 1987; Vasef et al., 1997). Others however, reported presence of EBV only in type II and III but not type I NPC by using EBER *in situ* and polymerase chain reaction (PCR) (Hording et al., 1993; Niedobitek et al., 1991). This controversy could be explained with the observation that all NPCs from endemic regions contain EBV whereas only 33% of NPC type I from low risk areas have shown any EBV association (Nicholls et al., 2004). Other factors such as smoking may also be involved in NPC type I pathogenesis but not in type II or III.

In the tumour, EBV expresses latency II in which EBNA1, LMP1, LMP2, EBERs and *Bam* HI A RNA transcripts are expressed. EBNA1 expression has been detected in all the NPC cases analysed and EBERs have been detected at high levels. LMP1 expression is more variable and depends on the detection method used. By RT-PCR 100% of primary NPC tumours (18 samples) showed LMP1 expression (Brooks et al., 1992). Only 60% of the tumours analysed led to LMP1 detection by protein *in situ* (Niedobitek et al., 1992; Sheen et al., 1999; Stewart and Arrand, 1993; Young et al., 1988) but 100% of premalignant NPC lesions showed LMP1 expression (Pathmanathan et al., 1995). S. Chinese NPCs that showed LMP1 protein expression grew faster and were larger than LMP1 negative NPCs. However, the LMP1 negative NPCs, had greater chances of recurring and metastasising.

LMP2A mRNA was detected in most primary NPC tumours analysed whilst LMP2B mRNA was detectable at low levels in only a subset of the tumours (Brooks et al., 1992). Using new antibodies for LMP2A, another group showed that 45.7% of the tumours analysed expressed LMP2A (Heussinger et al., 2004).

Bam HI RNA transcripts are also implicated in NPC (Gilligan et al., 1991) but protein detection is unclear. Older studies (Fries et al., 1997) detecting BARFO protein in NPC biopsies used an antibody that cross reacts with a cellular protein (Schroder et al., 2002). This issue needs further clarification. BARF1 transcripts and protein have been detected in 85 % of

a sample range of Algerian NPC biopsies. Aside from LMP1, BARP1 may be another oncogenic protein playing a role in NPC formation and development.

Expression of the early lytic gene BZLF1/ZEBRA has been detected in 100% of NPC biopsies analysed by RNA *in situ* whereas the protein has been detected in 90% of the samples analysed showing that there is EBV reactivation in these tissues (Cochet et al., 1993).

In NPC tumour cells several chromosomal rearrangements have been described. Loss of 3p, 9, 11q, 13q, 14q, 16q and gain of 12 are some of the commonest chromosomal abnormalities observed in NPCs. A number of tumour suppressor genes map to the chromosomes that are lost and are therefore possible candidates in tumourigenesis. RASSF1a maps to 3p, p14^{ARF} and p16^{INK4a} map to 9p, TSLC-1, MLL and ATM map to 11q and loss of 13q,14q and 16q lead to loss of EDNRB and changes in E-Cadherin expression. Aberrant promoter hypermethylation in NPC is another way by which tumour suppressors are not expressed (Lo et al., 1996).

No p53 mutations have been detected in NPC biopsies to date (Effert et al., 1992; Spruck et al., 1992). However, consistent p53 overexpression of the wild type form has been reported (Muroso et al., 1999; Niedobitek et al., 1993). There are two theories to explain this observation; one is that due to loss of p14^{ARF}, the MDM2 protein is free to bind and target p53 for destruction however this is not the case as there is p53 overexpression and levels of MDM2 detected in NPCs are low (Kouvidou et al., 1997). The other more likely theory is that overexpression of a dominant negative homolog of p53- Delta Np63- may bind to p53 and block its function (Crook et al., 2000).

Precancerous lesions and invasive tumours show upregulation of Bcl-2 but there is no indication that there is any relationship between LMP1 expression and Bcl-2 upregulation. Other factors that are upregulated and may contribute to inhibition of apoptosis are upregulated metallothionein (MT), inhibitors of differentiation 1 (Id) and loss of death associated protein kinase (DAPK) (Jayasurya et al., 2000; Kwong et al., 2002). Further factors that are found to be upregulated in NPC are epidermal growth factor receptor (EGFR), matrix metalloproteases (MMPs), hypoxia factors (HIF-1a and CAIX), Cox-2 (Muroso et al., 2001; Thornburg et al., 2003) and for some this upregulation is due to LMP1.

Whether *ras* mutations occur in NPC is still unclear. Immunohistochemistry studies to detect Ras overexpression in NPC biopsies gave conflicting results (Porter et al., 1994a; Yung et al., 1995).

The proposed mechanism for NPC onset and progression is that chemical carcinogens in food lead to accumulation of mutations that together with genetic predisposition and EBV infection lead to NPC onset. For example, pre-invasive dysplastic lesions both low and high grade show 3p and 9p deletions. EBV infection is only seen in high grade dysplasias implying that the genetic changes happen first and then EBV infection takes place. Loss of 3p and 9p could lead to clonal expansion of the epithelial cell population leading to low grade dysplasias. When an EBV latent infection is established in the epithelium, this leads to high grade dysplasia. Loss of other tumour suppressors such as ENDBR, TSLC1 leads to invasive carcinoma. Changes in E-Cadherin expression, MMP9 and other metastatic factors contribute to invasion and metastasis.

Other carcinomas that have similarities to undifferentiated NPC have been described and these include carcinomas of the thymus, stomach, lungs, tonsils, skin and cervix and are known as lymphoepitheliomas but are EBV negative.

LMP1 strains

LMP1 genes from the different EBV strains are relatively well conserved and are almost identical in amino acid sequence. There are several LMP1 strains and here I will describe the prototype B95-8 and CAO, 1510 and C15 which have been associated with NPC. The B95-8 strain of EBV was isolated from an IM case and the LMP1^{B95-8} is 386aa, 63kDa. It has 4.5 repeats of the 11aa repeat in the C-terminus. LMP1^{CAO} was isolated from a S.Chinese NPC biopsy (Hu, 1991). It is 404aa, 66kDa and has three extra 11aa repeats. In total it has 7 11aa repeats. LMP1^{CAO} has a point mutation in its first exon that leads to the loss of an *XhoI* restriction site that is present in LMP1^{B95-8}. LMP1^{CAO} has several point mutations in the transmembrane domains, a point mutation in the CTAR1 (G212 to S) and three point mutations in the CTAR2 region relative to LMP1^{B95-8}. LMP1^{CAO} has a 10aa deletion (343-352) just N-terminal to the CTAR2 region and a further 5aa deletion in the carboxy terminus (Hu, 1991). The LMP1¹⁵¹⁰ comes from an Asian NPC biopsy and is 95% homologous in sequence to LMP1^{B95-8}. LMP1¹⁵¹⁰, has 5 11aa repeats and has a 10aa deletion in the carboxy terminus (Chen et al., 1992). LMP1^{C15} comes from a Mediterranean NPC that has been passaged in nude mice. This strain also has the 10aa deletion seen in CAO and 1510 strains.

Both CAO and 1510 variants when transformed in rodent fibroblasts, showed increased transforming ability (formed larger and more colonies) compared to B95-8. The transforming ability of LMP1^{B95-8} was increased when aa343-352 were deleted. The opposite was true when those aa were substituted in LMP1¹⁵¹⁰ thus implying that the 10aa deletion renders the protein

more tumourigenic (Hu, 1991; Li et al., 1996; Zheng et al., 1994b). Since the 10aa deletion maps in a domain necessary for NF- κ B activation (Mitchell and Sugden, 1995), the ability of deletion variants isolated from HD to affect the NF- κ B pathway was examined with negative results (Rothenberger et al., 1997). The 10aa deletion LMP1 variants were isolated from other malignancies such as HD and peripheral T cell lymphoma thus leading to the hypothesis that the 10aa deletion plays an important role in transformation but more recent studies suggest not (Brousset et al., 1994; Knecht et al., 1995). Furthermore, LMP1^{CAO} was shown to be less immunogenic than LMP1^{B95-8}. The latter could convert a non immunogenic mammary carcinoma cell line (S6C) into an immunogenic tumour rejected by the immune system whereas LMP1^{CAO} could not (Trivedi et al., 1994) implying that LMP1^{CAO} is less immunogenic. Further experiments using LMP1 proteins isolated from LMP1 positive NPC and LMP1 negative (LMP1 gene is hypermethylated) showed that LMP1 proteins from LMP1 positive NPCs were less immunogenic (Hu et al., 2000). However, the 10aa deletion was not responsible for this as LMP1 proteins that were not deleted for the 10aa were also less immunogenic.

From the above results, it is not clear if the 10aa deletion is playing a role in increased tumourigenicity or immunogenicity of the deletion variants; CAO, 1510 or C15. Instead, studies have focused on the transmembrane domains of the protein which show point mutations from one strain to another. Transfection of LMP1^{CAO}, LMP1^{C15}, or LMP1^{B95-8} in epithelial cells, showed that LMP1^{CAO} and LMP1^{C15} could lead to increased NF- κ B and AP1 signalling when compared to LMP1^{B95-8} and this was proposed to be due to the increased half life of LMP1^{CAO} (7.25hrs) compared to LMP1^{B95-8} (2.9hrs) (Blake et al., 2001; Dawson et al., 2000; Miller et al., 1998a). Use of chimeras, led to the conclusion that the transmembrane domains of LMP1^{CAO} and LMP1^{C15} are responsible for the increased stability and thus the increased signalling. Transfection of B cells with either LMP1^{CAO} or LMP1^{B95-8}, showed that LMP1^{CAO} leads to decreased CD40 and CD54 induction but it increases NF- κ B signalling two-fold when compared to LMP1^{B95-8}. Removal of the 10aa from LMP1^{B95-8} and replacement of the 10aa on LMP1^{CAO}, showed that the 10aa deletion was not important for these functional changes (Johnson et al., 1998). Similarly in epithelial cells, stable transfection of LMP1^{B95-8} led to growth inhibition, block of differentiation, morphological changes and production of

CD40, 54, 44, IL-6 and -8 whereas LMP1^{CAO} did not induce any of these effects (Dawson et al., 2000)¹.

It has also been shown that LMP1^{B95-8} can induce cell death via activation of caspase-3 in an NF-κB dependant manner whereas LMP1^{CAO} does not (Nitta et al., 2003; Sheu LF, 1998). Chimeras were created by swapping the amino, transmembrane and carboxy domains of LMP1^{CAO} and LMP1^{B95-8} in order to identify the domain responsible for apoptosis. The transmembrane domain of LMP1^{B95-8} was responsible for apoptosis induction and this was due to the presence of Ile the 85th aa and Phe at 106th aa. LMP1^{CAO} has Leu at 85th aa and Tyr at 106th aa. The LMP1^{B95-8} pattern is seen in LMP1 from healthy EBV carriers whilst the LMP1^{CAO} pattern is seen in LMP1 from NPC patients. When the two aa were interchanged between the two variants, it was shown that they were critical for cell death but not responsible for affecting NF-κB activation levels. Since LMP1^{CAO} leads to increased signalling of factors such as NF-κB and possibly AP1 that activate genes involved in proliferation and metastasis and at the same time inhibits apoptosis, it has an additive advantage over LMP1^{B95-8} in leading to tumourigenesis. An extensive analysis of 9 different strains of LMP1 including LMP1^{B95-8}, LMP1^{CAO} and other European NPC strains showed that there are differences between them in NF-κB and AP1 signalling but these differences do not correlate with a particular sequence variation (Fielding et al., 2001).

An interesting idea that has been examined by Hu *et. al.*, is that initially all cells leading to an NPC express LMP1. Due to hypermethylation of the LMP1 regulatory sequence (LRS) in the LMP1 negative NPC, the LMP1 protein is no longer expressed. The LMP1 protein that mutates to avoid immune recognition does not need to be switched off by hypermethylation. This supplies a reason why LMP1 positive NPCs express LMP1 protein that is highly mutated but less immunogenic whereas LMP1 negative NPCs, have extensive LMP1 hypermethylation, LMP1 gene has fewer mutations and the protein is more immunogenic (Hu et al., 2000). This theory is compatible with what is observed with LMP1 positive and negative NPCs. LMP1 positive NPCs are larger and grow faster than negative NPCs, but negative NPCs have an increased risk of metastasis (Hu et al., 1995).

¹ Note that AP1 activity of LMP1^{CAO} was shown not to have any significant difference from LMP1^{B95-8} by Dawson et al, 2000. This is the same laboratory that published Blake et. al., 2001 indicating that different cell types respond differently to LMP1^{CAO} and the response it has on AP1 signalling.

1.5 Ras

Ras proteins are members of a superfamily of low-molecular weight guanine nucleotide binding proteins. The other members are Rho and Rac. There are three mammalian Ras proteins, Harvey-ras (H-ras), Kirsten-ras (K-ras) and N-ras. These proteins are 21kDa, are highly conserved among different species and show about 85% homology between them. They are all expressed in all mammalian cells at low basal levels and under normal conditions they control cell proliferation and cell terminal differentiation (Barbacid, 1987). K-ras is expressed in almost all cell types and knock out studies have shown that K-ras is essential for proper development (Johnson et al., 1997).

Ras proteins bind guanine nucleotides (GTP and GDP) and have a very low intrinsic GTPase activity. GTPase activating proteins (GAPs) catalyse hydrolysis of GTP from Ras while guanine nucleotide exchange factors (GEFs) catalyse the replacement of GDP for GTP (fig.1.4). Initially Ras proteins are released in the cytosol but post-translational modification by farnesylation is needed to make them functional. Farnesylation, enables Ras to be localised to the inner plasma membrane and thus recruit its appropriate target enzymes. Failure to localise to the plasma membrane leads to non functional Ras proteins.

Ras activation results from activation of receptor tyrosine kinases such as EGFR. The activated (tyrosine phosphorylated) receptor binds the src homology domain (SH) 2 of growth factor receptor bound protein 2 (GRB2) and GRB2 via its SH3 domain binds son of sevenless (SOS) (Buday and Downward, 1993). This brings SOS to close physical proximity with Ras leading to an increased nucleotide exchange on Ras (fig.1.4). Ras oscillates from GDP bound and thus inactive to GTP bound and activated. This dynamic equilibrium is vital to keep Ras activation under control. When it is disturbed by having Ras constitutively GTP bound and thus constitutively active, it can lead to aberrant proliferation.

Activated Ras can activate four downstream signalling pathways: the Raf/MAPK, the PI3K pathway, the RALGDS and the PLC ϵ pathways (fig.1.5). Effects of the activation of these pathways include cell cycle progression, transcriptional activation, cytoskeletal signalling, vesicle transport and calcium signalling control. Some of these pathways will be described later.

All three Ras proteins (H, K, and N) have been found to be activated in different human tumours. About 25% of all human tumours have a Ras activating mutation. Usually K-ras mutations are found in pancreatic cancers whereas epithelial type cancers show H-ras mutations. 85% of human tumours with Ras mutation show a mutation in K-ras, 14% in N-ras and about 1% in H-ras. All mutations prevent hydrolysis of GTP from Ras thus locking it in

its active state. Mostly mutations in codons 12,13 and 61 are responsible for activating Ras (Downward, 2003).

Activated Ras can transform rodent cell lines in culture (Barbacid, 1987; Varmus, 1984). In mouse skin chemical carcinogenesis studies, application of the tumour initiator 7,12-dimethylbenzanthracene (DMBA) led to 99.5% of the tumours developed, to have an activated H-ras gene. Activation of Ras genes is an early event during tumour development (Bizub et al., 1986).

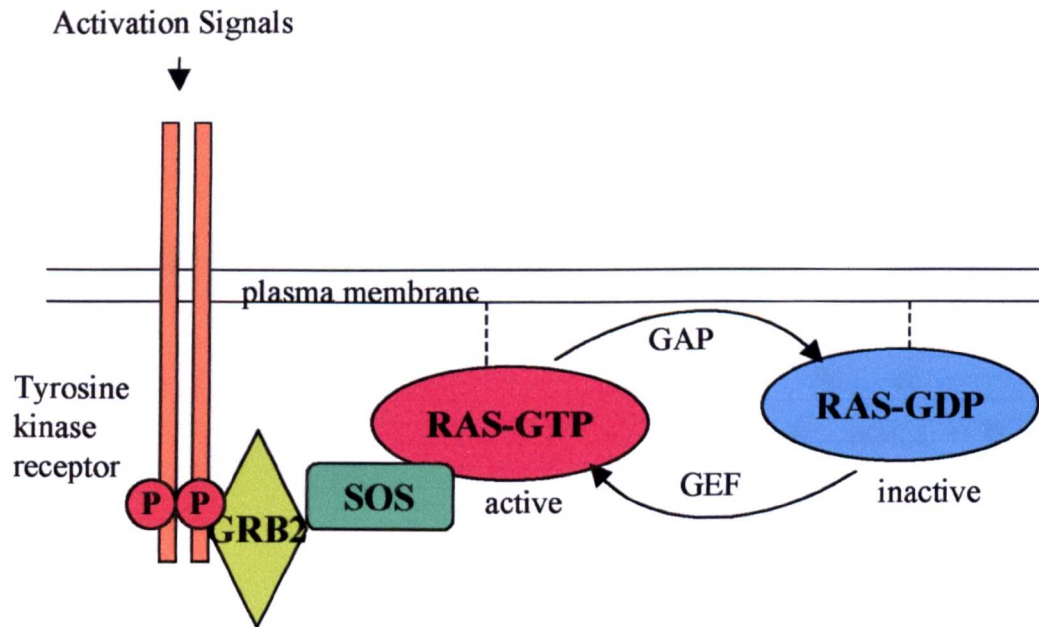


Figure 1.4: Ras Activation

External stimuli such as growth factors bind to and activate tyrosine kinase receptors. Activated receptors such as EGFR, can recruit effector proteins such as GRB2 and SOS that can activate Ras. GAPs catalyse hydrolysis of the GTP from Ras in order to return it to its inactive GDP bound state. GEFs catalyse hydrolysis of GDP to allow GTP to bind to Ras and activate it. Note that Ras proteins are connected to the plasma membrane via an isoprenoid chain represented by a disconnected line.

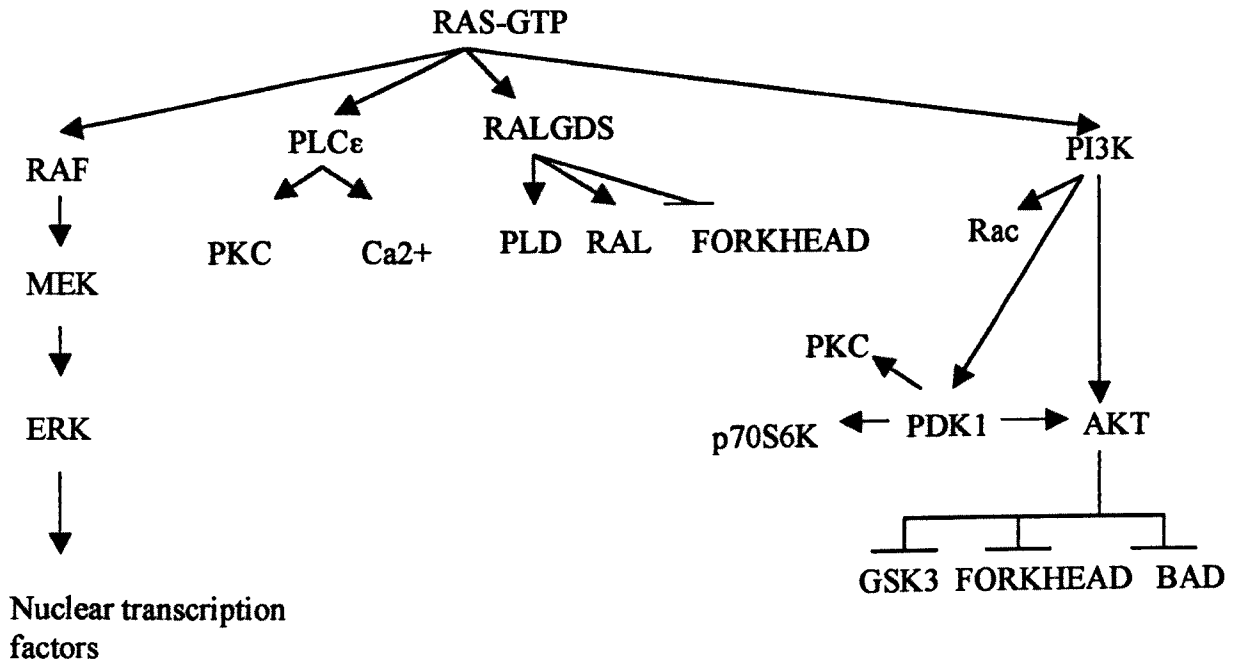


Figure 1.5: Signalling pathways activated by Ras

The figure shows the four main pathways that are activated by Ras. Ras leads to activation of the MAPK/ERK1/2 pathway and the PI3K/Akt pathway which are involved in gene transcription, survival and cell cycle progression. The PLCε and RALGDS pathways are involved in vesicle transport, calcium signalling and cytoskeletal signalling. (Figure adapted from Downward *et. al.*, 2003).

RAS transgenic mouse models

Several Ras transgenic mouse models have been created. Here I will discuss only the ones that are relevant for skin carcinogenesis.

Overexpression of oncogenic H-ras to the skin under the direction of different promoters has given different results. Directing H-ras to the suprabasal epidermal layer (using the bovine K10 promoter) gave rise to skin hyperkeratosis and papilloma formation at sites of mechanical irritation (Bailleul et al., 1990), whereas directing expression to the basal layer (using a truncated human K1 promoter) led to epidermal hyperplasia and hyperkeratosis in the neonates and juveniles that regressed by 5 weeks of age. Adults developed papillomas over time and their K1 and K13 staining patterns were consistent with benign lesion formation. This shows that an activated Ras by itself is not enough to lead to malignant conversion and that a secondary event is needed (Greenhalgh et al., 1993a). However directing expression of H-ras to the follicular and interfollicular cells of neonates and to the hair follicles of adults (using a truncated K5 promoter) gave newborn mice acanthotic areas that progressed to carcinomas and spontaneous papillomas and keratoacanthomas in adults (Brown et al., 1998). Similar results were obtained when the v-H-ras oncogene was directed for expression to the hair follicles (using the zeta-globin promoter). Spontaneous papilloma formation was seen at sites of mechanical irritation and when the mice were treated with a chemical promoter 4 beta-phorbol 12-myristate 13-acetate (PMA) more than 90% of the mice developed multiple papillomas that went on to form SCC and sarcomas. This study demonstrated that an activated Ras can replace the need for an initiation step in a chemical carcinogen treatment (Leder et al., 1990). These mice also develop a variety of tumours including squamous cell carcinomas, odontogenic tumours and dermal spindle cell tumours. Use of the native Ras promoter to direct expression of the human H-ras gene led to 50% of the offspring developing tumours within 18 months and those tumours had mutations at codon 61 (A-T transversion) and codon 12 showing that overexpression of somatic Ras does not necessarily lead to tumorigenesis but it is the activation of Ras that causes proliferation (Saitoh et al., 1990).

From the above studies, it is clear that the cell context in which activated Ras is found plays a very important role as to whether there will be a malignant conversion or not. From the transgenic animal work, it is concluded that benign tumours are more likely to show malignant conversion if they originated from the hair follicle cells or from the basal proliferating layer. Use of dominant negative Ras transgenic animals showed that spatial expression of Ras alters its effects and that normally Ras functions in the basal layer of the epidermis and its primary

role is in epidermal cell renewal and inhibition of differentiation of cells early in the differentiating pathway. Ras function divides the epidermis into two segments; the basal proliferating segment and the differentiating segment (Dajee et al., 2002). In the Dajee *et al.*, study, two sets of transgenic mice harboring a dominant negative form of Ras (RasN17) directed for expression at the basal layer (using the K14 promoter) or at the suprabasal layer (using the truncated human K10 promoter) were created. A control transgenic mouse harboring activated Ras (RasV12) in the basal layer (K14 promoter) was also created. Whereas HK10.RasN17 mice were normal, K14.RasN17 mice showed hypoplasia with widespread skin erosion by 6 weeks of age and non healing loss of epidermis. This is consistent with a role for Ras in cell proliferation and epidermal self renewal. The K14.RasV12 mice showed massive epidermal hyperplasia with no differentiating epidermal layers and all mice died at birth. Further *in vitro* experiments using primary epithelial cells and modulating doses of active Ras showed that Ras regulates epidermal proliferation and inhibits differentiation. Where a transgene is expressed is therefore, of the utmost importance when interpreting what the gene's normal function may be.

Due to the fact that the different Ras proteins can compensate for each other null animals for H-ras, K-ras and N-ras showed no skin defects (Esteban et al., 2001; Ise et al., 2000; Johnson et al., 1997; Umanoff et al., 1995). Triple null animals however, could not be created as the N-ras -/- / K-ras -/- combination is embryonic lethal (Johnson et al., 1997).

Ras and chemical carcinogenesis

A classical chemical carcinogenesis regime in the mouse involves a single topical application (usually on the back) of a chemical initiator followed by repeated applications of chemical promoters. An initiator, is a chemical that can change the structure of DNA in such a way that will lead to an irreversible mutation thus creating a population of "primed" cells. One of the most common chemical initiators used is DMBA, a polycyclic aromatic hydrocarbon. DMBA is metabolised to diol epoxides that are reactive electrophiles and covalently interact with DNA causing mutations (Dipple et al., 1984). About 99.5% of DMBA initiated mouse skin tumours have a mutation that activates the H-ras gene (Balmain et al., 1988; Balmain et al., 1984; Bizub et al., 1986; Brown et al., 1990). 95% of these activating H-ras mutations are an A-T transversion in codon 61. The rest are mutations at codon 61,60,12 and 13. Thus if an H-ras mutation is involved in the initiation of mouse skin tumours, then by overexpressing a gene that affects the Ras pathway *in vivo* in the epithelium, this will make experimental use of a chemical initiator such as DMBA redundant (Quintanilla et al., 1986). Promoters do not alter

DNA structure but can activate proliferative pathways. A promoter can stimulate those “primed” cells to clonally proliferate and form premalignant lesions. Other genetic or environmental events are then needed for these premalignant lesions to convert to malignant carcinomas. A common tumour promoter is 12-O-tetradecanoyl phorbol-1,3-acetate (TPA) which is a phorbol ester and a structural homolog of diacylglycerol (DAG). One of the targets of TPA is Protein Kinase C (PKC). PKC is a ser/thr protein kinase that is activated by Ca^{2+} . DAG increases the affinity of PKC for Ca^{2+} thus activating it. TPA is a structural homolog of DAG and can activate PKC in the same way (Nishizuka, 1984). Activation of PKC leads to activation of several downstream pathways such as MAPK, JNK, PI3K and downstream targets include AP1, cyclic AMP-binding protein (CREB), NF- κ B and more. Thus the first event of promotion is a general epidermal hyperplasia that occurs about 24hrs after first promoter application, peaks 48-72hrs and disappears 7 days after application.

Relationship between Ras, LMP1 and NPC

There is no clear evidence for association of activated Ras and NPC. There is however a single report suggesting that LMP1 acts in a similar way as activated Ras, producing similar phenotypes in transfected cells (Dawson et al., 1990). SCC12F cells (derived from an immortalised non-tumorigenic subclone of the squamous cell carcinoma line SCC12) were transfected with either LMP1 or activated H-ras. Both cell populations showed similar levels of CD40 and ICAM-1 (markers elevated in NPC) which were increased when compared to control cells, both populations failed to form stratified epithelia when grown on collagen rafts and were impaired in their ability to undergo terminal differentiation as they failed to form cross-linked envelopes. These experiments suggest that LMP1 and Ras can cause similar effects. On the contrary, when NIH3T3 cells transfected with NPC DNA were analysed, H-ras mutations were evident suggesting that activation of *ras* is a way by which some NPCs may gain their malignant properties (Hu et al., 1986). Staining primary NPC for Ras showed that only 19% of the samples gave intense staining suggesting that Ras is expressed, however this reflects only whether there is Ras present or upregulated and not whether *ras* is activated (Porter et al., 1994b; Yung et al., 1995).

Ras mutations are not common in Western head and neck tumours or nasopharyngeal angiofibroma. Only 5% of head and neck tumours show any correlation with activated Ras and it may be that upregulation of Ras protein plays a role in these kinds of cancers and not its activation (Coutinho et al., 1999; Sheng et al., 1990; Yarbrough et al., 1994).

Ras, apoptosis and senescence

Overexpression of activated Ras can lead cells to senesce (eg. human and rodent fibroblasts) (Feig and Buchsbaum, 2002) to differentiate (eg. pheochromocytoma rat cells (PC12) into neuron-like cells) (Bar-Sagi and Feramisco, 1985) or apoptose (eg. rat embryo fibroblasts) (Joneson and Bar-Sagi, 1999).

Ras induced senescence is mediated by Raf and MEK1/2 leading to accumulation of p16, p53 and p21 (Lin et al., 1998; Lin and Lowe, 2001; Serrano et al., 1997; Sewing et al., 1997; Zhu et al., 1998). Cells lacking p53 or p16^{INK4a} are readily transformed by Ras suggesting that p53 or p16^{INK4a} overexpression may serve as a cancer protective mechanism.

Recently, other Ras effectors (RASSF1 and NORE1A) have been discovered that may mediate Ras induced apoptosis. In 293 cells, RASSF1c could bind activated Ras and induce apoptosis (Vos et al., 2000), however most studies argue that RASSF1 cannot directly bind Ras but instead it heterodimerises with NORE1A or mammalian sterile20-like (MST)1/2 that can both bind Ras and induce apoptosis (Khokhlatchev et al., 2002; Ortiz-Vega et al., 2002).

Initially activated Ras overexpression leads to proliferation but its excessive and prolonged activation leads to cell cycle arrest, senescence, differentiation or apoptosis as a means of controlling aberrant proliferation. Already immortalised cell lines can be readily transformed by activated Ras whereas primary cell lines with an activated Ras require a secondary genetic mutation in order to become immortalised and transformed. This can also explain why so many human tumours have mutated or non functional p53 and p16^{INK4a} products.

1.6 Ras Association Domain Family (RASSF)

The RASSF family of proteins consists of six members; RASSF1-6. The founding member of this family was RASSF5A or NORE1A (Hesson et al., 2003; Tommasi et al., 2002; Vavvas et al., 1998). RASSF1 has several splice variants; RASSF1a-e. Only RASSF1a along with NORE1a have been characterised as tumour suppressors. Their role as tumour suppressors was unveiled when several studies pointed to the fact that hypermethylation of their promoters led to their silencing in a variety of human tumours such as NPC (Chow LS, 2004; Chow et al., 2004), pancreatic carcinoma (Dammann et al., 2003), neuroblastoma and non-small cell lung carcinoma (Agathangelou et al., 2003), melanomas (Spugnardi et al., 2003), oesophageal carcinoma (Kuroki et al., 2003), HD, myeloma, gliomas (Hesson et al., 2004), brain (Horiguchi et al., 2003) breast and kidney. RASSF1a – which is located on chromosome 3p21- is thought to play a role in NPC onset and development as its expression is lost by deletion or by hypermethylation. To support the hypothesised role of RASSF1a as a tumour

suppressor, RASSF1a was reintroduced into a human lung cancer cell line where the promoter of the endogenous RASSF1a was hypermethylated. Re-expression led to a reduction in cell proliferation, decrease in the number of transformed cells and inhibition of tumour formation when these cells were introduced into nude mice (Burbee et al., 2001; Dammann et al., 2000). A single report indicated that RASSF1c may be a tumour suppressor but this has not been confirmed as yet (Vos et al., 2000).

Both RASSF1a and NORE1A proteins contain a Ras association domain (RA) and a conserved carboxy terminus. Despite having an RA, RASSF1a cannot directly bind to Ras. Instead it has to heterodimerise with NORE1A which can bind activated Ras and simultaneously bind to MST1/2 (a pro-apoptotic kinase) and induce apoptosis (Khokhlatchev et al., 2002; Ortiz-Vega et al., 2002). RASSF1a can also lead to cell cycle arrest at G1 (Shivakumar et al., 2002), microtubule stabilisation and protection from inappropriate spindle formation and genomic translocation. Its association with Cdc20 ensures that the cells do not enter metaphase until the spindle apparatus is properly in place (Song et al., 2004a). RASSF1a interacts with p120^{E4F} (an E1A regulated transcription factor). Transfection of NIH3T3 cells with both RASSF1a and p120^{E4F} led to increased S phase inhibition (Fenton et al., 2004). It is also important to note that p120^{E4F} can associate simultaneously with p14^{ARF} (the human homolog of p19^{ARF}) and p53 and induce growth arrest (Rizos et al., 2003). A further interaction of RASSF1a is with the scaffold protein CNK1. Both NORE1A and RASSF1a can associate with CNK1. Coexpression of RASSF1a and CNK1 in HEK293 cells leads to an increase in apoptosis. It is thought that CNK1 binds the RASSF1a-MST1 complex and brings it in touch with activated Ras (Rabizadeh et al., 2004).

To conclude, RASSF1a protects from aberrant proliferation by activating apoptosis and inducing cell cycle arrest. The exact mechanisms involved in these processes are not clear yet.

1.7 TGF α and EGFR signalling

Epidermal Growth Factor Receptor (EGFR)

Epidermal growth factor receptor (EGFR) belongs to the EGFR family of receptors. The other three members of the family are HER2(ErbB2), HER3(ErbB3) and HER4(ErbB4) (Carpenter and Cohen, 1990). They are all transmembrane receptors with an extracellular ligand binding domain and a cytoplasmic domain containing a tyrosine kinase activity region. EGFR has at least seven ligands including EGF, TGF α and amphiregulin (AR) (that preferentially bind EGFR), heparin binding EGF (HB-EGF), epiregulin, epigen and betacellulin (fig.1.6). The

ligands are all produced as transmembrane forms and after proteolytic cleavage by metalloproteases, they are released as the mature soluble growth factor. The mature forms contain six conserved cysteine residues that make up the EGF motif, via which they can bind to EGFR members. Although the ligands are similar in sequence they have distinct roles as animal knock out models have shown. The one ligand that has been shown to have an effect on the role EGFR has in the epithelium is TGF α which is described in more detail later.

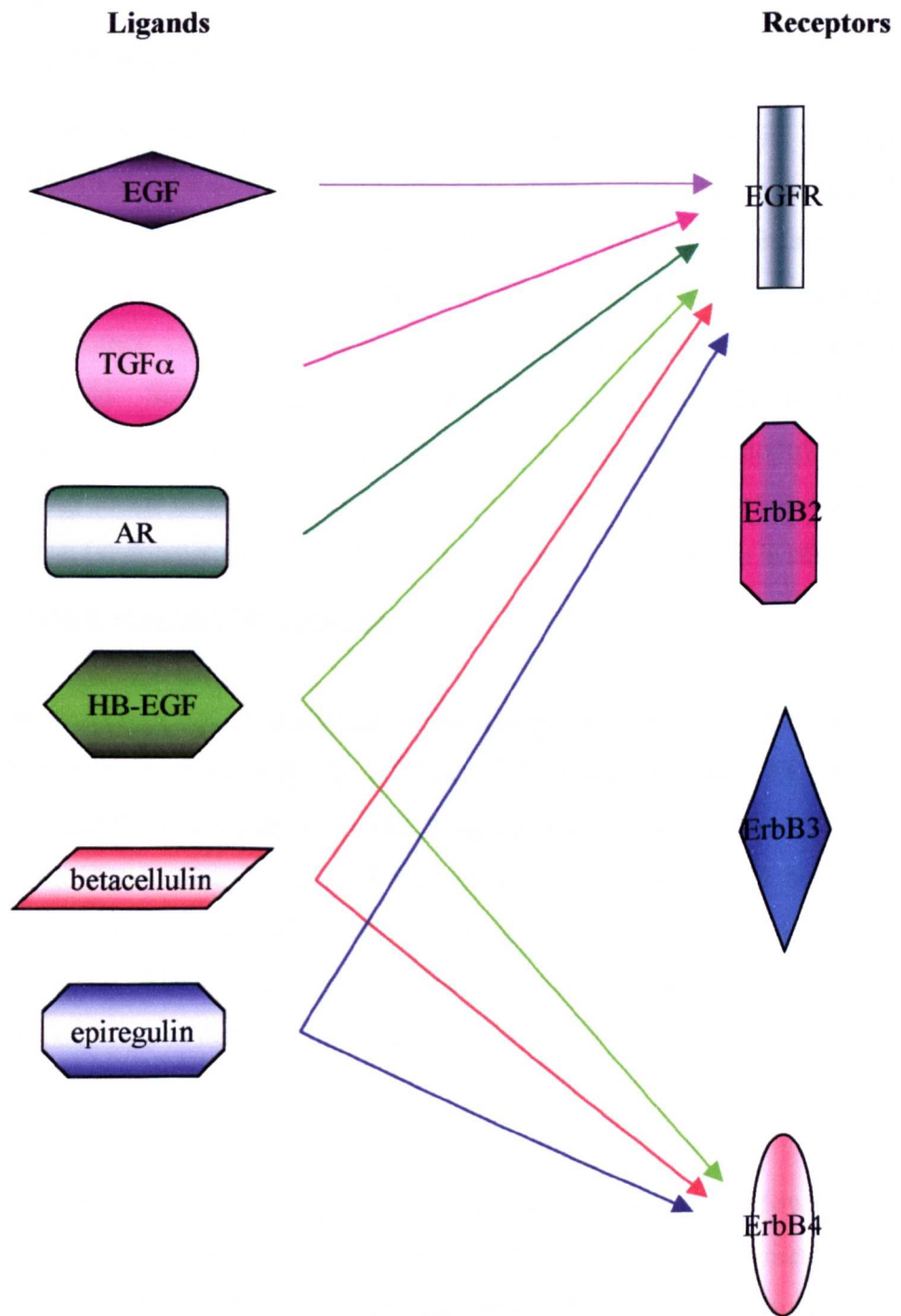
The classical route of activation of EGFR is binding of growth factors such as EGF and others, to the extracellular domain causing receptor homo/heterodimerisation and activation of the tyrosine kinase domain by autophosphorylation. Activation of the tyrosine kinase domain enables transfer of the γ phosphate ATP group to tyrosine kinase domains of both the receptor and other downstream substrates. Tyrosine phosphorylation leads to activation of several signalling pathways via downstream adaptor molecules and also to receptor internalization and recycling allowing modulation of downstream signalling pathways (Cohen et al., 1982; Wiley et al., 1991). Other stimuli apart from growth factors can activate EGFR (reviewed in (Carpenter, 1999). These other stimuli include G protein-coupled receptor (GPCR) agonists (working via c-Src), cytokine receptors (via Jak2), adhesion receptors, membrane depolarization (increased flux of calcium that brings about EGFR activation via c-Src) and stress response.

EGFR is a 170kDa protein initially produced from cleavage of the N terminus of a 1210 residue precursor followed by insertion of the 1186-residue protein in the cell membrane. 20% of the size of the mature EGFR is due to glycosylation of the N terminus. This glycosylation is necessary for protein translocation to the cell membrane (Slieker et al., 1986). An EGFR molecule consists of two ligand binding and two cysteine rich extracellular domains and an intracellular tyrosine kinase. EGFR sequence is about 64% similar to the other receptors of the family and can form heterodimers with them upon activation, thus expanding the possible pathways that it can activate.

Figure 1.6: Ligands of the EGFR family

There are six ligands binding to members of the EGFR family. These are shown on the left column and are EGF, TGF α , AR, HB-EGF, betacellulin and epiregulin. EGF, TGF α and AR bind preferentially to EGFR leading to its homo/heterodimerisation. The rest of the ligands are not EGFR specific but can bind to ErbB4 as well. The arrows are colour coded according to their respective ligand and show with which receptors the ligands can associate.

Figure adapted from Olayioye *et. al.*, 2000, *Oncogene*19(13):3159-3167.



There are several pathways activated by EGFR (fig1.7):

1. The Shc, Grb2, Ras/MAPK pathway
2. c-Src
3. JAK/STATs
4. PLC γ , PLD and PI3K

In the epidermis, EGFR signaling plays a major role in normal epithelial development. Some of the EGFR growth factors are synthesized by normal epithelial cells. EGFR is strongly expressed in the basal layer of the epidermis and the outer root sheath of hair follicles. Moving on to the suprabasal layer where less proliferation takes place, the number of EGFR receptors decreases. EGFR signalling regulates keratinocyte survival and protects them against apoptosis. Several animal models of EGFR ligands as well as dominant negative EGFR animal models show impaired epidermal and hair follicle development, implicating the EGFR pathway in the normal development of epithelial cell proliferation and differentiation. Which pathway(s) downstream of EGFR are important in this function is still unclear.

The Shc, Grb2, Ras/MAPK pathway

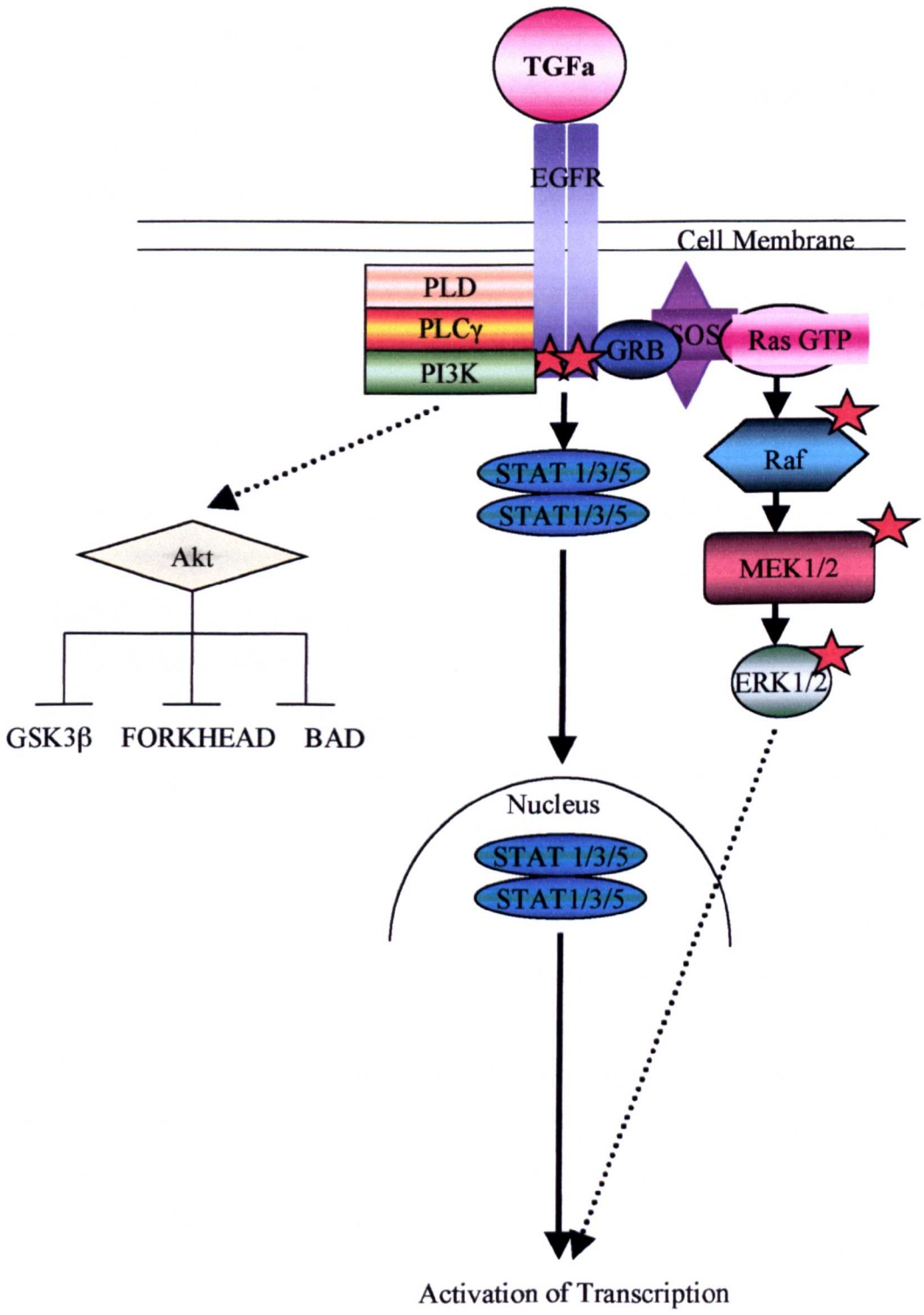
Upon ligand binding, EGFR is activated by phosphorylation and as a result the SH2 domain of Grb2 binds EGFR either directly via Y¹⁰⁶⁸ or Y¹⁰⁸⁶ or indirectly by first binding Shc that is associated to EGFR (Sasaoka et al., 1994a; Sasaoka et al., 1994b). The Grb2 association with EGFR leads to the association of SOS with Ras which leads to GTP binding on Ras thus leading to Ras activation. Usually, Grb2 is constitutively bound to SOS and localized in the cytosol preventing SOS from releasing active Ras. Activation of Ras leads to activation of downstream pathways as described in section 1.5.

The Src pathway

Src is both contributing to EGFR activation and acting as a downstream effector. Overexpression of Src proteins in fibroblasts or epithelial cells, leads to increased proliferation and transformation that is EGF mediated. Inhibition of Src, leads to decreased proliferation and to reversal of the transformed phenotype observed in cells overexpressing EGFR. Phosphorylation of Y⁸⁴⁵ of EGFR by Src leads to receptor activation. Src phosphorylates EGFR on other tyrosine residues and allows EGFR mediated activation of STAT5b and PI3K (Kloth et al., 2003).

Figure 1.7: EGFR signalling pathways

Binding of an EGFR ligand such as TGF α , leads to EGFR homodimerisation and activation by phosphorylation (indicated by a red star). Activated EGFR can recruit PLD and PLC γ , activating them and thus enabling them to carry their function in phospholipid metabolism. Physical interaction of activated EGFR and PI3K leads to activation of the latter which leads via other intermediate molecules to activation of Akt that plays a role in apoptosis inhibition. Association of activated EGFR and Grb2 via their SH2 domains and SOS recruitment leads to Ras activation by preferential binding to GTP. Activated Ras, phosphorylates and activates Raf, which in turn phosphorylates and activates MEK1/2, which leads to phosphorylation and activation of ERK1/2. Activated ERK1/2 leads to transcriptional activation of several downstream genes. Activated EGFR leads to homo/heterodimerisation of STATs 1/3/5 and their translocation to the nucleus where they play a role in transcriptional activation of downstream genes.



The JAK/STAT pathway

Mammals have seven STAT genes (1-4,5a,5b,6). STATs are inactive transcription factors when in the cytosol but translocate to the nucleus upon activation. STATs 1, 3 and 5 are usually constitutively associated with inactive EGFR via their SH2 domains. Activation of EGFR leads to homo/heterodimerisation of STATs. This association activates them and leads to their nuclear translocation. Activation of STAT by EGFR is independent of JAK activation which is the standard for STAT activation in cytokine signalling.

PLD, PLC γ and PI3-K

EGFR directly activates three enzymes involved in phospholipid metabolism; phospholipase- γ (PLC γ), phosphatidylinositol-3-kinase (PI3K) and phospholipase D (PLD). Upon EGFR activation, PLD physically associates with EGFR and gets activated by phosphorylation. PLD hydrolyses phosphatidylcholine to create choline and phosphatidic acid.

PLC γ binds to phosphorylated EGFR via Y¹¹⁷³ or Y⁹⁹² and gets activated. Activation of PLC γ leads to hydrolysis of Ptd Ins(4,5)-P₂ to give 1,2 diacylglycerol (DAG) and inositol 1,3,5-triphosphate (IP₃). IP₃ can release Ca⁺² from intracellular compartments and DAG plays a role in activation of PKC.

PI3K phosphorylates phosphatidylinositol at the 3' position. There are three classes of PI3 Kinases depending on structure but only PI3K class Ia gets activated by tyrosine kinase receptors. Phosphorylated ErbB receptors physically interact with the PI3K p85 subunit via its SH2 domain. p85 preferentially binds ErbB3, so it is believed that there is heterodimer formation of EGFR/ErbB3 that mediates this interaction. Also Src phosphorylation of EGFR can lead to activation of PI3K. PI3K Ia leads to phosphatidylinositol-3, 4, 5-triphosphate (PIP₃) formation which plays a role in Akt translocation to the plasma membrane and its activation via phosphorylation by phosphoinositide-dependent kinase 1 (PDK1). Akt could be the major route by which EGFR exerts its antiapoptotic effects. PI3K γ also binds Ras via its catalytic subunit p110. Maybe via this association EGFR can activate and control both the MAPK and PI3K pathways.

EGFR and Cancer

Several studies have shown that alterations in EGFR such as amplification, rearrangements and overexpression occur at high frequencies in human squamous cell carcinomas, glioblastomas, breast, pancreatic, liver and colorectal cancers (Derynck, 1992; Libermann et al., 1985; McKay et al., 2002). It has been shown that about 30% of human cancers express elevated levels of EGFR and it has been correlated with poor prognosis and decreased disease-free and overall survival rate. A natural mutant of EGFR, EGFRvIII, has a deletion of exons 2-7 and lacks the extracellular domain therefore it is constitutively active and is not internalized thus being capable of long term signalling. This is the most common mutation in human cancers and is detected in 50% of glioblastomas and 70% of medulloblastomas. Transfection of EGFRvIII in glioma cell lines increases their tumorigenicity in nude mice. EGFRvIII action is also linked to the anti-apoptotic protein Bcl-xL. *In vivo* expression of EGFRvIII in inhibitors of CDK4 (INK4a) knock out mice, led to glioma formation. This shows that EGFRvIII on its own is not enough for tumor formation but promotes proliferation.

EGFR animal models

Several knock out EGFR mice have been developed but their phenotype is strain dependent and they do not reach weaning age. They show peri-implantation, mid-gestational death, skin, lung, brain, liver and gastrointestinal tract abnormalities as well as disorganized hair follicles and curly coats. Fetal death is due to placental defects or failure of epithelium maturation in several tissues (Miettinen et al., 1995; Sibilian and Wagner, 1995; Threadgill et al., 1995).

Dominant negative EGFR models have been created to overcome the premature death observed in EGFR null animals. One of these models where the transgene under control of K5 promoter is directed for expression at the basal layer and the outer root sheath of hair follicles, the animals that develop are smaller with short, waved hair and curly whiskers initially, progressing to atrophic and sparse hair and finally to alopecia. Absence of EGFR has thus prevented entry of the hair follicles into the catagen stage leading to follicle necrosis, infiltration of the epidermis with inflammatory elements and epidermal hyperplasia (Murillas et al., 1995).

Inducible expression of ErbB2 in the K14-rtTA/TetRE-ErbB2 mouse led to skin hyperplasia after 2 days of doxycycline exposure that regressed upon withdrawal of the chemical. In prolonged induction of ErbB2, hyperplasia of the corneas, eyelids, tongue and oesophagus

developed and the animals showed increased TGF α expression, implying that ErbB2 cooperates with EGFR in the regulation of hair follicle and skin architecture (Xie et al., 1999).

EGFR and LMP1

Human epithelial cells (C33A and HNE2) showed upregulation of EGFR at the protein and mRNA level upon transient or stable expression of LMP1 (Miller et al., 1995). CTAR1 is essential for EGFR induction but not CTAR2. Overexpression of TRAF3 (a negative regulator of the TRAF pathway) or an amino truncated TRAF3 that inhibits NF- κ B activation from the CTAR1, led to inhibition of EGFR expression. Since the CTAR2 mediated NF- κ B is still active, this implies that the LMP1 mediated EGFR activation may involve the TRAF signalling pathway and not NF- κ B signalling only (Miller et al., 1998b; Miller et al., 1997). A recent study confirms that CTAR1 is essential for EGFR induction and showed that LMP1 can modulate the EGFR promoter activation via NF- κ B (Tao et al., 2004b). When 60 NPC specimens were studied by means of immunohistochemistry (IHC), 41 of the samples tested positive for LMP1 and 44 tested positive for EGFR upregulation. The EGFR upregulation was closely correlated with LMP1 expression, implicating LMP1 in the control of EGFR expression in NPC (Sheen et al., 1999). Also Zheng *et. al.*, showed that positive LMP1 NPC specimens expressed EGFR strongly and that there was an increase of EGFR expression in the later stages of NPC (Zheng et al., 1994a).

Regulators of EGFR ligand shedding

Metalloproteases with a disintegrin domain (ADAMs) are responsible for regulating the cleavage of EGFR ligands and thus regulating EGFR activation and the effects this has on tumour progression (reviewed in (Gee and Knowlden, 2003). TNF α -converting enzyme (TACE or ADAM17) has been shown to be necessary for TGF α shedding. Absence of TACE or non functional TACE leads to defective TGF α shedding. It has been shown that TACE is upregulated in human breast cancer, indicating it plays a regulatory role in activating EGFR (Borrell-Pages et al., 2003). It was thought that GPCR activated EGFR independently of its ligands but it has been shown that ADAM10 and ADAM17 regulate cleavage of HB-EGF and AR respectively activating the MAPK cascade and Akt signalling (Yan et al., 2002).

TGF α

TGF α is a mammalian growth factor that was first isolated from the culture medium of growing retrovirally transformed fibroblasts. It is first synthesized as a 160aa transmembrane precursor (proTGF α). The extracellular domain of TGF α contains the receptor binding motifs and is cleaved by ADAM 17 to produce the mature soluble form of TGF α that is 50aa and other TGF α molecules of different sizes. Usually, TGF α is detected as a polypeptide between 5kDa –20 kDa (reviewed in (Derynck, 1988)). The difference in size its due to differences in glycosylation. The membrane bound forms of TGF α are biologically active but act on adjacent cells rather than at cells at a distance. (Anklesaria et al., 1990)(reviewed in (Massague, 1990)). An experiment in which the two cleavage sites that release soluble TGF α were modified so that no soluble TGF α could be released showed that transmembrane TGF α could still activate EGFR. The transmembrane form is about 50-100 times less active than soluble TGF α (Brachmann et al., 1989). Defective cleavage of TGF α in two human colon cancer cell lines, led to the transmembrane form inducing increased phosphorylation of EGFR, a slower EGFR internalization and transmembrane TGF α was more resistant to tyrosine phosphatases thus enhancing activation of EGFR and giving a growth advantage to the cells.

It has been shown that TGF α can be synthesized by various oncogenically transformed fibroblasts and by tumour cells such as renal, squamous carcinoma, melanomas etc. There is evidence showing that TGF α may contribute to the conversion of a normal cell to a malignant one. However, TGF α plays an important role in normal embryonic development. It is normally expressed in the unfertilized oocyte, the developing embryo and tissues such as the placenta, the kidney and the oral cavity of the developing mouse. In adult mice TGF α is expressed in skin, brain, breast and the gastrointestinal mucosa among other organs. TGF α also plays a role in wound healing, angiogenesis and keratinocyte proliferation and migration. It has been suggested that TGF α can promote skin tumorigenesis and there are several animal models that support this as well as other experiments, for example, elevated TGF α levels have been detected in DMBA/TPA treated mice skin tumours. Furthermore, papilloma cells transfected with human TGF α , when grafted to nude mice produce larger tumours than untransfected papilloma cells. In addition, there is evidence that TGF α and TPA synergise in enhancing epithelial proliferation.

EGFR ligands animal models

Several animal models have been created to determine the action of each of the EGFR ligands and clarify whether they complement each other or have distinct functions.

Gain of function models

Overexpression of TGF α to the stratified squamous epithelia (using the human K14 promoter) led to ear, scrotum, tail, foodpad and body skin hyperplasia, stunted hair growth, localised psoriasis symptoms and spontaneous papilloma formation at sites of mechanical irritation. Upon TPA treatment papillomas were formed that did not display any Ras mutations, showing that overexpression of TGF α in the epidermis can act as an initiator in tumorigenesis (Vassar and Fuchs, 1991; Vassar et al., 1992). Increased expression levels of EGFR (in the olfactory epithelium), cyclin D1, retinoblastoma, cyclin E and E2F-1 was observed suggesting a response due to increased levels of TGF α (Getchell et al., 2000). Similarly, when TGF α was expressed in the basal epidermal layer (human K1 promoter), epidermal hyperplasia and hyperkeratosis was evident in the newborn mice as well as spontaneous papilloma formation in the young adult, mostly at wounding sites. Upon TPA treatment papillomas formed that had no H-ras mutations. However when these mice were crossed with HK1.v-fos mice, the resulting bitransgenic animals showed a severe hyperplastic neonatal epidermis and developed spontaneous papillomas as adults much faster. TPA treatment of these mice led to a rapid onset of papillomas that progressed to squamous cell carcinomas that had H-ras mutations, suggesting that v-fos and TGF α cooperate in tumorigenesis but need an additional genetic event such as H-ras mutation for progression (Dominey et al., 1993; Greenhalgh et al., 1993b; Wang et al., 1994; Wang et al., 1995; Wang et al., 1999).

Other TGF α transgenic mice under the control of the MT promoter were created (Shibata et al., 1997). Without any treatment these mice showed no phenotype, however, bromodeoxyuridine (BrdU) treated mice showed increased DNA synthesis indicative of increased proliferation. In DMBA/TPA treated transgenic mice, the tumour load and volume was higher than that of wild type mice. Application of only DMBA or TPA was not enough to promote tumour formation but TPA alone, produced epidermal hyperplasia in 63% of transgenic mice as opposed to only 20% of wild type mice. Western analysis of tumours and skin, led to detection of EGFR downregulation in transgenic papillomas as opposed to wild type skin tumours suggesting that a tight homeostatic control is in place to compensate for ligand overexpression. Western analysis also led to detection of the phosphorylated forms of

EGFR only in transgenic skin tumours and not in wild type tumours showing that TGF α overexpression led to the activation of EGFR. There were no inactivating p53 mutations in any of the lesions but there were *ras* codon 61 mutations in both transgenic and wild type skin tumours.

Overexpression of EGF under the direction of β -actin, gave mice that were smaller than wild type littermates and had necrotic regions in some regions of their liver. No lesions were observed. However to be able to directly compare these mice to the TGF α overexpressing mice, the EGF has to be under the direction of a promoter specifically leading to its expression in the epithelium (Chan and Wong, 2000).

Mice overexpressing AR under the K14 promoter showed a psoriasis like phenotype with reddening, scaly skin, alopecia and rare spontaneous papilloma formation. AR overexpressing mice using the involucrin enhancer/promoter to direct expression of the transgene to the suprabasal epidermal layer, also showed a psoriasis like phenotype and synovial inflammation (Cook et al., 2004; Cook et al., 1997).

Loss of function models

Two groups have developed TGF α null mice (Luetteke et al., 1993; Mann et al., 1993). The resulting mice from both groups, were viable and fertile and it was shown by radioassay that they had no detectable TGF α levels in skin, small bowel or kidney. Phenotypically, the mice, showed waviness of fur and whiskers evident from day 1, more pronounced after day 12 and less evident beyond 8 weeks of age. The null mice showed eye abnormalities such as precocious eyelid opening and corneal inflammation in older animals. There was no diminished wound healing ability in those mice as seen by examination of the tail stamps after tail clipping. By cross breeding experiments it was shown that waved-1 recessive mutation and TGF α are allelic. These mice have been used in cross breeding experiments in this study and are referred to as line 125 in this thesis.

EGF null mice have no phenotype. AR null mice show no phenotype but when crossed with EGF null (EGF/AR null) or TGF α null mice (AR/TGF α null) or with both EGF and TGF α null mice (EGF/AR/TGF α null) an essential role of AR in mammary ductal morphogenesis was revealed. The triple null mice also show eye defects, dermatitis and skin ulcerations.

1.8 INK4a Locus

The INK4a locus encodes two distinct proteins that are both involved in cell cycle arrest and growth inhibition (Quelle et al., 1995). These overlapping genes are transcribed from different promoters and have different first 5' exons. Even though they share their second and third exons, these are read in different frames so the two gene products p16^{INK4a} and p19^{ARF} (p14^{ARF} is the human homolog) have no amino acid similarity (fig1.8). The locus is highly conserved among species thus showing its importance.

p19^{ARF} has been implicated in the regulation of the p53 tumour suppressor and p16^{INK4a} has been implicated in the cyclin-D dependent kinase (CDK4)/CyclinD1/Rb pathway.

The INK4 family

The INK4 family of proteins includes; the p16^{INK4a}, p15^{INK4b}, p18^{INK4c} and p19^{INK4d}. The first two are located on human chromosome 9p21 and share 40% homology, p18^{INK4c} is located on 1p32 and p19^{INK4d} is located on 19p13. The mouse and the human proteins are 90% homologous showing how well the INK4 family members have been conserved among species. They all have characteristic ankyrin repeat motifs. Ankyrin motifs mediate protein-protein interactions. p16^{INK4a} and p15^{INK4b} have four ankyrin repeats whilst p18^{INK4c} and p19^{INK4d} have five ankyrin like repeats. All of the INK4 family members have a similar structure as shown by X-ray crystallography and similar biochemical functions. They all bind and inhibit CDK 4 or 6. Initially p16^{INK4a} was discovered because of its binding to CDK4. Crystallography data have shown that the third ankyrin repeat is crucial for the interaction of p16^{INK4a} with CDK4/6 (Koh et al., 1995; Noh et al., 1999).

Many human tumours carry mutations affecting p16^{INK4a}. These range from homozygous deletions (14% of all human tumours), intragenic mutations (5% of all human tumours) and promoter silencing by methylation (19% of all human tumours). Mutations of the other family members in human cancers are rare suggesting that p16^{INK4a} is the member of the family with the major tumour suppressive role. Most human tumours show inactivation of p16^{INK4a} by one of the three ways described above with a frequency between 25-70%. About 98% of spontaneous pancreatic tumours have p16^{INK4a} inactivation and cases of familial melanoma and pancreatic cancer also show p16^{INK4a} inactivation.

Each of the four family members are regulated by different signals and show different expression patterns during development. Normally p16^{INK4a} expression is kept at very low levels but during senescence or oncogenic stress p16^{INK4a} levels increase. The p15^{INK4b} is

specifically upregulated by TGF β . The other two members, p18^{INK4c} and p19^{INK4d} show a cyclic pattern of expression with maximum expression in the S phase. So far studies have indicated that the four family members are not functionally redundant.

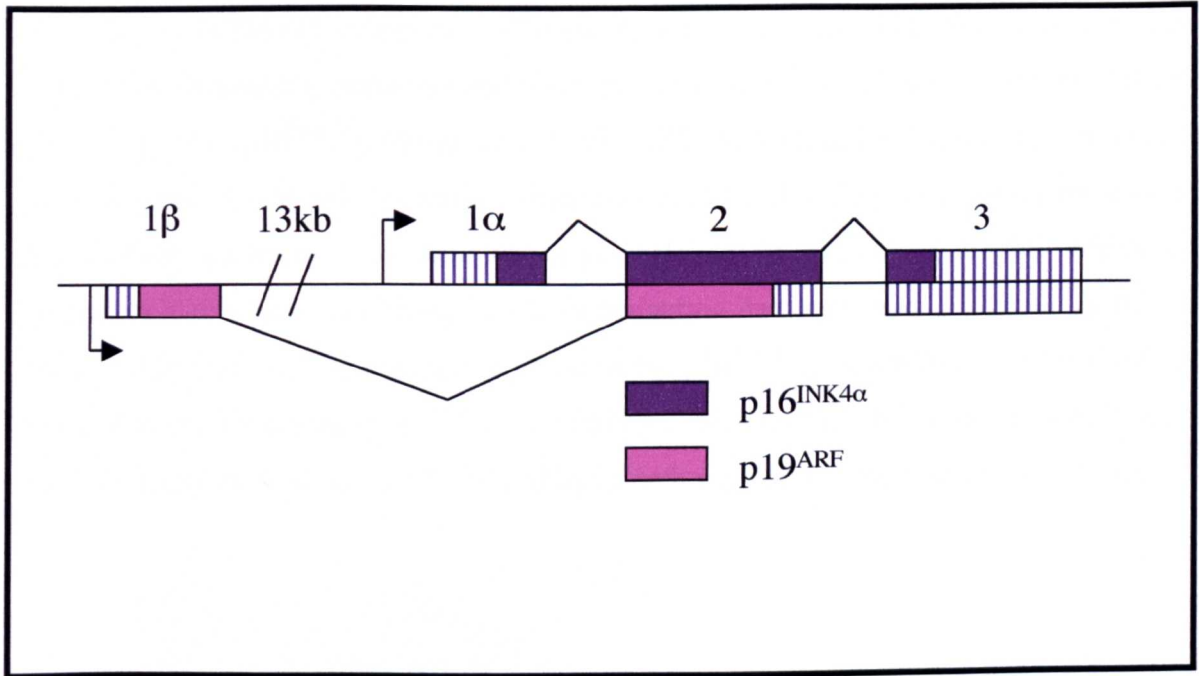


Figure 1.8: The INK4a locus (not to scale)

The diagram depicts the organisation of the two genes and their encoded products, p16^{INK4a} and p19^{ARF}. p16^{INK4a} is encoded by exons 1 α , 2 and 3 (ORF in purple). p19^{ARF} is encoded from exons 1 β , 2 and 3 (ORF in pink). Introns are indicated by angled lines. The two promoters are indicated by arrows and are separated by approximately 13kb.

The p16^{INK4a}/CDK4/CyclinD1/Rb pathway

Under normal conditions, Rb is unphosphorylated and bound to E2F transcription factors preventing them from activating their downstream target genes. Rb can be phosphorylated by the CyclinD/CDK4/6 complex. Phosphorylation releases E2F that can now activate downstream signalling pathways and allow progression of the cell cycle from G0/G1 to the S phase (fig.1.9). p16^{INK4a} preferentially binds CDK4/6, forcing the CDK4/6/CyclinD complex to dissociate. Unbound CyclinD is then degraded by the ubiquitin dependent proteasome degradation pathway. In this way CyclinD cannot activate CDK4/6 which cannot phosphorylate Rb thus inhibiting E2F from activating its targets and thus arresting the cells in G0/G1. Most of the inactivating mutations of the p16^{INK4a} gene are found in the third ankyrin repeat thereby preventing p16^{INK4a} from binding CDK4/6 (fig.1.9). Release of E2F also plays a role in the control of the p19^{ARF}/MDM2/p53 pathway and this will be discussed later.

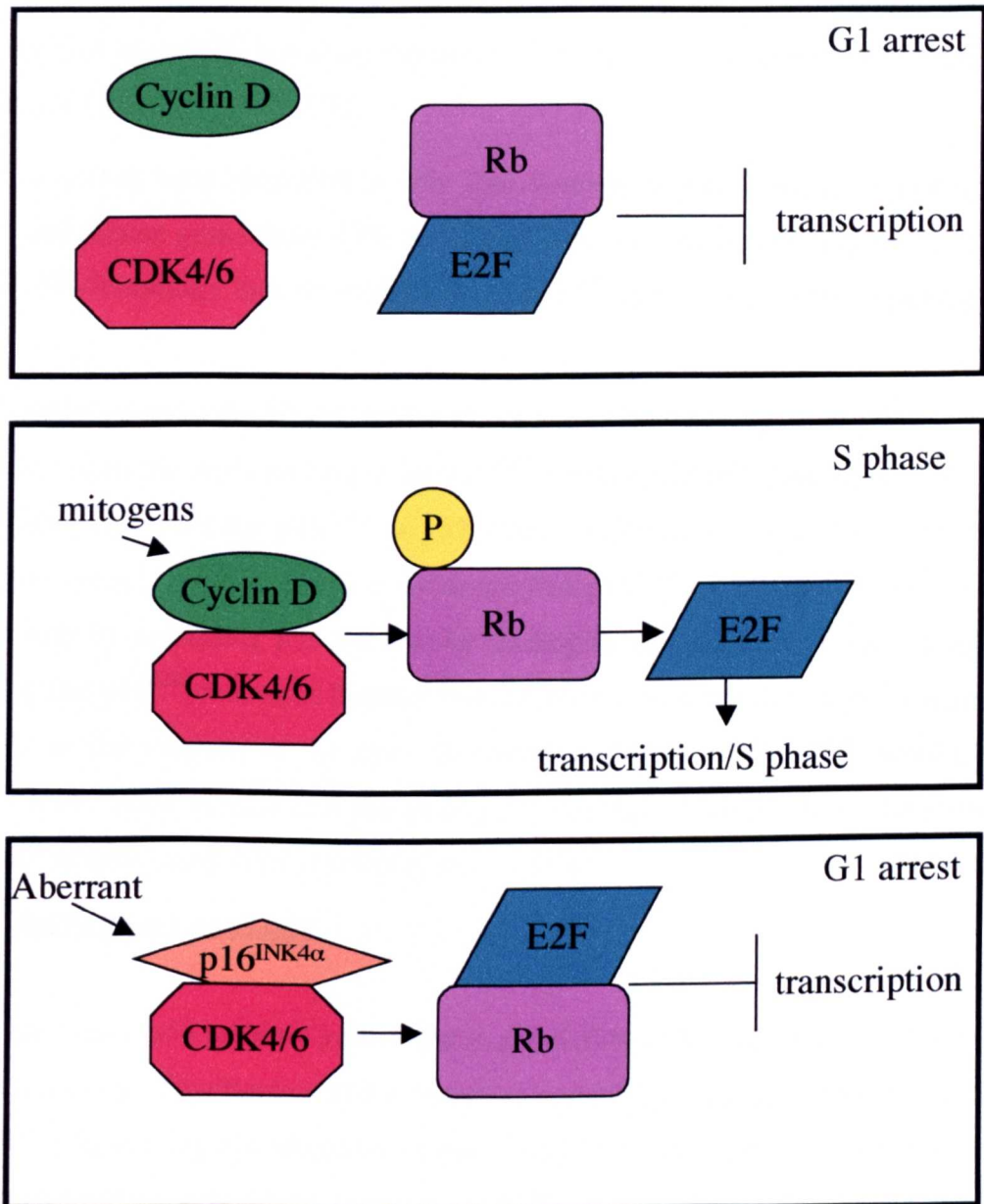


Figure 1.9: The p16^{INK4α} role in inhibiting S phase entry

In G0/G1, Rb binds E2F factors preventing them from transcribing genes that would promote S phase entry. On mitogenic signals, Cyclin D complexes with CDK4/6 to phosphorylate Rb and release E2Fs that can promote S phase entry. Abnormal mitogenic signals lead to activation of p16^{INK4α} that prevents association of Cyclin D and CDK4/6 thus inhibiting Rb phosphorylation and inhibiting S phase progression leading to G1 arrest.

The p19^{ARF} protein

The p19^{ARF} protein was discovered after p16^{INK4a} when it was realised that the INK4a locus could encode a further protein in another reading frame (ARF). It was shown early on that the ectopic expression of p19^{ARF} could also inhibit cell cycle progression both at G1 and G2 via the p53 pathway (Kamijo et al., 1997).

The p19^{ARF} gene has been identified in only four species; human, mouse, rat and opossum. The human and mouse genes have 49% homology whereas the human and mouse p16^{INK4a} genes show 63% homology thus showing that the p19^{ARF} gene is less well conserved among species.

The p19^{ARF} protein acts in the MDM2/p53 pathway as well as having other p53 independent functions. For example triple null mice for p19^{ARF}, MDM2 and p53 develop a wider variety of tumours than mice null for p19^{ARF} or p53 alone, implying that the p19^{ARF}/MDM2/p53 pathway is not entirely linear. There is evidence that p19^{ARF} exerts its tumour suppressor function not only by stabilising p53 but also by leading to regression of vessels as suggested by the finding that p19^{ARF} null mice become blinded soon after birth due to the persistence of blood vessels in the vitreous of the eye. Normally expression of p19^{ARF} would lead to regression of these blood vessels thus preventing any damage to the eye from the subsequent proliferation of neighbouring cells (McKeller et al., 2002).

The p19^{ARF}/MDM2/p53 pathway

The tumour suppressor p53 is found inactivated in about 50% of human cancers. The levels of p53 are determined by ubiquitination and subsequent proteolytic cleavage. p53 can negatively regulate itself by activating the ubiquitin ligase MDM2 (MDM2 is the human homologue). MDM2 can target p53 for proteolytic cleavage. p19^{ARF} can prevent this cleavage in two ways; by binding to MDM2 and preventing it from targeting p53 for degradation and by actively sequestering MDM2 into the nucleolus thus physically separating it from p53. In this way p19^{ARF} leads to stabilisation of p53 levels. Usually the levels of p19^{ARF} are very low. This is believed to be the result of repression of p19^{ARF} by E2F3 (Aslanian et al., 2004) or by E2F1 (Bates et al., 1998). Oncogenic stimuli such as activated Ras, c-myc, E2F, E1A and v-Abl (de Stanchina et al., 1998; Dimri et al., 2000; Kamijo et al., 1998; Palmero et al., 1998; Radfar et al., 1998; Serrano et al., 1997; Zindy et al., 1998) lead to increased levels of p19^{ARF} thus ensuring that p53 is unbound. The tumour suppressor p53 exerts its anti-oncogenic function in

two ways; first it can induce cell cycle arrest and second it can induce apoptosis. Unbound p53 can act as a transcriptional activator of genes such as the cell cycle inhibitor p21^{Cip1} and the pro-apoptotic gene *bax*.

The two pathways p19^{ARF}/MDM2/p53 and p16^{INK4a}/CDK4/6/CyclinD/Rb do not act in isolation but in a synergistic way. Interaction is at two levels, the first being E2F factors activating or repressing p19^{ARF} and the second being p53 activating p21^{Cip1} that can inhibit Cyclins E/A interaction with CDK2 thus inhibiting entry into the Sphase. p16^{INK4a} also mobilises p27^{kip1} that can inhibit the activity of CDK2 (fig.1.10). Using siRNA against either p16 or p19 in MEFs, Carnero et. al., showed that p16^{INK4a} and p19^{ARF} have overlapping roles. siRNA against p16 or p19 only, led to colony formation, no senescence and immortalisation. Restoration of function of p16^{INK4a} in MEFs that were treated with siRNA against p16^{INK4a} and subsequent treatment with siRNA against p19^{ARF}, led to continuous proliferation. When the p19^{ARF} function was restored in MEFs treated with p19^{ARF} siRNA and their subsequent treatment with p16^{INK4a} siRNA led to growth arrest. These results show that p19^{ARF} suppression of immortalisation overlaps with the function of p16^{INK4a} but that p19^{ARF} has also another role in suppressing immortalisation that is independent of p16^{INK4a} function.

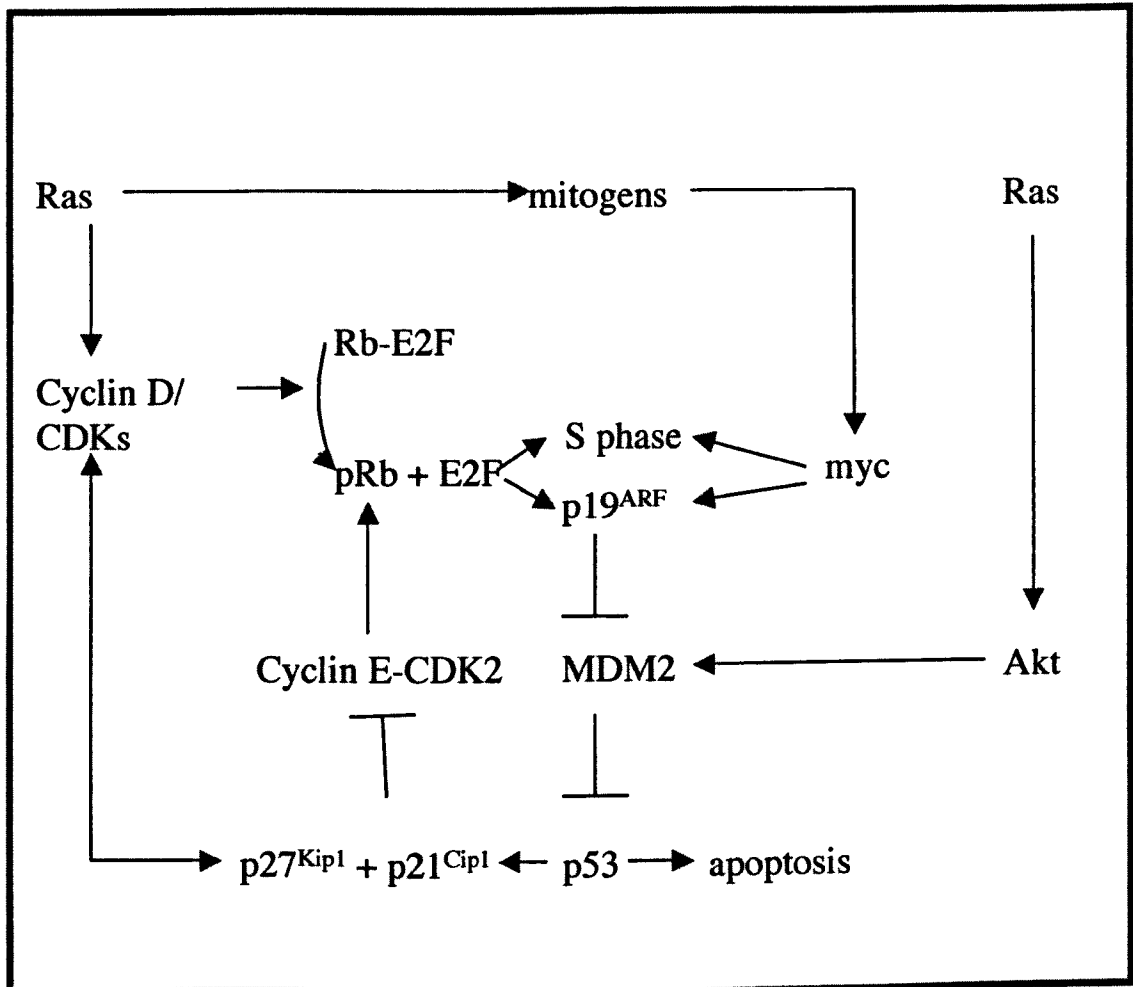


Figure 1.10: p19^{ARF} signalling and p16^{INK4a} adapted from Lowe and Sherr, Curr. Opin. Genet. Dev., 2003, 13(1): 77-83

Activation of p19^{ARF} leads to the inhibition of MDM2 mediated degradation of p53. Active p53 can induce apoptosis. Ras activated CyclinD/CDK leads to Rb phosphorylation and release of E2F allowing for progression of cell cycle and at the same time reinforcing p19^{ARF} activation.

Transgenic Mouse Models of INK4a locus

The first mouse model to be developed was the INK4a null model where exons 2 and 3 of the INK4a locus were replaced with a neomycin cassette (Serrano et al., 1996). The mice lack p16^{INK4a} protein. It is not clear whether they lack p19^{ARF} completely since there is an intact exon 1 β , and these mice may express a truncated p19^{ARF} product. The mice are viable and fertile. However, 69% of the mice spontaneously show tumour formation by 29 weeks of age, mostly lymphomas. When these mice are carcinogen treated almost all of them succumb to tumours such as sarcomas and lymphomas. When MEFs from these mice were compared to wild type MEFs or heterozygous MEFs, they showed an increase in growth rate, higher cellular densities, higher efficiency in colony formation and they could also escape senescence. They could also form foci in culture when *Ras* but not *c-myc* was introduced and these cells could form tumours in nude mice. These experiments showed that the INK4a locus is powerful in tumour suppression. (Note these mice have been used in the studies described in this thesis and are referred to as line 113).

Subsequently, mice lacking specifically the p19^{ARF} gene were created (Kamijo et al., 1997). These mice become blind soon after birth but they are viable and fertile. They develop sarcomas, T-cell lymphomas, carcinomas and neurological tumours and about 80% of them are dead within a year of birth²(Sharpless et al., 2004). Since the phenotype between INK4a null and p19^{ARF} mice was quite similar it was suggested that p19^{ARF} maybe more important in tumour suppression in mice.

More recent models include one that leads to production of an unstable form of p16^{INK4a} protein (due to a stop codon insertion in exon 2) (Krimpenfort et al., 2001) and mice that are null only for p16^{INK4a} (due to exon 1 β deletion) (Sharpless et al., 2001). MEFs from both of these models had the same growth rate, same Rb phosphorylation and same pattern of growth arrest when serum starved as wild type MEFs but p19^{ARF} null MEFs were very susceptible to transformation and could escape growth arrest whilst p16^{INK4a} null MEFs were not acting in this manner.

² Sharpless et al, 2004, reported the generation of p19^{ARF} null mice. These mice were created only for comparison reasons with the p16^{INK4a} null mice (Sharpless et al., 2001). These new p19^{ARF} null mice were also more prone to tumours than wild type animals.

Both mouse models showed increased tumour load after chemical carcinogen treatment when compared to wild type siblings but the mice harboring the mutant p16^{INK4a} showed no difference in spontaneous tumour formation unlike the INK4a null mice.

Comparing these results between p16^{INK4a} null or mutated protein and p19^{ARF} null mice it is shown that both p16^{INK4a} and p19^{ARF} are important as tumour suppressors but they play a different role in different tumour types. A recent study argues that in humans the most important tumour suppressor is p16^{INK4a} and not p19^{ARF}. This is consistent with epidemiological studies that have shown point mutations, deletions and promoter hypermethylation affecting only p16^{INK4a} and not p14^{ARF} (the human homolog of p19^{ARF}) (Ruas and Peters, 1998). In the study by Voorhoeve and Agami, 2003, human primary fibroblasts were used along with siRNAs against Rb, p53, p14^{ARF} or p16^{INK4a}. It was shown that inhibition of p14^{ARF} leads to fibroblast increased growth only in the presence of p53 but these cells do not readily form tumours in nude mice (Voorhoeve and Agami, 2003). In contrast inhibition of p16^{INK4a} does not play a role on fibroblast growth rate but instead cooperates with the loss of p53 to increase growth rate and cause transformation, thus suggesting that loss of p16^{INK4a} is more important for human tumours.

LMP1 , NPC and p16^{INK4a}

NPC primary tumours and xenografts show homozygous deletion of the INK4a locus as well as silencing of p16^{INK4a} due to promoter hypermethylation (Lo et al., 1996; Lo et al., 1995). When NPC cell lines were treated with 5'-aza-2'-deoxycytidine that reverses hypermethylation, p16^{INK4a} protein levels increased. It was therefore implied that p16^{INK4a} could be involved in the development of NPC.

As described in section 1.3, LMP1 inhibits p16^{INK4a} expression in rodent fibroblasts by relocalising its effectors (Ohtani et al., 2003; Yang et al., 2000a; Yang et al., 2000b). However, inhibition of p16^{INK4a} was not observed in LCLs, implying that either LMP1 cannot inhibit p16^{INK4a} or it is not sufficient for p16^{INK4a} inhibition (Hayes et al., 2004). Data generated from chemical carcinogenesis treatment of mice expressing LMP1 in the epidermis but with INK4a null mutation, showed that INK4a locus products (either p16^{INK4a} or p19^{ARF}) inhibit lesion growth. Heterozygous loss of INK4a leads to intermediate growth, therefore a cell with an INK4a mutation (ie.heterozygous) and EBV infection with LMP1 expression will grow faster than an EBV infected cell with no mutation. Also loss of INK4a in the absence of

EBV shows reduced risk of lesion outgrowth. It is therefore the specific combination of loss of INK4a and EBV/LMP1 that leads to increased risk (Macdiarmid et al., 2003).

1.9 Mouse models of LMP1 expression in the epithelium

In order to investigate the role LMP1 plays in the formation and the development of EBV associated carcinoma *in vivo*, mouse models were developed that would express LMP1 in the epithelium. There are many advantages to using an *in vivo* model to study a disease. An *in vivo* model enables the researcher to gain access to affected tissues and study the different stages of the disease from the outset. Directing expression to epidermis allows ready observation and monitoring of a developing phenotype. Moreover, carcinogenesis in the mouse skin has been extensively characterised as described in section 1.5.

The Structure of the Skin

Epidermis is a type of stratified epithelium. Epithelia line all the cavities and free surfaces of the body. Cells in epithelia are tightly bound together and provide a barrier to environmental agents and bacteria as well as regulating water, solute and cell movement. All epithelia are avascular and depend on the underlying connective tissue for nutrients. Simple epithelia are single sheets of cells while stratified epithelia consist of layers of multiple cells usually of different types. Pseudostratified epithelia appear to consist of different layers whereas in reality they consist of a single layer of cells. Epithelia are categorised according to the shape of the cells that make them up. There are cuboidal epithelia where the cells are cubed shaped, columnar epithelia where the cells are rectangular and squamous epithelia where the cells are flat. Epithelia can contain cells that can form keratins or not. The epidermis is a stratified keratinising epithelium whilst the epithelium lining the mouth, the nasopharynx and the gastrointestinal tract consists of simple squamous or columnar non keratinising epithelium. NPC arises from the simple squamous non keratinising epithelium of the nasopharynx. In the transgenic mice, we are modelling EBV associated disease in the stratified keratinising epithelium of the skin and the gastrointestinal tract.

The skin consists of the epidermis, the underlying dermis and the skin appendages which include hair follicles and sweat glands (fig.1.11). Its purpose is to protect internal organs from injury, infectious agents and dehydration and serve for insulation, vitamin D production, sensation and excretion (Fuchs and Byrne, 1994; Fuchs and Raghavan, 2002).

The dermis is developmentally derived from the mesoderm and is usually much thicker than the epidermis. It consists of two layers; the innermost thicker layer is the reticular dermis and

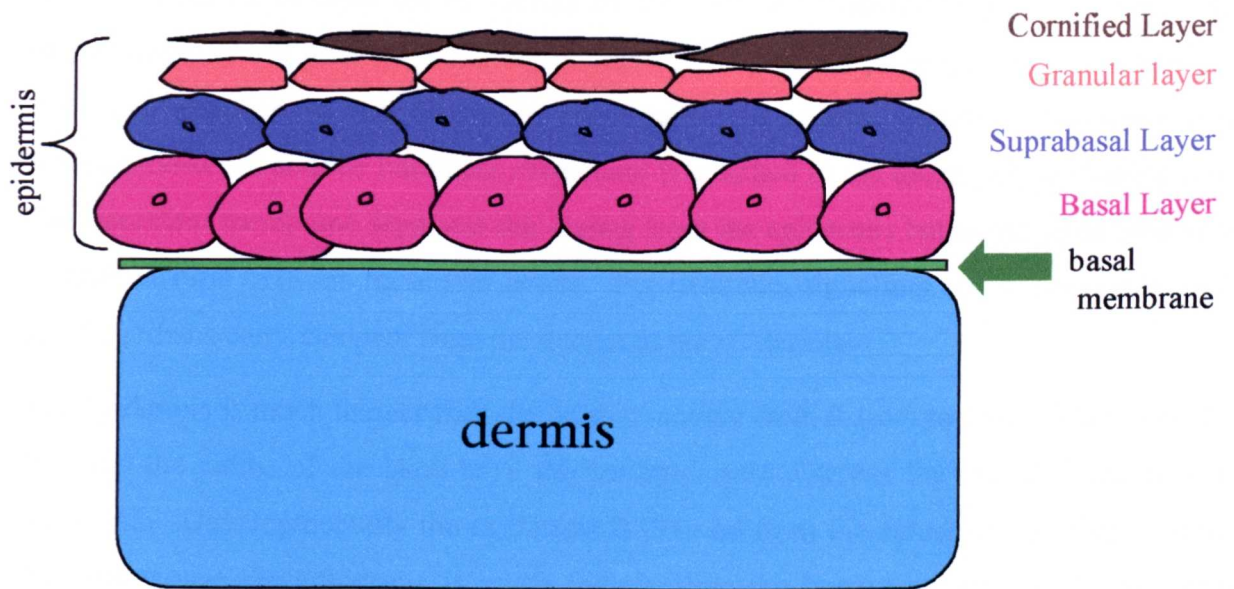


Figure 1.11: Structure of the skin

The diagram shows the structure of the skin; consisting of the epidermis the dermis and the basement membrane. The skin appendages like hair follicles and sweat glands are not shown. The different epidermal layers are depicted. The proliferating basal layer is shown in pink, the differentiating suprabasal layer in purple, the granular layer in peach and the cornified layer in brown.

the outermost thinner layer is the papillary dermis. The dermis consists mainly of collagen and elastic fibers, capillaries and blood vessels. It is in the reticular dermis that all the epidermal appendages such as hair follicles and sweat glands lie. The dermis main cell type is the fibroblast which is responsible for producing collagen elastic fibers. Other cell types found in the dermis include macrophages and mast cells that play a role in immunity.

Dermis is separated from the epidermis by the basement membrane which is made up of extracellular matrix proteins including laminins, collagen and proteoglycans. The epidermal cells are attached to the basement membrane via special adherens junctions called hemidesmosomes and the basement membrane is attached to the dermis via anchoring fibrils. The basement membrane separates the dermis from the epidermis but at the same time allows communication between these two layers. For example, signalling molecules, lymphocytes and Langerhans cells can pass from the dermis to the epidermis.

The epidermis is much thinner than the dermis ranging from 0.1mm to 1mm. The soles of the feet and the palms of the hand have thicker epidermis whereas the eyelids have very thin epidermis. Developmentally the epidermis is derived from the ectoderm. In furry mammals like the mouse the epidermis is much thinner than the human epidermis. The epidermis consists of mainly of keratinocytes (85%), Langerhans cells, Merckel cells and melanocytes. The primary role of keratinocytes is to produce keratins. Melanocytes produce melanin which protects the keratinocytes from UV light. Langerhans cells can present foreign antigens to the immune system. Merckel cells are found in certain parts of the epidermis and allow pressure to be felt. The epidermis is a stratified keratinised squamous epithelium that is replaced every 3-4 weeks and is made up of five distinct layers. These are:

- Stratum basale (basal cell layer)

Stratum basale (the innermost layer of the epidermis) is composed of a single layer of columnar or cuboidal keratinocytes that are attached to the basement membrane via hemidesmosomes. These keratinocytes are mitotically active and can proliferate. These cells detach from the basement membrane and move further up the surface of the skin to the spinous layer where they are terminally differentiated. In the stratum basale one can find melanocytes, Langerhans and Merckel cells.

- Stratum Spinosum (spinous layer or suprabasal layer)

Stratum spinosum consists of 8-10 layers (humans, 1-2 layers in the mouse) of irregularly polygonal flattened cells. These cells are alive and are separated by clefts that are spanned by spine like cytoplasmic extensions of cells.

- Stratum Granulosum (granular layer)

Stratum granulosum consists of 3-5 layers (humans, 1-2 layers in mouse) of flattened polygonal cells with disintegrating nuclei. These cells accumulate keratohyalin granules. They also contain lamellar granules that shed their lipid contents into the interstitial space and form a seal that prevents entry of water or foreign objects in the skin. The cells of this layer are not dividing.

- Stratum Lucidum

Stratum lucidum is a translucent, thin layer of extremely flattened dead cells. In some cells the nuclear outline may be slightly visible but most of these cells are enucleated. Only the intermediate filaments and desmosomes are retained.

- Stratum Corneum (cornified layer)

The stratum corneum consists of 25-30 (human, 10 layers in mouse) layers of dead, enucleated, flattened, keratinised cells. The cells closer to the surface of the epidermis are loosely connected to each other and are constantly shed from the skin in a process called desquamation.

The epidermis is constantly in a state of dynamic equilibrium and growth and differentiation must be tightly regulated in order for this equilibrium to function properly. Increase in the number of dividing cells can lead to epidermal hyperproliferation and disorders such as psoriasis, and basal- and squamous-cell carcinomas. On the other hand, premature differentiation can lead to very thin skin. The epidermis is also receiving signals that affect its homeostatic control from the underlying dermis. Therefore, when one studies epithelial abnormalities all these factors must be taken into account.

One of the important roles of keratinocytes within the epidermis is to produce different keratins. There are two types of keratins; type I are acidic (pKi = 4.5-5.5) and small (40-56.5kDa) whilst type II are basic (pKi = 5.5-7.5) and larger (53-67kDa). The keratins form heterodimers of these two types. About 20,000 pairs assemble into an intermediate filament that give the epidermis its structure. At the different layers of the epidermis different keratin

pairs are expressed. In the basal layer only keratins 5,14 and 15 are expressed. As the cells enter the suprabasal layer, expression of these keratin pairs is downregulated and other keratin pairs such as keratins 1, 10 and 11 are expressed. In response to injury, retinoic acid treatment or hyperproliferative diseases like cancer, the subbasal layer can produce keratins 6 and 16 (K16 has no murine homologue). Therefore keratin pairs can serve as markers of proliferation or differentiation (Fuchs, 1995; Fuchs and Byrne, 1994; Fuchs and Raghavan, 2002).

The other components of the skin are the epidermal appendages which are derived from the epidermis and include hair follicles, sebaceous glands, eccrine, apocrine glands, nails and teeth. Their function is to protect the skin and to regulate skin homeostasis.

LMP1 transgenic models

With the above in mind, several transgenic mice were created in order to study the role of LMP1 in carcinoma genesis and progression.

The first series of mice were created using the Py promoter to direct expression of the LMP1^{B95-8} to the epidermis. 12 founders were created that gave rise to 9 lines. Out of these, 2 lines expressed the LMP1 in the epidermis and these were lines 5 and 53 (Wilson et al., 1990). Line 5 showed high levels of LMP1 expression but also showed insertional mutation that led to line extinction. Line 53 showed a lower LMP1 expression and was viable and therefore subsequent studies were performed using line 53. Transgenic pups of this line are slightly smaller initially than their wild type siblings and also show an epidermal hyperplasia that is most evident from day 3 to day 7 (fig.1.12). They also show a delay in eye opening and fur growth. These phenotypes resolve as the mouse matures and are not evident in adults of the line. The adults show a progressive increase in claw growth and in the C57BL/6 strain, a colour coat change from black to patches of ginger as they age. Expression analysis performed on tissues of mice of this line and line 5 showed that the transgene was expressed in the skin both at the mRNA and protein level and at low levels in the tongue. Consistent with hyperplasia, keratin 6 and 14 levels (proliferation markers) in the skin of transgenic mice were upregulated by 2.5 times compared to wild type sibling skin in line 53 (higher in line 5) (Curran et al., 2001; Wilson et al., 1990). In further studies in which these mice (in FVB strain) were treated with topical chemical carcinogens, the transgenic mice developed more papillomas than the wild type siblings and it was shown that LMP1 could augment the activity of TPA (Curran et al., 2001). However, growth expansion of these small papillomas into larger lesions was inhibited in the LMP1 expressing mice. When these mice were bred into an

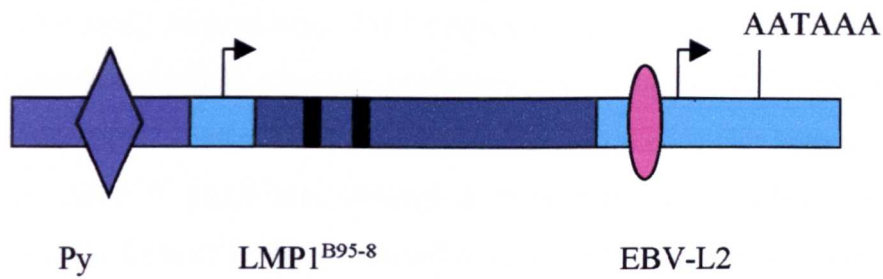


Figure 1.12a: Construct used to generate line 53

The purple rectangle and diamond represent the polyoma enhancer and promoter, the turquoise coloured area represents EBV sequence, the blue area represents the LMP1^{B95-8} sequence. The black bars represent the two introns found in the LMP1 gene. The pink oval represents the EBV-L2 promoter.

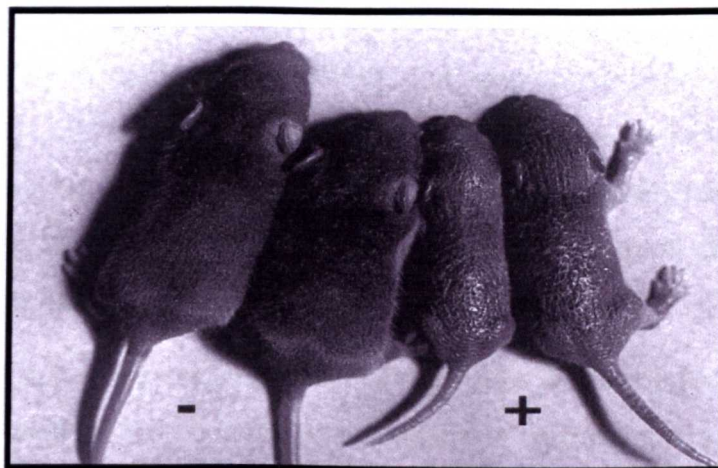


Figure 1.12b: Phenotype of line 53 pups

In the above picture, 4 pups of line 53 are shown. The two on the left are wild type (-) whilst the two on the right are transgenic (+) for LMP1^{B95-8}, as indicated. The pups shown above are 3-7days old and the transgenic ones are smaller than their wild type siblings, showing epidermal hyperplasia.

INK4a null background, the growth inhibition was removed, demonstrating that the LMP1 induced inhibition of lesion growth was mediated by products of the INK4a locus (p16^{INK4a} and/or p19^{ARF}). Loss of INK4a also promoted carcinoma progression (Macdiarmid et al., 2003). This study showed that LMP1 plays a role in the early stages of tumourigenesis, acts as a promoter and exerts a growth inhibitory effect via p16^{INK4a} and/or p19^{ARF} and therefore implies that LMP1 is not sufficient to inhibit expression of one or both of these products.

Since the LMP1^{CAO} strain was isolated from an NPC and has been postulated to be more oncogenic, this form of LMP1 was used to create further transgenic lines in order to explore its activity *in vivo*. The LMP1^{CAO} gene (Hu, 1991) was expressed under the control of the EBV ED-L2 promoter to drive expression of LMP1^{CAO} in the epithelium (Stevenson *et al*, in press)(fig.1.13). 5 lines of mice were created. These were lines 104, 117, 105B, 105A and 106, the strength of phenotype indicated according to their order. For example, line 104 showed the strongest expression and more intense phenotype and all the mice of this line died before further breeding. Line 106 had little or no phenotype. Here I will describe only the lines that have been used in this PhD study: lines 117, 105A and 105B. Line 117 and 105B transgenic animals show extensive epidermal hyperplasia on the ears and the tail with evident vascularisation as adults. The ear phenotype progressively worsens with age. For the purpose of the study described in this thesis, the progressive phenotype was categorised in stages (fig.1.14). When line 117 and 105B were bred into the FVB background, the transgenic animals started developing dorsal papillomas spontaneously (see fig.1.15).

Line 105A animals do not show any hyperplastic epidermal phenotype but develop a wasting phenotype starting at around 1 year or older.

Note that due to the importance of the strain variation in epithelial carcinogenesis, all line 117 animals used in the chemical carcinogenesis experiments and the spontaneous papilloma studies were mostly in FVB strain (backcross 5 or 6, the original strain being C57BL/6). However, the cross of line 117 to 125 mice was in a mixed strain background (FVB/129/C57) as the line 125 animals were in a mixed 125/C57 strain.

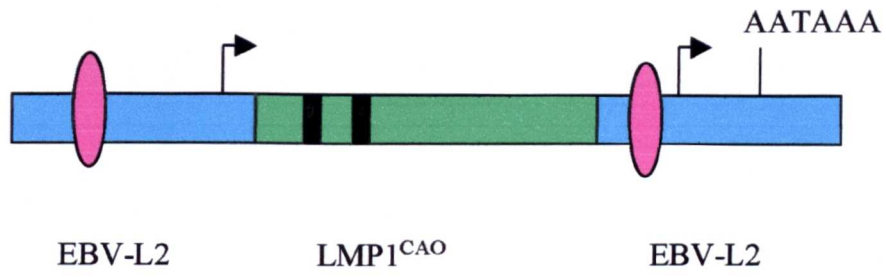
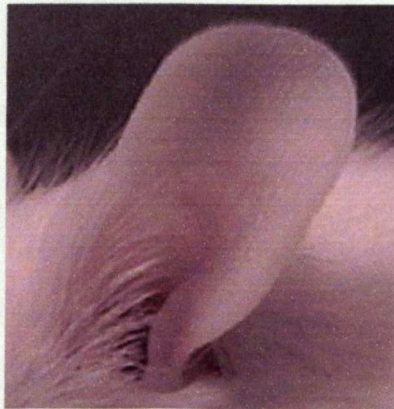


Figure 1.13: Construct used to generate lines 117, 105A and 105B

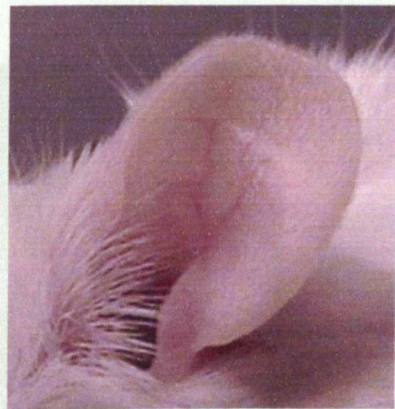
The pink oval represents the EBV-L2 promoter. The blue rectangle represents EBV sequence. The green rectangle represents LMP1^{CAO} sequence. The black bars in the green rectangle represent the two introns of the LMP1^{CAO} gene.

Figure 1.14: Ear phenotype of line 117 mice

The top left corner shows an ear from a wild type mouse of same age and strain to the L2LMP1^{CAO} transgenic ear shown on the top right corner. Stage 1 transgenic ear, is showing vascularisation when compared to the wild type ear, whereas stage 2 shows hyperplasia, stage 3 ear shows the beginning of necrosis and stages 4 and 5 transgenic ears show extensive ulceration and necrosis like a keratoacanthoma and can progress to carcinoma. The approximate age at which the specific phenotype is observed is given.



wild type ear



stage 1 ear (4 weeks old)



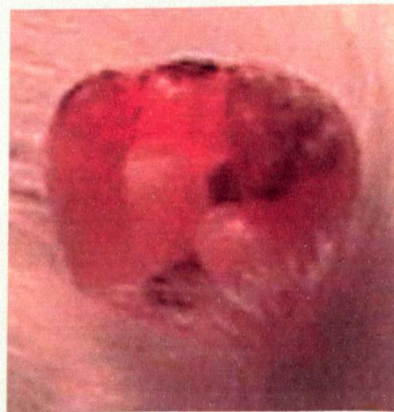
stage 2 ear (8 weeks old)



stage 3 ear (4-6 months old)



stage 4 ear (7-12 months old)



stage 5 ear (10 months or older)



Figure 1.15: Phenotype of a 117 mouse bred into the FVB background

This mouse is backcross 3 into FVB background (87.5% FVB). At least 6 spontaneous papillomas have developed on its back at sites not related with mechanical irritation (figure from Stevenson *et. al.*, in press).

1.10 Aims

The purpose of my thesis was to investigate the role LMP1 plays in the onset and progression of carcinoma *in vivo*, using the transgenic mouse models. The investigation was subdivided into the following analyses:

- (1) To characterise the expression patterns of LMP1^{CAO} in the transgenic lines generated and evaluate whether the observed phenotypes correlate with the expression patterns.
- (2) To investigate the action of LMP1 in conjunction with loss of the INK4a locus in order to explore cooperative effects.
- (3) To test the hypothesis that LMP1 exerts its oncogenic action via upregulation of TGF α , a ligand of EGFR. It is known that EGFR is upregulated by LMP1 in epithelial cells and that it is also found upregulated in NPC biopsies. Upregulation of an EGFR ligand could lead to faster cycling of the receptor and thus increased activation of the pathways affected by EGFR. One such pathway is the Ras/MAPK pathway. The effect LMP1 has on this pathway was explored.
- (4) To examine the status of other signalling pathways known to be affected by LMP1 in B cells. LMP1 plays a role in many cellular processes and it was important to dissect which pathways are impacted in the tissues and therefore which may be responsible for the induced phenotype and thus which might be implicated in NPC development.

Chapter 2: Materials and Methods

2.1 Materials

Chemicals were purchased from Sigma except where stated otherwise. Tissue culture reagents were from GibcoBRL.

2.1.1 Antisera

Table 2.1: Primary Antibodies Used

Antibody/Control/Hybridoma Cell Supernatant	Supplier/ref.	Catalogue Number	Species	Dilution used	Protein size kDa
Phospho-Akt (Thr308)	Cell Signaling	9275	Rabbit	1:1000	60
Phospho-Akt (Ser473)	Cell Signaling	9271	Rabbit	1:1000	60
Total Akt	Cell signaling	9272	Rabbit	1:1000	60
Cleaved caspase-3	Cell Signalling	9661	Rabbit	1:1000	17, 19
Total caspase-3	Cell Signalling	9662	Rabbit	1:1000 (Western) 1:50 (IHC)	35,17, 19
Phospho-p38	Promega	V121A	Rabbit	1:1000	38
Cyclin A	Santa Cruz	sc-751	Rabbit	1:1000	50
Cyclin B1	Santa Cruz	sc-752	Rabbit	1:1000	50-55
Cyclin D1	Cell Signalling	2926	Rabbit	1:1000	36
Elk-1	Santa Cruz	sc-355	Rabbit	1:1000	62
Phospho-EGFR (Tyr845)	Cell Signaling	2231	Rabbit	1:1000	170
Phospho-EGFR (Tyr1068)	Cell Signaling	2234	Rabbit	1:1000	170
Total EGFR	Cell Signaling	2232	Rabbit	1:1000	170
Phospho-ERK1/2 (Thr202/Tyr204)	Cell Signaling	9101	Rabbit	1:1000	44, 42
Total ERK1/2	Cell Signaling	9102	Rabbit	1:1000	44, 42
Fra-1	Santa Cruz	sc-183	Rabbit	1:1000	42
Fra-2	Santa Cruz	sc-604	Rabbit	1:1000	43
c-fos	Santa Cruz	sc-253-G	Rabbit	1:1000	62
FosB	Santa Cruz	sc-48X	Rabbit	1:1000	36
Phospho-GSK3 β	Cell Signaling	9336	Rabbit	1:1000	46

Phospho-HER2 (Tyr1112)	Cell Signaling	2245	Rabbit	1:1000	185
JunB	Santa Cruz	sc-46X	Rabbit	1:1000	45
c-Jun	Santa Cruz	sc-45X	Rabbit	1:1000	39
LMP1 (1G6)	(Nicholls et al., 2004)		Rat	1:100	60
LMP1 (S12)	(Mann et al., 1985)		Mouse	200µl (IP) 1:500 (Western)	63
LMP1 (CAO) cocktail	(Nicholls et al., 2004)		Rat	1:100	66
Phospho-MEK1/2 (Ser217/221)	Cell Signaling	9121	Rabbit	1:1000	45
Total MEK1/2	Cell Signaling	9122	Rabbit	1:1000	44, 42
NF-κB p50	Santa Cruz	sc-1190	Goat	1:1000	50
NF-κB p65	Santa Cruz	sc-372	Rabbit	1:1000	65
PCNA	Novocastra	NCL-PCNA		1:50 (IHC)	36
Phospho-PTEN	Cell Signaling	9551	Rabbit	1:1000	54
p53	Santa Cruz	sc-1312	Goat	1:1000	53
p16	Santa Cruz	sc-1207	Rabbit	1:1000	16
B-Raf	Santa Cruz	sc-9002	Rabbit	1:1000	95
Phospho-c-Raf	Cell Signaling	9421	Rabbit	1:1000	74
c-Raf-1	Santa Cruz	sc-227	Rabbit	1:1000	74
Rassf 1	Santa Cruz	sc-18724	Goat	1:1000	43
Total Rb	Santa Cruz	sc-50	Rabbit	1:1000	110
Phospho-Rb	Cell Signaling	9307	Rabbit	1:1000	110
Phospho-SAPK/JNK	Cell Signaling	9251	Rabbit	1:1000	54, 46
Phospho-SEK1/MKK4	Cell Signaling	9151	Rabbit	1:1000	46
β tubulin	Santa Cruz	sc-9935	Rabbit	1:500	54
TACE	Santa Cruz	sc-13973	Rabbit	1:1000	74
TGFα	Santa Cruz	sc-9043	Rabbit	1:1000	11

Table 2.2: Secondary Antibodies used

Goat anti-rabbit IgG-HRP	Santa Cruz	sc-2030	1:4000
Donkey anti-goat IgG-HRP	Santa Cruz	sc-2020	1:4000
Goat anti-mouse IgG-HRP	Santa Cruz	sc-2031	1:4000
Goat anti-rat IgG-HRP	Santa Cruz	sc-2032	1:4000

2.1.2 Oligonucleotides

Table 2.3: Factor Binding Sites

OLIGONUCLEOTIDE NAME AND COMPANY	SEQUENCE
ETS (Santa Cruz)	5'-GGG CTG CTT <u>GAG GAA</u> GTA TAA GAA T-3'
NF-κB Forward (Sigma Genosys)	5'-G AGC AGT TGA <u>GGG GAC TTT CCC</u> AGG C-3'
NF-κB Reverse (Sigma Genosys)	3'-TCA ACT CCC CTG AAA GGG TCC GGA TG -5'
SRE Forward (Sigma Genosys)	5'-GAG CGG ATG <u>TCC ATA TTA</u> GGA CAT CT-3'
SRE Reverse (Sigma Genosys)	3'-CCT ACA GGT ATA ATC CTG TAG AGA TG-5'
SRE (Santa Cruz)	5'-GGA TGT <u>CCA TAT TAG</u> GAC ATC T -3'
TRE Forward (Sigma Genosys)	5'-G AGC CGC TTG <u>ATG ACT CAG</u> CCG GAA- 3'
TRE Reverse (Sigma Genosys)	3'-GCG AAC TAC TGA GTC GGC CTT GAT C-5'

Table 2.4: PCR oligos

PCR FRAGMENT	PRIMER NAME	PRIMER SEQUENCE
Neomycin	Neo Forward	5'- TGA ATG AAC TGC AGG ACG AGG- 3'
	Neo Reverse	5'- AAG GTG AGA TGA CAG GAG ATC- 3'
p16 exon 2	p16 Forward	5'- GTG ATG ATG ATG GGC AAC GT- 3'
	p16 Reverse	5'- CTG GGC GAC GTT CCC AGC GG- 3'
TGF α exon 3	TGF α KO1	5' -GAC TAG CCT GGG CTA CAC GT G- 3'
	TGF α KO2	5' -CCG CTT CCT CGT GCT TTA CGG T- 3'
	TGF α KO3	5'- ACA TGC TGG CTT CTC TTC CTG C- 3'
v-H-ras	v-H-ras Forward	5'- GGA TCC GAT GAC AGA ATA CAA GC- 3'
	v-H-ras Reverse	5'- ATC GAT CAG GAC AGC ACA CTT GCA- 3'
c-H-Ras	c-H-ras Ex2A	5'- CTA AGC CTG TTG TGT TTT GCA GGA C- 3'
	c-H-ras Ex2B	5'- GCT AGC CAT AGG TGG CTC ACC GT- 3'
LMP1	DS1	5'- ATG GAA CAC GAC CTT GAG AG- 3'
	DS2	5'- TAG GCC TTG CTC TCC TTC TC- 3'
	DS3	5'- AGA TGG TGG CAC CAA GTC GC- 3'
	DS4	5'- GAA GAA GGC TAG GAA GAA GG- 3'

2.1.3 Cell Lines

All cell lines were developed from carcinomas following topical DMBA/TPA carcinogen treatment of transgenic positive and negative mice as listed.

Table 2.5: Cell lines and their transgenic status

Cell Line	Description	LMP1 Transgenic status
CarB	Spindle (NIH mouse carcinoma)	-
53.217	Cuboidal	-
117.30	Spindle	-
105.60	Spindle	-
105.113	Spindle	-
53.278a	Spindle	+
53.278b	Spindle	+
53.279	Cuboidal	+
53.234a	Cuboidal	+
53.191	Cuboidal	+
53.220	Cuboidal	+
53.226a	Cuboidal	+
105.92	Cuboidal	+

2.1.4 Frequently used solutions

Church buffer (pH7.2)	1%(w/v) BSA 1mM EDTA 500mM NaPO ₄ 7%(w/v) SDS
Denaturing Solution	0.6M NaCl 0.4M NaOH
0.5% Dispase	0.5%(w/v) Dispase in PBS
10x ETS binding buffer	10mM Tris-HCl pH7.5 50mM KCl 5mM MgCl ₂ 1mM EDTA pH8.0 12.5% (v/v) glycerol 0.1% Triton X 1mM DTT
2FC	49.45%(v/v) Chloroform 0.1%(w/v) 8-hydroxyquinoline 1%(v/v) Isoamyl Alcohol 49.45% Buffer Saturated Phenol
4M GT	250g guanidium thiocyanate 293ml dH ₂ O 17.6ml 0.75M sodium citrate, pH 7.0 26.4ml 10% sarcosyl
High Salt buffer (EMSA)	20mM Hepes pH7.9 0.4M NaCl 1mM EDTA pH8.0 1mM DTT 1mM PMSF Vanadate Aprotinin Protease inhibitor

Buffered Neutral Formalin	50ml of 40%(v/v) Formaldehyde 1.75g NaH ₂ PO ₄ 3.25g Na ₂ HPO ₄ dH ₂ O up to 500ml
10x Loading dye (DNA or RNA)	50%(v/v) Glycerol 0.1%(v/v) Bromophenol Blue 0.1%(w/v) Xylene Cyanol in TE pH7.5 (DEPC-treated for RNA)
10x Loading buffer (RNA)	100µl 10x MOPS (0.001M) 500µl pure deionised formamide 178µl formaldehyde pH4.0 22µl DEPC-treated H ₂ O
10x MOPS-E	200mM MOPS 10mM EDTA 50mM NaOAc pH7.0 in dH ₂ O pH7.0 wrap in foil and autoclave
PBS	2.7mM KCl 1.4mM KH ₂ PO ₄ 137mM NaCl 4.3mM Na ₂ PO ₄ pH/HCl/7.3
Protein Blocking buffer	5%(w/v) milk powder TBST
Protein Blotting buffer	25mM Tris 192mM Glycine 20%(v/v) Methanol (analytical grade)
2x Protein Gel Sample buffer (GSB)	125mM Tris-HCl, pH6.8 20%(v/v) Glycerol 10%(v/v) Sodium 2-Mercaptoethanol 4%(w/v) SDS 0.004%(w/v) Bromophenol Blue
4x Protein Gel Sample buffer (GSB)	200mM Tris-HCl, pH6.8 30%(v/v) Glycerol 8%(w/v) SDS 10%(v/v) Sodium 2-Mercaptoethanol 0.04%(w/v) Bromophenol Blue
Protein MENSA buffer	62.5mM Tris-HCl, pH6.8 2%(w/v) SDS 50mM Sodium 2-Mercaptoethanol
Protein extraction: NET-N buffer	150mM NaCl 5mM EDTA pH8.0 50mM Tris-HCl pH8.8 0.05%(v/v) NP40

Protein extraction: Ripa buffer	150mM NaCl 5mM EDTA pH8.0 20mM Tris-HCl pH7.5 0.5%(w/v) Deoxycholic Acid 1.5%(v/v) NP40 0.1% SDS
8M Urea buffer	8M urea 5% (v/v) Sodium 2-Mercaptoethanol 25mM Tris, pH9.5
Protein SDS-PAGE Running buffer	50mM Tris 380mM Glycine 0.1%(w/v) SDS
10x Santa Cruz binding buffer	100mM Tris pH7.5 500mM NaCl 10mM DTT 10mM EDTA pH8.0 50%(v/v) glycerol
Southern Stripping Solution A	0.1x SSC 0.5% SDS
Southern Stripping Solution B	0.1x SSC 0.1% SDS
Southern Washing Solution A	2x SSC 0.1% SDS
Southern Washing Solution B	0.1x SSC 0.1% SDS
Solution D	0.36ml Sodium 2-Mercaptoethanol 50ml 4M GT
2x Sp1 binding buffer	30mM Hepes pH7.5 8mM MgCl ₂ 1.2mM EDTA 20% (v/v) glycerol dH ₂ O
2/3x SRE binding buffer	10mM Hepes pH7.9 2mM EDTA pH8.0 1M NaCl 1mg/ml BSA 10%(v/v) glycerol
20x SSC	150mM NaCl 150mM Tri-Sodium Citrate
STE buffer	1mM EDTA 10mM NaCl 10mM Tris-HCl pH7.5
TAE (50x stock solution, 1 litre)	5.71% (v/v) Glacial Acetic Acid 100mM EDTA 2000mM Tris-HCl pH8.5

Tail Solution	100mM EDTA pH8.0 150mM NaCl 1%(w/v) SDS 10mM Tris-HCl pH7.5
TBE(10x stock solution, 1litre)	890mM boric acid 4% (v/v) 0.5M EDTA pH8.0 890mM Tris
TBS	140mM NaCl 20mM Tris
TBST	140mM NaCl 20mM Tris 0.1%(v/v) Tween-20
TE	1mM EDTA pH8.0 10mM Tris-HCl pH8.0
Trypsin Solution	25%(v/v) Trypsin 0.02%(v/v) Versene
Versene	0.54mM EDTA 2.7mM KCl 1.4mM KH ₂ PO ₄ 137mM NaCl 4.3mM Na ₂ PO ₄ pH/HCl/7.3

2.1.5 Frequently used growth media

Agar Plates	250ml dH ₂ O 10g Tryptone Oxoid L42 5g Yeast Extract (Oxoid) 10g NaCl make up to 1L with dH ₂ O pH7.54 (NaOH)
Luria-Bertani (LB)	1% (w/v) Bacto-tryptone 0.5% (w/v) Bacto-yeast extract 1% (w/v) NaCl
Complete Tissue Culture Medium	DMEM medium 5-20% (v/v) FCS 2% (v/v) L-glutamine (200mM stock) 2% (v/v) Penicillin/Streptomycin (10000U/mL stock)
Freezing Medium	Per ml of medium added 920µl FCS 80µl DMSO

2.2 Methods

2.2.1 Animal procedures

All mouse procedures were conducted in accordance with the Home Office regulations and as detailed in the covering project licence. Unless otherwise stated, the procedures were conducted by me, or the animal technicians (where indicated) as covered by my Home Office

personal licence. Where the use of brief anaesthesia was required, a halothane/oxygen mixture was used in an anaesthesia chamber.

A) Breeding and record keeping of transgenic mice

All food, water and bedding requirements were handled by the animal technicians. Litters were monitored by the animal technicians and all animals were regularly health checked. Usually, at three weeks of age the mice were weaned and males and females separated. The mice were given consecutive numbers for each line. The mice were anaesthetised using halothane/oxygen before being numbered by ear punching. A small tail biopsy was taken (a tail tip of 0.5cm) and the mouse tail was cauterised with a hot iron to prevent bleeding and sterilize the wound. The tail tip was used to extract DNA and analyse the transgenic status of the animal by Southern blotting or PCR. In mice of several transgenic lines that developed a serious ear phenotype the animals were not ear punched. Instead, the scruff of the neck was shaved, the animal anaesthetized and a microchip was injected subcutaneously. The microchip had a unique six-digit identification number that could be read with an appropriate reader (microchips obtained from MID-FingerPrint Ltd cat. no: ID100 transponders).

B) Animal health

Animal health was monitored in accordance with procedures described in the Home Office project licence. All animals were monitored regularly for signs of ill health and discomfort. Animals which were subject to the development of lymphomas, hind paralysis and excessive papilloma growth and conversion to carcinomas were monitored at least once a week. Any animal suffering or deviating from the health status outlined in the UK guidelines for the use of experimental animals was euthanised without delay.

C) Mouse lines

Line Number	Transgene	Expression	References
53	PyLMP1 ^{B95-8}	LMP1 expressed in the epithelium	(Wilson et al., 1990)
113	Neomycin cassette has replaced exons 2 and 3 of INK4a locus	p16 ^{INK4a} not expressed p19 ^{ARF} truncated mRNA	(Serrano et al., 1996)
117	L2LMP1 ^{CAO}	LMP1 ^{CAO} expressed in the epithelium and some lymphoid tissues	Stevenson <i>et al.</i> , (in press)
1205	HK1-H-ras	H-ras expressed in the basal layer of the epidermis	(Wang et al., 2000)
125	Neomycin cassette replaced exon 3 of TGF α gene	No TGF α expression	(Mann et al., 1993)

Table 2.6: Mouse lines used

Offspring from cross breeds are indicated eg. as 117/113 indicating that line 117 has been crossed to line 113.

D) Sample collection from mice

Animals were euthanased by a schedule 1 method according to Home Office guidelines.

D.1 Dispase epidermis separation

Mouse pups 3-7 days old were euthanased, and immediately placed in a 7ml sterile plastic Bijoux and stored on ice. The limbs and tail were amputated and stored for subsequent DNA extraction and identification of transgene status. The body was rinsed in 70% ethanol and dried with a tissue. The skin was removed in a single sheet by a ventrical longitudinal excision. If total skin was needed, then it was snap frozen in liquid nitrogen. For epidermal separation, the skin sample was floated dermis side down on a 0.5% dispase solution in a 5cm petri dish (if samples were to be used for RNA extraction, ribonucleoside vanadyl complexes (RVC) Sigma cat no: R3380, was added to the 0.5% dispase solution. RVC inhibits RNase A activity but not DNase I). The sample was incubated at 4°C overnight. The skin was then placed on a dry sterile petri dish epidermis side down, so that the epidermis could adhere to the plastic. The thicker dermis was then removed from the epidermis with forceps leaving the

thin, translucent epidermis on the plate. The separate epidermal and dermal samples were placed in screw cap Nunc tubes and snap frozen in liquid nitrogen and stored indefinitely at -70°C (Macdiarmid and Wilson, 2001).

D.II Removal of papillomas and carcinomas

The fur of the euthanased animal was wetted in 70% ethanol. Using surgical tweezers and scissors the area around the lesion was cleared of fur and the lesion was excised removing any excess skin. Part of the lesion was placed in 10% buffered neutral formalin fixative and the remainder was placed immediately in a screw cap Nunc tube and snap frozen in liquid nitrogen and stored at -70°C . A sample of tail tissue was also taken from each animal for confirmation of transgene status if needed.

D.III Removal of internal tissues

Following incision of the abdomen, any peripheral lymph nodes were collected and the layer of skin was pulled back and internal organs were revealed. The organ of interest was then excised and if necessary washed in 1xPBS and snap frozen in liquid nitrogen and stored at -70°C or fixed in 10% neutral buffered formalin for subsequent pathological analysis.

E) Chemical Carcinogen Treatment of mice

Mice that were treated with chemical carcinogens were dorsally shaved the day before application of the agent. TPA was kept as a 40x stock (1.25mg/ml) dissolved in acetone at -20°C . The working solution was 1x (31.25 $\mu\text{g}/\text{ml}$) and was made by dissolving the 40x solution in appropriate amounts of acetone. The 1x solution was also kept at -20°C in a glass universal wrapped in aluminium foil. 200 μl of 1x TPA solution was applied to the shaved back of each mouse. The procedure was performed in a ventilated sink, wearing all the appropriate protective clothing and double gloves. The mice were left in their cage in the ventilated sink for 45 min. after treatment so that the acetone would evaporate and were then caged in a dedicated room for chemically treated animals in filter top cages. TPA application was performed according to a minimal regime of twice a week for four weeks. The mice were observed once every week and appearance and size of any papillomas or carcinomas was recorded.

F) Papilloma monitoring of mice

Lines 117, 117/113 and 117/113/1205 developed acanthomas or papillomas spontaneously in the FVB strain. The lesion number and size was monitored usually by touch once every two weeks. Lesions were observed from the start of the study until the animal was removed from the study. A lesion was classified as papilloma if it was raised above the surface of the skin (although several were later characterized as acanthomas). Visually papillomas look like cauliflower-type warts. Carcinomas were classified by eye, since they have a smoother, firmer appearance than papillomas and do not “wobble”. Subsequently, lesions were examined by histopathological analysis. Lesions were categorized subjectively by size according to the following specifications:

Category	Approximate Lesions Diameter
Size 1	<0.2cm
Size 2	0.2cm-0.5cm
Size 3	0.5cm-1.0cm
Size 4	>1.0cm

Table 2.7: Lesion sizes

Mice were taken off the study and euthanased according to the project license, when their lesion load reached a maximum, or when a single papilloma or carcinoma had reached a diameter of 1cm, or had become ulcerated or when a lesion occurred at an orifice or a site of irritation. Mice were also removed from the study if they were generally unhealthy.

G) Ear Monitoring of mice

The ear phenotype of line 117/125 was monitored once a week. The mice were visually observed and their ear phenotype was compared to a chart containing the different stages of ear phenotype as observed in line 117 (fig.1.14). The study was performed blind without knowledge of the genotype of the animal.

2.2.2 Bacterial cell culture techniques

A) Bacterial cell culture

All plasmid propagation was performed in the *E.coli* strain DH5. Plasmids containing *E.coli* clones were stored as viable glycerol stocks at -70°C. *E.coli* was cultured by taking about 1ml of the relevant glycerol stock and adding it to 2.5ml of LB medium, supplemented with 50mg/ml ampicillin. The culture was incubated overnight at 37°C, with constant shaking. If a

single sub-clone was required, the culture was then streaked onto an agar plate containing 50mg/ml ampicillin, and incubated overnight at 37°C. A single colony was then picked with a sterile toothpick and used for subsequent propagation.

B) Transformation

DH5 competent cells as prepared by the laboratory technician were used. 200ml of competent cells were thawed on ice for 10 min. 100ng plasmid DNA was added and the cells were incubated on ice for 15 min. They were heat shocked for 90 sec. at 42°C and left on ice for 1-2 min. Warm (37°C) LB (500ml) with no antibiotics was added and the cells were incubated at 37°C with gentle shaking for 20 minutes. This step allows for recovery of the bacteria and plasmid gene expression. The cells were centrifuged at 9,000 xg for 1 min. and most of the medium was removed. 10ml was plated on one agar plate and the remainder (about 90µl) on another, which were incubated overnight at 37°C. The following day, distinct colonies from each plate were picked and inoculated in 10ml of L-broth containing 10ml ampicillin overnight at 37°C with gentle shaking.

2.2.3 DNA techniques

A) Small scale extraction of plasmid DNA

The Sigma Plasmid Miniprep DNA purification kit was used for small scale plasmid DNA isolation according to the manufacturer's protocol. It is based on a modified alkaline-SDS lysis procedure (Birnboim and Doly, 1979) followed by adsorption of the DNA on silica in the presence of high salts.

A colony of the desired plasmid containing bacteria was picked and inoculated overnight in 5ml of selective LB with vigorous shaking. The bacteria were then harvested in a pellet by centrifugation at 12,000 xg for 1min. and resuspended in 200µl of resuspension buffer. After that 200µl of lysis buffer, containing SDS-NaOH was added. The SDS solubilises the cell membrane thus leading to lysis of the bacterial cell and release of the cell contents. The NaOH denatures chromosomal and plasmid DNA. The mixture is neutralized by addition of 350µl of the neutralization solution containing acidic potassium acetate causing the covalently closed plasmid to reanneal and remain in solution whilst the high salt concentration leads to SDS, chromosomal and bacterial protein-salt complexes that precipitate and are removed by centrifugation at 12,000 xg for 10min. The plasmid DNA is allowed to bind onto the silica matrix of the column whilst debris is washed away by addition of 750µl of wash solution and elution takes place in 100µl of water or Tris-EDTA buffer.

B) Large scale extraction of plasmid DNA

The Quiagen Plasmid Maxiprep DNA purification kit was used for large scale plasmid DNA isolation as per manufacturer's protocol. It is based on a modified alkaline-SDS lysis procedure followed by adsorption of DNA on an anion-exchange resin under low salt and appropriate pH conditions (Birnboim and Doly, 1979). The same principles apply as in section 2.2.3A. As before, a colony with the plasmid containing bacteria was picked and inoculated in 5ml of selective LB. The 5ml culture was subsequently added to 200ml of selective LB and inoculated overnight. The bacteria were harvested into a cell pellet in a 250ml Nalgene tube by centrifugation at 6,000 xg for 15min. at 4°C (in a Beckman JA-14 rotor). After centrifugation, the plasmid DNA was resuspended in 20ml of buffer P1 (50mM Tris-HCl, pH 8.0, 10mM EDTA, 100µg/ml RNase A) and lysed in 20ml of buffer P2 (200mM NaOH, 1%SDS (w/v)) by inverting the Nalgene tube 4-6 times. The lysate was neutralized by addition of 20ml of chilled buffer P3 (3.0M potassium acetate, pH 5.5) and chilled on ice for 20min. A fluffy, white precipitate consisting of genomic DNA, proteins, cell debris and SDS was formed. The lysate was centrifuged at 20,000 xg for 30min. at 4°C and was then passed through a column that had been equilibrated with buffer QBT (750 mM NaCl, 50mM MOPS, pH 7.0, 15% isopropanol (v/v), 0.15% Triton-X (v/v)). The lysate was allowed to bind the Quiagen Resin whereas debris, cellular proteins and degraded RNA flowed through. The column was washed twice with 30ml of buffer QC (1.0M NaCl, 50mM MOPS, pH7.0, 15% isopropanol (v/v)). 30ml of the high salt buffer QF (1.25M NaCl, 50mM Tris-HCl, pH 8.5, 15% isopropanol (v/v)), was used to elute the plasmid DNA from the column and the plasmid was desalted by isopropanol precipitation (0.7 volumes ie 21ml). The DNA pellet was washed with 10ml of 70% ethanol and dried by centrifugation at 15,000 xg for 10min. The DNA was air dried and resuspended in a suitable volume (usually 100µl) of water, TE pH, 8.0 or 10mM Tris-HCl, pH 8.5. The columns used contain positively charged diethylaminoethanol (DEAE) groups that interact with the negatively charged phosphate backbone of the DNA. Elution of plasmid DNA takes place in high salt buffers during which the cations of the column are occupied by anions provided by the high salt buffer.

C) Purification of plasmid DNA by caesium chloride (CsCl) gradient

Plasmid DNA was added to a solution of CsCl and ethidium bromide (EtBr)(2.1ml plasmid DNA, 270ml of 15mg/ml EtBr, 5g CsCl, 3ml TE buffer) and centrifuged for 20 hrs at 49K in a Ti70 rotor. The EtBr forms a complex with protein that shows up as a red precipitate at the

top of the tube. Supercoiled plasmid DNA forms a band in the middle of the tube, where its density equals that of the CsCl gradient. Chromosomal DNA forms a band above the supercoiled DNA band. The supercoiled DNA was extracted with a syringe, and if required added to a second CsCl gradient, and further centrifuged for 20hrs. A clearer band was visible in the middle of the tube which was extracted with a syringe. The EtBr was removed by adding TE/butan-1-ol saturated. EtBr goes in the organic phase and can be removed. The aqueous phase was repeatedly extracted in this way until there was no red colour indicating that all the EtBr had been removed. The DNA was precipitated by adding 2 volumes of 100% EtOH at room temperature.

D) Extraction of genomic DNA

Phase Lock Gel™ tubes (supplier VWR cat. no: 427353P) were used to extract protein from mouse tissue, tail segments and cell pellets. Phase Lock Gel™ tubes contain a quantity of Phase Lock Gel™ that effectively separates organic phenol and interphase from the aqueous layer. This is due to the density of the Phase Lock Gel™ which is higher than the aqueous layer and lower than the organic layer. The tissue samples were digested by adding 700ml of tail solution (2.1.4) and 35ml of Proteinase K (10mg/ml), and shaking overnight at 55°C in an Eppendorf thermomixer. The Phase Lock Gel™ tubes were briefly centrifuged and the digested sample was added to them. The proteins were extracted by adding 750 ml of 2FC, shaking the samples vigorously about 20 times and then centrifuging for 15 min. at 18,000 xg in a Beckman microcentrifuge. Phenol is used to extract proteins and chloroform to stabilise the boundary between aqueous and organic layer. Phenol is trapped under the gel of the Phase Lock Gel™ tubes and the aqueous solution was then transferred to a new Phase Lock Gel™ tube that had been briefly centrifuged and 750 ml of chloroform: isoamyl alcohol solution was added, shaking the samples vigorously for about 20 times and then centrifuging for 15 min. at 18,000 xg. Isoamyl alcohol aids the separation of the organic and aqueous layers. Chloroform was trapped under the gel of the Phase Lock Gel™ tubes and the aqueous solution was transferred to microfuge tubes and 100ml of 10M NH₄OAc and 750ml of ice cold 100% ethanol was added, shaking vigorously and centrifuging for 2 min. at 9,000 xg. A white precipitate was visible. The ethanol was carefully decanted and 1ml of ice cold 70% ethanol was added, shaken vigorously and the DNA was pelleted by centrifugation at 9,000 xg for 2 min. The supernatant was removed, the samples were left to air dry for 15 min. and resuspended in 215ml of TE pH8.0. The samples were then heated at 65°C for 30 min. with gentle agitation and stored at 4°C indefinitely. Ethanol precipitation is used as a purification

step for the DNA and to remove any residual phenol and chloroform. Washing the precipitate with 70% ethanol removes any excess salts from the precipitation step.

E) Quantification of DNA

The concentration of DNA in a sample was obtained by measuring the optical density (OD) of a dilution of the sample at 260nm. 10ml of sample was added to 290ml of TE buffer, thoroughly resuspended and transferred to a quartz cuvette measured in a spectrophotometer.

The concentration of the sample was calculated using the formula:

DNA concentration = $OD_{260} \times 50 \times \text{dilution factor (=30)} \times 1/\text{light path (=0.5)}$

Genomic DNA samples were then adjusted to 0.33 $\mu\text{g/ml}$ and stored at 4°C. Plasmid DNA samples were adjusted to 1 $\mu\text{g}/\mu\text{l}$ (or appropriate concentration) and stored at -20°C.

F) Restriction Digestion of Genomic DNA for Southern blotting

5 μg of genomic DNA was restriction digested in a total volume of 40ml. For the various transgenic lines the enzymes listed in table 2.8 were used for the digest. A typical reaction mixture consisted of 15 μl of DNA, 4 μl of 10x buffer, 2-4 μl of restriction enzyme and 19ml of dH₂O. The samples were mixed by brief centrifugation and incubated overnight at 37°C. Next morning, the reaction was stopped by heating at 65°C for 5 minutes and 10% (v/v) of 10x Loading Buffer was loaded to each sample.

G) Agarose Gel Electrophoresis of DNA

The restricted digested DNA samples were electrophoresed through an agarose gel in order to separate the fragments by size. For high molecular weight genomic DNA 0.8% agarose gels were used. To separate smaller fragments, for example PCR samples and plasmid DNA, higher percentage of agarose gels, up to 3% (Nusieve gels), were used. 5 μl of 10mg/ml EtBr/100ml was added to the gel before it was poured to visualize the DNA. The gel was placed in a horizontal electrophoresis tank and 1xTAE was poured to cover it. DNA samples that were prepared by adding 10%(v/v) 10x DNA loading buffer, were loaded into the slots alongside 1mg of 1kb DNA ladder as size control. The gel was run at 120V (0.8A) for 3.5 hrs or 50V (0.3A) overnight (for genomic DNA) and at 100V (0.6A) for 1 hr (for low molecular weight DNA). DNA was visualized on a short wave UV transilluminator and a photograph was taken. The long wave UV transilluminator was used for visualising plasmid fragments that would be collected and used for probe production.

H) Southern blotting of DNA

The agarose gel was trimmed to remove the 1kb DNA ladder, the loading wells and any excess gel. The gel was then soaked in denaturing solution for 30 min. on a shaking platform to denature the dsDNA. The gel was then washed 2 x 15 min. in a 1x TAE buffer. The DNA was then transferred onto a Biodyne B membrane by electroblotting for 3 hrs at 1.5A, (34V) in 0.5x TAE in a Hoeffer electroblotting tank. The DNA was then baked for 2 hrs at 80°C and then cross linked onto the membrane using a Stratalinker. The blot was stored at room temperature.

I) Generation of specific probe fragments

The DNA fragments used for generating probes for Southern blotting were derived from recombinant plasmid vectors propagated in *E.coli*. To generate a probe fragment, the relevant plasmid (see table 2.8) was propagated in *E.coli*, a large scale plasmid prep was performed to extract the plasmid DNA and then the plasmid DNA was restriction digested to isolate the relevant fragment. The digested DNA was electrophoresed at 80V on a 1% low-gelling temperature agarose (LGT-agarose) gel in 1x TAE with 5ml of 10mg/ml EtBr/100ml. The gel was run until the relevant fragment was well separated from other fragments and visualised on a long wave transilluminator to prevent degradation of the DNA. The DNA quantity was estimated by comparing the intensity of the band with that of a known standard. The fragment was cut out, placed in a microfuge tube and melted at 70°C. The volume was estimated and concentration was adjusted to 5ng/ml with TE buffer and stored at -20°C.

Line	Probe	Plasmid#	Genomic DNA Digests	Plasmid Digests	Fragments Generated	Probe Fragment
53	LMP1	139	<i>Bgl</i> III	<i>Bam</i> HI+ <i>Eco</i> RI	3.8kb 2.8kb	3.8kb
113	p16	454	<i>Bam</i> HI	<i>Xho</i> I	1kb 3kb	1kb
1205	Ras	233	<i>Xba</i> I	<i>Sac</i> I	3.5kb 2.4kb 2.5kb 1.6kb	2.4kb

Table 2.8: Genomic Digests and Probe Fragments

J) ³²P radioactive Labelling of probe fragment and hybridisation

The probe fragment generated was radioactive labelled with $\alpha^{32}\text{PdCTP}$ using the Stratagene Prime It II Random Primer Labelling Kit (cat. no: 300385).

The probe fragments were used as the template for Klenow polymerase with random hexanucleotide primers and dATP, dGTP, dTTP and the $\alpha^{32}\text{PdCTP}$. The reaction was incubated for at least 30 min. at 37°C, after which the reaction reaches a plateau and no more new DNA strands are generated. The DNA probe was purified to remove any unincorporated nucleotides by passing it through a NucTrap®Probe purification column, (Stratagene cat. no: 400701). Unincorporated small nucleotides are trapped in the column resin whereas the probe passes through the column with STE buffer (2.1.4) and is collected. 1µl of purified probe was used to count the specific activity of the labelled DNA and the specific activity was calculated. The probe was used for hybridisation only if the specific activity was greater than 5×10^8 cpm. The blot was prehybridised by placing it in a hybridisation tube and adding 10ml of Church buffer. The Bovine Serum Albumin (BSA) in Church buffer coats the membrane thus inhibiting non specific binding of the probe. The tube was rotated in a hybridisation oven for at least 2 hrs at 65°C. The purified probe was denatured at 95°C for 5 min. and was then added to the hybridisation tube with the blot. The tube was rotated overnight in a hybridisation oven at 68°C. The single stranded radioactively labelled probe will hybridise to complementary DNA fragments on the blot.

K) Washing of Southern blots

After hybridisation the blot was washed to remove any probe that did not specifically bind to the DNA and any non specific DNA that bound at low melting temperature. The blot was first washed 4 x 10 min. at room temperature on a shaking platform in solution A. The blot was then washed 2 x 30 min. in solution B at 68°C in a shaking water bath. The blot was then wrapped in a polythene bag, placed in an autoradiography cassette with an intensifying screen and exposed to Kodak XAR film at -70°C for the appropriate time and the film was developed in a Kodak X-Omat developer.

L) Stripping of Southern blots

Southern blots were stripped of hybridised probe in order to re-hybridise with a different probe. The blot was washed 2x 15 min. at 90° in southern stripping solution A (2.1.4). The

blot was then washed 1x30 min. in southern stripping solution B (2.1.4) at 65°C. The blot was either prehybridised directly for reprobing or stored in a sealed bag at -20°C until further use.

M) Amplification of DNA fragments using PCR

PCR was used to amplify short DNA fragments. PCR 1.1x Reddy mix™ PCR Master Mix (Abgene cat. no: AB0575) was used as the master mix in all the PCR reactions in order to increase reliability and uniformity of the reactions. Reddy mix gives a final reaction composition of 1.5mM MgCl₂, 0.2mM of each of the 4 deoxynucleotide triphosphates (dNTPs), 1.25 units of thermostable *Taq* DNA polymerase, 0.01% (v/v) Tween 20, 75mM Tris-HCl pH8.8 and 20mM ammonium sulphate. Each reaction was set up with 45ml 1.1x Reddy mix™ PCR Master Mix, the two primers, DNA and water to a total volume of 50ml. DNA and primer concentration for each amplified fragment is shown in tables 2.9 and 2.10.

The reactions were placed in a PTC200 thermocycler for 35 cycles of amplification. The first step in any PCR reaction is to denature the template strand and this is done at 95°C for 15sec. to 2 min. The next step is annealing the primers to the two single stranded templates and this is conducted at a reduced temperature of 40-60° (depending on the melting temperature of the oligos) for 60sec. This step allows annealing of the oligos to the template. Polymerisation of the new strand is conducted at an increased temperature of 72° for as long as needed to create the size required (roughly 30 sec per 500bp). A final 72°C step is often included to allow polymerisation reaction completion.

Each PCR reaction was optimised depending on the length of the fragment that needed to be amplified. 10 or 20 µl of PCR product was electrophoresed through a 1.5% TAE agarose gel or a 2% NuSieve, 1% agarose TBE gel for very small fragments (eg. <200bp).

Table 2.9: Reverse transcribed (RT)-PCR programs

PCR Name	PCR reaction components	PCR Program
CDNA step	RNA- 2µl DNase treated Anchored oligo dT-1µl dNTPs- 1µl RT (or water) - 1µl	1. 47°C for 1hr 2. 75°C for 10 min 3. 4°C unlimited
DNase step	RNA – 2µg DNase- 5µl DEPC H ₂ O- up to 100µl total volume	1. 42°C for 30min 2. 75°C for 10min 3. 0°C unlimited
LMP1 DS1 and DS4	DNA-300ng(1µl) dH ₂ O- 1µl Forward primer DS1 - 1µl Reverse primer DS4 - 1µl	1. 94°C for 2min 2. 94°C for 30sec 3. 50°C for 30 sec 4. 72°C for 1min Go to step 2-3, 4 times 5. 94°C for 30 sec 6. 55°C for 30sec 7. 72°C for 1 min Go to step 6-7, 29 times 8. 72°C for 5 min 9. 4°C unlimited
LMP1 NESTED DS2 and DS3	DNA-300ng(1µl) dH ₂ O- 1µl Forward primer DS2 - 1µl Reverse primer DS 3 - 1µl	1. 94°C for 2min 2. 94°C for 30sec 3. 50°C for 30 sec 4. 72°C for 1min Go to step 2-3, 4 times 5. 94°C for 30 sec 6. 55°C for 30sec 7. 72°C for 1min Go to step 6-7, 29 times 8. 72°C for 5 min 9. 4°C unlimited

Table 2.10: PCR programs

PCR Fragment	PCR reaction components	PCR Program
Neomycin/p16	DNA-300ng (1µl) dH ₂ O- 1µl Forward primer - 1µl (10pmoles) Reverse primer- 1µl (10pmoles) Reddy Mix- 45µl	91°C 30s 2. 53°C 30s 3. 72°C 30s Go to step 2-3, 35 times 4. 72°C 10min 5. 4°C unlimited
TGFα-knock out	DNA-300ng(1µl) dH ₂ O- 1µl TGFαKO1- 1µl (10pmoles) TGFαKO2- 1µl (10pmoles) Reddy Mix- 45µl	1. 95°C 150s 2. 95°C 50s 3. 63°C for 50s 4. 72°C for 70s Go to step 2-4 , 34 times 5. 4°C unlimited
TGFα-wild type	DNA-300ng(1µl) dH ₂ O- 1µl TGFαKO1- 1µl (10pmoles) TGFαKO3- 1µl (10pmoles) Reddy Mix- 45µl	1. 95°C 150s 2. 95°C 50s 3. 63°C for 50s 4. 72°C for 70s Go to step 2-4 , 34 times 5. 4°C unlimited
v-H-ras (transgene)	DNA-300ng (1µl) dH ₂ O- 1µl Forward primer- 1µl (25pmoles) Reverse primer- 1µl (25pmoles) Reddy Mix- 45µl	1. 95°C for 5min 2. 93°C for 1min 3. 50° for 1min 4. 72°C for 2min Go to step 2-4, 34 times 5. 72°C for 15 min 6. 4° unlimited

N) Purification of DNA for PCR

Genomic DNA samples that were to be genotyped using the neomycin/p16 program were first purified using the Bio-101 GeneClean kit as per manufacturer's instructions (Anachem, cat. no: 1101-400). Briefly, DNA binds to a silica matrix in high concentrations of chaotropic salt and is eluted in low salt. Removal of the salt and rehydration of the silica matrix breaks the cation bridges that formed between the silica matrix and the negatively charged phosphate backbone of the DNA thus allowing the DNA to be eluted. Using this method any impurities can be removed and the purified DNA can be used in sensitive applications such as PCR. Empirically, it was found that for these particular PCR reactions Genecleaning of the DNA was needed for success.

2.2.4 Protein techniques

A) Protein sample preparation from tissue

For most analyses, protein was extracted in RIPA buffer containing freshly added phosphatase inhibitors (Sigma cat. no: P5726) and protease inhibitors (Sigma cat. no: P2714). Phosphatase inhibitor cocktail contains sodium vanadate, sodium molybdate, sodium tartrate and imidazole that can inhibit acid/alkaline and tyrosine protein phosphatases. The protease inhibitor cocktail contains AEBSF, E-64, bestatin, leupeptin, aprotinin and sodium EDTA that can inhibit serine/cysteine/aspartic and metalloproteases. 1ml of RIPA buffer and inhibitors was added to the tissue sample in a 4ml Falcon tube. The sample was homogenised using a Kinematica polytron homogeniser. Skin samples are tougher than soft tissues and need to be homogenised at higher settings usually 8-10 and for longer. Before and after each sample was processed, the polytron was washed with 1% (v/v) SDS, 3 washes of dH₂O and finally 70% (v/v) ethanol. Once homogenised, the samples were transferred to microfuge tubes, vortexed and left to stand on ice for 5 min. The samples were then centrifuged at 18,000 xg in a microfuge for 10 min. at 4°C. The supernatant was removed to new microfuge tubes and 5µl of it was used for protein quantification. Once concentration of the protein was known the sample was aliquoted in 100µg aliquots and stored at -70°C. The same process as above was followed when samples were extracted in 8M urea buffer except that no protease or phosphatase inhibitors were added and after homogenisation the samples were transferred to microfuge tubes and heated at 55°C overnight with shaking. The rest of the procedure was the same as for RIPA extracted samples.

B) Protein sample preparation from cultured mammalian cells

Mammalian adherent cells were grown on 100mm² plates. When confluent, the medium was removed, the cells washed with ice cold 1x PBS and the cells were scraped off the plate using a silicon cell scraper. The cells were collected in 1x PBS, washed, pelleted, PBS removed, frozen in liquid nitrogen and stored at -70°C. 300ml of RIPA buffer with phosphatase and protease inhibitors was added to the cell pellet and it was vortexed thoroughly until a homogenate was formed and then left to stand on ice for 5 minutes. Then it was microfuged at 18,000 xg for 10 min. at 4°C. The supernatant was transferred to a new microfuge tube and 5ml of the supernatant was used for protein quantification. Once the sample concentration was established, it was aliquoted in 100µg aliquots and stored at -70°C.

C) Protein Immunoprecipitation (IP)

Sepharose-G beads (Sigma cat. no: P3296 Protein G on Sepharose® 4B fast flow resuspended in 20% ethanol, 45-165µm) were used for protein IP. The beads were rotated for 1hr at 4°C in either Ripa buffer or Net-N at 50% (v/v) (50% beads, 50% buffer). The beads were centrifuged at 18,000 xg for 5min. at 4°C and the supernatant discarded. This wash step was repeated twice in order to completely remove the ethanol in which the beads were stored. The beads were then resuspended in equal volume of the appropriate buffer (50%(v/v)) and stored at 4°C for future use. If not immediate, prior to use, the beads were washed one more time. Usually 500µg of protein was used for the IP per sample. If the sample was prepared in 8M urea, the appropriate volume of NET-N and protease inhibitors was added to dilute the urea to 1M and allow renaturation of proteins. Appropriate amounts of phosphatase inhibitors were added to each sample and 70µl of 50%Protein-G sepharose beads were added. The samples were rotated for 2hrs at 4°C and were then centrifuged at 18,000 xg for 10min. at 4°C. The supernatants were transferred to fresh microfuge tubes. To the clarified samples, 30µl 50%Protein-G sepharose beads washed in Ripa buffer (or NET-N in the case of urea samples) were added. The samples were rotated for 2hrs at 4°C and were then centrifuged at 18,000 xg for 10min. at 4°C. The supernatants were transferred to fresh microfuge tubes and appropriate amounts of antibody were added (in the case of S12 ascites 2µl were added, for other antibodies 200µl were added). The samples were rotated overnight at 4°C. The next day, 30µl washed 50%Protein-G sepharose beads were added and rotated for 30min. at 4°C. The samples were centrifuged at 18,000 xg for 10min. at 4°C and the supernatants were discarded. The precipitates were washed by vortexing in 1ml of NET-N, pH8.0 and centrifuged at 18,000 xg for 1min at 4°C. The supernatant was discarded and the wash step was repeated with 1ml of TBS (table 2.1.4). To elute the protein from the beads, 30µl of 2X GSB was added. The samples were vortexed and heated for 5min. at 95°C. The samples were centrifuged at 18,000 xg for 1min. at room temperature. The sample supernatant was then either directly loaded onto an acrylamide gel or frozen at -70°C for future use.

D) Quantification of protein concentration

Protein concentration was determined using the Bradford assay. A set of protein concentration standard reactions was prepared using BSA as shown on table 2.11. 5µl of the sample was diluted in 795µl of the appropriate lysis buffer. 200µl of Biorad dye was added, the samples were vigorously mixed and left to stand for 5 minutes for the colour to develop. Then the

protein concentration was read at $\lambda=595\text{nm}$. A standard curve was drawn using the values obtained from reading the set of standard protein concentration samples, and the concentration of each test sample was determined.

BSA μg	BSA 100 $\mu\text{g/ml}$ added (μl)	Lysis Buffer (μl)
16	160	635
8	80	715
4	40	755
2	20	775
1	10	785
0	0	795

Table 2.11: Standard Protein Curve Reactions

E) SDS Polyacrylamide Gel Electrophoresis of protein samples

Polyacrylamide gels were made up as shown on table 2.12. First the running gel was poured, overlaid with saturated butan-1-ol and allowed to set. Then, the butan-1-ol was discarded, washed off with dH_2O and the stacking gel was poured and then the combs were placed. The gels were 2mm thick and were made up of about 25ml running gel and 5ml stacking gel.

Reagents	5% Stack Gel	7.5% Running Gel	10% Running Gel	15% Running Gel
Bis-Acrylamide	2.4ml	9.4ml	12.5ml	18.75ml
Tris pH 6.8	2.5ml	-----	-----	-----
Tris pH 8.8	-----	12.5ml	12.5ml	12.5ml
10% SDS	0.2ml	0.5ml	0.5ml	0.5ml
H ₂ O	14.8ml	27.35ml	24.25ml	18ml
TEMED	0.05ml	0.05ml	0.05ml	0.05ml
10% APS	0.500ml	0.250ml	0.250ml	0.250ml

Table 2.12: The composition of running and stack gels for Western blotting

F) Western blotting of protein gel

Usually, 100mg of total protein extract was used per track. An equal volume of 2xGSB or 1/5 of the final volume of the sample of 5xGSB was added to each extract. The samples were heated for 5 mins at 95°C and placed on ice until loaded. 10ml of markers (Gibco BRL BenchMark™ pre-stained protein ladder cat.no: 10748-010, New England Biolabs Prestained Protein Marker cat. no: P7708G) were loaded along with the samples and separated by variable percentage SDS PAGE with 5% stacking gel at 200V for 3 V until the dye front reached the bottom of the gel. The Immobilon-P membrane (Millipore cat.no: IPVH 00010) was pre-wet in methanol for 15seconds, dH_2O for 2 min. and transfer buffer for at least 5 min.

Following transfer, non-specific sites on the membrane were blocked in blocking buffer containing TBST and 5% non-fat dried milk overnight at 4°C with gentle agitation. The membrane was then incubated overnight with primary antibody (see table 2.1.1) at the indicated dilution in blocking buffer at 4°C, usually overnight and then washed 1x15min. and 3x5min. in TBST buffer. The secondary antibody (that is HRP conjugated – see table 2.1.1) was added, diluted in blocking buffer, for 1hr at room temperature. The membrane was then washed as for the primary antibody.

To visualise antibody binding, 8ml of Solution A (containing ECL + substrate in Tris buffer) and 250ml of solution B (acridan solution in dioxane and ethanol) of the ECL+ System kit (Amersham, cat.no: RPN 2132) were mixed and added to the membrane. This reaction converts acridan with the use of peroxide and horseradish peroxidase in slightly alkaline conditions, to acridinium esters that produce a high intensity chemiluminescence that can be detected on a photographic film. The solution was left on for 5mins at room temperature. The membrane was then drained of excess solution and was placed in a plastic bag and sealed. The membrane was exposed to X-AR photographic film in cassette for the required time and the film developed in an X-Omat developer. Densitometric analysis of the scanned autorads was performed using the program Kodak 1D 3.5.2 USB as described in the relevant chapters. Note that once the film has been exposed, it cannot get any blacker so many of the high intensities that were observed in certain autorads have been underestimated when calculating the fold difference. Also since the densitometric analysis was performed on a computer image and not the actual autorad the values obtained are not entirely accurate.

G) Stripping and reprobing of western blots

The membrane was incubated at 55°C with 20ml pre-heated MENSA buffer for 30mins. The membrane was rinsed with SDS wash buffer to remove the excess stripping buffer, and it was then washed 2x20mins with TBST at room temperature. The membrane was then blocked and reprobed as described above. Membranes were stored in plastic wrap at 4°C.

H) Electrophoretic Mobility Shift Assay (EMSA)

H.1 Protein sample preparation from tissues

Protein was extracted in high salt buffer containing fresh phosphatase and protease inhibitors. 0.5ml of the high salt buffer plus inhibitors was added to the frozen tissue sample in a 4ml

Falcon tube. The sample was homogenised in a Kinematica polytron homogeniser. Before and after each sample was processed the polytron was washed with 1% (v/v) SDS, 3 washes of dH₂O and finally 70% (v/v) ethanol. Once homogenised the samples were transferred to microfuge tubes, vortexed and let to stand on ice for 5 min. The samples were then centrifuged at 14,000 xg in a microfuge for 10 min. at 4°C. The supernatant was removed to fresh microfuge tubes and 5µl of it was used for protein quantification. Once concentration of the protein was known the sample was aliquoted in 10µg aliquots and stored at -70°C.

H.II Labeling Oligonucleotide and probe purification

For annealing single stranded sticky ended oligos to create the double stranded oligo, 2ml (200pmoles) each of forward and reverse oligos, 10µl 5M NaCl (250mM) and 186µl TE were added and heated at 80°C for 10min. They were allowed to cool down at room temperature, aliquoted 10µl per tube and frozen at -20°C. Two different labelling reactions were performed for probe preparation depending on whether the double stranded oligos were blunt or sticky ended. Blunt ended oligos were kinase labelled, 50ng of oligos were mixed with 2µl of 10x T4 Polynucleotide kinase (PNK) buffer and dH₂O up to 20µl. 20mCi of γ ³²P dATP and 1µl of T4 PNK was added to the reaction. The reaction was incubated at 37°C for 45min. To prepare the probe using the annealed sticky ended oligos, 1pmol annealed oligo (1µl) was mixed with 33µl dH₂O, 10µl dCTP buffer, 50µCi α ³²P dCTP and 1µl Klenow and incubated at 37°C for 30min. For both types of oligo the same procedure was followed for probe purification. A NICK™ Column (Amersham, cat. no: 17-0855-01) was equilibrated with 3ml TE that was allowed to run through the column but without allowing the matrix to dry. The labelled probe was added to the column. 400µl TE was added and allowed to run through the column. A further 400µl TE was added and this time the eluent was collected in a microfuge tube. The purified probe was stored in a lead container at -20°C. NICK™ columns are packed with Sephadex® G-50 and are used for the separation of oligonucleotides from unincorporated nucleotides.

H.III Polyacrylamide Gel preparation for EMSAs

A 6% non-denaturing polyacrylamide gel was used for electrophoresing EMSA samples. 7.5ml of 40%(v/v) acrylamide was mixed with 2.5ml 10xTBE, 39.625ml dH₂O, 350ml (v/v) 10%APS and 25ml TEMED. The gel was 2mm thick and its volume was 30ml. The gel was polymerised for an hour and then pre-run with 0.5xTBE buffer at 200V for 30minutes to warm the gel.

H.IV Sample Preparation for EMSAs

dH₂O was added to each sample to bring them all to the same volume of 10µl. Then for each sample 20µl of the appropriate binding buffer was added along with 2µl of polydI.dC (2mg/reaction) or 0.2µl salmon sperm (2µg/reaction) according to the protocols used. Competitor (unlabelled oligo) was added to one aliquot of each test sample (usually between 50 to 200x in excess of hot oligo was needed for successful competition) and the samples were left to incubate on ice for 10min. The probe (0.2-1ng) was added and the samples were left to incubate on ice for a further 30min. (For the SRE oligo, samples were incubated on ice 15min., and a further 15min. at room temperature.) The samples were loaded on the gel that had been pre-run (H.III). 10µl of dye was loaded in the first well to visualise a dye front during running. The samples were run at 150V for about 2hrs until the dye was about 5cm from the bottom of the gel. The buffer was discarded in the “radioactive sink” and the plates were separated. Using double thickness 3MM paper, the gel was carefully lifted, wrapped in saran wrap and dried for 2 hrs at 80°C. The dried gel was exposed to X-AR Kodak film for the required time and developed in an X-Omat developer.

2.2.5 RNA techniques

RNA extraction

To avoid RNA degradation all solutions were made up using diethyl-polycarbonate (DEPC)-treated and autoclaved water. DEPC inactivates ribonucleases by covalent modifications. Microfuge tubes and tips were autoclaved. All surfaces and equipment to be used were washed with 1% (w/v) SDS and then 75% (v/v) ethanol made with DEPC-treated water. Gloves were worn and frequently changed to avoid contamination with RNAses.

A) Total RNA Extraction

Two methods were used by me for extracting RNA; the Chomczynski and Sacchi method and the Tri-Reagent™ method. For the first method, the sample was vortexed or homogenised using a polytron as appropriate in 1.5 ml of solution D (0.36ml 2ME, 50ml 4M GT). The sample was kept on ice and 0.1 volume (150µl) of 2M NaOAc, pH4.0 in acetic acid, was added and thoroughly mixed. Then 1 volume (1.5ml) of H₂O saturated pure grade phenol was added and thoroughly mixed. Finally, 0.2 volumes (300µl) of chloroform:isoamyl alcohol (49:1) were added and thoroughly mixed. The sample was microfuged at 10,000 xg for 20min. at 4°C and the aqueous phase was transferred to fresh tubes. 1 volume of isopropanol

(1.5mL) was added and kept at 4°C overnight. The sample was microfuged at 10,000 xg for 20min at 4°C and the supernatant was discarded. The wet pellet was resuspended in 300µl of solution D and vortexed. 600µl of 100% ethanol was added and the solution was kept at -20°C for 2hrs or overnight if needed. The sample was microfuged at 10,000 xg and the pellet washed twice in 1ml of 75% ethanol. The pellet was allowed to air dry and was resuspended in 220µl of 0.5%TE,1% SDS or dH₂O. The sample was heated at 65°C for 10min. with vortexing. The RNA was stored at -70°C for subsequent use (Chomczynski and Sacchi, 1987).

The second method used to extract RNA was using the Tri-Reagent™ (Sigma cat. no: T-9424). This is a kit form modification of the Chomczynski and Sacchi method. Use of Tri-Reagent™ which is a phenol and guanidine thiocyanate solution, enables RNA, DNA and protein to be extracted and isolated after tissue homogenisation simultaneously. In this case only the RNA was used. Chloroform addition, separates RNA and DNA into the aqueous layer and proteins in the organic layer. In subsequent steps only the aqueous phase was collected. To frozen tissues of 50-100mg or cell pellets, 1ml of Tri-Reagent™ was added and the tissue or cell pellet was homogenised in a Kinematika polytron homogeniser. The sample was kept at room temperature for five min. to ensure dissociation of all nucleoproteins. Chloroform, 0.2ml for every 1ml of Tri-Reagent™ used, was added to the sample, mixed for 15 sec. and the sample was left at room temperature for 15 min. Chloroform allows separation of RNA, DNA and proteins into different phases. The sample was centrifuged at 8,000 xg for 15 min. at 4°C in a Beckman JA-14 rotor. The sample was separated into an upper aqueous layer containing the RNA, a middle fatty layer and an organic layer containing proteins. The aqueous layer was transferred to a new Falcon tube and isopropanol (0.5ml for every 1ml Tri-Reagent™ used) was added. The sample was mixed and left at room temperature for 10 min. It was then centrifuged at 8,000 xg for 10 min. at 4° in a Beckman JA-14 rotor. The supernatant was discarded and the pellet was washed and suspended in 1ml 75% ethanol for every 1ml Tri-Reagent™ used and transferred to 1.5ml microfuge tubes. The sample was centrifuged in a microguge at 14,000 xg for 5 min. at 4°C. The pellet was allowed to dry and resuspended in 300µl TE/0.1%SDS at 65°C for about 10 min. Lithium chloride (100µl from 10M stock) was added and the sample left at 4°C overnight to selectively precipitate RNA. The following day, the sample was centrifuged at 16,000 xg for 30 min. at 4°C. The pellet was then washed in 1ml 75% ethanol and microfuged at 16,000 xg for 10 min. at 4°C. The pellet was allowed to dry at room temperature and resuspended in an appropriate volume of TE/0.1%SDS and stored at -70°C.

B) Quantification of RNA

The concentration of RNA in a sample is obtained by measuring the OD of a dilution of a sample at 260nm. 5 μ l of sample was added to 295 μ l of TE/0.1%SDS buffer and transferred to a quartz cuvette where its concentration was measured in a spectrophotometer. The concentration of the sample was calculated using the formula:

RNA concentration = $OD_{260} \times 40 \times \text{dilution factor (=60)} \times 1/\text{light path}$

To determine the purity of RNA the optical density of a sample was also measured at 280nm. The ratio between OD_{260}/OD_{280} gives the purity of RNA or DNA, ie whether there are any proteins in the sample. Pure RNA or DNA samples give a ratio of OD_{260}/OD_{280} of 2.0 while proteins increase the OD_{280} reading.

C) Formaldehyde gel electrophoresis of RNA

To determine quality of RNA samples are run on an agarose gel. Pure RNA samples show the 28, 18 and 5S bands. The RNA samples that were extracted were electrophoresed in a mini 1% agarose gel containing formaldehyde in order to check the integrity of RNA (presence of three ribosomal bands). 10mg/mlEtBr/100ml was added to the gel before it was poured to visualize the RNA. For a 100ml gel, 10ml 10x MOPS-E, 84.5ml water and 1.0g of agarose were mixed and melted. When the temperature was 60°C, 5.2ml formaldehyde was added and allowed to set. The gel was placed in a horizontal electrophoresis tank and 1xMOPS-E was poured to cover it. 1 μ g RNA samples were prepared by adding 16ml of RNA loading buffer, mixed and heated at 65°C for 10 minutes to denature any secondary structure. Then 2 μ l of 10x loading dye (RNA) was added, the samples were briefly centrifuged and loaded on the gel along with 1kb DNA ladder and run at 100V for 30 minutes. RNA was visualized on a short wave UV transilluminator and a photograph was taken.

D) Electrophoresis and Northern blotting of RNA gels

The gel tank and combs were washed in 1% SDS overnight and rinsed with DEPC-treated water and ethanol before use. 20 μ g of total RNA was precipitated with 3M NaOAc. The RNA pellet was resuspended in 4 μ l DEPC-treated water by heating at 65°C and vortexing well. 16 μ l of 10x loading buffer (RNA) was added and the sample was heated to 68°C for 10minutes and then placed on ice. 2 μ l of 10x RNA loading dye was added and the samples loaded on a formaldehyde gel. 1% (w/w) agarose in 95ml 1x MOPS was melted and cooled to

60°C before adding 17.8% (v/v) formaldehyde (of the 38% stock solution) and poured. The gel was electrophoresed in 1x MOPS buffer at 100V for 1hr in the cold room.

The gel was then viewed on a UV transilluminator, trimmed and soaked 3x20mins in 1xTAE and electroblotted onto a Biodyne B membrane as described for Southern blotting in section 2.2.3H but using only RNase free solutions. The membrane was then hybridised exactly as described previously for Southern blots.

2.2.6 Cell culture techniques

All culture techniques were performed either by myself or by Liz Hill, the laboratory technical manager.

A) Explantation of papillomas and carcinomas

The explantation of papillomas and carcinomas was performed under sterile conditions with all the surfaces washed with 100%(v/v) ethanol. Part of the papilloma or carcinoma was washed with 100%(v/v) ethanol allowed to dry briefly and placed in transfer medium on ice. The rest of the lesion was snap frozen in liquid nitrogen or fixed in formalin for histopathological analysis.

The lesion was transferred to a Petri dish, cut in small pieces with a sterile scalpel and trypsinised in 10ml trypsin solution with agitation, for 30 minutes at room temperature. Then the sample was centrifuged at 194 xg for 5min. and the cells resuspended in 10ml of 20%FCS and plated in a Petri dish where it was incubated for 5-10 days. Cell growth was monitored and when the cells were confluent they were sub-cultured and later frozen in 10% DMSO in FBS.

B) Sub-culturing of mammalian cells

When the adherent cell cultures reached 90% confluence, they were sub-cultured onto fresh tissue culture plates. The medium was aspirated from the cells, and the cells were washed once in versene, which removes residual serum, and the EDTA chelates calcium and magnesium ions. Trypsin, a protease, was then layered on the cells and the plate was agitated to dislodge the cells. The cells were resuspended in fresh complete tissue culture medium (serum aids to inactivate the trypsin) and transferred to new plates at the required density. Cells were incubated at 37°C and 5% CO₂.

C) Freezing viable cells in liquid nitrogen

Cells were cultured on 5cm² plate. One plate of cells (about 2x10⁶ cells) was stored per cryotube. The medium was aspirated from a confluent plate. The cells were washed once in cold PBS. Using a cell scraper most of the cells were dislodged from the plate. The cells were collected in cold PBS, transferred in a Falcon tube and pelleted in a Heraeus 400 centrifuge at 194 xg for 5 min. The cell pellet was resuspended in 1ml freezing medium (10%DMSO, 90% FBS) and the cells transferred to a cryotube and frozen in a cryoflask at -70°C overnight. The cryoflask ensures gradual (1°C/min.) chilling of the cells. The vials were then transferred to liquid nitrogen for long term storage.

D) Revival of frozen stocks

Cells were stored in liquid nitrogen tanks. When cells were required, they were brought up from liquid nitrogen then quickly defrosted in the tube at 37°C in a water bath. The cells were then washed in complete tissue culture medium to remove DMSO and were pelleted by centrifugation in a Heraeus 400 centrifuge at 194 xg for 5 min. The cells were resuspended in 6ml of complete tissue culture medium and transferred to a 25cm² tissue culture flask. Cells were incubated at 37°C and 5% CO₂.

E) Transfection of cells with plasmid and selection

Cells were grown on tissue culture dishes until they were about 70% confluent. 5µg of linearised plasmid DNA (in TE) was diluted in medium without serum or antibiotics to a maximum volume of 150µl. The solution was mixed and spun briefly. 20µl of Superfect® transfection reagent (Quiagen cat.no:301305), was mixed with the DNA solution. The Superfect® transfection reagent is an activated dendrimer that has a spherical shape with branches coming out from a central core and terminating at charged amino groups. In this way, the DNA is assembled into compact structures thus making it easier for DNA to enter the cell. The Superfect-DNA complex is positively charged and this enables binding to negatively charged receptors on the cell surface thus enabling entry. Superfect has a second property, that upon entry into the cell it can buffer the lysosome thus inhibiting lysosomal nucleases from working and allowing greater stability of the Superfect-DNA complex.

The solution was incubated for 10 minutes at room temperature to allow for Superfect-DNA complex formation to take place. Meanwhile, the growth medium was removed from the cells and the cells were washed with 4ml PBS. After incubation, 1ml of medium containing serum

and antibiotics was added to the DNA solution, mixed and transferred to the cells. The cells were incubated at 37C and 5% CO₂ for 2hrs. Then the medium was removed and the cells were washed 4 times with PBS. Fresh medium was added with serum and antibiotics and the cells were left to incubate for 48hrs. Then they were passaged with the appropriate selection reagent (depending on what antibiotic the transfected plasmid was resistant to, usually geneticin or hygromycin) and clones were picked as they appeared.

Before, proceeding with the transfection, a death assay was performed on each cell line that was to be transfected in order to determine what concentration of the selection agent would be used after transfection. In that assay, cells were allowed to grow in tissue culture dishes until they were approximately 70% confluent. Different antibiotic concentrations (usually from 50µg/ml to 400µg/ml in 50µg/ml increments) were added to each plate. The antibiotic and medium was refreshed every three days. Every day, the cell population was counted by using Trypan Blue. This was repeated every day for fifteen days. The number of viable cells was plotted against the number of days and the lowest antibiotic concentration at which all the cells were dead at the end of the fifteen days was chosen to be used later

F) Viable Cell Counting with Trypan Blue

Adherent cells were brought into suspension using trypsin and resuspended in a volume of complete media as described in section 2.2.6B. 20µl of the cell suspension was removed and added to 80µl of Trypan Blue (0.4% Trypan Blue stain in 0.85% saline, from Gibco BRL cat. no: 15250-061). The haemocytometer was cleaned with 70% ethanol and the coverslip was moistened and placed over the chamber of the haemocytometer until Newton's refraction rings appeared. 10µl of the cell suspension in trypan blue was loaded onto the chamber and the cells were viewed under a light microscope at x20 eyepiece magnification. The number of viable cells that do not take up the stain (bright cells) was counted. Dead cells absorb trypan blue and are stained blue. Usually the cells in 5 squares were counted. The total number of viable cells per ml was calculated in the following way:

$$\text{Cells/ml} = (\text{Total viable cells counted} / \text{number of squares}) \times \text{dilution factor} \times 10^4$$

2.2.7 Immunohistochemistry

Tissue collection was performed by myself whereas tissue sectioning and staining was performed by Mr Colin Nixon, a trained histotechnologist. Pathological analysis was performed by Dr Adrian Phelby, a trained pathologist. Tissue was collected and fixed in 10% neutral buffered formalin and embedded in paraffin wax. Paraffin sections of 2µm were cut

from the tissue block and placed onto coated slides. The immunohistochemical analysis used an indirect two-step technique that was performed using DakoCytomation EnVision kits (cat no:K4007 for mouse monoclonal antibodies and K4011 for rabbit polyclonal antibodies). The sections were placed in Histo-clear to remove excess paraffin wax and then through a series of decreasing graded alcohols to water before starting the staining procedure. The antibodies that were used were the proliferating nuclear cell antigen (PCNA) and total caspase-3. For antigen retrieval, the sections were heated in 0.01M Sodium Citrate (pH6.0) buffer in a microwaveable pressure cooker for 2 min. in order to allow exposure of the antigen site. The buffer was allowed to cool down for 20 min. and the sections were placed in dH₂O. The endogenous peroxidase activity of the sections was blocked using the peroxidase block solution (0.03% hydrogen peroxide) of the DakoCytomation kit. This buffer was washed with 0.01M TBST (pH7.5) for 5 min. After the wash step the primary antibody (PCNA or total caspase-3) was applied on the sections in the appropriate dilution (1:50) which was determined before hand. The antibody was diluted in 0.01M TBS (pH7.5). The sections were incubated with the antibody for an hour at room temperature. After incubation, the samples were washed with TBST (pH7.5) for 5 min. The secondary antibody, as supplied in the DakoCytomation kit, was applied to the samples for 30 min. at room temperature. Application of the secondary antibody allows complex formation between primary and secondary antibody that will enable subsequent visualisation of the staining pattern of the primary antibody. The secondary antibody is either a goat anti-mouse polyclonal (in the case of PCNA) or rabbit polyclonal (in the case of total caspase-3) and is HRP conjugated. To visualise the complex, 3,3 diaminobenzidine (DAB) chromogen solution and the DAB substrate buffer (in hydrogen peroxide, pH7.5), supplied in the DakoCytomation kit were mixed and used as per manufacturer's instructions. DAB is applied on the sections for ten minutes at room temperature. The sections are microscopically monitored to allow for the desired staining to develop. DAB allows formation of a brown insoluble complex (the complex cannot dissolve in alcohol or other organic solvents) and allows the antibody-antigen complex to be visualised. The sections were counterstained with Gills Haematoxylin (cat no: 261103G, BDH) and mounted in DPX mountant for microscopy (cat no: 360294H, BDH). A negative control (ie. no primary antibody was applied) was run in parallel. For each antibody a known positive control was run beforehand to confirm that the primary antibody was working and to optimise the dilution of the antibody.

Chapter 3: Characterisation of LMP1 transgenic mouse lines

The aim of the work presented in this chapter was to characterise the expression patterns of LMP1 in the transgenic mouse lines 117, 105A and 105B and determine if this correlates with the observed phenotype.

These mouse lines harbour the transgene LMP1^{CAO} under the L2 EBV promoter (as described in section 1.9). When the PyLMP1^{B95-8} mice were created (Wilson et al., 1990), it was evident from Northern blots that a transcript derived from the ED-L2 promoter was showing relatively high expression in epithelial tissues including skin. Given the epithelial specificity of the ED-L2 promoter in those mice, ED-L2 was used to drive expression of the Cyclin D1 gene to mucosal stratified squamous epithelia such as tongue, oesophagus and forestomach (Nakagawa et al., 1997). As such, a similar pattern of expression may be predicted for the L2LMP1^{CAO} mice, but transgene expression patterns and levels cannot be precisely predetermined and must be characterised for each line.

Elucidating transgene expression is important as it will allow an understanding of the phenotype observed in these lines and enable the design of further relevant experiments.

3.1 Outline of approach

For the expression analyses three techniques were employed: RT-PCR, Northern and Western blotting. RT-PCR can be used to detect low levels of RNA. Northern blotting is not so sensitive as RT-PCR but can reveal the full size transcript and Western blotting shows whether there is any translation of the transgene message to produce the protein.

Tissues were collected from transgenic and wild type siblings from each line investigated and stored at -70°C until processed for the technique employed.

The purpose of these experiments was to answer the following questions:

1. In which tissues of the transgenic mice is LMP1^{CAO} expressed ?
2. What is the pathology/phenotype of tissues from these transgenic lines and does it correlate with transgene expression?

3. Does LMP1^{CAO} lead to a similar response in the tissue as LMP1^{B95-8} does after chemical carcinogen treatment of the mice? In this context can it replace the need for an activated *ras* in a chemical carcinogenesis setting?
4. Does loss of the INK4a locus cooperates with LMP1^{CAO} in a similar fashion to LMP1^{B95-8}?

For the phenotypic studies of LMP1 transgenic lines three approaches were taken:

1. In order to examine tissue pathology, tissues were collected and stained for histological examination.
2. In order to monitor the incidence of spontaneous papilloma formation on lines 117 and 117/113, mice were monitored once every two weeks and lesion load was recorded.
3. In order to determine if LMP1^{CAO} acts as a tumour initiator, a minimal carcinogen treatment was performed on line 117 animals.

3.2 Histopathology Analysis

Tissues were collected, fixed in formalin, paraffin embedded and stained for histological examination. Dr Adrian W. Philbey, a trained pathologist, performed the pathological examination and interpretation of the sections.

Following histological examination, it was deduced that ears of 117 wild type mice showed a normal pathology whereas ears of line 117 transgenic mice showed a variety of phenotypes ranging from epidermal hyperplasia (stage 1-3, see fig.1.14 for staging) to keratoacanthomas (stage 3-5) to squamous cell carcinomas (stage 5)(fig.3.1). Keratoacanthomas are rapidly growing spontaneous lesions that resemble inverted papillomas that can regress spontaneously, whilst a squamous cell carcinoma is a neoplastic tumour of the squamous cells (flat, thin cells found on the outer layer of the skin). An ear classified as keratoacanthoma was described by the pathologist “as a proliferative epidermal mass consisting of a large irregular central crateriform depression, lined by hyperplastic stratified squamous epithelium and filled with keratin laminae, along with degenerate cells and scattered colonies of bacteria. Shallow islands of stratified squamous epithelium with central keratinisation extent into the surrounding dermis. Rupture of these islands with release of keratin into the dermis is associated with locally extensive infiltrates of neutrophils, macrophages, lymphocytes and

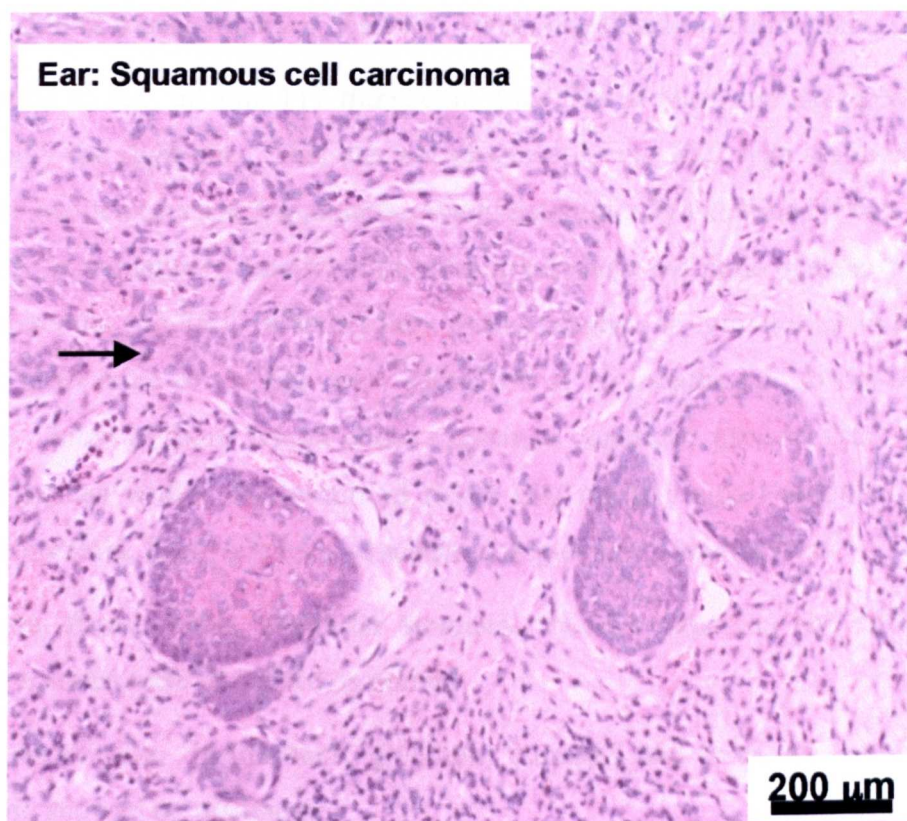


Figure 3.1: A Haematoxylin & Eosin staining of an ear of a transgenic mouse of line 117

An ear from a transgenic mouse of line 117 was fixed in formalin, embedded in paraffin, sectioned (2μm) and stained with haematoxylin and eosin. This section shows a squamous cell carcinoma. For example, the black arrow is indicating rupture of a keratin island indicative of progression to carcinoma.

plasma cells, along with fibrovascular hyperplasia and fibrosis.” Many of the ears also showed ulcerative dermatitis accompanied by necrosis. The phenotype resembles trauma to the ear with secondary bacterial infection, as there is fibrovascular hyperplasia of the dermis along with neutrophils and other inflammatory cells. Lesions that spontaneously developed on the dorsal skin of transgenic mice of line 117 were classified as acanthomas.

By 8 months of age, all line 117 transgenic mice had at least one enlarged cervical lymph node, usually the right one. This was not observed in the wild type siblings. When several samples of swollen cervical lymph nodes were histologically examined it was shown that they were mildly or moderately reactive indicating hyperplasia but none of them were classified as a lymphosarcoma (fig.3.2). Whether they would progress to lymphomas in older mice is not known as most mice of the line were sacrificed at 16 months due to the extent of the ear phenotype. Most of these lymph nodes examined contained pseudocysts, which consist of expanded spaces within the lymphoid tissue that contain small amounts of eosinophilic proteinaceous fluid, fibrin strands and scattered degenerate lymphocytes.

Oesophagus, forestomach, glandular stomach, trachea, pancreas and spleen of line 117 transgenic animals were described as normal.

Tongue, oesophagus, forestomach, glandular stomach and liver, of line 105B transgenic animals also showed no pathology.

Tongue, trachea, oesophagus, salivary gland, stomach and pancreas of one transgenic mouse of line 105A showing the wasting phenotype, were described as normal. However, lymph nodes, thymus, spleen, liver, glandular stomach and the junction of forestomach and glandular stomach of another transgenic mouse of line 105A exhibiting the wasting phenotype, were described as showing evidence of lymphosarcoma. The architecture of the tissues was replaced by dense sheets of large neoplastic lymphocytes that had large round nuclei, a high ratio of nucleus to cytoplasm and 10-20 mitoses per high power field. Macrophages were also seen that gave rise to a “starry sky” appearance. This was an individual case and the phenotype has not been followed for mice of this line as yet.

Most of the dorsal lesions collected and examined from line 117/113 were described as keratoacanthomas but on a single instance out of 5 cases examined, one of the larger lesions (size >4) was classified as a squamous cell carcinoma (Appendix 1).

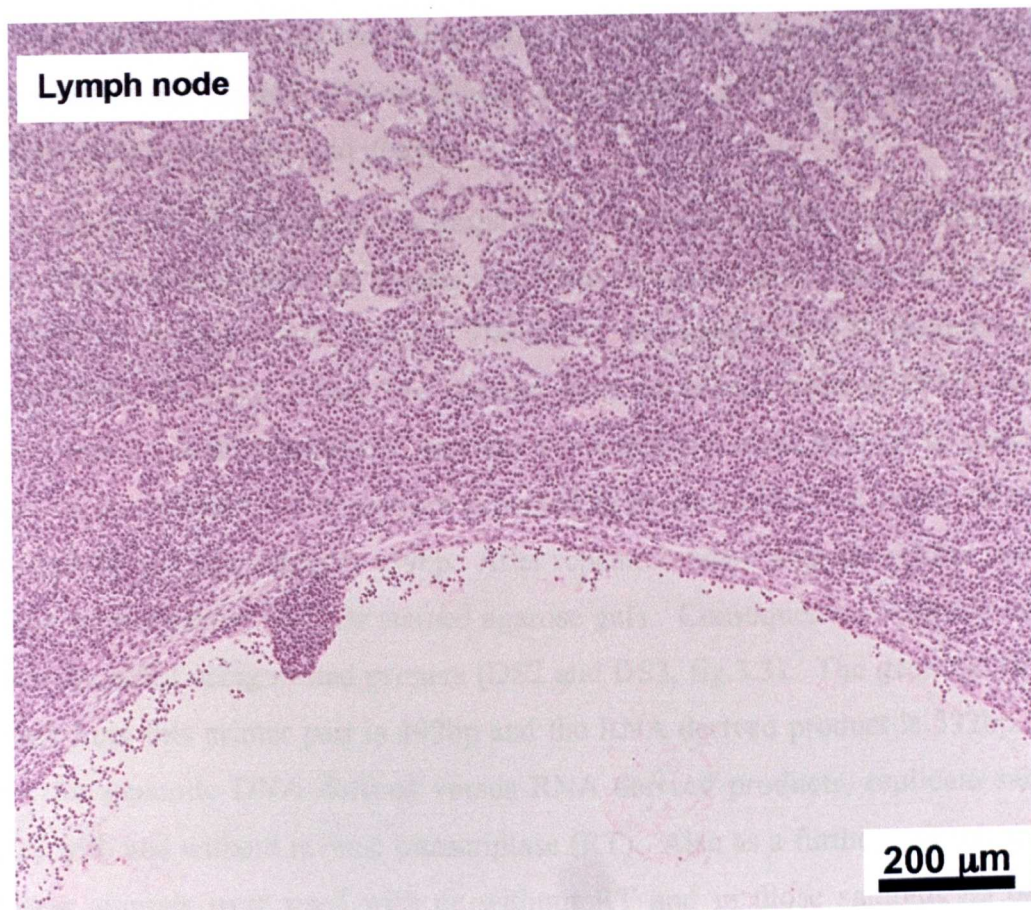


Figure 3.2: A Haematoxylin & Eosin stained section through an enlarged cervical lymph node of a transgenic mouse of line 117.

An enlarged cervical lymph node from a transgenic mouse of line 117 was fixed in formalin, paraffin embedded, sectioned (2 μ m) and stained with haematoxylin and eosin. The staining reveals lymphoid follicles with active germinal centers. There is mild expansion of lymphocytes in the paracortical zone and a moderate number of plasma cells in medullary cords. This lymph node is mildly hyperplastic.

3.3 LMP1 expression patterns in transgenic lines 117, 105A and 105B mice

3.3A RNA Expression

RNA was extracted from frozen tissue using Tri-Reagent™ or according to the method of Chomczynski and Sacchi (Chomczynski and Sacchi, 1987) (see section 2.2.5) using guanidium thiocyanate and acid phenol.

Initially the RT-PCR technique was employed to examine LMP1 specific RNA expression. Briefly, RNA obtained from the tissues was DNase I treated and used to make complementary DNA (cDNA) using a polydT primer. The cDNA was used in a PCR reaction using primers DS1 and DS4 (fig. 3.3). These two primers span the second exon of LMP1 and the small introns 1 and 2 and allow amplified genomic DNA and processed RNA to be distinguished by the size of the product. The product expected from genomic DNA using these primers is 599bp and the cDNA product is 439bp. After repeated assays with this primer pair, no visible products were detected on EtBr stained agarose gels. Consequently, a further amplification step was included using nested primers (DS2 and DS3, fig.3.3). The genomic DNA product expected from this primer pair is 492bp and the RNA derived product is 332bp. To further control for genomic DNA derived versus RNA derived products, replicate samples were assayed with and without reverse transcriptase (RT). Also as a further control, samples from wild type animals were used with or without RT and in those samples no bands of the appropriate size either from DNA or RNA products were observed. It was repeatedly observed that a 492bp band was seen in the RT samples but not in the no RT samples (eg. fig. 3.4 tongue). Despite the size, this suggested the product was derived from RNA and not from DNA contamination of the samples. It is possible that the 492bp band is derived from unprocessed nuclear LMP1 RNA. If this is the case, the transgene is expressed in these tissues but it is not clear to what degree the RNA is processed or translated. Some tissues yielded RT-PCR products of the expected size from an LMP1 RNA transcript (332bp). These include line 117 ears, heart, (fig. 3.4) and line 105A heart (fig. 3.5). The 492bp product was seen in line 117 tongue, lymph node, forestomach, lung and heart; line 105A ear, oesophagus (fig.3.5); line 105B thymus, spleen, forestomach, lymph node, ear, heart, lung, trachea, brain, glandular stomach and liver (fig.3.6). Due to DNA contamination in the samples from line 117 testicle, liver; line 105A lymph node, tongue, kidney, lung, testicle and liver no conclusion could be drawn for LMP1^{CAO} expression in these tissues. Blotting some of the gels and probing with an LMP1 probe did not reveal any other bands of the RNA product size.

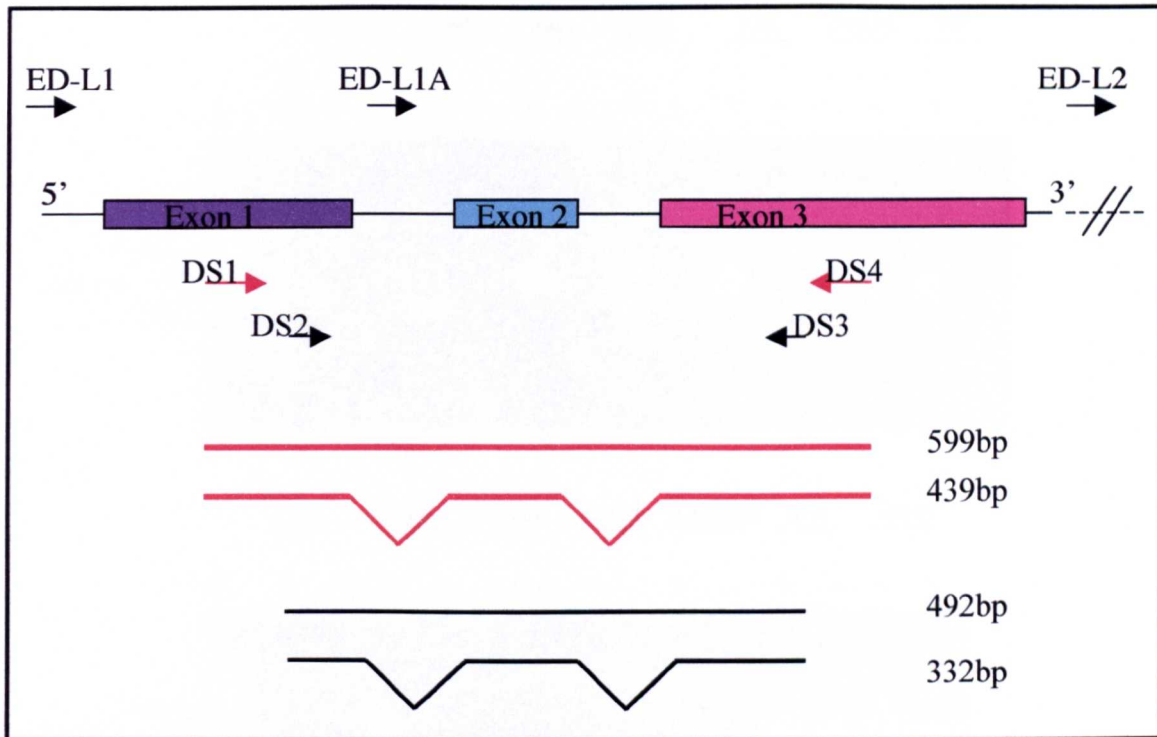


Figure 3.3: Diagram depicting the three exons of LMP1 and where the primer pairs used for RT-PCR correspond

Primers DS1 and 4 start at nucleotide 169474 and 168876 of exons 1 and 3 respectively. The DNA product expected from this pair is 599bp where as the cDNA product is 439bp. Nested primers DS2 and 3 start at nucleotide 169400 and 168909 of exons 1 and 3. The expected genomic DNA product from this pair is 492bp and the cDNA product is 332bp. The respective positions of the three LMP1 promoters are shown as EDL-1, 1A and 2. Note that the diagram is not to scale.

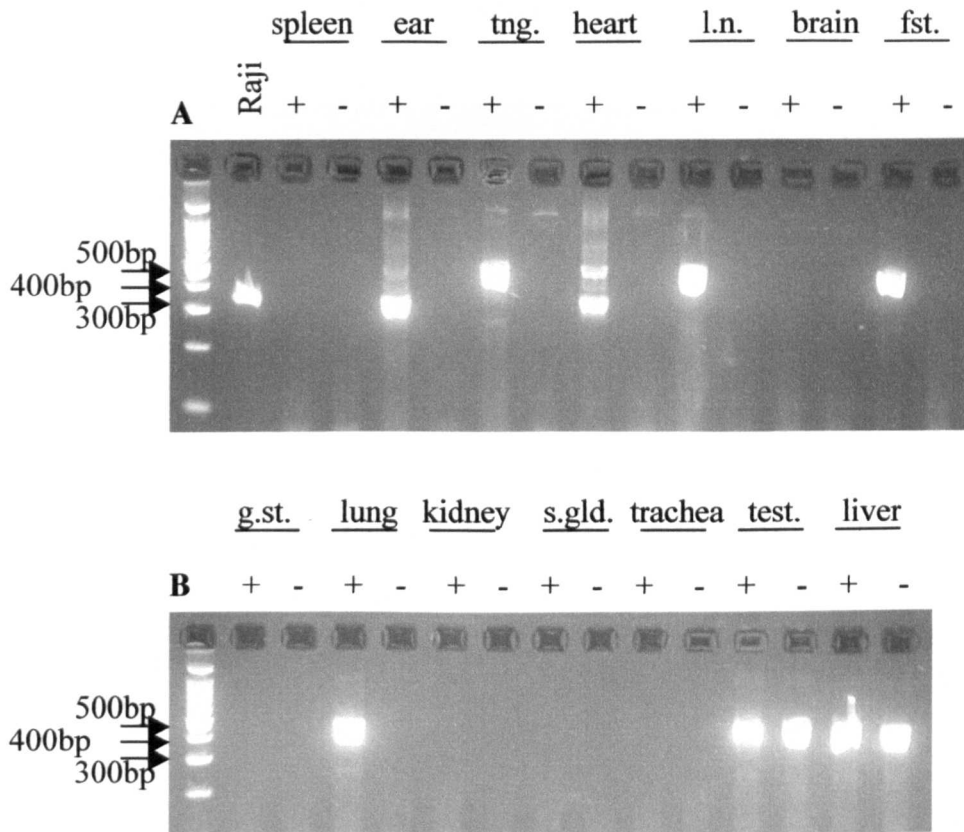


Figure 3.4: A nested RT-PCR of tissues from line 117

2% Nuseve, 1% agarose TBE gels stained with EtBr, showing the products of nested RT-PCR. Tissues from a transgenic animal of line 117 were used. RNA was extracted and DNaseI treated. A first round of amplification with primers DS1 and 4 was conducted, followed by a second round of amplification using nested primers DS2 and 3. A positive control (Raji) was included. RNA samples were incubated with (+) or without (-) RT. The RNA derived product should be seen at 332bp whilst any genomic DNA product should be seen at 492bp. Note that testes and liver samples show clear evidence of DNA contamination within the RNA sample as bands are evident in the no RT (-) tracks.
 tng. =tongue, l.n. = lymph node, fst. = forestomach, g.st. = glandular stomach, s.gld = salivary gland, test. = testes

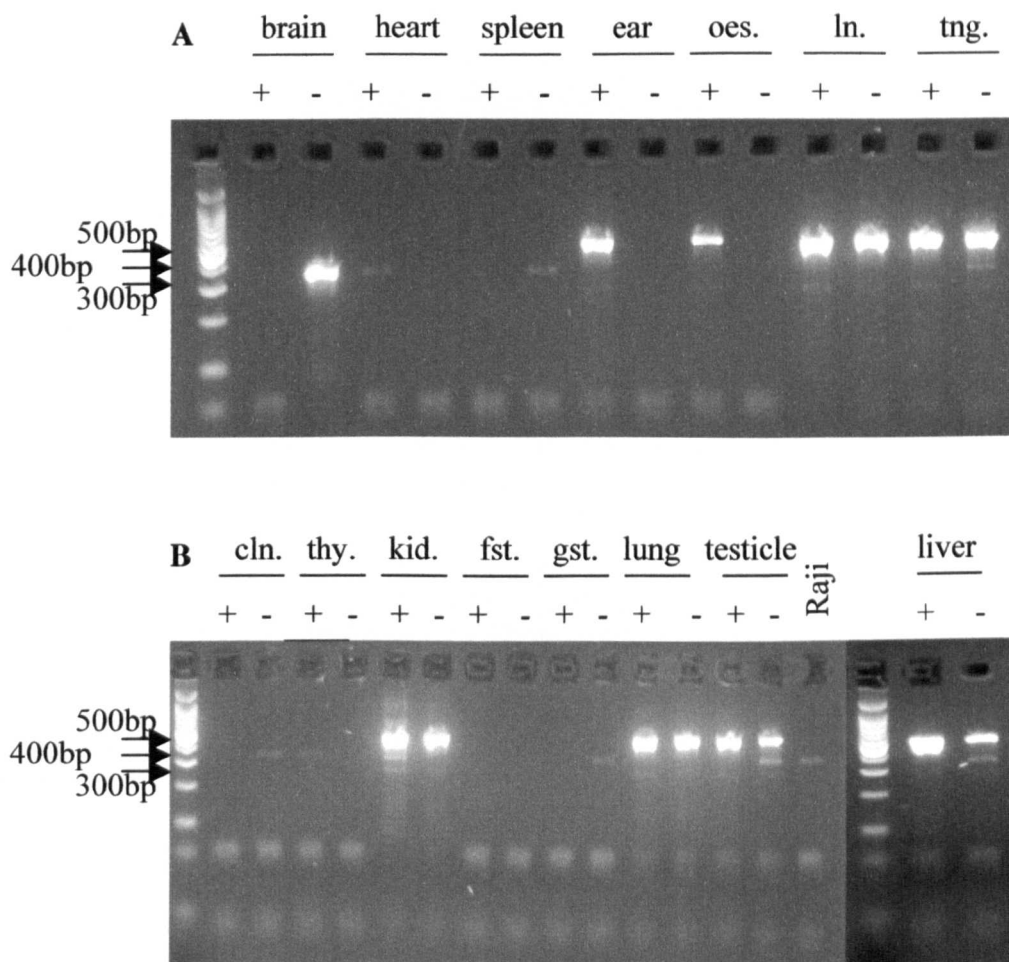


Figure 3.5: A nested RT-PCR of tissues from line 105A

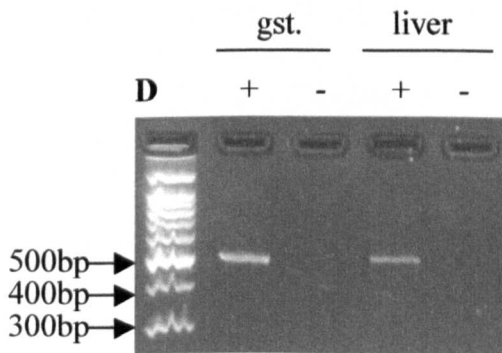
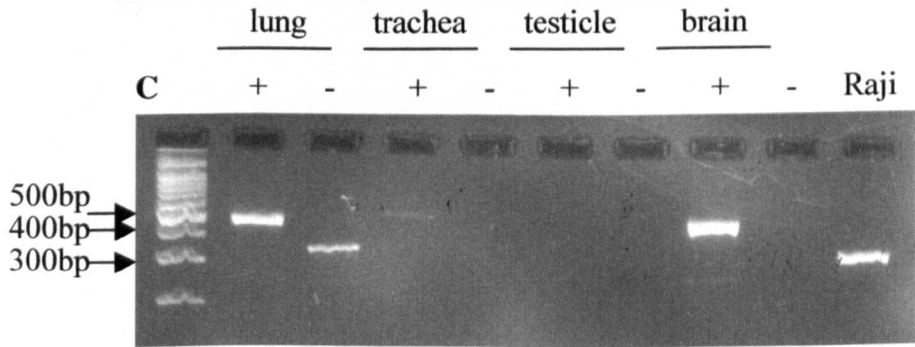
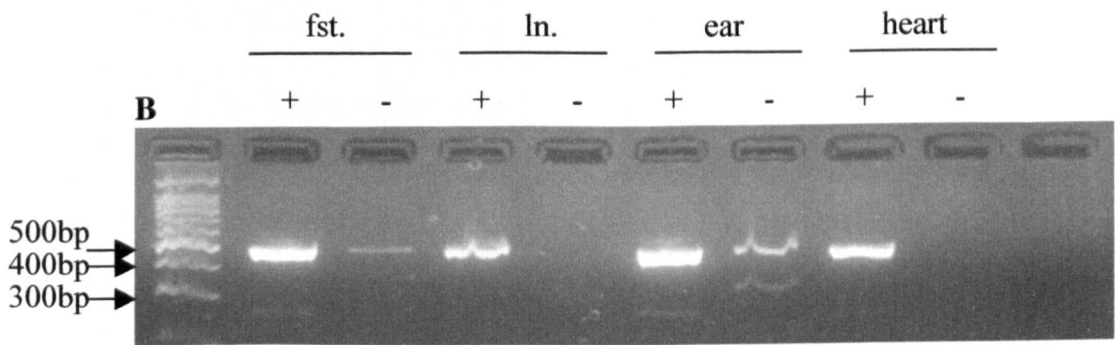
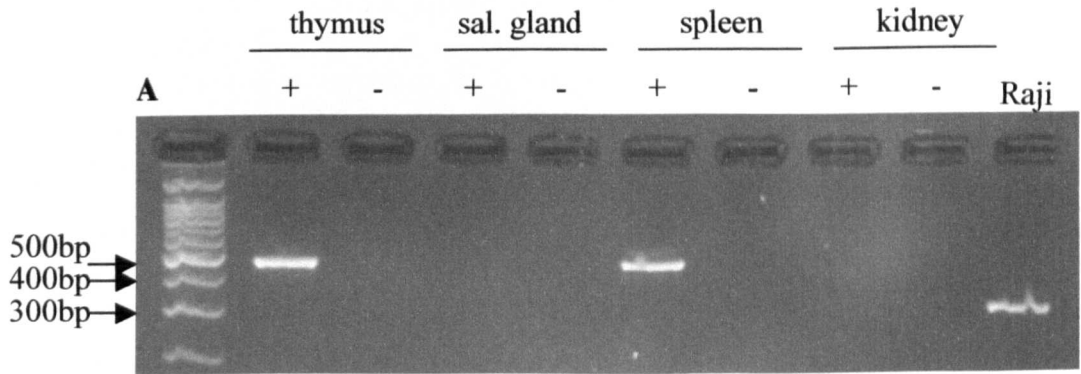
2% Nuseve, 1% agarose TBE gels stained with EtBr, showing the products of nested RT-PCR. Tissues from a transgenic animal of line 105A were used. RNA was extracted and DNaseI treated. A first round of amplification with primers DS1 and 4 did not give any visible products on an EtBr stained gel. A second round of amplification using nested primers DS2 and 3 gave the products shown. A positive control (Raji) was included. RNA samples were incubated with (+) or without (-) RT. The RNA derived product should be seen at 332bp whilst the genomic DNA product band should be seen at about 492bp. Note that lymph node, tongue, kidney, lung, testicle and liver samples show clear evidence of DNA contamination within the RNA sample as bands are evident in the no RT (-) tracks.

oes. = oesophagus, ln.= lymph node, tng. = tongue, cln. = cervical lymph node, thy. = thymus, kid.= kidney, fst. = forestomach, gst. = glandular stomach.

Figure 3.6: A nested RT-PCR of tissues from line 105B

2% Nuseve, 1% agarose TBE gels stained with EtBr, showing the products of nested RT-PCR. Tissues from a transgenic animal of line 105B were used. Two rounds of amplification as for lines 117 and 105A were used. RNA samples were incubated with (+) or without (-) RT. The RNA derived product should be seen at 332bp whilst the genomic DNA product band should be seen at about 492bp. Note that ear sample shows clear evidence of DNA contamination within the RNA sample as bands are evident in the no RT (-) tracks.

sal. gland = salivary gland, fst. = forstomach, ln.= lymph node, gst.= glandular stomach.



While this approach gave some indication of LMP1^{CAO} expression, due to persistent DNA contamination and the possibility of detecting unprocessed RNA it was not conclusive. Therefore, it was decided to investigate LMP1^{CAO} expression using Northern and Western blotting, to determine whether the unprocessed RNA was finally processed and translated.

Northern blotting is not as sensitive as RT-PCR. However, it was thought important to use it as RT-PCR was giving inconclusive results. Using Northern blotting, LMP1 expression is evident in the Raji positive control but not in Ramos negative control as expected. From the tissues examined, ear, tongue, forestomach, swollen lymph node, glandular stomach, heart, oesophagus and kidney show the 2.5kbp transcript corresponding to full length LMP1^{CAO} (fig.3.7). Lung, salivary gland and testicle show a smaller transcript. Note, that it was repeatedly observed in this lab that the Chomczynski and Sacchi method gave more and better quality RNA than the Tri-reagent™ for Northern blotting.

3.3B Protein expression

Standard protein extraction buffers such as RIPA buffer or boiling mix (see section 2.2.4) failed to yield detectable epidermal LMP1 as was seen from initial Western blotting experiments, even though these methods were efficient in extracting LMP1 from B cells. It is known that LMP1 co-localises with vimentin and possibly does so with the keratins of keratinocytes (Liebowitz et al., 1987). Keratins in skin become cornified and are difficult to solubilise, requiring denaturing extraction buffers. This may also be true of epidermal LMP1. Given these difficulties, it was decided to use extraction buffers that are used to detect keratins. Initially, three different buffers were used in a trial. The conventional keratin extraction buffer (8M urea, 5% 2ME, 25mM Tris, pH9.5), Shindai buffer (5M urea, 2.6M thiourea, 5% 2ME, 25mM Tris, pH 8.5) and a “New” buffer (9M urea, 2M thiourea, 2%CHAPS) (Nakamura et al., 2002) were used. Proteins were extracted from the samples in these buffers at 55°C overnight as detailed in section 2.2.4. Extracts were separated by SDS-PAGE, Western blotted and probed with anti-LMP1 antibodies.

Extracting LMP1 using the “New” buffer was the most successful in terms of specific versus non specific band detection (i.e. transgenic versus wild type tissue)(fig.3.8). However, the “New” buffer extracted the least amount of specific protein compared to the other two buffers used. Since the aim of these experiments was to detect LMP1^{CAO} expression in tissues, the buffer that extracted the most LMP1^{CAO} was chosen for further experiments and this was the conventional buffer.

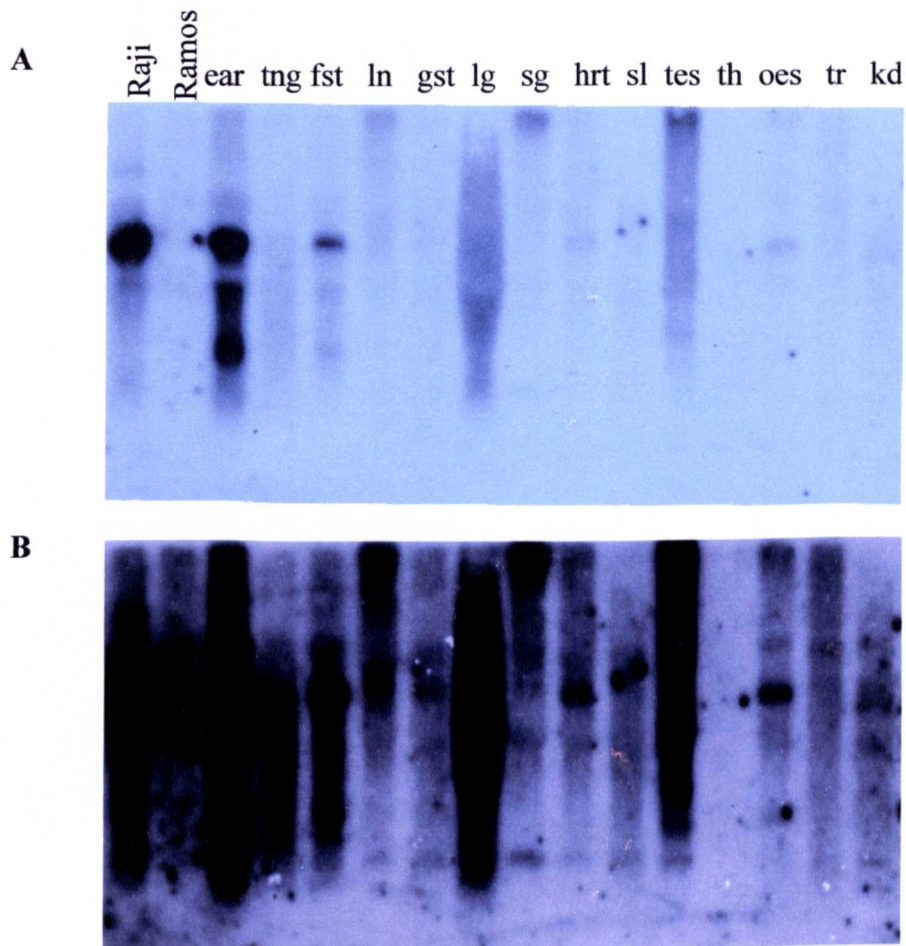
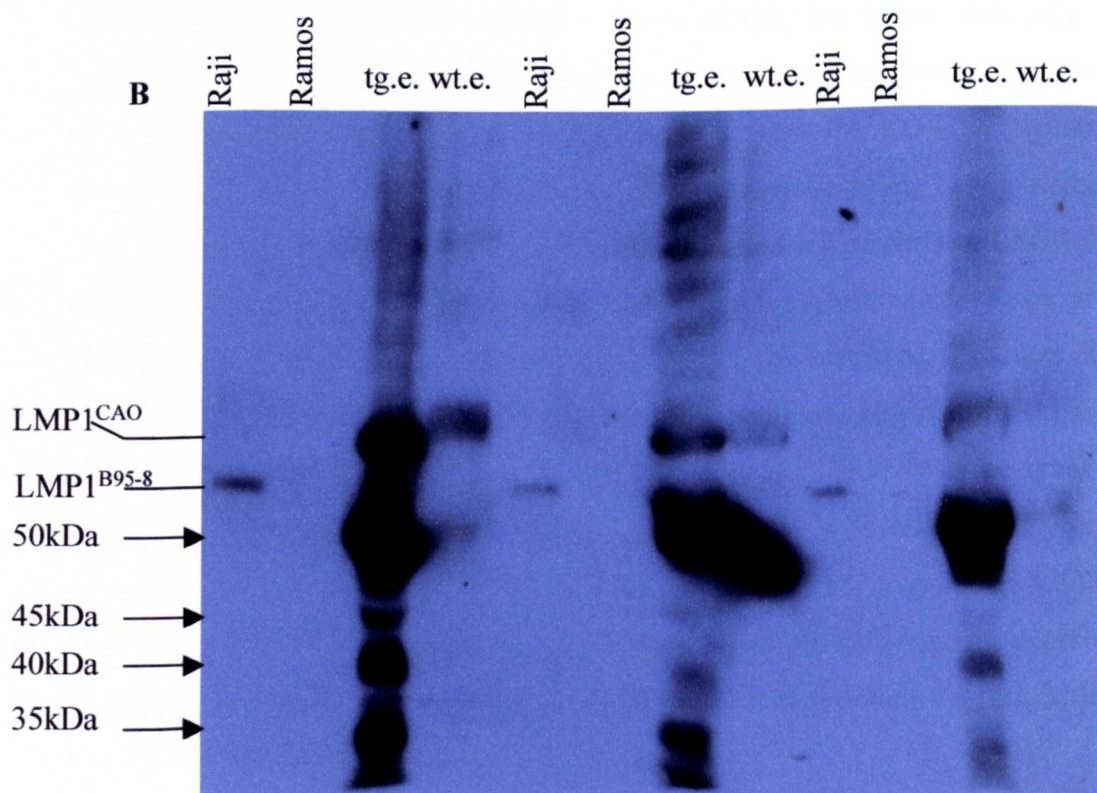
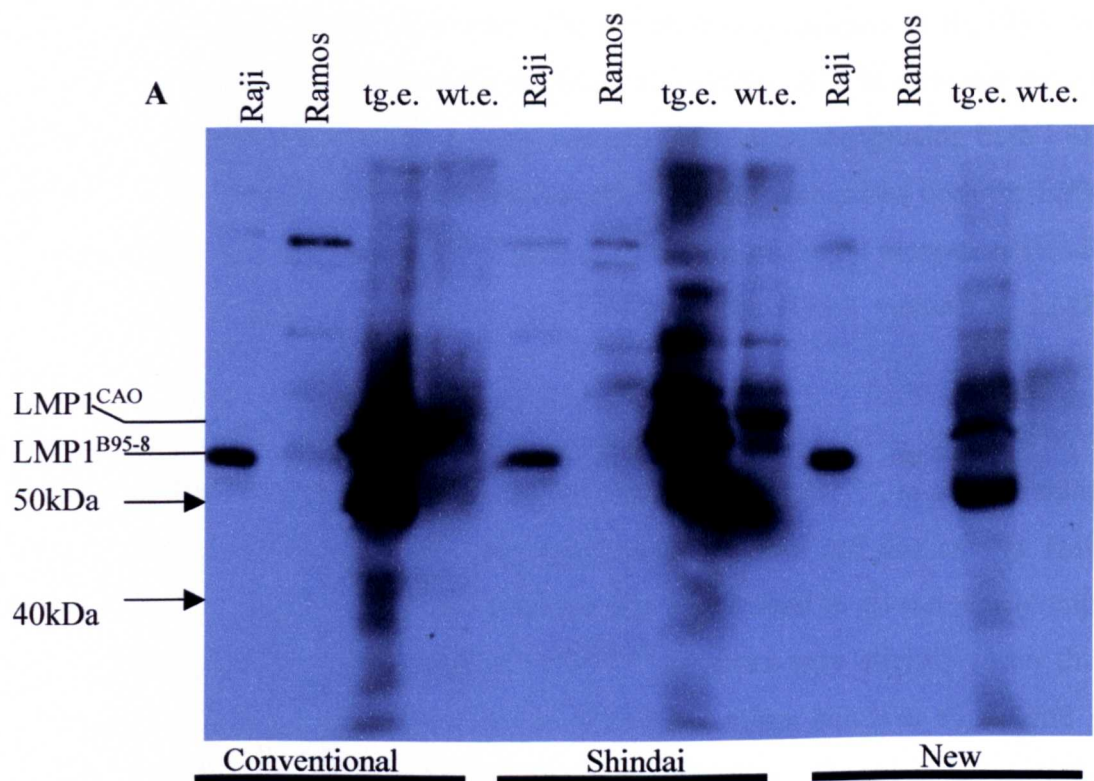


Figure 3.7: A Northern on tissues from a 117 transgenic mouse

20 μ g of total RNA extracted using the Chomczynski and Sacchi method, were electrophoresed through a 1% formaldehyde gel, transferred onto a nylon membrane and probed with an LMP1 specific probe (probe 139). A film was exposed to the blot for varying time periods and developed through an X-Omat developer. Raji positive control and Ramos negative for LMP1 control were included. Autorad A was underexposed whilst autorad B was overexposed. As can be seen, the 2.5 kb LMP1 transcript is observed in the Raji, ear, forestomach, glandular stomach, oesophagus, lymph node, heart, tongue, kidney. Lung, salivary gland and testicle show a smaller product. tng= tongue, fst= forestomach, ln= lymph node, gst= glandular stomach, lg= lung, sg= salivary gland, hrt= heart, sl = spleen, tes= testicle, th= thymus, oes= oesophagus, tr= trachea, kd= kidney.

Figure 3.8A and B: Western blot of trial extraction buffers probed with anti-LMP1 S12 (A) and 1G6 (B) antibodies

100µg of protein extract was separated by 10% SDS-PAGE and blotted. A Raji (EBV+ BL cell line) positive control, a Ramos (EBV - BL cell line) negative control, a 117 transgenic ear sample (tg.e) and a wild type ear sample (wt.e) were extracted with three different buffers; conventional, Shindai and “new” buffers were tested. Blot A was probed with the primary antibody S12 (1:500). The secondary antibody used was goat anti-mouse IgG-HRP (1:4000) and visualised with ECL+. The Western blot was stripped and re-probed with the 1G6 antibody (1:100)(B). The secondary antibody used was goat anti-rat IgG-HRP (1:4000) and visualised with ECL+. Transgenic and wild type tissue samples were electrophoresed in adjacent tracks to allow direct comparison. The Raji positive control gives an LMP1^{B95-8} specific band at 63kDa whilst the transgenic ear sample gives a band at 66kDa corresponding to LMP1^{CAO}. Smaller bands of about 50, 40 and 35kDa are also observed in the transgenic ear sample. Note, that there is a cross reacting band of about 67kDa observed in the transgenic and wild type ears irrespective of the method or antibody used for detection.



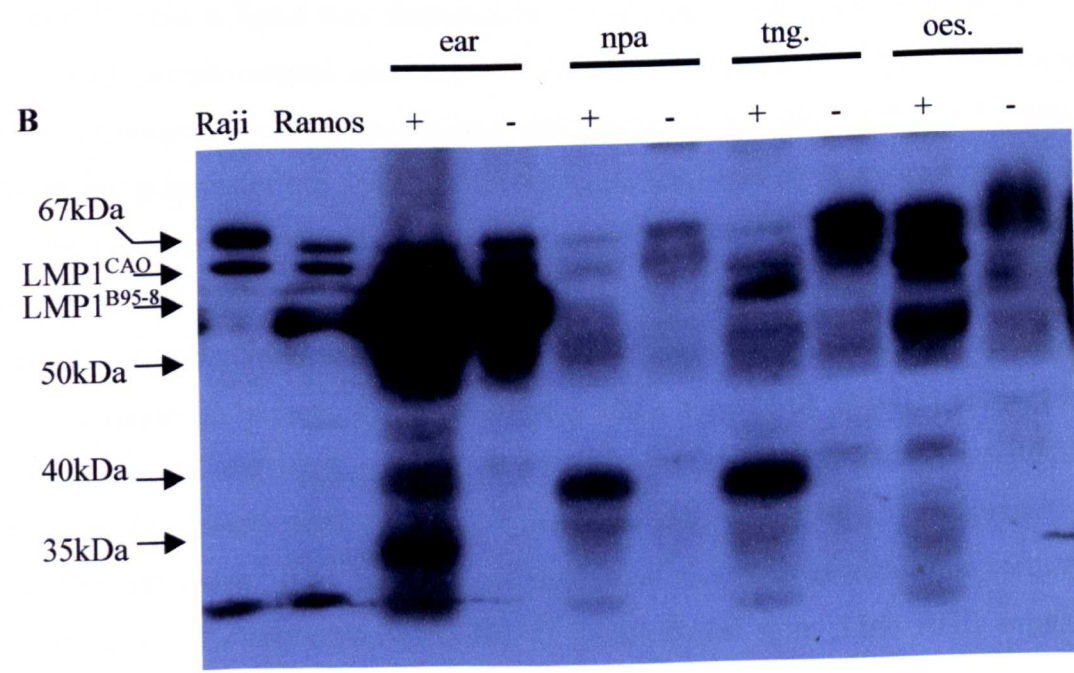
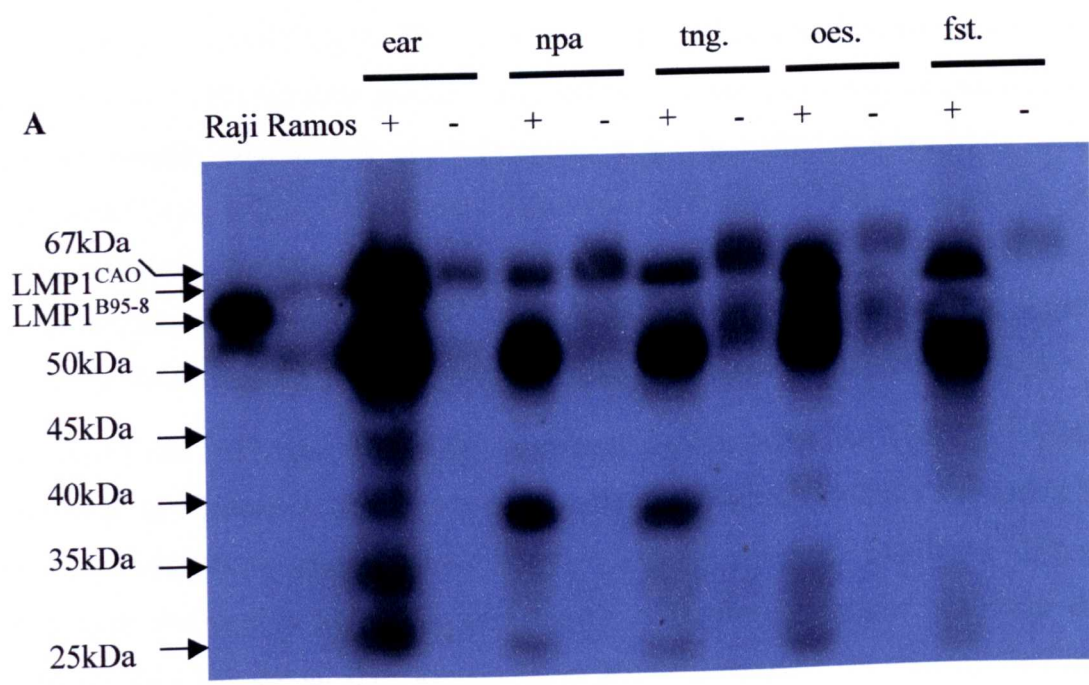
In order to confirm the results obtained from this Western blotting analysis, three different antibodies directed against LMP1 were used. These were S12 (Hennessy et al., 1984; Mann et al., 1985), 1G6 and the CAO cocktail (Nicholls et al., 2004). S12 is a mouse monoclonal IgG2a antibody directed towards the carboxy terminus of LMP1, recognising both LMP1^{CAO} and LMP1^{B95-8}. 1G6 is a rat monoclonal IgG2a antibody that recognises both the B95.8 and CAO version of LMP1. The CAO cocktail antibody consists of the rat monoclonal antibodies 5G5, 7F8 and 7D7. This cocktail does not recognise the B95.8 version of LMP1 but recognises CAO.

LMP1^{CAO} is larger than LMP1^{B95-8}, comprising 404 amino acids instead of 386 (Hu, 1991). As seen from fig.3.9, a band at about 66kDa, predicted for LMP1^{CAO}, is seen in transgenic ears, larger than the 63kDa band seen in the Raji positive control cell line extract. However, there is also a cross reacting band at about 67kDa that is observed in all samples (compare to wild type tracks) albeit at lower intensity. LMP1^{CAO} migrates very slightly faster than this band. Smaller products, a predominant one of 50kDa and minor bands at 40, 35 and 25kDa are observed with the S12, 1G6 and CAO cocktail antibodies. Bands at about 45kDa are observed with the 1G6 and the CAO cocktail. These smaller bands are seen only in the transgenic samples. As such they could either be cleaved products of LMP1, *in vitro* breakdown products or products derived from transcripts from the ED-L1A promoter of LMP1. Moorthy and Thorley-Lawson (Moorthy and Thorley-Lawson, 1990), detected a 25kDa cytoplasmic product that they demonstrated to be a cleaved product of LMP1. They also detected a 35kDa cell membrane product that was not always extracted. Since in these experiments 8M urea was used, this 35kDa product is likely to be extracted. Products derived from LMP1^{CAO} may be larger than LMP1^{B95-8} and therefore migrate slower through an SDS gel. Further reports (Baichwal and Sugden, 1987; Wang et al., 1985) describe breakdown products of 54kDa, 43kDa and 49kDa whereas a 52kDa product is described as the product derived from the ED-L1A promoter. Hudson *et al.*, also predicted LMP1 size to be 42kDa and the ED-L1A product to be 28kDa (Hudson et al., 1985). Given that subsequent experiments showed that LMP1^{CAO} migrates slower through an SDS gel it is possible that the LMP1^{CAO} ED-L1A product migrates at about 50kDa.

A prominent band of about 50kDa is observed in 117 transgenic ears (fig. 3.9). Identification of the 66kDa band was difficult at times due to the cross-reacting bands seen in both transgenic and wild type samples with the different antibodies used. However, reprobing blots with all 3 antibodies allowed the LMP1^{CAO}, 66kDa band, to be unequivocally identified. The

Figure 3.9A and B: Western blot of line 117 tissues using S12 (A) and CAO cocktail (B) antibodies

100µg of protein extract was separated by 10% SDS-PAGE and blotted. The primary antibody used in A was S12 ascites (1:500). The secondary antibody used was goat anti-mouse IgG-HRP (1:4000). The Western blot was stripped and reprobed with the CAO cocktail antibody (1:100) (B). The secondary antibody used was goat anti-rat IgG-HRP (1:4000). A positive control for LMP1 (Raji) and a negative control (Ramos) were used. Transgenic tissue samples (+) and wild type tissue samples (-) were electrophoresed in adjacent tracks to allow direct comparison. The 63kDa LMP1^{B95-8} band is seen in the Raji sample in A. The LMP1^{CAO} 66kDa band as well as further smaller products are seen in the transgenic ear extract but not in the wild type ear extract. The LMP1^{CAO} band is detected in nasopharyngeal area (npa), tongue (tng.), oesophagus (oes.) and forestomach (fst.). There is also a prominent 50kDa band that is present only in transgenic tissue extracts. A smaller product of about 40kDa is observed in the transgenic ears, npa and tng (A). No LMP1 specific band is observed in the Raji positive control in B as the CAO cocktail antibody does not recognise the LMP1^{B95-8}. A band at about 66kDa is clearly seen in transgenic tongue (tng.) and oesophagus (oes.) but not in wild type tissue. An extensive cross reacting band in ear sample does not allow ready detection of the LMP1^{CAO} band. Smaller bands of about 40kDa are clearly seen in transgenic ear, npa, tng. and oes. Note, that S12 cross reacts with a non specific protein at about 67kDa that is present in all tracks making it hard to identify the LMP1^{CAO} band in A. The CAO cocktail also cross reacts with non specific bands seen in the wild type samples (-) in B.



smaller products observed are possibly products of transcription of the lytic ED-L1A promoter or proteolytic products of LMP1^{CAO}, were much easier to identify and were only present in transgenic samples thus indicating that in that tissue LMP1^{CAO} or derivatives were expressed.

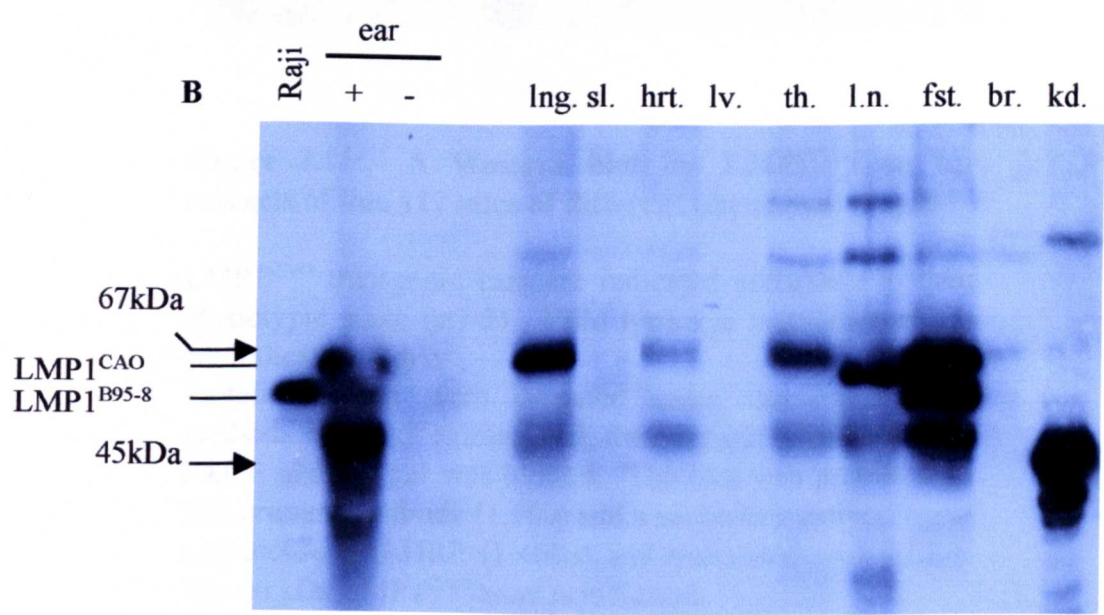
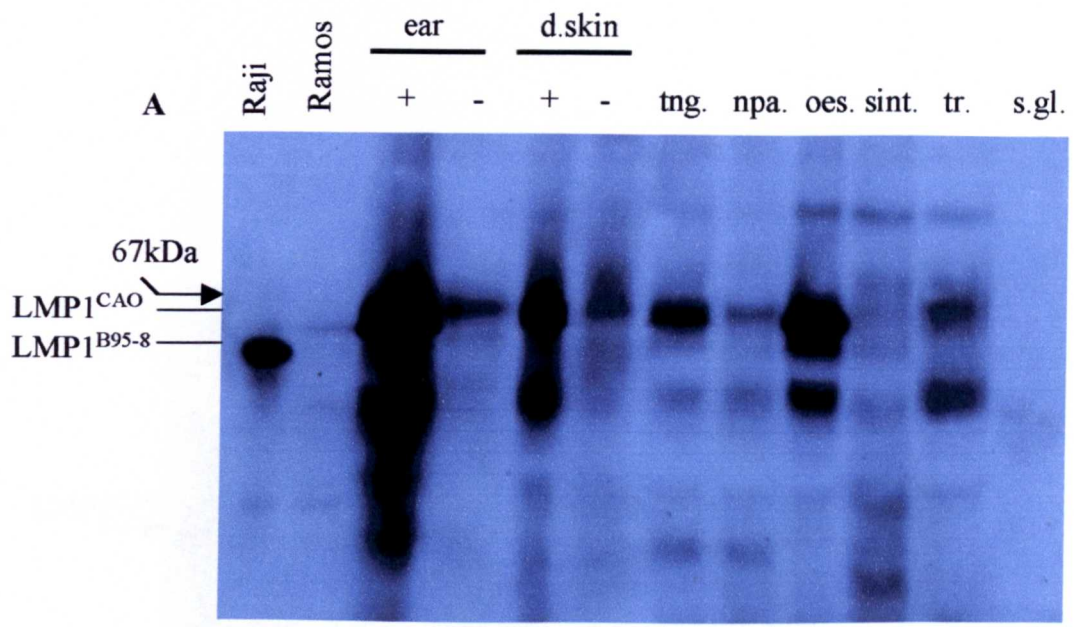
First tissues from line 117 were examined. The LMP1^{CAO} specific band at 66kDa is detected in transgenic ears, nasopharyngeal area, tongue, oesophagus, forestomach (fig.3.9), dorsal skin, swollen lymph node (fig.3.10B), testicle, thymus, kidney and small intestine (data not shown). Smaller LMP1 specific products are detected in transgenic ear, nasopharyngeal area, tongue, oesophagus, forestomach (fig.3.9), dorsal skin (fig.3.10A), trachea (data not shown), lung and heart (fig.3.10B). The strongest expression of LMP1^{CAO} 66kDa band was observed in transgenic ears. In order to examine if this expression varied with age and phenotypic stage, ear extracts of phenotypic stages 1-3 were examined (fig.3.11). From that examination, it was concluded that LMP1^{CAO} expression is strong irrespective of phenotypic stage.

Tissues from lines 105A and B were also examined. In line 105B, the LMP1^{CAO} 66kDa band was observed in transgenic ears, trachea, oesophagus, tongue, glandular stomach (fig.3.12) forestomach, nasopharyngeal area and testicle (data not shown). Smaller LMP1 specific products were observed in transgenic ears, trachea, oesophagus, tongue, glandular stomach, forestomach (fig.3.12), dorsal skin, kidney, heart and thymus (data not shown). In line 105A, the LMP1^{CAO} 66kDa band was detected in transgenic oesophagus, forestomach, tongue (fig.3.13) and nasopharyngeal area (data not shown). Smaller LMP1 specific products were observed in transgenic trachea, lung, kidney and heart (data not shown). Table 3.1 summarises the expression patterns of the tissues of the different lines that show expression of LMP1^{CAO} and related products by using all three antibodies (fig.3.9, 10, 12, 13). The expression pattern shows consistency with the phenotype. For example, line 117 and 105B animals show a hyperplastic ear phenotype whereas line 105A animals do not. This is consistent with LMP1^{CAO} expression as only ears of 117 and 105B transgenic animals show LMP1^{CAO} expression whereas line 105A ears do not. Line 117 transgenic animals consistently show enlarged cervical lymph nodes and this is in agreement with LMP1^{CAO} expression in the expanded lymph nodes. Also line 117 animals show spontaneous papilloma formation and this is consistent with expression of LMP1^{CAO} in the dorsal skin. Line 105B animals show spontaneous papilloma formation but to a lesser extent and much later in life and this is consistent with the lower level of LMP1^{CAO} expression in this line compared to line 117. Note that the western blots shown are representative samples of several repetitions with all transgenic positive samples showing the specific pattern of expression.

Figure 3.10A and B: Western blot of line 117 tissues using anti-LMP1 S12 antibody.

100µg of protein extract was separated by 10% SDS-PAGE and blotted. The primary antibody used was rabbit anti-mouse LMP1 S12 ascites (1:500). The secondary antibody used was goat anti-mouse IgG-HRP (1:4000). A positive for LMP1 control (Raji) and a negative control (Ramos) were used. Transgenic tissue samples (+) and wild type tissue samples (-) were electrophoresed in adjacent tracks to allow direct comparison. The 63kDa LMP1^{B95-8} band is seen in the Raji samples. The LMP1^{CAO} 66kDa band as well as further smaller products are seen in the transgenic ear extract but not in the wild type ear extract. The LMP1^{CAO} band is detected in ear, dorsal skin (d.skin), trachea (tr), lung (lng.) and heart (hrt.). There are also smaller breakdown products of about 50kDa and 45kDa observed in transgenic ear, d.skin, oesophagus (oes.) and forestomach (fst.) tissue extracts. An extensive cross reacting band that runs at about 67kDa makes identification of the 66kDa LMP1^{CAO} band extremely hard.

Tng. = tongue. npa.= nasopharyngeal area, sint.= small intestine, s.gl.= salivary gland, sl. = spleen, lv.= liver, th.= thymus, l.n. = lymph node, br. = brain, kd. = kidney.



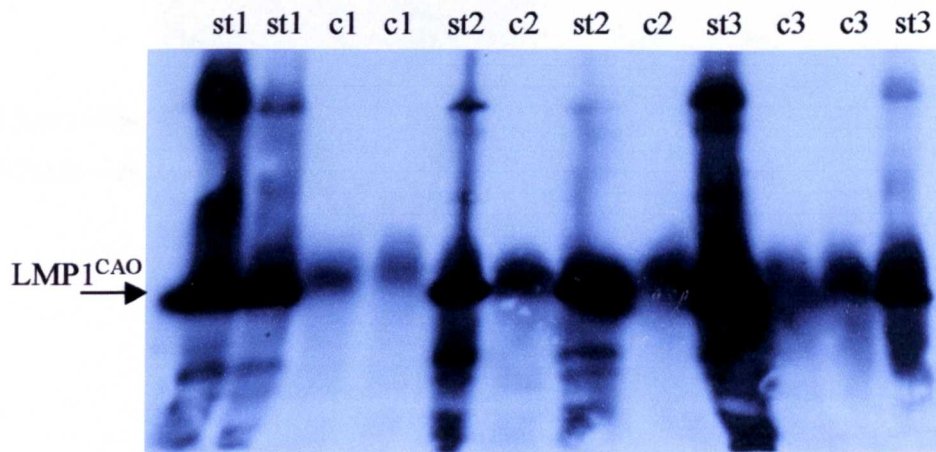


Figure 3.11: A Western blot for LMP1^{CAO} on ear extracts of line 117 mice of different phenotypic stages

LMP1^{CAO} transgenic ears are indicated according to their phenotypic stage (st1-3) . Wild type age matched controls are indicated with c.

Protein extracts were prepared using the conventional method. 100µg of extract/track were separated by 10%SDS-PAGE and the gel was blotted. The blot was probed with S12 primary antibody (1:500) and a secondary antibody goat anti-mouse IgG-HRP (1:4000) and visualised with ECL⁺. The 66 kDa LMP1^{CAO} band is indicated.

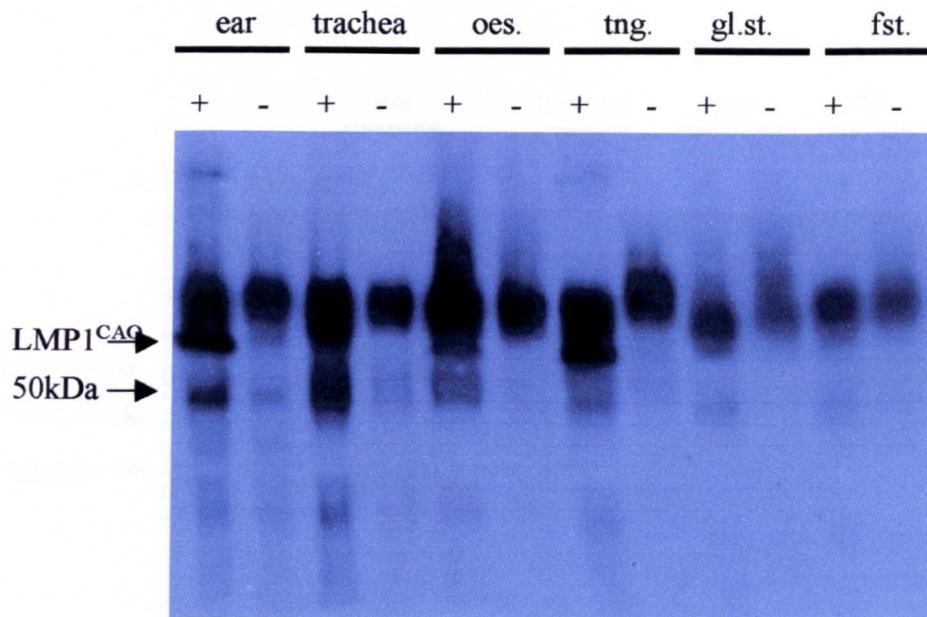


Figure 3.12: Western blot of line 105B tissues using S12 antibody

Protein was extracted using the conventional extraction buffer. 100µg of protein from both transgenic (+) and wild type (-) tissues was separated by 10% SDS-PAGE and blotted. Primary antibody used was rabbit anti-mouse S12 ascites (1:500). The secondary antibody was goat anti-mouse IgG-HRP (1:4000). A band at 66kDa corresponding to LMP1^{CAO} is detected in the transgenic ears, trachea, oesophagus (oes.), tongue (tng.) and faintly in the glandular stomach (gl.st.) and forestomach (fst.). There is also a 50kDa band present in transgenic ears, trachea, oesophagus, tongue and faintly in transgenic glandular stomach and forestomach.

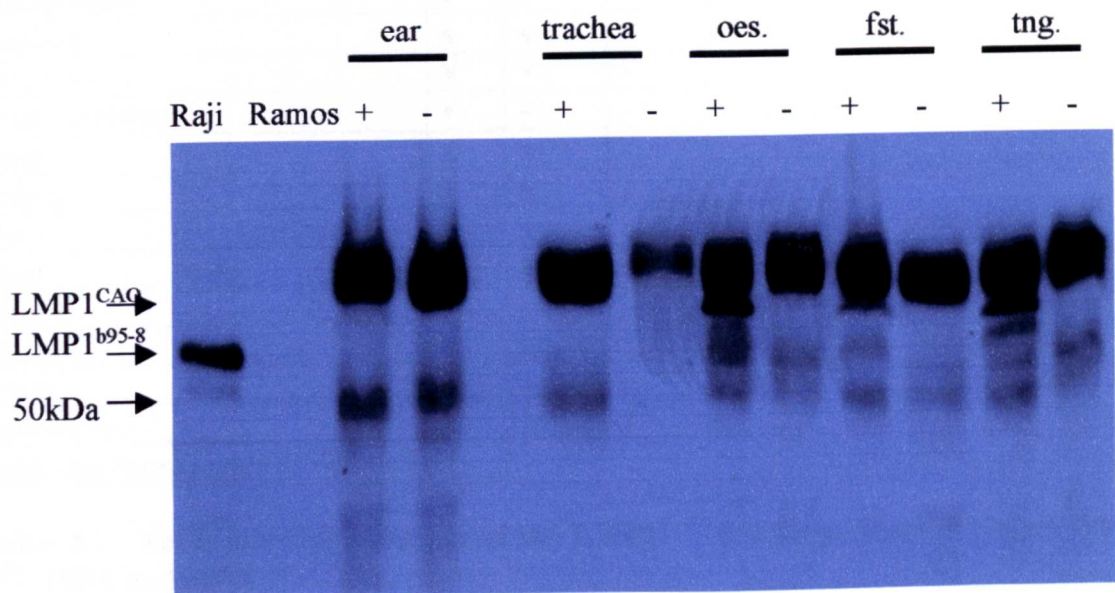


Figure 3.13: Western blot of line 105A tissues using S12 antibody

Protein was extracted using the conventional extraction. 100µg of protein from both transgenic (+) and wild type (-) tissues were separated by 10%SDS-PAGE and blotted. The primary antibody used was rabbit anti-mouse S12 ascites (1:500). The secondary antibody used was goat anti-mouse IgG-HRP (1:4000). A positive control (Raji) and a negative control (Ramos) were included. The 63kDa LMP1^{B95-8} band is seen in the positive control. No 66kDa LMP1^{CAO} can be detected in transgenic ears and this is consistent with the phenotype of this line. The 66kDa LMP1^{CAO} is clearly detected in transgenic oesophagus (oes.), forestomach (fst.) and tongue (tng.).

Tissue	117	105A	105B
Ear	√	-	√
Dorsal skin	√	-	s
Tongue	√	√	√
Nasopharyngeal area	√	√	√
Salivary gland	-	-	-
Oesophagus	√	√	√
Trachea	s	s	√
Forestomach	√	√	√
Small intestine	√	-	-
Lung	s	s	-
Kidney	√	s	s
Heart	s	s	s
Liver	-	-	-
Spleen	-	-	-
Thymus	√	nt	s
Brain	-	-	-
Testes/ovary	√	nt	√
Expanded lymph node (117 only)	√		

Table 3.1: Table showing presence of the LMP1^{CAO} 66kDa product in tissues from lines 117, 105A and 105B.

This table gives a summary of all the LMP1 products either full length or smaller that have been detected using the various antibodies.

The symbol (√) indicates presence of the LMP1^{CAO} 66kDa product. The letter (s) indicates expression of smaller LMP1 specific products detected in the absence of detection of the 66kDa product. The symbol (-) indicates that no LMP1 expression was detected.

(nt) = not tested.

3.4 Spontaneous papilloma formation on lines 117, 117/113 and 117/113/1205

It has been well documented that mice from different genetic backgrounds have a different susceptibility to developing lesions after topical chemical carcinogen treatment and have different resistances to malignant conversion of such lesions. Studies have indicated that FVB strain mice that developed cutaneous papillomas following chemical carcinogen treatment were much more prone to show malignant conversion to carcinomas than C57BL/6 mice (DiGiovanni et al., 1991; Hennings et al., 1993). In our lab, it was noted that when line 117 mice were brought into an FVB background (backcross 2, approx. 75% FVB), 40% of the mice spontaneously developed cutaneous papillomas. Initially the line 117 colony was maintained in a C57BL/6 background and no papilloma formation was observed.

In order to characterise this observation further, a cohort of 21 transgenic and 10 wild type 117 mice at backcross 3 (87.5% FVB) were monitored from 6 weeks of age up to 65 weeks of age for spontaneous papilloma formation. The mice were monitored once every fortnight and the lesion load was recorded in size categories as shown in table 3.2. Note that this categorisation is subjective, however it should be internally consistent.

Category	Lesion diameter
Size 1	<0.2 cm
Size 2	0.2-0.5 cm
Size 3	0.5- 1.0 cm
Size 4	>1.0 cm

Table 3.2 Categorisation of lesions by size

Of the 21 transgenic mice in the study, a total of 12 (57.14%) transgenic mice had developed papillomas by the end of the study (fig.3.14A). No papillomas developed on the wild type siblings throughout the study period. Of these 12 mice that did develop papillomas the average maximum number of papillomas per mouse was 2.58. The first onset of papillomas was at 6 weeks of age. The papillomas that formed remained small, mostly in category 1 (fig. 3.14B,C). Note that the severity of the ear phenotype, necessitated removal of animals from the study at different time points. Sudden drops on the curve indicate that papillomas

A

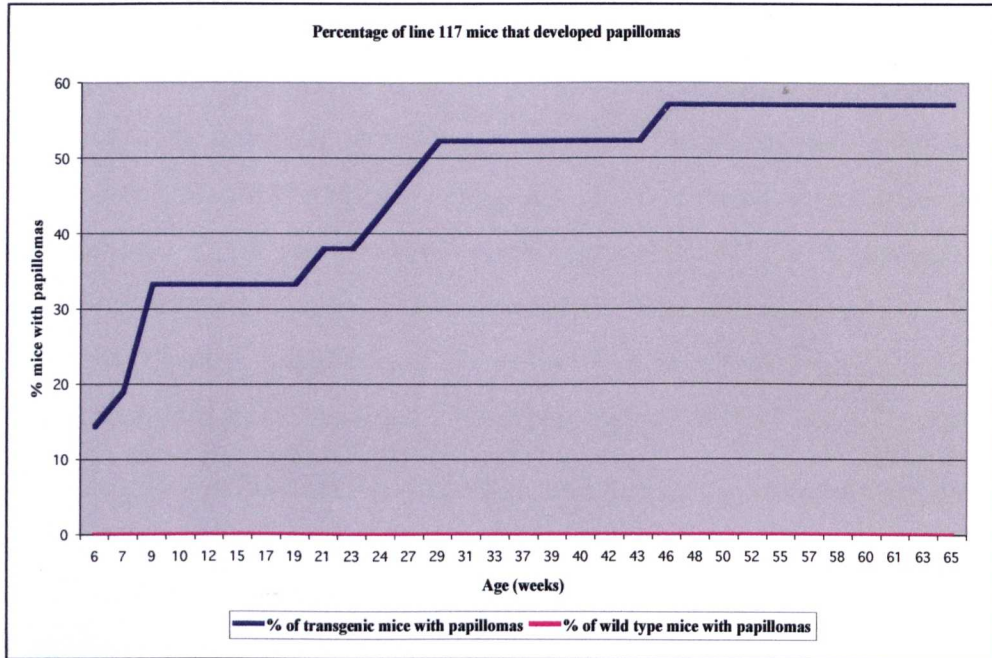


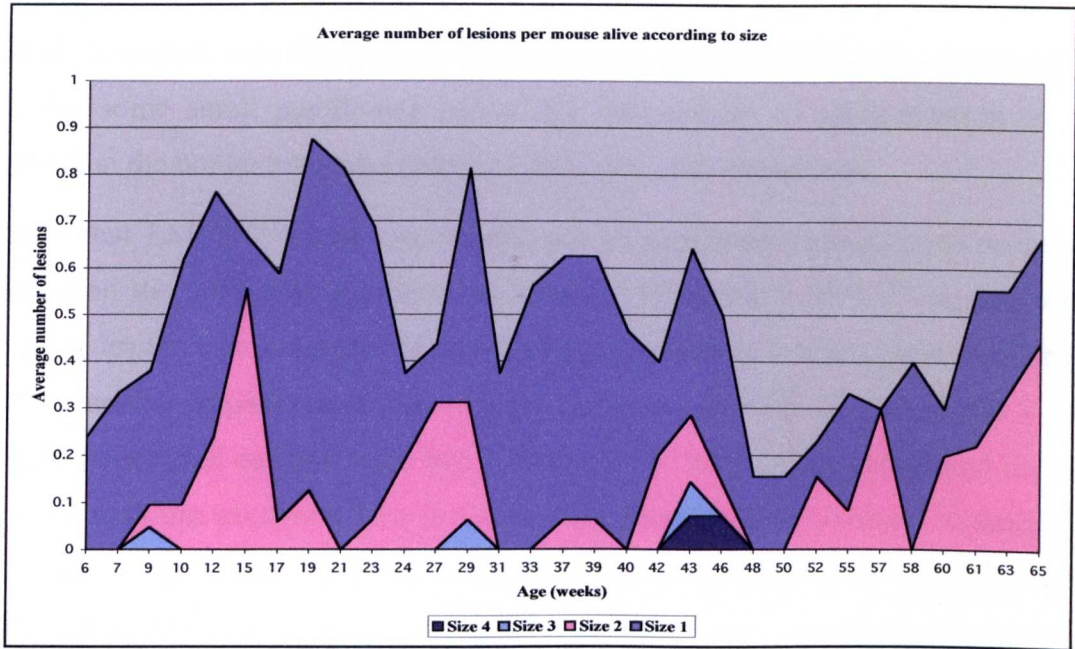
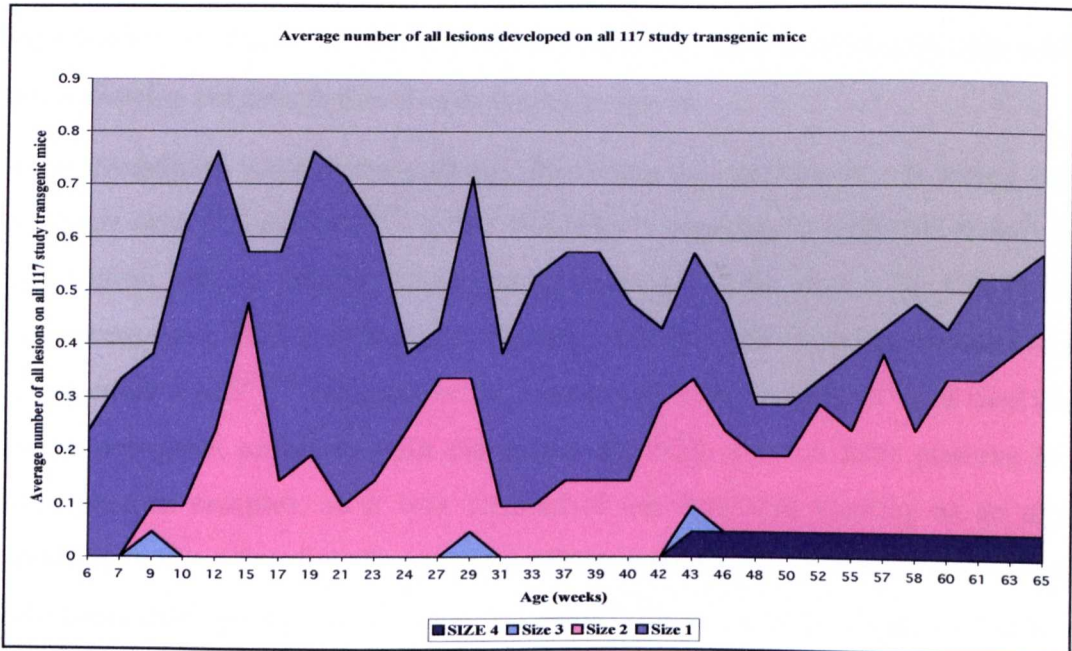
Figure 3.14: Development of spontaneous cutaneous lesions in mice of line 117

21 transgenic and 10 wild type siblings of line 117 mice, were monitored for 59 weeks (from 6 weeks old) for the appearance of cutaneous lesions.

A) The percentage of mice developing a lesion through the study period is shown, at the age of first lesion appearance. Transgenic mice are shown by a blue line and wild type mice are shown by a pink line.

B) A graph showing the average (mean) number of lesions per mouse alive at each weekly count according to lesion size; size 1 (purple), size 2 (pink), size 3 (light blue), size 4 (dark blue). Note that sudden drops indicate papilloma regression or removal of a mouse bearing lesions from the study.

C) A graph showing the cumulative average (mean) number of all lesions that developed on all transgenic mice during the study according to size; size 1 (purple), size 2 (pink), size 3 (light blue), size 4 (dark blue). In this representation, if a mouse was removed from the study, its lesion load is shown as a constant to the end of the study period. As such, drops in the average lesion load represent lesion regression.

B**C**

regressed or changed size category or that a mouse that had papillomas was withdrawn from the study. In order to allow for this, the cumulative lesion load is shown in the graph in fig.3.14C in which the lesion load of a mouse at the time of removal from study is shown as a constant to the end of the study period. As seen from this graph (fig. 3.14C) some lesions regressed. However, some fluctuation in the count can also be attributed to experimental error in missing some small papillomas and to the subjectivity of categorisation of a lesion particularly at the border between categories from one week to the next.

It is seen that LMP1^{CAO} alone can pre-dispose to papilloma formation as no papillomas developed on the wild type sibling control mice. However, LMP1^{CAO} on its own is not sufficient to lead to a large number of papillomas per mouse or to many large papillomas. The maximum number of papillomas that a mouse on this study ever developed was 4 (although more have been noted on some mice not in this cohort). Most of the papillomas formed were size 1 or 2 with the exception of a few size 4 papillomas that developed towards the later stages of the study. Finally, no papillomas from the ones sent for pathological examination showed evidence of conversion to carcinomas but larger lesions (size>4) were not examined. Further details about the animals used in this study can be found in Appendix 2.

These results suggest that LMP1^{CAO} can initiate a proliferation pathway that leads to papilloma formation. However, this proliferation pathway must be limited as only a few small papillomas develop per mouse that do not readily progress.

In order to investigate whether the pathway that limits this proliferation is acting via INK4a locus products (p16^{INK4a} and p19^{ARF}), line 117 mice were crossed with INK4a null, line 113 mice (see section 1.8). In order to determine the genotype of the mice at the INK4a locus two techniques were used, PCR and Southern blotting. For the PCR reaction, two sets of primers recognising either a p16^{INK4a} fragment or the neomycin insertion cassette, were used (fig.3.15). There were persistent problems with the neomycin PCR, since a false positive band was frequently seen in samples, so it was decided to use Southern blotting as an alternative genotyping method. After digesting genomic DNA with several enzymes, and probing with an INK4a containing probe, it was shown that *Bam*HI digest gave the clearest results. A band at about 2.8kbp is observed in wild type samples, this band is observed in heterozygotes at half the intensity and no band is seen in the null (fig.3.16). However, due to unequal loading and the fact that distinguishing wild type from heterozygote was based on band intensity, it

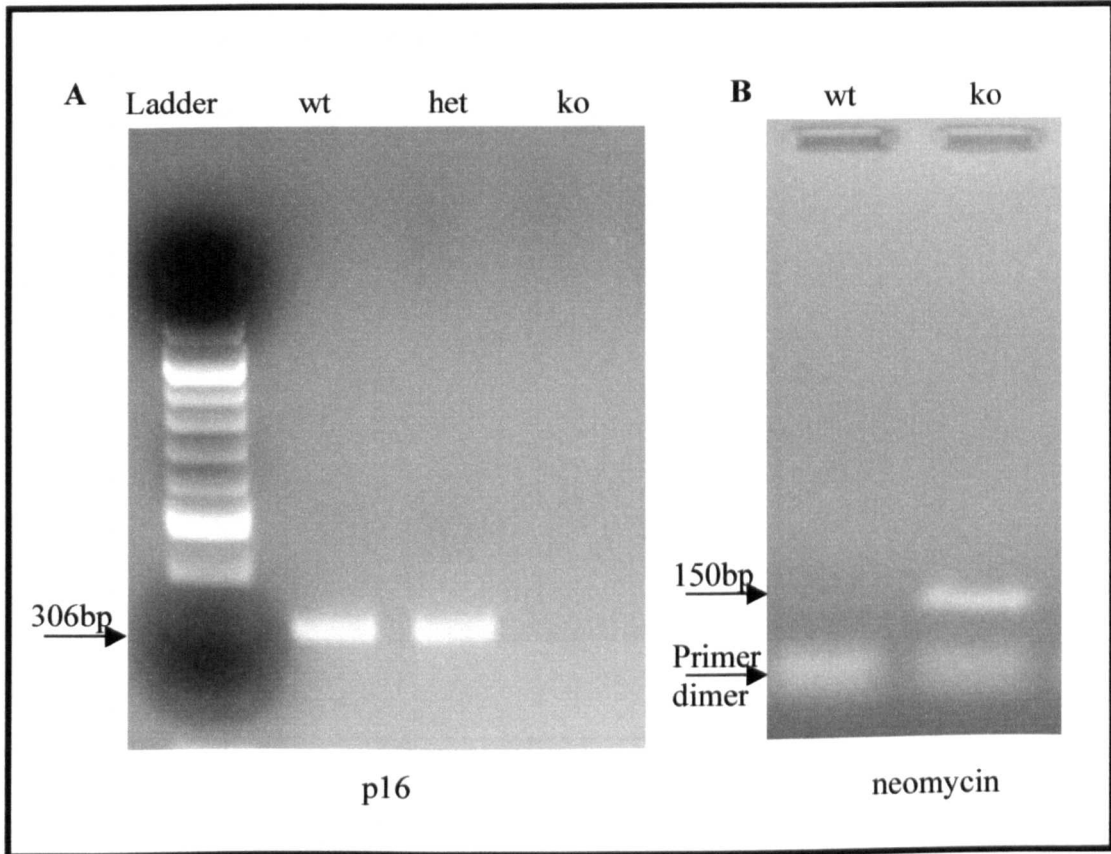


Figure 3.15: Genotyping of line 117/113 mice using PCR

300 ng of genomic DNA are used along with p16 (A) or neomycin (B) primers for PCR assays. 10 μ l of the product were run on a 1.5% EtBr stained agarose gel. Gel A shows the DNA ladder along with PCR samples using p16 primers for wild type (wt), heterozygous (het) or knock out (ko) mice for the INK4a locus. The 306bp product of the p16 primers is indicated and is observed in wt and het samples only.

Gel B shows the PCR samples with neomycin primers for wt and ko mice for the INK4a locus. The 150bp product of the neomycin primers is indicated and is observed in the ko sample only. Presence of the p16 band only indicates wt, presence of both bands indicates het and presence of the neomycin band only indicates ko genotype.

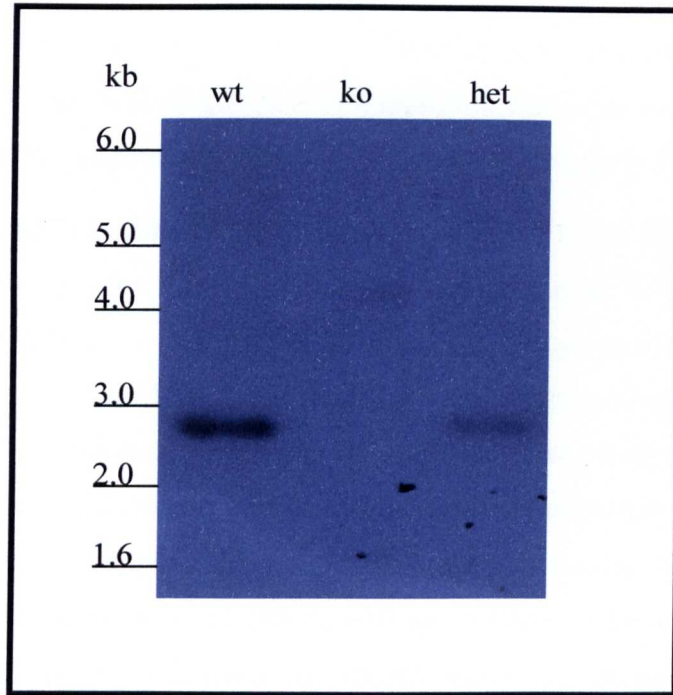


Figure 3.16: Southern blot genotyping of line 117/113

Genomic DNA (5 μ g) was digested with *Bam*HI overnight and separated by electrophoresis on a 0.8% agarose gel. A probe comprising exon 2 of the INK4a locus genes was used to detect wild type (wt), or heterozygous (het) samples. The wt or het band was observed at about 2.8kb. The knock out (ko) sample showed no such band. Note that the intensity of the band observed in the het sample, is less than the intensity of the band observed in the wt sample. This banding pattern was repeatedly observed on a number of known control samples. The Southern gel showed equal DNA loading of similar quality in all tracks shown in this figure.

was quite hard to reliably determine whether genomic DNA displaying that band corresponded to a wild type or a heterozygous mouse. As a consequence it was decided to group wild type and heterozygous for INK4a mice together in order to observe the effects of the null on lesion formation. Although this approach is not optimal, as there may be a heterozygous effect, it was the only approach that could reasonable be taken with this data set. 6 LMP1^{CAO} / INK4a null, 40 LMP1^{CAO} / INK4a heterozygous or wild type, 17 LMP1^{CAO} wild type / INK4a null and 40 LMP1^{CAO} / INK4a heterozygous or wild type mice, were monitored for spontaneous papilloma formation from 5 weeks of age to 70 weeks old.

No papillomatous lesions were formed on any of the mice that were wild type. The papillomatous lesions formed on LMP1 transgenic mice were grouped according to size as previously (table 3.2). As seen from figure 3.17, the average number of lesions developing on LMP1^{CAO} / INK4a null mice is always higher than the average number of lesions developing on LMP1^{CAO} / INK4a heterozygous or wild type mice. With the small number of mice in the null group it is difficult to conduct a meaningful statistical significance test at single time points. Using the nonparametric Mann-Whitney Confidence Interval and Test to compare the lesions that developed on all INK4a null and all INK4a heterozygous and wild type mice at weeks 9 and 28, no statistical significant difference between the two groups was found (P=0.5123 and 0.1262 respectively). However, as can be seen from the graph (fig.3.17), the average number of lesions that developed on the INK4 null mice was always more than the average number of lesions that developed on the INK4a heterozygous and wild type mice, throughout the study period (over 42 weeks while INK4a null were on study). If the values between the two groups were randomly distributed, it would be expected that from one sampling (week) to the next, either group could show the higher average. This is clearly not the case. In order to show this statistically a Runs Test was used comparing the distribution of a pattern over time. If the values in one group are consistently higher (or lower) than the other group, the Runs Test will evaluate the probability that this pattern can happen by chance. When a Runs Test was performed on the difference between the average number of lesions developed on INK4 null and INK4 heterozygous and wild type mice from week 5 to week 47 it is evident that there is a “single Run”. That is, at no time did the average for the INK4a null group fall below the average for the INK4a heterozygous and wild type group. As such P=0 and therefore the pattern between the two groups shows very high statistical significant difference. Only one of the 6 INK4a null mice did not develop any papillomas but was removed from study (due to lymphoma) early in the study at week 26. By contrast 8/40 (20%)

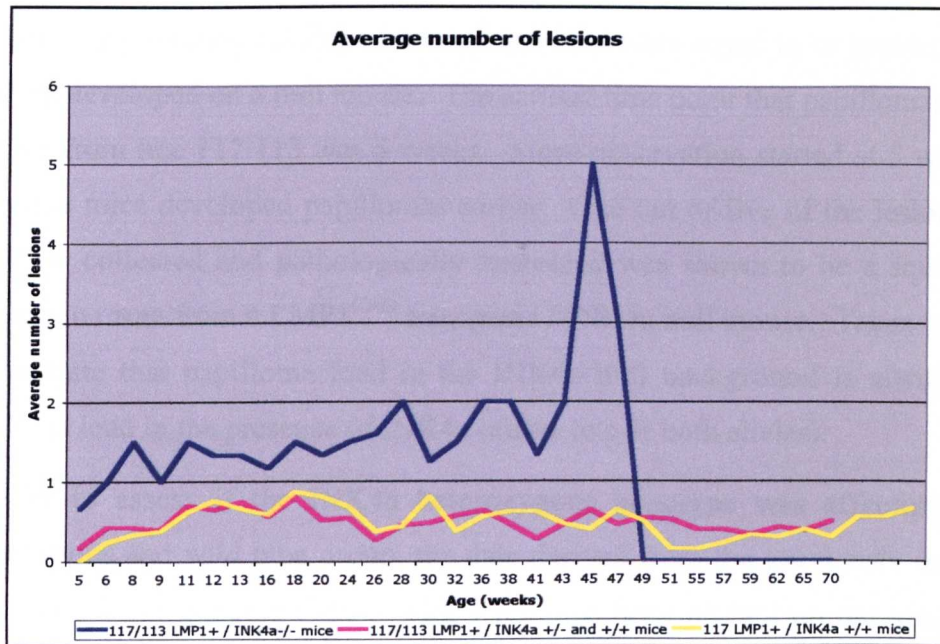


Figure 3.17: Development of spontaneous cutaneous lesions in mice of line 117/113 and line 117

6 INK4a locus null (-/-)(blue line) and 40 INK4a locus wild type (+/+) or heterozygous (+/-)(pink line) mice were monitored for 65 weeks (from 5 weeks old) for the appearance of spontaneous cutaneous lesions. Note that all the mice shown here are LMP1^{CAO} transgenic.

The graph shows the average number of lesions per mouse alive at each weekly count. The yellow line shows the data derived from the line 117 mice, transgenic for LMP1^{CAO} and wild type for the INK4a locus (previously shown in figure 3.14). Note that sudden drops indicate papilloma regression or removal of a mouse from the study.

mice in the INK4a heterozygous and wild type group never developed a lesion throughout the study period. The highest lesion load on a single mouse in the study was recorded on an INK4a null mouse which developed a maximum of 9 papillomas. By comparison the highest lesion load on a single INK4a heterozygous and wild type mouse was 6. The maximum number of papillomas developed on a mouse that were equal to or greater than size 2 was 7 and they developed on a null mouse. The earliest time point that papillomas could be detected on mice from line 117/113 was 5 weeks. Since observation started at 5 weeks, it is possible that some mice developed papillomas earlier. One out of five of the lesions of line 117/113 that were collected and pathologically examined was shown to be a squamous carcinoma. This lesion came from a LMP1^{CAO} transgenic / INK4a null mouse. Taken together, these data demonstrate that papilloma load in the INK4a null background is always larger than the papilloma load in the presence of INK4a (either one or both alleles).

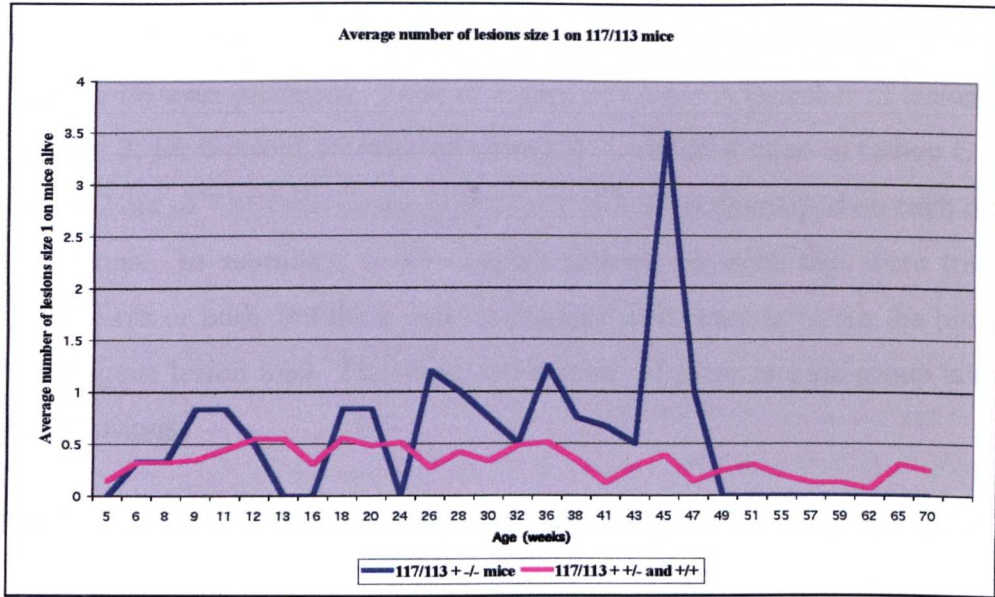
In order to assess if the INK4a heterozygous genotype was affecting the data in the heterozygous and wild type group, the data derived from the previously described cohort of mice, line 117 transgenic INK4a wild type have been plotted on the graph in figure 3.17. Since these data are very similar, to the data from the wild type and heterozygous grouped mice of the cross 117/113 it suggests that the heterozygous genotype is not affecting the observed phenotype.

Figure 3.18A shows no obvious differences between INK4a null or heterozygous and wild type in size 1 lesions that developed except at one time point between weeks 43-49. The most striking difference is observed when the lesions equal or greater than size 2 for the INK4a null, heterozygous and wild type mice are plotted. The INK4a null mice appear to show development of more larger (>size 2) lesions than the heterozygous and wild type mice (fig.3.18B). Lesions greater than size 2 presented a similar picture as the total number of lesions. Also at the beginning of the study when the mice are 5 weeks old, the null mice have a higher average number of papillomas (0.67) that are equal to or greater than size 2, whereas the wild type and heterozygous mice start with fewer lesions equal to or greater than size 2 (0.05). Note that at 49 weeks all the null mice have been removed from the study due to the incidence of lymphoma in this strain. Sudden drops in the curve represent the removal of a mouse bearing lesions from the study.

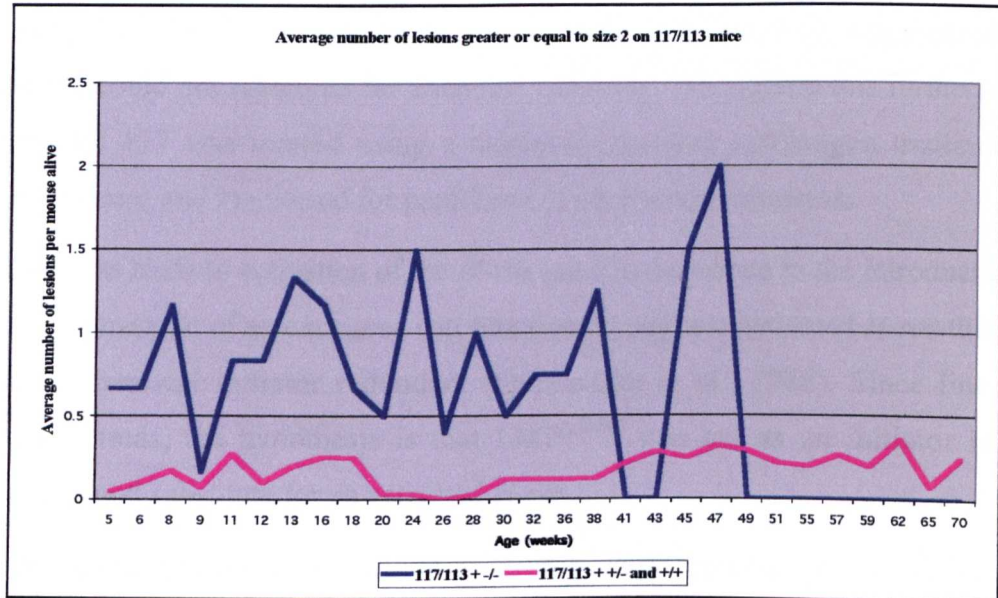
Figure 3.18: Development of spontaneous cutaneous lesions in mice of line 117/113

A graph showing the average (mean) number of lesions size 1 (A) or equal to size 2 or greater (B) per mouse alive at each weekly count. INK4a null mice are shown by a blue line and wild type and heterozygous for INK4a locus mice are shown by a pink line. All the mice included in this graph are LMP1^{CAO} transgenic positive. Note that sudden drops indicate papilloma regression or removal of a mouse from the study.

A



B



In order to investigate whether LMP1^{CAO} can activate Ras, an indirect approach was taken to cross mice of line 117/113 to line 1205 mice. Line 1205 mice bear an activated *H-ras* transgene under the control of the HK1 promoter, directing oncogenic Ras expression to the skin epithelium (see section 1.8). As a result of this preliminary study, 4 LMP1^{CAO} + / H-ras + (Group A), 15 LMP1^{CAO} + / H-Ras - (Group B), 4 LMP1^{CAO} - / H-Ras + (Group C) all of which were in a heterozygous or wild type INK4a background and 7 LMP1^{CAO} +/- INK4a -/- / H-Ras - (Group D) were produced. 2 out of 4 mice of Group A (number of lesions developed on each mouse: 2, 6), 0 out of 15 mice of Group B, 1 out of 4 mice in Group C (number of lesions: 6) and 2 out of 7 mice in Group D (number of lesions developed on each mouse: 2, 3), developed lesions. In summary, a few lesions formed on mice that were transgenic for LMP1^{CAO}, or H-ras or both, but there was no obvious difference between the bitransgenic or the single transgene lesion load. However, the number of mice in each group is too small to draw any conclusions.

3.5 Does L2LMP1^{CAO} act as a chemical initiator?

Mice of line 117 show spontaneous papilloma formation when in an FVB strain background. It was therefore hypothesised, that LMP1^{CAO} could act as a weak tumour initiator. Previous studies using PyLMP1^{B95-8} mice demonstrated that LMP1 activity augmented chemical promotion but could not substitute for chemical initiation. To explore this further, a cohort of mice from line 117 was treated using a minimal chemical carcinogen treatment without carcinogen initiator and monitored for papilloma or carcinoma formation.

DMBA initiation leads to activation of the *H-ras* gene as described in the introduction (section 1.5). If overexpression of an oncogene can functionally replace activated *H-ras* this will make the use of a chemical initiator redundant (Quintanilla et al., 1986). Since line 117 mice develop papillomas, the hypothesis is that LMP1^{CAO} can act as an initiator in chemical carcinogenesis and substitute for an activated *H-ras*.

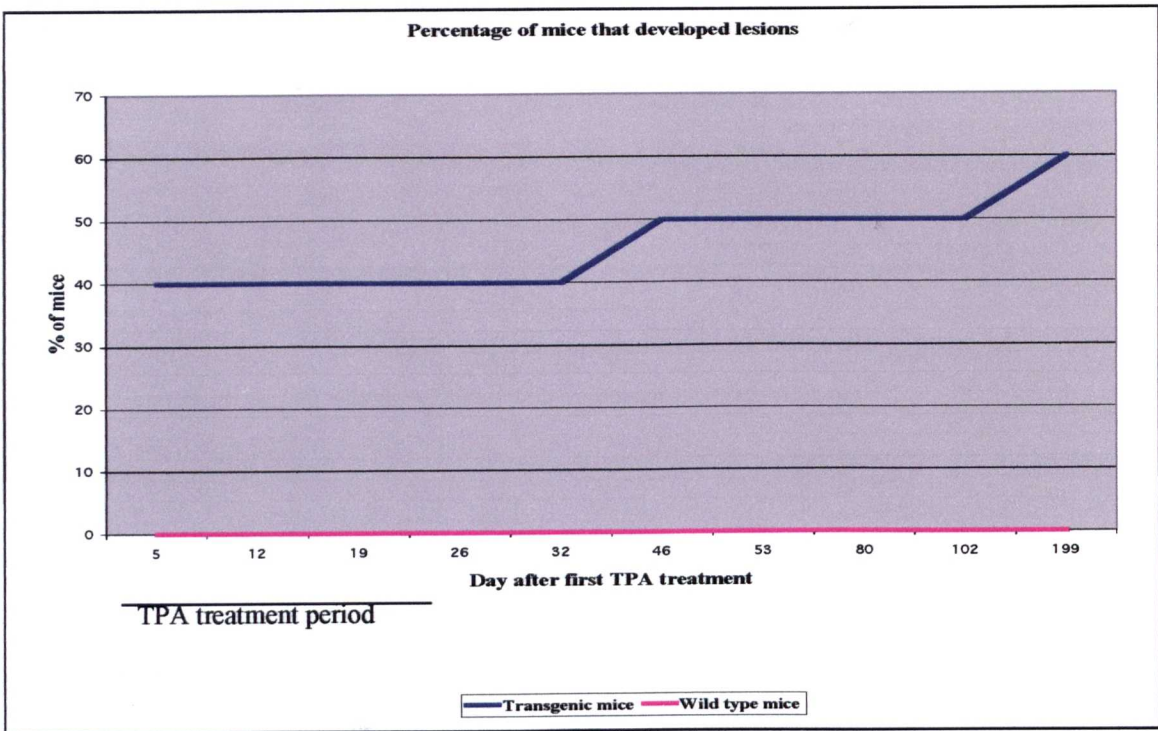
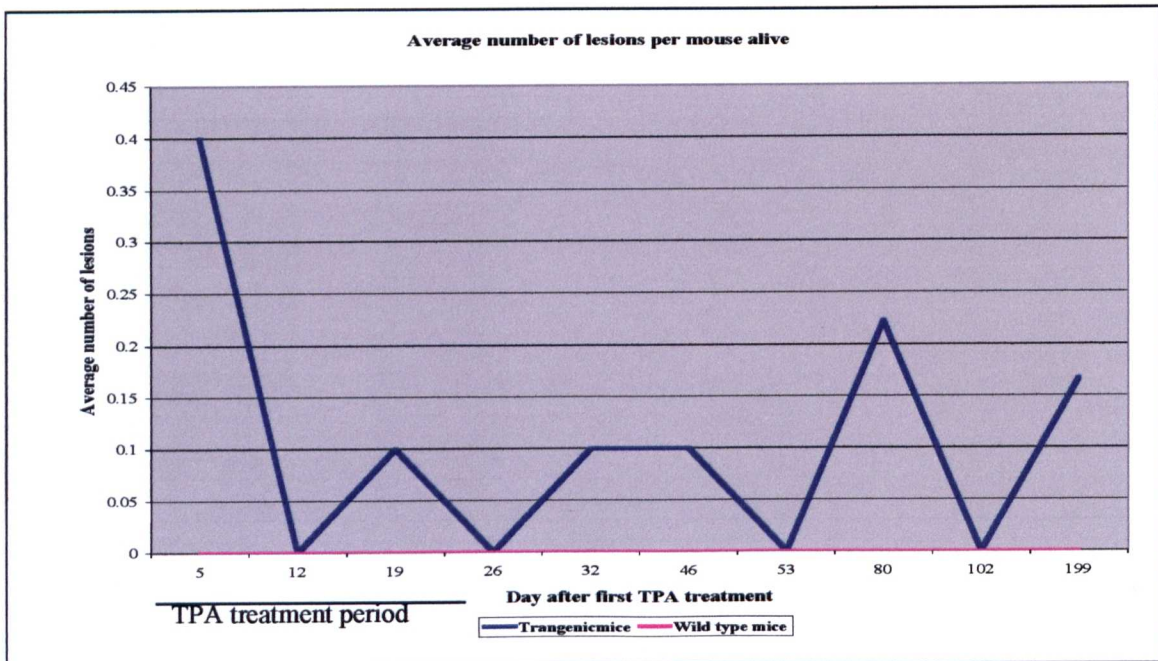
A complete topical carcinogenesis regime involves a single application of DMBA followed by 20 biweekly applications of TPA. Different minimal regimes were previously used with line 53 (PyLMP1^{B95-8}) mice showing that LMP1 can partially substitute for the promotion stage (Curran et al., 2001). In order to test if LMP1^{CAO} in line 117 can act as an initiator, a minimal regime was followed of TPA treatment without initial application of DMBA. If LMP1^{CAO} can indeed act as an initiator, then the transgenic mice treated with TPA would show a larger papilloma load than wild type siblings treated with TPA (section 1.5). In total, 23 animals of

FVB backcross four (93.75%) and five (96.88%) at 5-6 months old were included in the study. 10 animals were transgenic positive and 13 wild type. The lesion load was monitored from week 1 after the first TPA application up to week 43 and lesions were recorded according to their size as previously described (section 3.4).

It was observed that upon TPA application the transgenic mice developed a rough, red and raised surface to the skin, described as papillomatosis. The papillomatosis phenotype was persistent throughout the TPA treatment and only evident on transgenic animals (fig.3.19.C).

60% of the transgenic mice in this study developed papillomas by the end of the study period and the average number of lesions developed was very small (fig.3.19.A, B). None of the wild type mice developed papillomas. This is not statistically significant ($P = >0.25$ $\chi^2 = 0.033$ $df=1$)³ when compared to the percentage of mice that spontaneously developed papillomas. This implies that minimal TPA treatment did not promote increased papilloma formation and suggests that LMP1^{CAO} is not acting as a powerful initiator able to replace the activation of the *H-ras* gene in chemical carcinogenesis. However, as seen from fig.3.19.C only the transgenic mice showed this papillomatosis upon TPA treatment. The last day of the TPA application was day 25 and 9/10 of the transgenic mice showed this hyperplastic response. A week later on day 32, 4/10 of the transgenic mice still showed this hyperplasia. Three weeks after the treatment had stopped (day 46) this phenotype had regressed completely. None of the wild type mice showed this phenotype so this cannot be a TPA effect alone. It implies that LMP1^{CAO} is augmenting the action of TPA as shown in previous studies using PyLMP1^{B95-8} (Curran et al., 2001). At this point, it is not clear why papillomatous lesions form on the L2LMP1^{CAO} mice and not on PyLMP1^{B95-8}.

³ The chi-squared test investigates whether a variance in a normal distribution has a specified value. The formula is $\chi^2 = \sum [(o-e)^2/e]$. In this case observed (o) value was 6 and expected (e) value was 5.714 (since 57.14% of line 117 spontaneously developed lesions and the transgenic size of this group is 10). This value is later compared on a table with P values at the appropriate degrees of freedom (df) to determine whether the P value is less than 0.05 and thus of statistical significance.

A**B**

C

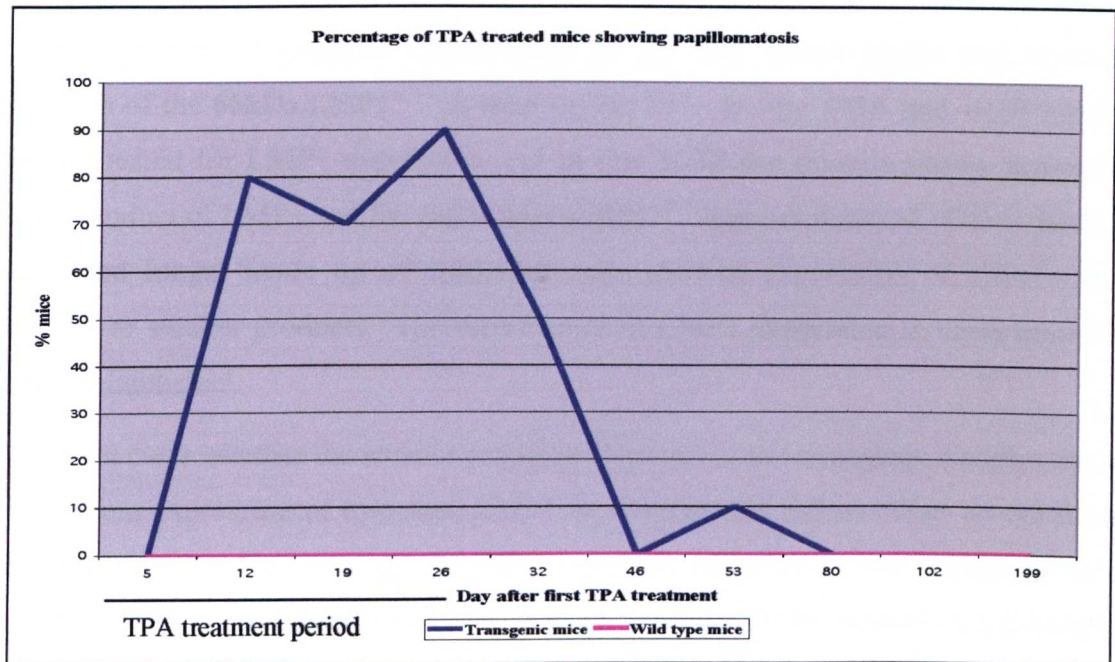


Figure 3.19A, B and C: Development of cutaneous lesions in mice of line 117 that have been TPA treated

10 transgenic and 13 wild type siblings of line 117 mice, were monitored for 43 weeks after the first TPA treatment for the appearance of cutaneous lesions.

A) The percentage of mice developing a lesion through the study period is shown, at the days following the first TPA treatment. Transgenic mice are shown by a blue line and wild type mice are shown by a pink line.

B) A graph showing the average (mean) number of lesions per mouse alive at each weekly count. Transgenic mice are shown by a blue line and wild type mice are shown by a pink line. Note that sudden drops indicate papilloma regression or removal of a mouse from the study.

C) A graph showing the percentage of mice that showed papillomatosis upon TPA treatment. Transgenic mice are shown by a blue line and wild type mice are shown by a pink line.

3.6 Conclusions and Discussion

From the above studies, it is shown that LMP1^{CAO} under the ED-L2 promoter, is expressed in a wide variety of tissues in the transgenic animals created and this is not restricted only to epithelial tissues. Lymphoid organs such as cervical lymph nodes and thymus show expression of the 66kDa LMP1^{CAO} at least in line 117. In line 105A and 105B lymph nodes were not tested for LMP1 expression and in line 105B the thymus shows expression of a smaller product of LMP1 and the full 66kDa LMP1^{CAO} was not detected. Other tissues (heart, kidney and lungs) made up of epithelial cells showed expression of either the 66kDa LMP1^{CAO} or smaller products. The significance of LMP1 expression in these tissues has not yet been established.

It is not yet clear whether the smaller products observed in the transgenic samples are actually derived from expression of truncated LMP1 or whether this has an effect on the function of full length LMP1. For example, the 50kDa product observed in the transgenic tissues by Western blotting could be the lytic LMP1 protein or a breakdown product of full length LMP1 or a product of another LMP1 promoter other than L2. To date this has not been clarified. There are at least three promoters associated with LMP1. The first to be detected was ED-L1 which is 5' upstream of exon 1 of LMP1 and gives rise to 2.8kbp mRNA and the 63kDa full length LMP1 polypeptide. ED-L1A is an internal promoter in intron 1 giving rise to a 2.6 kbp mRNA and a 50kDa polypeptide (Chen et al., 1995). Also a promoter 5' upstream of ED-L1 and situated into the first terminal repeat was discovered (L1-TR) that gives rise to a 3.5kbp mRNA that is preferentially detected in NPC cell lines rather than LCLs (Sadler and Raab-Traub, 1995). Another group has discovered another 5' of ED-L1 promoter, the ED-L1E, that gives rise to a 3.5kbp mRNA and is specifically activated in epithelial cells. This promoter has about 5x increased activity when compared to ED-L1 (Chang et al., 1997). An early lytic cycle promoter that is found 3' of the LMP1 gene and just 5' of the LMP2A gene- the ED-L2, and gives rise to a 0.6kbp mRNA was used to generate the LMP1^{CAO} transgenic mice.

A recent study (Pandya and Walling, 2004) has revealed that presence of the 50kDa lytic LMP1 protein along with full length LMP1 leads to decreased half life of the latter and also decreased LMP1 induced activation of NF- κ B, AP1 and STAT in RHEK-1 epithelial cells. It is therefore possible that this occurs in the transgenic tissues of line 117. If the 50kDa band observed is the lytic form, then the ratio between full length LMP1 and lytic LMP1 protein may play a role as to whether there is an observed phenotype in a tissue or not. For example, both ears and tissues of the gastrointestinal (GI) tract of transgenic animals of line 117 show

the 66kDa LMP1^{CAO} protein. However, a phenotype is observed only in ears and not in the GI. It could be that this has to do with the fact that in ears the 66kDa protein is expressed at much higher levels than the GI tract tissues or it could be that a smaller ratio between 66kDa and 50kDa protein leads to decreased LMP1^{CAO} function. Note however, that the 50kDa is not seen strongly in 105A or B transgenic tissues and this argues against any role that the 50kDa may have.

The expression patterns of LMP1^{CAO}, is consistent with the observed phenotype. Line 117 transgenic mice show hyperplastic ears and enlarged lymph nodes. This is consistent with the observation that LMP1^{CAO} is expressed at high levels in the ears and it is also expressed in the lymph nodes. Similarly, line 105B transgenic animals show the hyperplastic ear phenotype whereas 105A transgenic animals do not. LMP1^{CAO} is expressed in ears of line 105B but not in ears of line 105A.

Some line 105A transgenic animals show a wasting phenotype as they grow older. Organs of the GI tract of transgenic animals of this line show LMP1^{CAO} expression. One hypothesis is that LMP1^{CAO} expression can lead to aberrant proliferation in those tissues disrupting the differentiation pattern of the lining of the digestive system leading to problems in nutrient absorption. However, this is not apparent from the pathological examination of those tissues and the GI tract tissues of transgenic animals of lines 117 and 105B also show LMP1^{CAO} expression but no wasting phenotype. An alternative explanation could be that the transgene in line 105A has disrupted a cellular gene and the observed phenotype is unrelated to the LMP1^{CAO} expression. Also, in one case, a lymphoma was observed in these tissues. Perhaps this interferes with GI function in other wasted animals but this has not been examined.

The appearance of spontaneous papillomas on line 117 prompted the investigation as to whether LMP1^{CAO} is acting as an initiator or as a promoter. It was subsequently shown that LMP1^{CAO} cannot act as an initiator in the context of chemical carcinogenesis but rather acts as a tumour promoter and replaces TPA. This is in agreement with previous data obtained in this laboratory using LMP1^{B95-8} transgenic animals in chemical carcinogen studies (Curran et al., 2001). However, the observed phenotype of line 117 mice where 57.14% of the mice spontaneously develop papillomas, shows that LMP1^{CAO} can lead to activation of signalling pathways that initiate the process of carcinogenesis but that LMP1^{CAO} does this to a low level, since only a few and small spontaneous papillomas develop per mouse and few ears go on to become squamous cell carcinomas.

From the data described here and published (Curran et al., 2001; Macdiarmid et al., 2003), it was found that the two LMP1 strains - B95-8 and CAO - show no significant differences in terms of initiation in the context of chemical carcinogenesis. A more progressed phenotype is observed on the LMP1^{CAO} animals when compared to the LMP1^{B95-8} animals. Even though we cannot at the moment exclude the hypothesis that LMP1^{CAO} may be more tumourigenic, as has been suggested by several groups in the past, we cannot confirm it either. The expression of the transgene in lines 53 and 117 is still not known. Initial studies performed in this laboratory using the LMP1^{B95-8} (line 53) transgenic animals indicated that the transgene expression is probably localised to the suprabasal layer. This is the non proliferative differentiating layer of the epidermis. Despite repeated attempts of mine to investigate expression patterns by RNA *in situ*, on tissues from line 117 these proved unsuccessful. It is possible however, that the LMP1^{CAO} transgene is expressed in the basal epidermal layer. This is the proliferating layer of the epidermis and so it is expected that if LMP1 plays any effects on proliferation, differentiation or apoptosis that these could be magnified just by the fact that the transgene is expressed in a proliferating compartment. This can be seen in other transgenic mouse models, for example the TGF α transgenic animals. As has already been discussed, suprabasal expression of TGF α leads to hyperkeratotic skin (Dominey et al., 1993) whilst basal TGF α expression leads to ear thickening and spontaneous papilloma formation (Vassar and Fuchs, 1991). Similarly, Ras transgenic animals show an increase in the severity of the phenotype when the transgene expression is in the basal layer than if the transgene expression is in the suprabasal layer (Bailleul et al., 1990; Brown et al., 1998; Dajee et al., 2002; Greenhalgh et al., 1993a). Elucidating the spatial expression of LMP1 transgene in lines 53 and 117 is of utmost importance as this will allow direct comparison of the effects of the two strains in the epithelium *in vivo*.

Upon removal of the INK4a locus (i.e. no p16^{INK4a} or p19^{ARF} expression), an increased lesion load both in terms of numbers and size is observed on the transgenic for LMP1^{CAO} mice. Furthermore, a spontaneous lesion that appeared on an LMP1^{CAO}+ / INK4a null mouse of line 117/113 was described as a squamous cell carcinoma rather than as a keratoacanthoma which was what was usually observed on mice of line 117. These results are in agreement with previous results obtained in the laboratory with mice of line 53 (PyLMP1^{B95-8}) crossed to an INK4a null strain (Macdiarmid et al., 2003). When the 53/113 mice were chemically treated and the lesion load recorded, it was observed that LMP1^{B95-8}+ / INK4a null mice developed more lesions faster that became larger in size and progressed to carcinoma. Taken together, these data show that there is a cooperation between the effects of LMP1^{CAO} and loss of INK4a

locus *in vivo*. This would explain what is observed in NPC where the INK4a locus is deleted or hypermethylated during the development of the lesion. The data presented here with respect to LMP1^{CAO} are in accord with published data from this laboratory concerning LMP1^{B95-8} indicating that LMP1 mediates a lesion growth inhibition effect through products of the INK4a locus (p16^{INK4a} or p19^{ARF}). However, this seems to be contrary to the published reports that LMP1 inhibits both p16^{INK4a} expression and function (Ohtani et al., 2003; Yang et al., 2000a). Nevertheless, it has been found that in LCLs, LMP1 does not lead to p16^{INK4a} inhibition, or its not sufficient for its inhibition (Hayes et al., 2004).

It is not clear if *ras* activation is part of tumourigenesis in line 117 mice. To examine this, sequencing of lesions that spontaneously developed on line 117 transgenic mice, with the focus on codons 12, 13, 60 and 61 of the *ras* gene that are known to develop spontaneous activating mutations, is needed.

Another phenotype observed is that of the reactive cervical lymph node. These lymph nodes do not show evidence of neoplasia at the stage analysed but appear to be reactive. This phenotype is not observed in the transgenic negative and is observed in 100% of the transgenic mice. Since LMP1^{CAO} is not a foreign protein to these mice, it could be that it leads to “fake” CD40 signalling thus simulating the interaction between B- and T-cells and showing this phenotype. It would be interesting to investigate this further by identifying whether it is the B or T cell compartments that are expanded in those lymph nodes and in which LMP1 is expressed.

To conclude, expression of LMP1^{CAO} in the transgenic animals, is predominantly directed to epithelial tissues as well as some lymphoid tissues. Its expression leads to hyperplasia and spontaneous papilloma formation when in a genetically susceptible strain background. However, LMP1^{CAO} expression is not sufficient to replace the need for a chemical initiator in the context of chemical carcinogenesis. Nevertheless, lesions developing in the ear can progress to carcinoma.

Chapter 4: Signalling Pathways Activated by LMP1

The primary aim of the work described in this chapter was to examine signalling pathways affected by LMP1^{CAO} in the epithelium *in vivo*, with an emphasis on the Ras/MAPK pathway.

Previous studies showed upregulation of EGFR levels in both NPC biopsies and epithelial cells (C33A) *in vitro* in response to LMP1 expression (Miller et al., 1998a; Miller et al., 1997; Sheen et al., 1999; Zheng et al., 1994a). Given these facts and the similarity in phenotype between LMP1 transgenic mice and TGF α transgenic mice (see 1.7), it was hypothesised that LMP1 may act via upregulating TGF α . Among the pathways activated by EGFR is the Ras/MAPK cascade. A previous report showed LMP1 activation of MAPK in a Ras-dependent way in Rat-1 fibroblasts (Roberts and Cooper, 1998), therefore, it was decided to investigate this pathway using the affected tissues from the transgenic mouse lines generated in the laboratory.

The aims of this chapter were:

1. Does LMP1^{CAO/B95-8} lead to upregulation of TGF α ?
2. Does LMP1^{CAO} lead to upregulation or increased activation of EGFR?
3. Does LMP1^{CAO} affect the Ras/MAPK in any way?
4. Does LMP1^{CAO} activate the PI3K/Akt pathway? (another major pathway activated by EGFR)
5. What other pathways are activated by LMP1^{CAO} in the epithelium *in vivo*?

4.1 Outline of Approach

In order to explore the status of several signalling pathways, affected tissues (ears) from mice of line 117 and (adult skin, pup epidermis, pup dermis) from line 53, both transgenic and age matched sibling controls were collected. The transgenic ears were staged according to their phenotype (see fig.1.14). Skin from 3-7 day old pups from mice of line 53 was collected and separated into the epidermal and dermal components. In order to detect the levels of total or activated protein, protein extracts were prepared using Ripa buffer and analysed by Western blotting. In order to examine DNA binding activity whole protein extracts from affected tissues were prepared as described previously (see 2.2.4H) and used in EMSA experiments.

Results

4.2 LMP1^{CAO} and the TGF α /EGFR/Ras/MAPK Signalling Pathway

Initially, expression levels of TGF α were examined. Figure 4.1 shows that TGF α is found upregulated in the phenotypic transgenic pup epidermis (5 days old) of mice of line 53 but not in transgenic dermis or adult skin or when compared to control samples. The cleaved soluble product of TGF α ranges from 5-20kDa depending on the degree of glycosylation. The 10kDa product observed in fig.4.1, could therefore be a soluble product of TGF α . Similarly, TGF α was also detected in ear protein extracts of line 117 mice (Stevenson *et. al.*, in press). Protein was also extracted from cell pellets derived from carcinomas that developed after chemical carcinogen treatment on transgenic and wild type mice of lines 53 and 117. When these samples were separated by SDS-PAGE, the gel blotted and probed with anti-TGF α antibody, there was no evidence of either the uncleaved or the cleaved form of TGF α (fig.4.2). It is possible that in these cell pellets the TGF α soluble form is secreted into the cell culture medium or it has a very fast turnover. In order to test this, cell culture medium from these cells could be examined for the presence of TGF α using an enzyme linked immunosorbent assay (ELISA) approach or by an IP followed by a Western blot. It is also possible that since these cells are established immortalised cell lines, that overexpression of TGF α is not selected for.

The next logical target was to investigate whether EGFR, the receptor for TGF α , was affected in any way as a result of increased expression of its ligand. Total EGFR levels were slightly higher in transgenic ears (fig.4.3). However, levels of total EGFR decreased as the phenotype progressed (stage 1: 1.36 fold, stage 2: 1.1 fold, stage 3: 0.85 fold when compared to controls normalised against β tubulin, see table 5.3). In contrast, smaller EGFR products (sizes approximately 70, 66 and 50kDa) were observed in transgenic ears of increasing phenotype severity (stage 1: 1.13, stage 2: 1.60, stage 3: 3 fold when compared to controls normalised against β tubulin, see table 5.3). Similar results were obtained when using line 53 tissues (fig.4.4). Total EGFR levels are higher in the wild type epidermis as compared to transgenic epidermis whilst using an antibody specific for the phosphorylated EGFR form, led to detection of increased possible breakdown products of EGFR (50, 45, 40kDa) in the transgenic epidermis as compared to the wild type epidermis. It is of interest that when cell pellet protein extracts were probed with anti-total EGFR, the 170kDa band did not show any

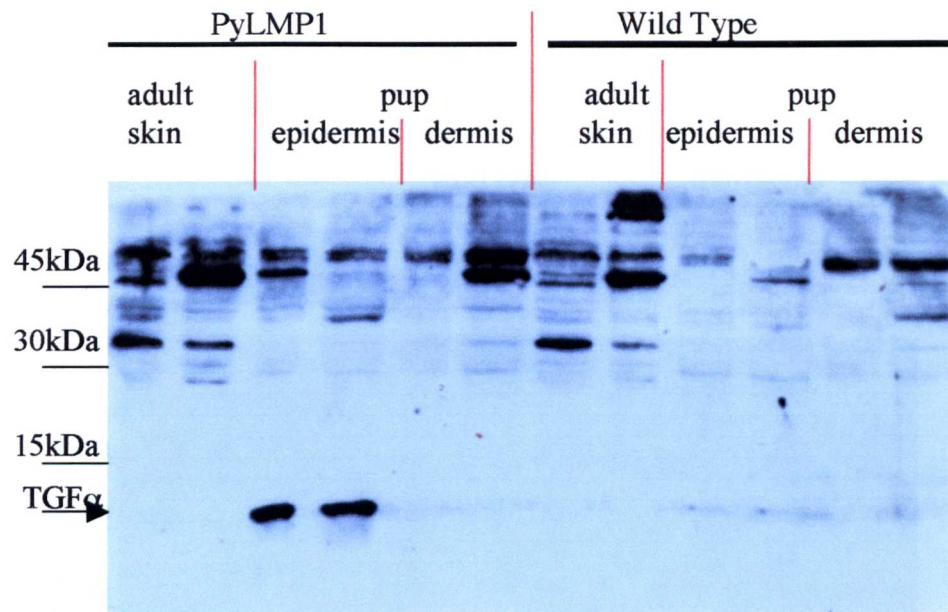


Figure 4.1: TGF α expression in the skin of line 53 mice (PyLMP1^{B95-8}).

5 day old pup skins were collected and separated into epidermal and dermal components. Whole adult skin was also collected. Protein was extracted using Ripa buffer. 75 μ g of protein extract/track was separated by 15% SDS-PAGE and the gel was blotted. The blot was probed with a rabbit anti-mouse TGF α primary antibody (1:1000) and a goat anti-rabbit IgG-HRP secondary antibody (1:4000) and visualised with ECL+. The 10kDa band corresponding to TGF α is indicated. Molecular weights according to the marker track are shown.

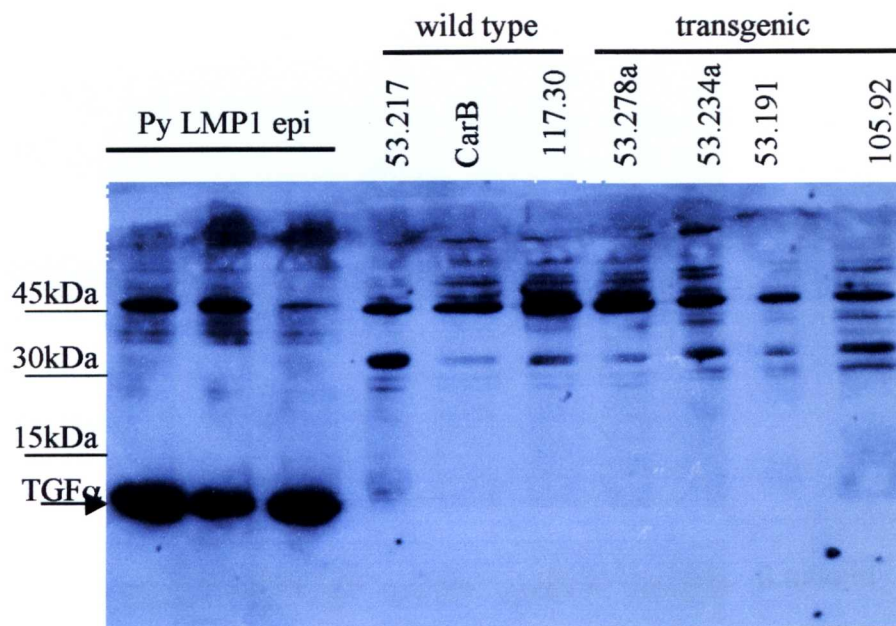


Figure 4.2: TGF α expression in LMP1 transgenic and control carcinoma derived cell lines.

Protein was extracted from 5 day old pup epidermis (epi.) and from cell pellets using ripa buffer. 100 μ g of protein extract/track was separated by 15% SDS-PAGE and the gel was blotted. The blot was probed with a rabbit anti-mouse TGF α primary antibody (1:1000) and a goat anti-rabbit IgG-HRP secondary antibody (1:4000) and visualised with ECL+. The 10kDa band corresponding to TGF α is indicated. Molecular weights according to the marker track are shown.

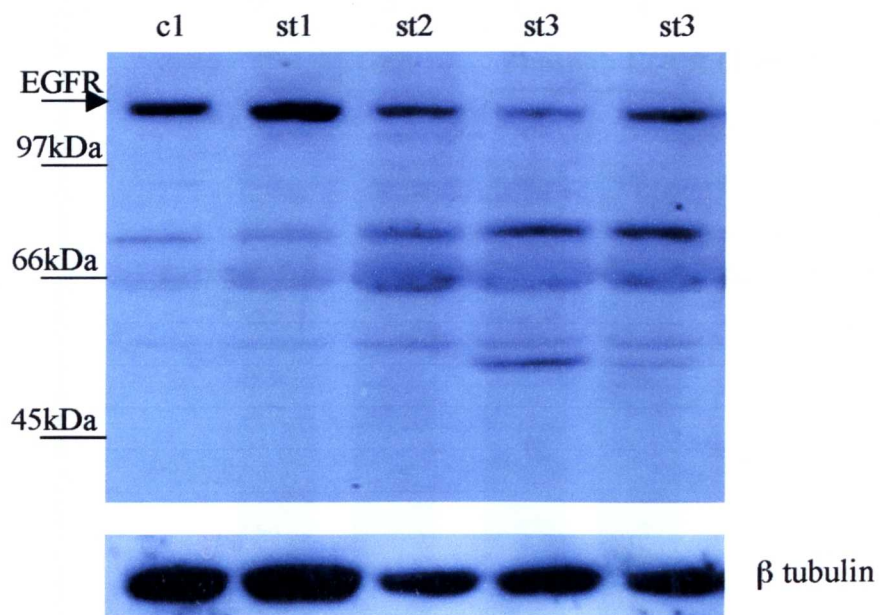


Figure 4.3: EGFR expression in the ears of line 117 (L2LMP1^{CAO}) mice.

Protein extracts were prepared from ear samples of increasing phenotypic stage, stage 1(st1), stage 2(st2), stage 3(st3) along with a stage 1 aged matched control (c1).

100µg of protein extract/track was separated by 7.5% SDS-PAGE and the gel was blotted. The blot was probed with a rabbit anti-mouse total EGFR primary antibody (1:1000) and a goat anti-rabbit IgG-HRP secondary antibody (1:4000) and visualised with ECL⁺. The 170kDa band corresponding to total EGFR is indicated. Molecular weights according to the marker track are shown.

The blot was stripped and re-probed with β tubulin as a loading control (shown below).

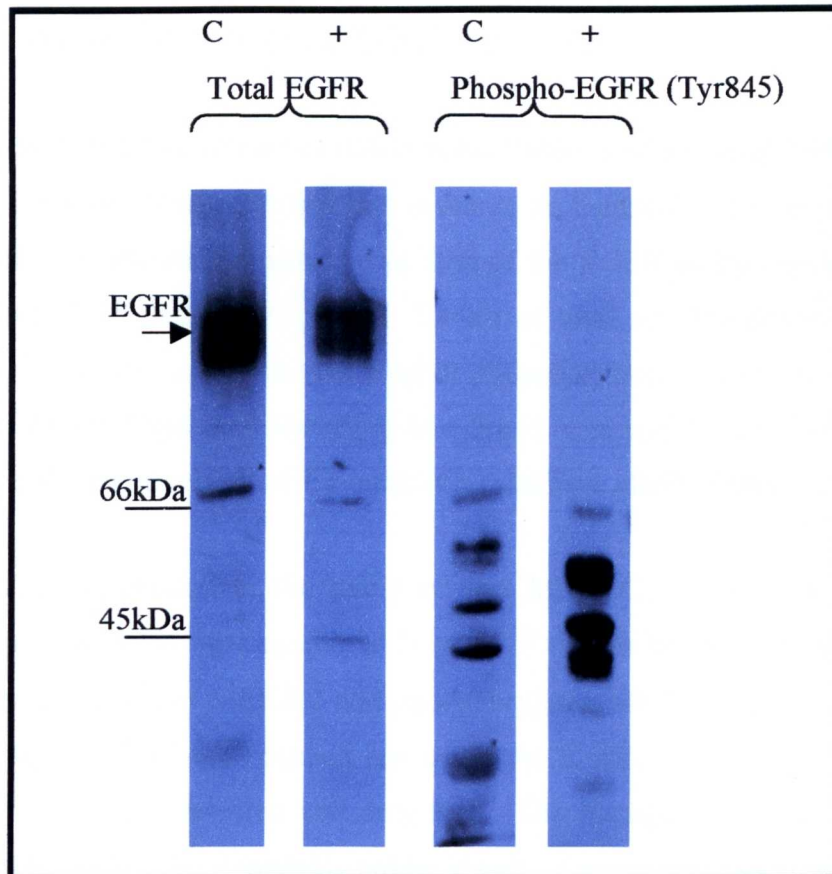


Figure 4.4: Total EGFR and phospho-EGFR (Tyr845) expression in the epidermis of 5 day old pups of line 53 (PyLMP1^{B95-8}).

Protein extracts were prepared from epidermis samples of 5 day old pups both transgenic (+) and wild type siblings (C). 100µg of protein extract/track was separated by 7.5% SDS-PAGE and the gel was blotted. The blot was probed with a rabbit anti-mouse total EGFR primary antibody (1:1000) or after stripping with a rabbit anti-mouse phospho-EGFR (Tyr 845) antibody (1:1000) as indicated and a goat anti-rabbit IgG-HRP secondary antibody (1:4000) and visualised with ECL+. The 170kDa band corresponding to total EGFR is indicated. Molecular weights according to the marker track are shown.

decrease in transgenic samples, instead levels of total EGFR were shown to be equivalent or higher in cell pellets derived from transgenic animals. The smaller products of EGFR are prominent in the cell pellets obtained from transgenic positive carcinomas (fig.4.5a) and when an antibody against the phosphorylated EGFR was used, it was shown that some of the smaller products are phosphorylated forms of EGFR (fig.4.5.b).

If the breakdown products observed reflect faster turnover of activated EGFR in the transgenic tissues, then this would suggest that this is due to an increase in EGFR activation and hence activation of downstream pathways. The first of the EGFR pathways that was investigated was the Ras/MAPK pathway (fig.4.6). Levels of total and phosphorylated c-Raf-1 were examined using antibodies against the total or phosphorylated form of the protein. However, the specific 74kDa band corresponding to c-Raf-1 was not detected on the blot (data not shown). Use of a positive control for c-Raf-1 would have clarified this.

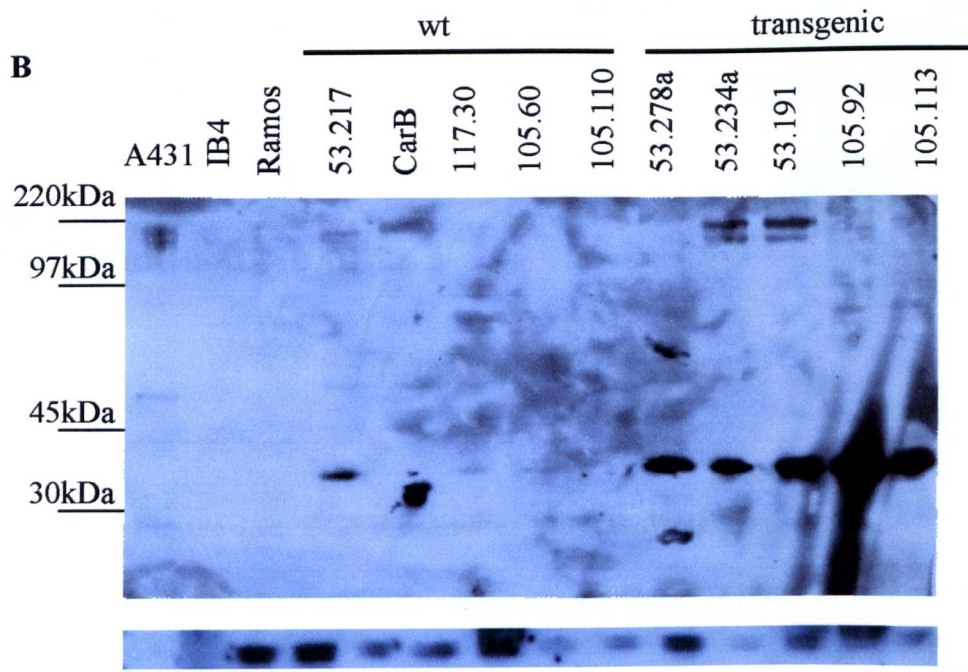
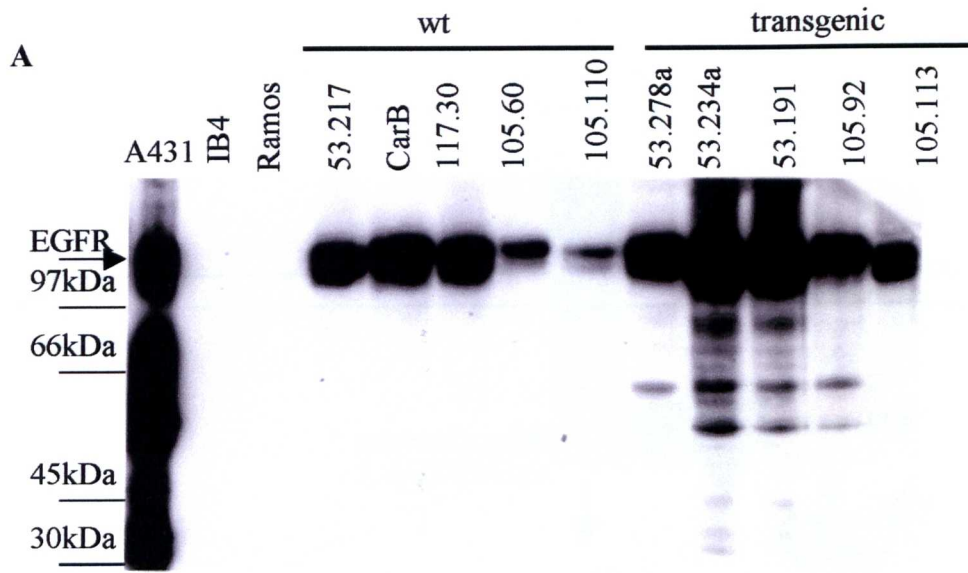
The next target examined in the pathway was MEK1/2. Levels of total MEK1/2 and phosphorylated MEK1/2 were examined in line 117 tissues (fig.4.7). In order to quantify the difference in the levels of MEK1/2 and phosphorylated MEK1/2 expression in ear samples, the respective autorads were scanned and using the Kodak 1D 3.5.2 program, the bands of interest were manually selected and analysed. The background sum intensity value was subtracted from the total sum intensity value of each of the bands to give the net sum intensity. The ratio of phosphorylated MEK1/2 band net intensity over total MEK1/2 band net intensity was calculated for each of the samples. For example the phosphorylated MEK1/2 net intensity of control 1 over the total MEK1/2 net intensity of control 1 gave a value of 0.173. For each of the transgenic phenotypic stages, this value was compared to the value of the corresponding control. For example transgenic stage 1 to control 1 ratio is 4.40 (0.762/0.173) (Table 4.1). In this way the levels of phosphorylated MEK1/2 to total MEK1/2 were calculated.

Sample	Ratio Phospho-MEK1/2: total MEK1/2	Stage x: control x
C1	0.173	
C2	0.264	
C3	0.226	
St1	0.762	4.40
St2	0.789	3.00
St3	0.167	0.74

Table 4.1: Densitometric analysis of phospho-MEK1/2 to total MEK1/2.

Figure 4.5: EGFR and phospho-EGFR expression in cell pellets derived from line 53, 117 and 105B carcinomas.

Protein was extracted from cell pellets and 100µg of protein extract/track was separated by 10% SDS-PAGE and the gel blotted. The blot was probed with a rabbit anti-mouse total EGFR primary antibody (1:1000) stripped and reprobed with a rabbit anti-mouse phospho-EGFR (Tyr 845) primary antibody (1:1000) and a goat anti-rabbit IgG-HRP secondary antibody (1:4000) and visualised with ECL+. The 170kDa band corresponding to total EGFR is indicated. Molecular weights according to the marker track are shown. The blot was tripped and reprobed with β tubulin to indicate loading levels (shown below).



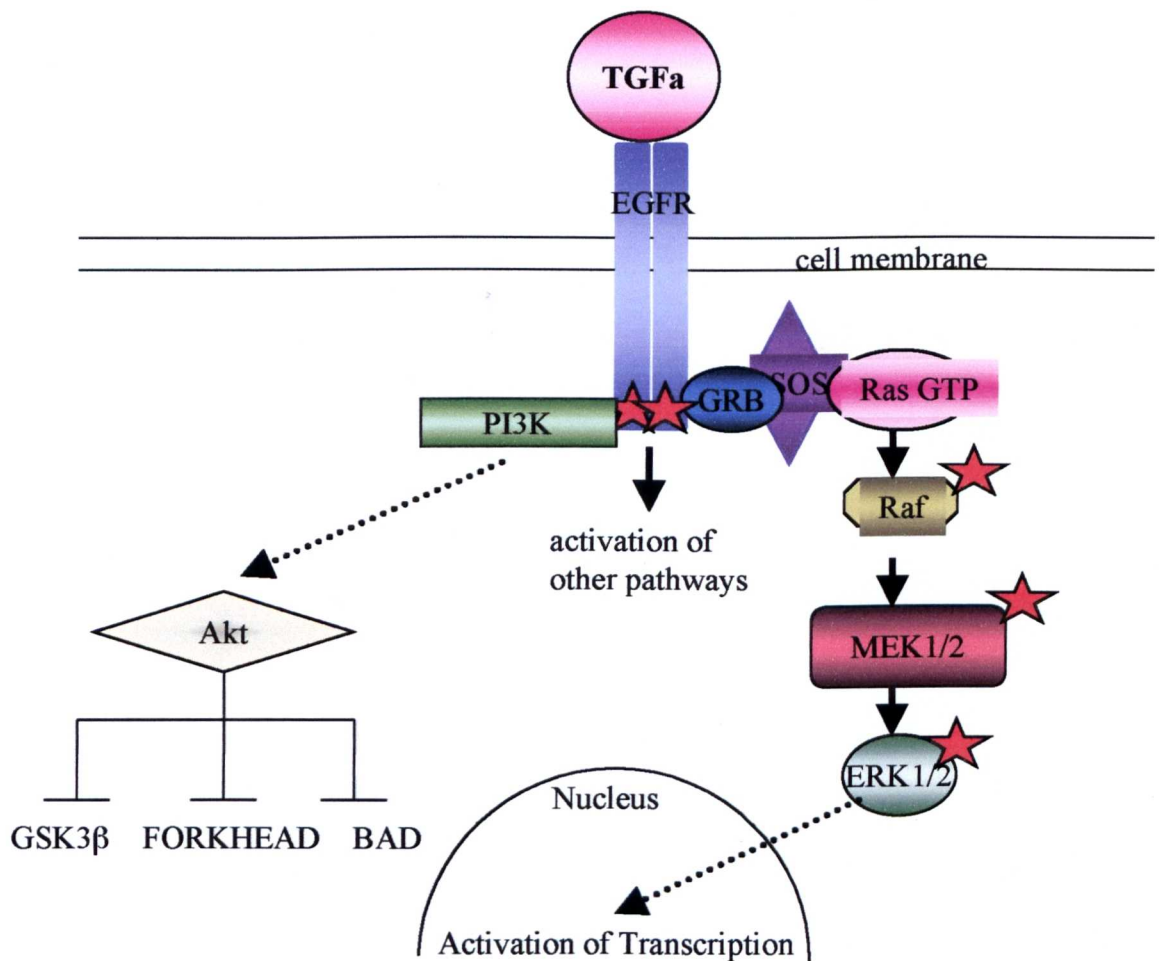
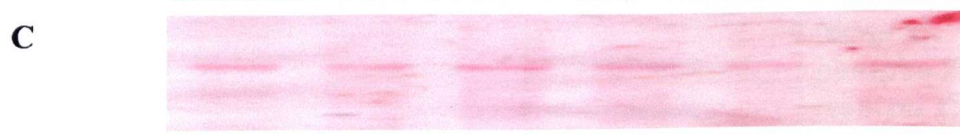
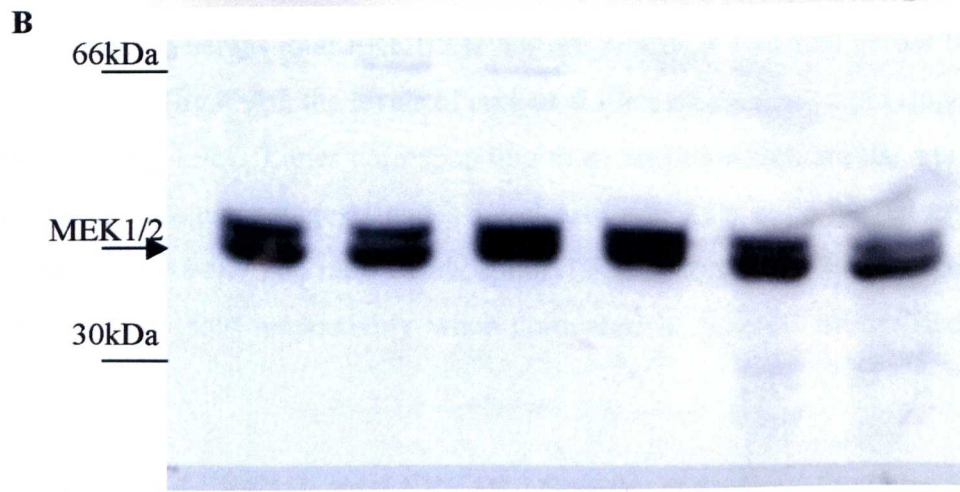
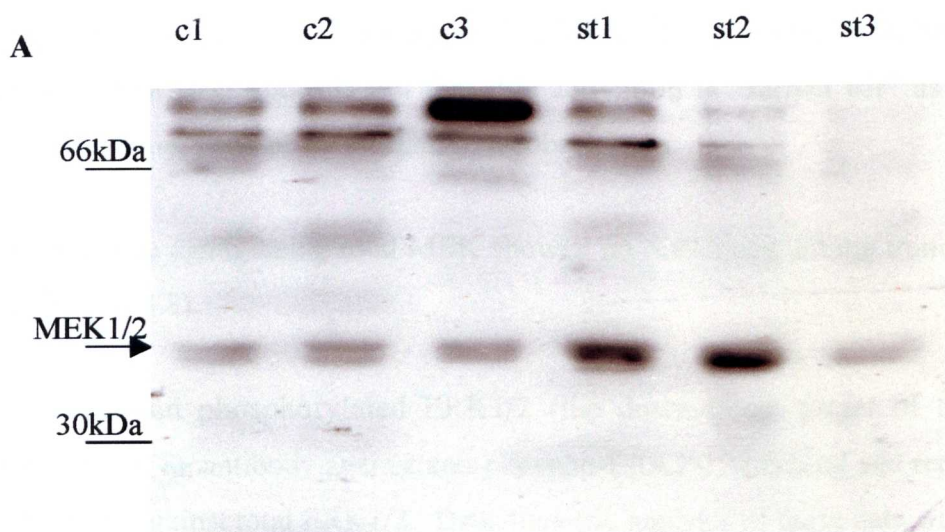


Figure 4.6: EGFR activates the Ras/MAPK cascade

A simplified pathway diagram indicates TGF α binding to EGFR causing the receptor to homo/heterodimerise. This leads to its autophosphorylation and activation. The activated receptor can recruit GRB and SOS that allow exchange of GDP for GTP thus activating Ras. Activated Ras leads to Raf activation by phosphorylation (indicated by a red star). Activated Raf can lead to phosphorylation and activation of MEK1/2 which in turn leads to phosphorylation and activation of ERK1/2. Downstream targets of ERK1/2 include transcriptional factors Elk-1, C-Myc, C-Jun, C-Fos and Sap-1.

Figure 4.7: Total MEK1/2 and phospho-MEK1/2 of ears of line 117 mice (L2LMP1^{CAO}).

Protein extracts were produced from ear samples of increasing phenotypic stage, stage 1(st1), stage 2(st2), stage 3(st3) and stage 1-3 age matched controls (c1-3). 100µg of protein extract/track was separated by 10% SDS-PAGE and the gel blotted. The blot was probed with a rabbit anti-mouse phosphorylated MEK1/2 primary antibody (1:1000) (A) and a goat anti-rabbit IgG-HRP secondary antibody (1:4000) and visualised with ECL+. The blot was stripped and reprobed with a rabbit anti-mouse total MEK1/2 (1:1000), followed by a goat anti-rabbit IgG-HRP secondary antibody (1:4000). The 45kDa doublet corresponding to MEK1/2 is indicated. Molecular weights as per marker track are shown. The blot was stained with Ponceau's stain to indicate loading levels (C).



It was found that the levels of phosphorylated MEK1/2 were higher in stages 1 and 2 of phenotypic ears (stage 1: 4.4 fold, stage 2: 3 fold, compared to controls normalised against total MEK1/2) but stage 3 phenotypic ears showed a decrease in levels of phosphorylated MEK1/2 down to control levels (stage 3: 0.74 fold). Levels of total MEK1/2 were relatively equal in all samples (fig.4.7). This suggests that MEK1/2 is activated in the phenotypic tissue to a greater extent than controls but that this activation is “turned off” as the phenotype progresses over time, perhaps by a negative feedback loop.

In cell pellets once again, using total MEK showed no difference among transgenic and wild type samples (fig.4.8).

Levels of total and phosphorylated ERK1/2 (the downstream target of MEK1/2) were examined by using an antibody against anti-phospho-ERK1/2, stripping and reprobing the blot with an antibody against total ERK1/2. Densitometric analysis of these data was performed as described earlier. Whereas total ERK1/2 levels are relatively constant across the control and transgenic samples (fig.4.9b), the levels of activated ERK1/2 increase from stages 1 to 3 of the transgenic ears (fig.4.9a). Lanes corresponding to c1 and c2 which are the age matched wild type controls of transgenic stages 1 and 2 are clearly relatively underloaded as seen from the Ponceau stain (fig.4.9c). The ratio of phosphorylated to total ERK2 for stage 1-3 ears was 1.49, 1.80 and 1.30 fold respectively when compared to controls normalised against total ERK1/2 (table 4.2).

Sample	Phospho-ERK1/2: total ERK1/2	Stage x: control x	Phospho-ERK1/2 (stage x): phospho ERK1/2 (control x)
C1 ERK2	0.296		
C2 ERK2	0.344		
C3 ERK2	0.465		
St1 ERK2	0.440	1.49	0.94
St2 ERK2	0.621	1.80	1.46
St3 ERK2	0.605	1.30	1.57
C1 ERK1	0.666		
C2 ERK1	0.475		
C3 ERK1	0.600		
St1 ERK1	0.626	0.94	1.10
St2 ERK1	1.160	2.44	2.02
St3 ERK1	0.500	0.83	2.17

Table 4.2: Densitometric analysis of phospho-ERK1/2 to total ERK1/2.

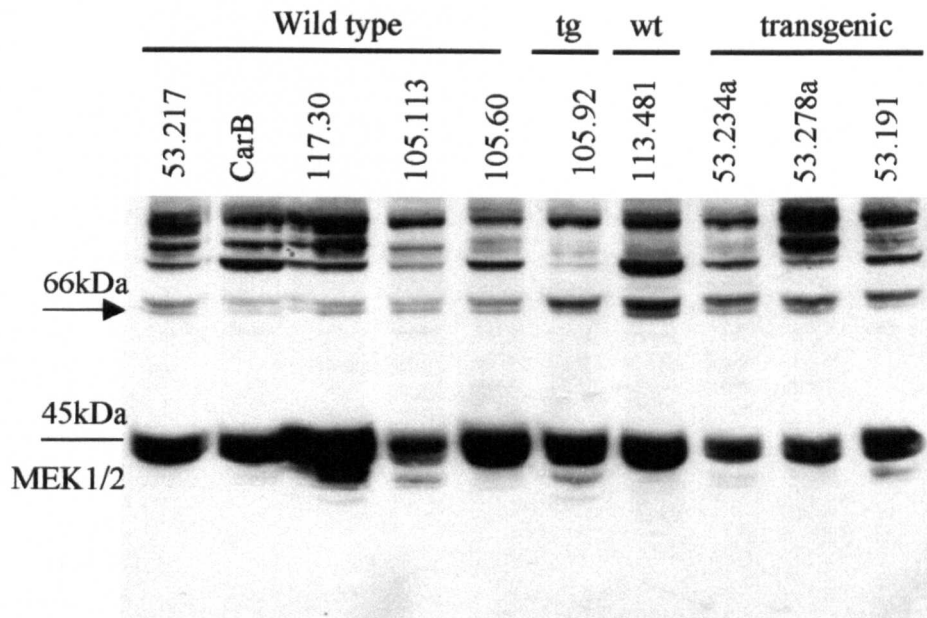


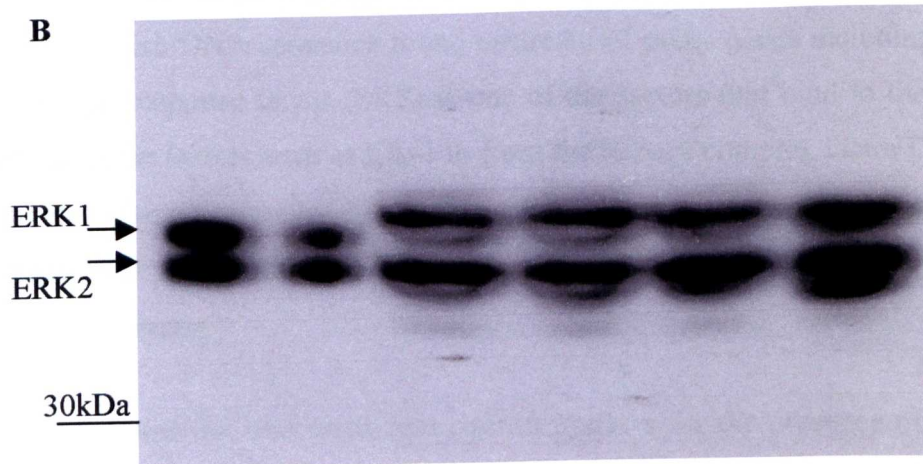
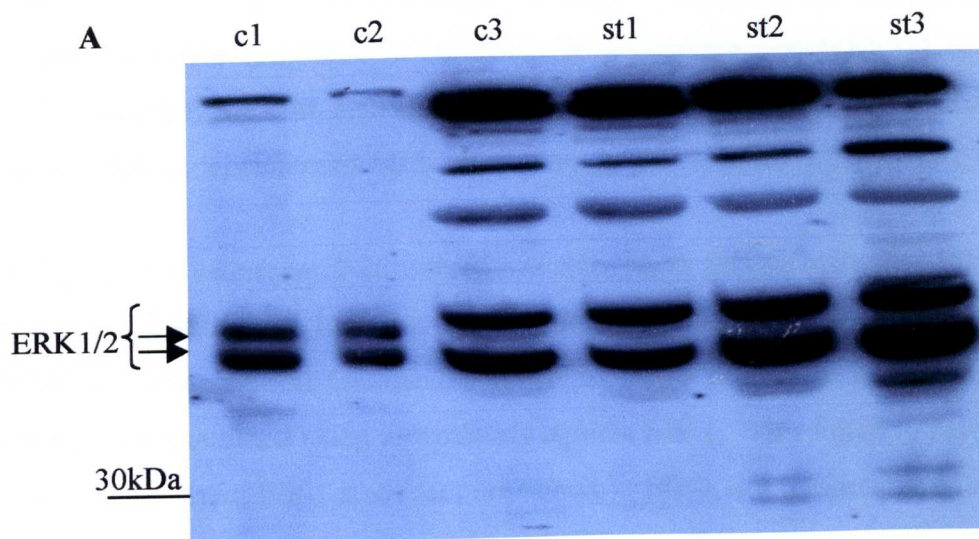
Figure 4.8: Total MEK1/2 expression in LMP1 and control carcinoma derived cell lines.

Protein extracts were produced from cell pellets. LMP1 status is indicated by wt = wild type; tg= transgenic.

100 μ g of protein extract/track was separated by 10% SDS-PAGE and the gel was blotted. The blot was probed with a rabbit anti-mouse total MEK1/2 primary antibody (1:1000) and a goat anti-rabbit secondary antibody (1:4000) and visualised with ECL+. The 45kDa doublet corresponding to MEK1/2 is indicated. Molecular weights according to the marker track are shown.

Figure 4.9: Total and phospho-ERK1/2 expression in the ears of line 117 (L2LMP1^{CAO}) mice.

Protein extracts were prepared from ears of increasing phenotype stages 1-3 and age matched controls c1-3. 100µg of protein extract/track was separated by 10% SDS-PAGE and the gel was blotted. The blot was probed with a rabbit anti-mouse phospho-ERK1/2 (A) primary antibody (1:1000) and a goat anti-rabbit IgG-HRP secondary antibody (1:4000) and visualised with ECL+. Subsequently, the blot was stripped and reprobed with a rabbit anti-mouse total ERK1/2 (B) primary antibody (1:1000). The 44 and 42kDa bands corresponding to ERK1/2 are shown. Molecular weights according to the marker track are indicated. The lower panel (C) is a Ponceau staining of part of the blot to indicate loading levels. Note that c1 and c2 are underloaded but c3 and st1-3 are equally loaded.



The ratio of phosphorylated to total ERK1 for stage 1-3 ears was 0.94, 2.44 and 0.83 fold respectively. This suggests that ERK1/2 is activated in the transgenic tissues compared to controls. For both ERK1 and ERK2 the activation is higher at stage 2 than at stage 1. From these data it is not clear if this activation is reduced again in real terms at stage 3, since (compared to the Ponceau stain) there may be more total ERK1/2 at stage 3. Comparing the levels of phospho-ERK1 and 2 at stage 3 to stage 2, suggests that ERK remains active in the transgenic samples compared to controls. It is possible that MEK1/2 is activating ERK1 directly since they are both activated in the transgenic samples but ERK2 must be activated by another kinase independent of MEK1/2 at later stages when MEK1/2 is no longer activated.

ERK1/2 can activate several downstream transcription factors including Elk-1, c-Myc, c-Jun, c-Fos and C/EBP beta. In order to investigate whether activated ERK1/2 could activate downstream transcription factors, the levels of Elk-1 protein in control and transgenic ear samples, were examined using an antibody against Elk-1. This failed to reveal any bands that correspond to correct Elk-1 size (data not shown). Elk-1 is a transcription factor that can bind the sequences of the serum response element (SRE) and activate transcription of linked genes. SRE is an A/T rich DNA sequence found upstream of many genes including genes of the *fos* family. Serum response factor (SRF) is one of the factors that bind to the SRE along with other transcription factors such as Elk-1 to form the ternary complex factor (TCF). SRF binds and activates transcription by binding to SRE sequences in a TCF dependent and TCF independent way. Activation of TCF can be achieved through the Ras/MAPK, p38 MAPK and the JNK pathways.

In order to examine the transgenic and control extracts for the presence of activated factors which can bind to specific DNA elements, an EMSA using an oligo containing the SRE site was performed.

Whole protein extracts from transgenic ears and age matched sibling controls, were incubated with a labelled SRE oligo. Specific binding was competed out using an excess (50x) of unlabelled oligo. A positive control extract from NIH3T3 cells, known to show SRE binding activity was used. A band (A) representing specific binding was detected in transgenic extracts (fig.4.10). This band was barely visible or not apparent in control samples.

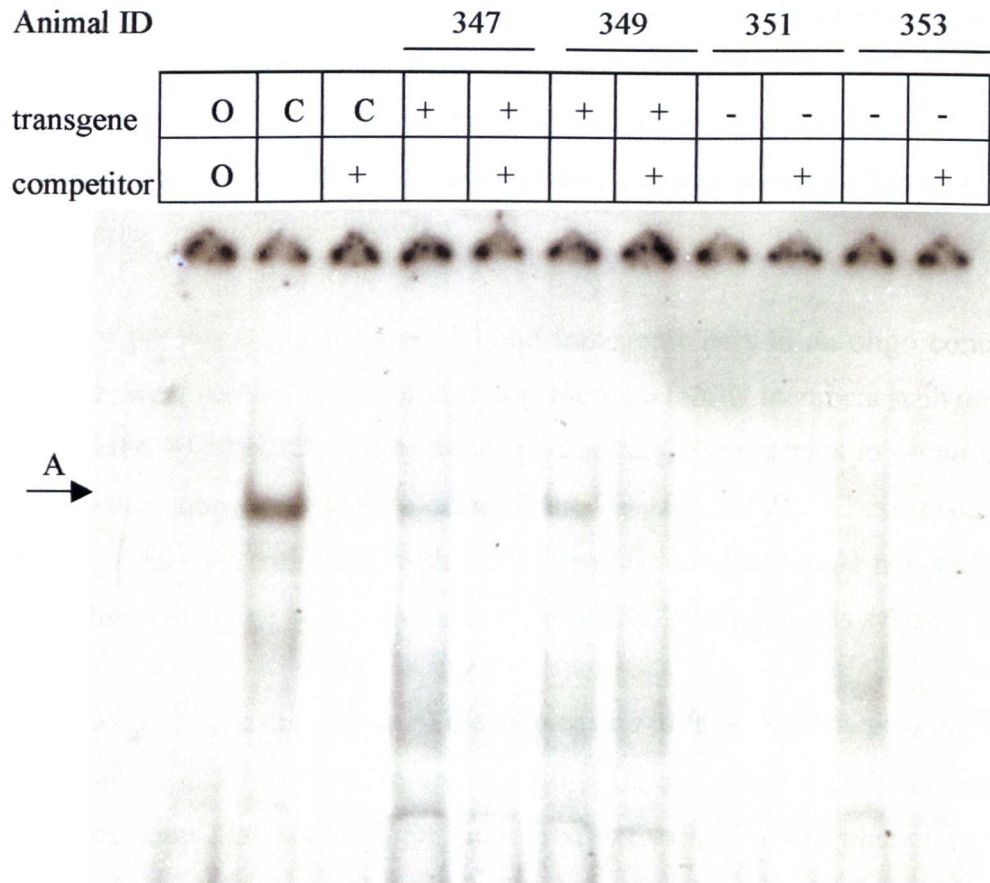


Figure 4.10: An EMSA showing specific binding of ear extracts of line 117 (L2LMP1^{CAO}) to SRE binding oligo.

Protein was extracted from transgenic (+) and wild type ears (-) (10µg/track) incubated with labelled SRE oligo and then separated by 6% PAGE. 10µg of NIH3T3 cell extracts were used as positive control (c). No extract is indicated by (O). 50x competitor (unlabelled oligo) was added to the samples indicated (+). The transgenic samples (mouse numbers: 347 and 349) show specific binding to the SRE sequence while the wild type samples (mouse numbers: 351 and 353) show comparatively little binding activity. The specific SRE binding band is indicated (A).

In order to ascertain if these extracts were of equal quality and quantity, binding to the recognition sequence for Sp1, a ubiquitous transcription factor, was conducted in parallel (fig.4.11). From this it can be seen that control extract 353 may be of lower quality and/or quantity than the transgenic extracts. However, control extracts 351, 375 and 362 (used in subsequent assays) show equal if not stronger Sp1 oligo binding activity compared to the transgenic samples. Therefore, the transgenic positive extracts shown in figure 4.10, show a greater SRE binding activity than controls.

Binding levels of protein extracts of control and transgenic ears to an oligo containing the ETS1 binding site were also investigated. Some of the ETS family members such as Elk-1 and SAP-1 are activated by ERK1/2. From the EMSA results, there seems to be no significant differences between transgenic and wild type samples (fig. 4.12). These results are not entirely clear as in the wild type samples the ETS1 specific band and other non specific bands are not clearly observed, so ETS1 remains a possible ERK1/2 target in this system.

In conclusion, LMP1^{CAO} can upregulate TGF α expression in these tissues, possibly leading to faster EGFR turnover and MEK1/2 activation. MEK1/2 activation may be countered by a negative feedback loop that prevents the increased activation as the phenotype worsens. LMP1^{CAO} can lead to activation of ERK1/2 and in the advancing stages of the phenotype this activation is independent of MEK1/2 activation. Downstream targets of activated ERK1/2 such as transcriptional factor Elk-1 may then be activated leading to increased binding to SRE. As seen from these results, LMP1^{CAO} can activate the Ras/MAPK pathway in the epithelium *in vivo*, possibly via TGF α upregulation and EGFR activation.

Figure 4.11: An EMSA showing specific binding of ear extracts of line 117 (L2LMP1^{CAO}) to Sp1 binding oligo.

Protein was extracted from transgenic (+) and wild type ears (-) and 5µg/track were separated by 6% PAGE. 5µg of A431 cell extracts were used as positive control (c). Labelled oligo without extract (O) was also added as an extra control. 100x competitor (unlabelled oligo) was added to the samples indicated (+). The transgenic samples (mouse numbers: 347,349,359) show specific binding to Sp1 sequence as indicated by the specific bands A and B and these are competed out upon addition of the competitor. The same is true for wild type samples (mouse numbers: 367,375,351, 353,362. Sample numbers 367 and 353 show weaker specific binding and this may reflect lower quality or quantity of these two samples. The non specific band C, is seen in all the samples.

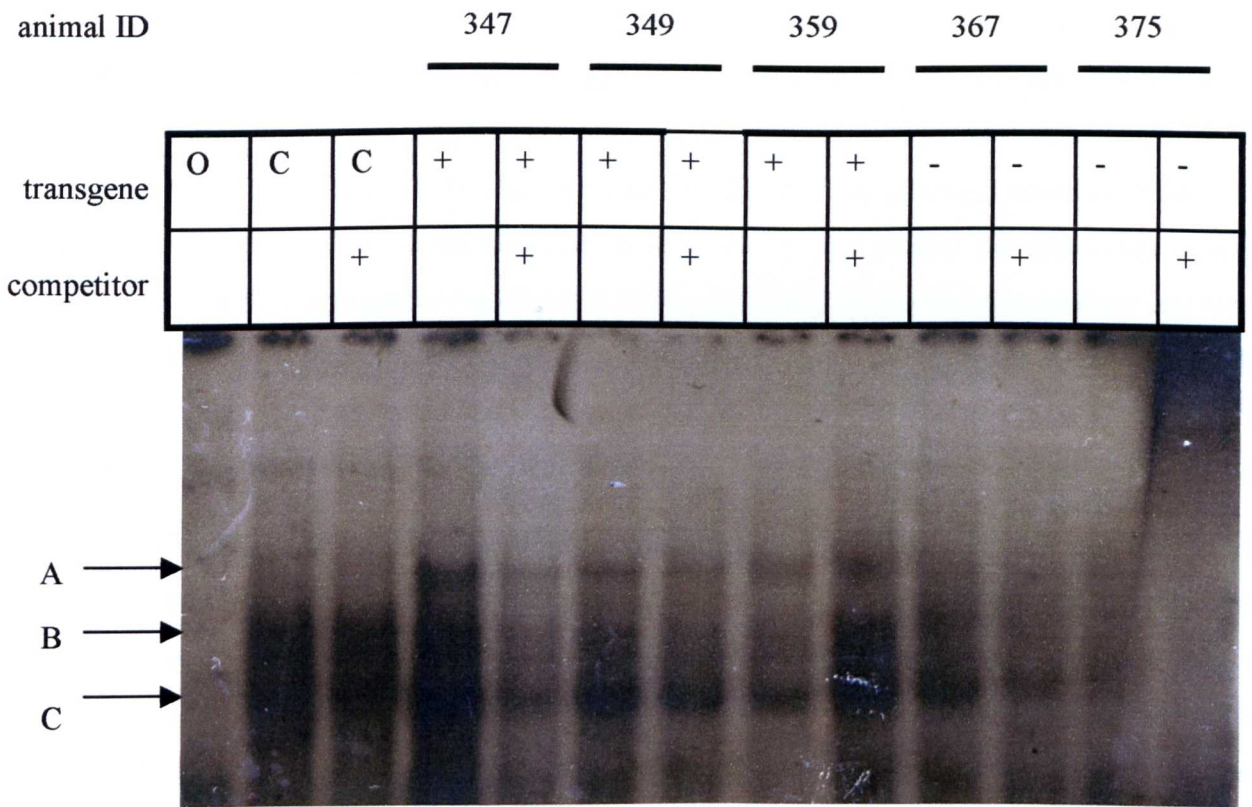


Figure 4.12: An EMSA showing specific binding of ear extracts of line 117 (L2LMP1^{CAO}) to ETS1 binding oligo.

Protein was extracted from transgenic ears (+) and wild type ears (-) and 5µg/track were separated by 6% PAGE. 5µg of NIH3T3 cell extracts were used as positive control (c). Labelled oligo without extract (O) was also added as an extra control. 100x competitor (unlabelled oligo) was added to the samples indicated (+). The ETS1 specific band A that is partially competed out upon addition of the competitor is seen in sample numbers 347, 349 and 359. Band A is not seen in samples 367 and 375 but these samples also show weaker bands B and C. The non specific bands B and C are indicated.

4.3 LMP1^{CAO} and PI3K/Akt pathway

Another target of EGFR signalling that plays a role in oncogenesis is the PI3K/Akt pathway. Ligand binding to EGFR, can activate PI3K by phosphorylation. Active PI3K can generate PIP3s that go on to activate PDK1, by phosphorylation. Active PDK1 and PIP3s together activate Akt by binding to its plekstrin homology domain and phosphorylating it at Thr308. Phosphorylation at Ser473 is also needed but it is still unclear whether PDK1 can phosphorylate Ser473 or whether another protein kinase specifically phosphorylates Ser473 (Hill et al., 2002). A negative regulator of PI3K and PDK1 is protein phosphatase and tensin homologue deleted on chromosome 10 (PTEN) that catalyses the dephosphorylation of PIP3s. Activated Akt, translocates to the cytosol where it is dephosphorylated and inactivated by PP2A. Activation of Akt affects several pathways. Active Akt inactivates Caspase-9 and Bad thus inhibiting apoptosis, it can activate NF- κ B and destabilise p53. It can also inhibit p21/cip1/waf1 and p27/kip1 from inducing cell cycle arrest by directly phosphorylating them thus leading to the release of cyclins. It also phosphorylates and inactivates glycogen synthase kinase 3 β (GSK3 β) thus inhibiting CyclinD1 degradation. Akt can also activate endothelial nitric oxide synthase (eNOS) that increases blood supply to tumour cells and increases metalloprotease production.

In order to investigate the activation status of this pathway in LMP1^{CAO} tissues, antibodies against activated Akt (Ser473 and Thr308), total Akt, PTEN and phosphorylated GSK3 β were used with both tissue and cell pellet extracts. Protein extracts from transgenic ears of increasing phenotype stages (st1-3) of line 117 and transgenic pup epidermis of line 53 alongside age matched sibling controls (c1-3) were separated by SDS-PAGE and the gels were blotted and incubated with the appropriate antibodies. Levels of phosphorylated Akt (Ser 473) in line 117 ear protein extracts, possibly show a slight decrease in stages 2 and 3 (fig.4.13). Levels of phosphorylated Akt (thr) also show a decrease in transgenic ears from stages 1-3 (fig.4.14). Levels of total Akt (fig.4.14) may be slightly reduced in stages 1-3, as the Ponceau staining of the blot suggests that each track is equally loaded, however, this is not unequivocal. Levels of total Akt show no difference among wild type and transgenic samples when further samples were analysed (fig.4.15).

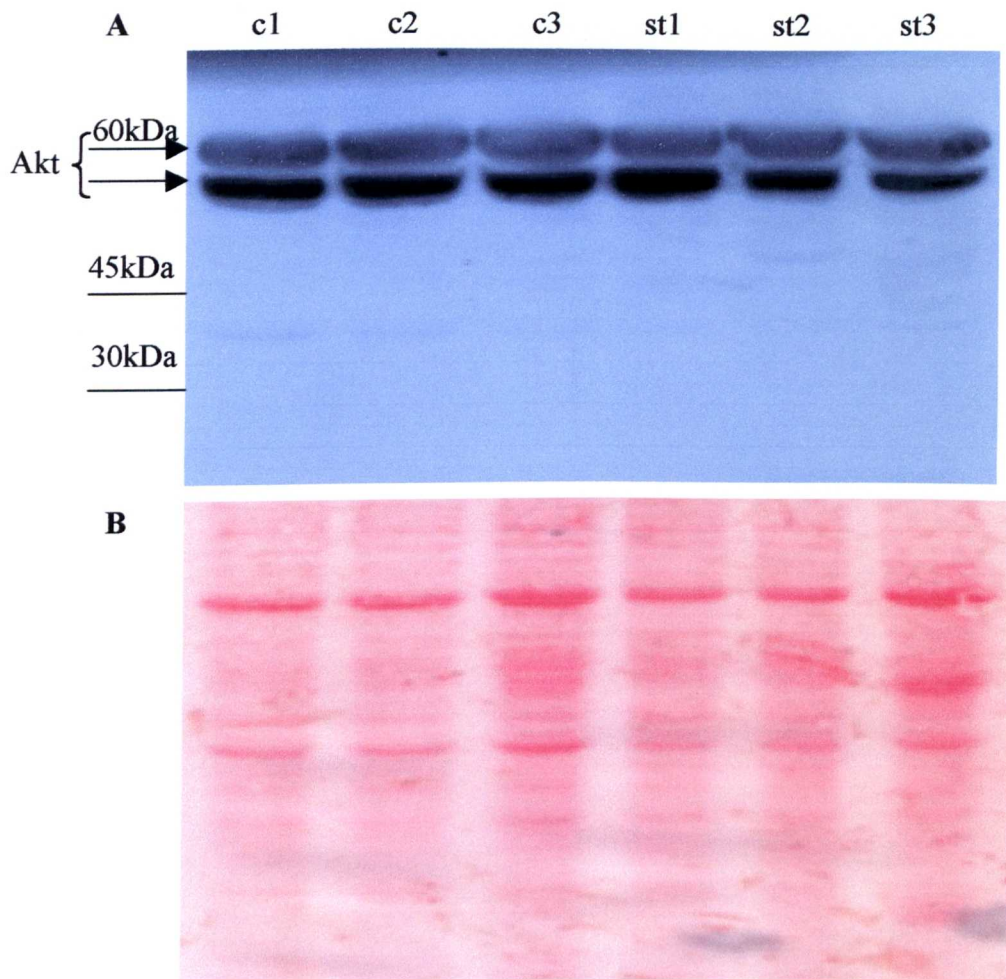
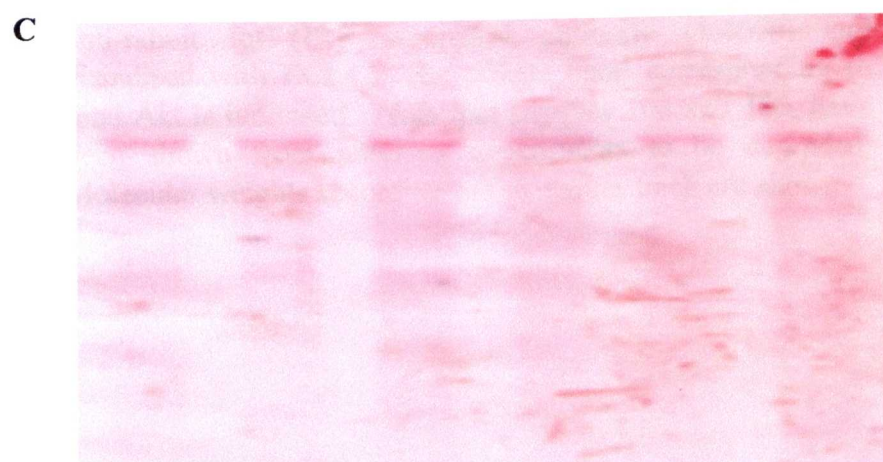
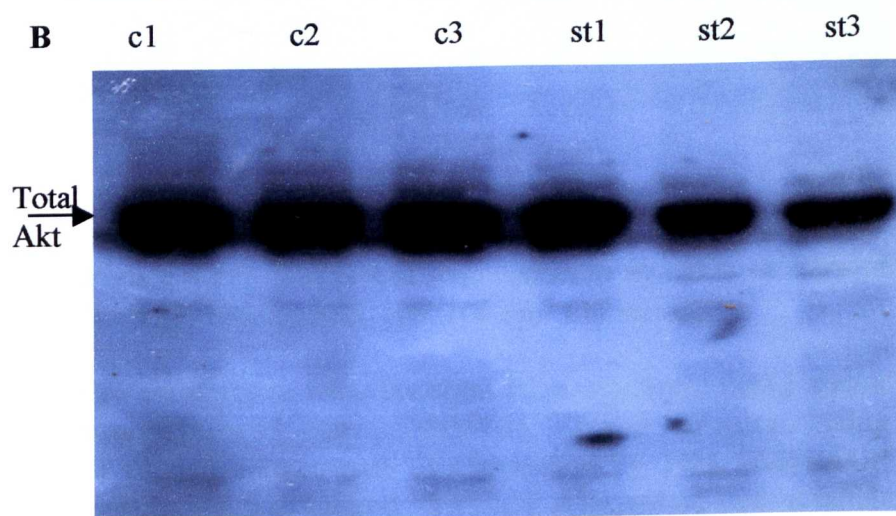
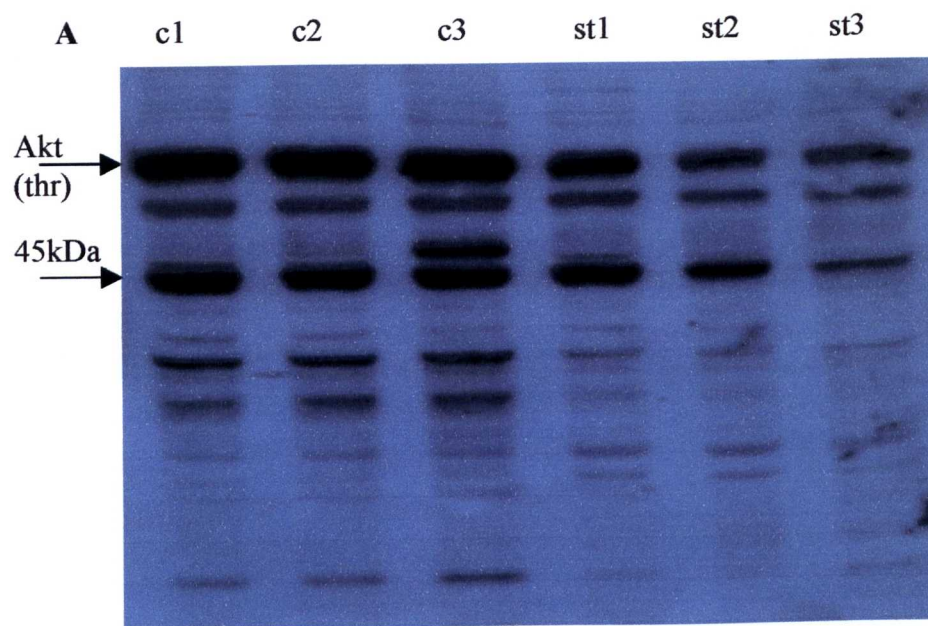


Figure 4.13: Phospho-Akt (ser) expression in the ears of line117 (L2LMP1^{CAO}) mice.

Protein extracts were prepared from ears of line 117 of increasing phenotypic stages 1-3 (st1-3) alongside age matched controls (c1-3). 100 μ g of protein extract/track was separated by 10% SDS-PAGE and the gel was blotted. The blot (A) was probed with a rabbit anti-mouse phospho-Akt (ser) primary antibody (1:1000) and a goat anti-rabbit IgG-HRP secondary antibody (1:4000) and visualised with ECL+. The 60kDa band corresponding to phospho-Akt is indicated. Molecular weights according to the the marker track are shown. A Ponceau's staining of the blot to indicate loading levels is shown (B).

Figure 4.14: Phospho-Akt (thr) and total Akt expression in ears of line 117 (L2LMP1^{CAO}) mice.

Protein extracts were prepared from ears of line 117 of increasing phenotypic stages 1-3 (st1-3) alongside age matched controls (c1-3). 100µg of protein extract/track was separated by 10% SDS-PAGE and the gel was blotted. The blot (A) was probed with a rabbit anti-mouse phospho-Akt (thr) primary antibody (1:1000) and a goat anti-rabbit IgG-HRP secondary antibody (1:4000) and visualised with ECL+. The blot was stripped and reprobed with rabbit anti-mouse total Akt (1:1000) primary antibody (B) and secondary antibody as before. The 60kDa band corresponding to Akt is indicated. Molecular weights according to the marker track are shown. A Ponceau's staining of the blot (C) used as a loading control is shown.



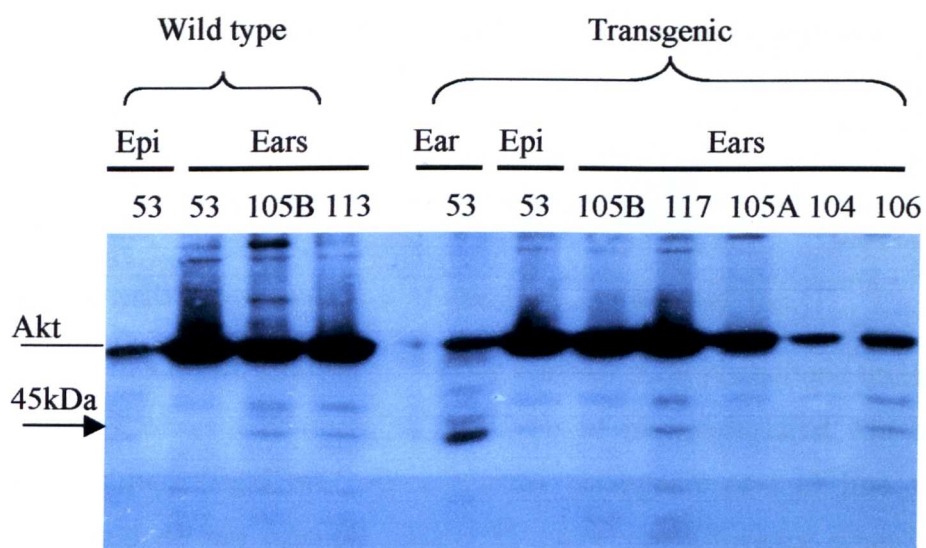


Figure 4.15: Total Akt expression in the skin or ears of lines 53, 105A, 105B, 104, 106 and 117 mice.

Protein extracts were prepared from epidermis (epi.) and/or ears of lines 53, 105A, 105B, 104, 106 and 117 mice. 100µg of protein extract/track was separated by 10% SDS-PAGE and the gel was blotted. The blot was probed with a rabbit anti-mouse total Akt primary antibody (1:1000) and a goat anti-rabbit IgG-HRP secondary antibody (1:4000) and visualised with ECL+. The 60kDa band corresponding to total Akt is indicated. Note that samples 104 and 106, have been shown from previous experiments to be degraded. Molecular weights according to the marker track are shown.

Densitometric analysis on the two blots shown in fig.4.14, showed that when the ratio of phosphoAkt (thr) to total Akt from stage 1 was compared to the corresponding ratio for control 1 there was a slight decrease as this comparison gave a value of 0.82 fold. Similarly, stage 2 and stage 3 ears when compared to their corresponding controls showed a reduced Akt (thr) activation (0.68 and 0.85 fold respectively)(Table 4.3).

Sample	Ratio Phospho-Akt (thr) : total Akt	Stage x: control x
C1	0.097	
C2	0.096	
C3	0.096	
St1	0.079	0.82
St2	0.065	0.68
St3	0.081	0.85

Table 4.3: Densitometric analysis of phospho-Akt to total Akt.

In support of this result, analysis of further samples from phenotypic transgenic ears of lines 105B and 117, show a decrease in the levels of phosphorylated Akt both at serine and threonine residues (fig.4.16). As a control, transgenic ears of line 105A that are not phenotypic and do not express LMP1^{CAO}, show no difference when compared to non transgenic sibling ears of line 105A. This indicates that the change in activation of Akt is due to the expression of LMP1 and phenotypic consequences. Levels of total Akt were investigated in cell pellets and were found to be comparable between transgenic positive and transgenic negative cell lines (data not shown). One of the effects activated Akt has is to induce an anti-apoptotic effect. The above results suggest that in transgenic tissues, apoptosis is not inhibited through the Akt pathway.

An inhibitor of Akt activation is PTEN. In order to investigate PTEN status in these tissues, a panel of tissue extracts from several LMP1 transgenic mouse lines generated in the laboratory was examined. Levels of PTEN appear to be equivalent in the control and the transgenic tissues examined (fig4.17a).

One of the downstream targets of Akt is GSK3 β . In order to investigate the status of phosphorylated GSK3 β , the same panel of tissue extracts from the LMP1 lines were examined. In the epidermis, both wild type and transgenic, phosphorylated GSK3 β is absent or below detection. In the ears examined, there is no difference in the levels of phosphorylated GSK3 β between wild type and transgenic samples (fig4.17b). Levels of phosphorylated GSK3 β in cell pellet extracts showed no difference (fig.4.18).

In conclusion, it seems that LMP1 leads to a reduction in the activation status of Akt in transgenic phenotypic tissues. This appears to be independent of the upstream inhibitor of Akt, PTEN and does not show any measured effect on the downstream factor GSK3 β .

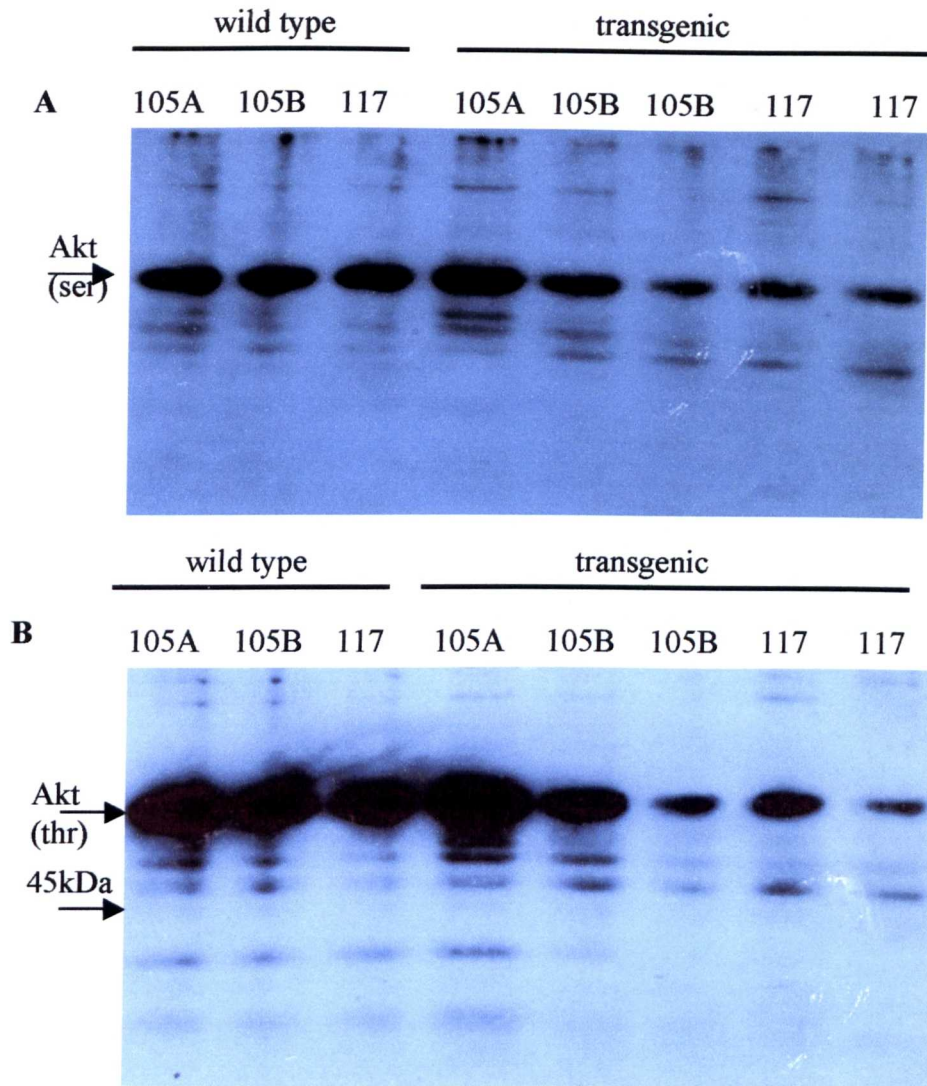


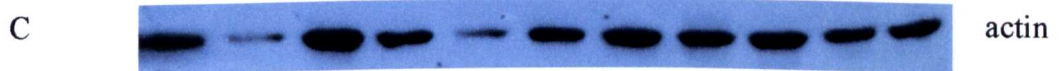
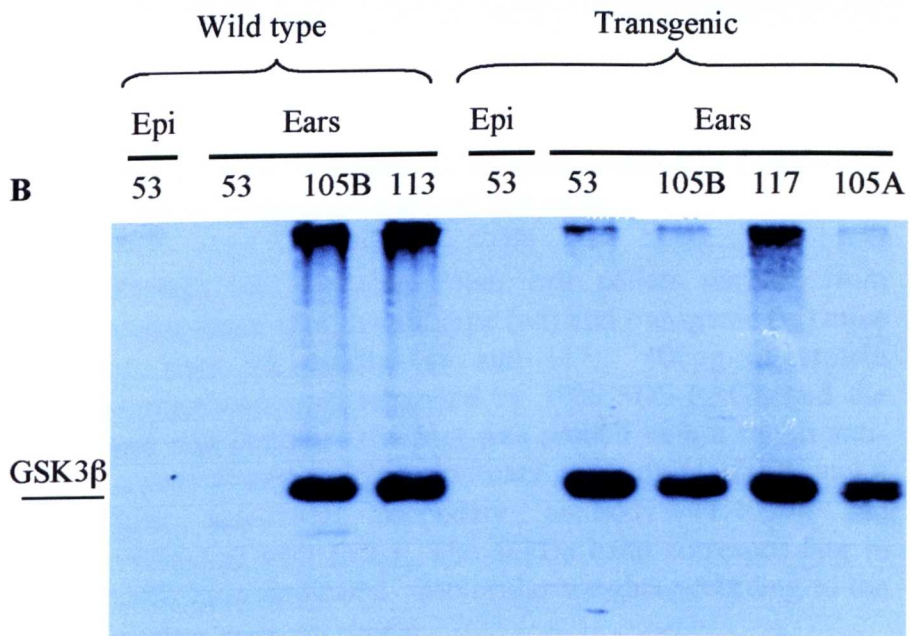
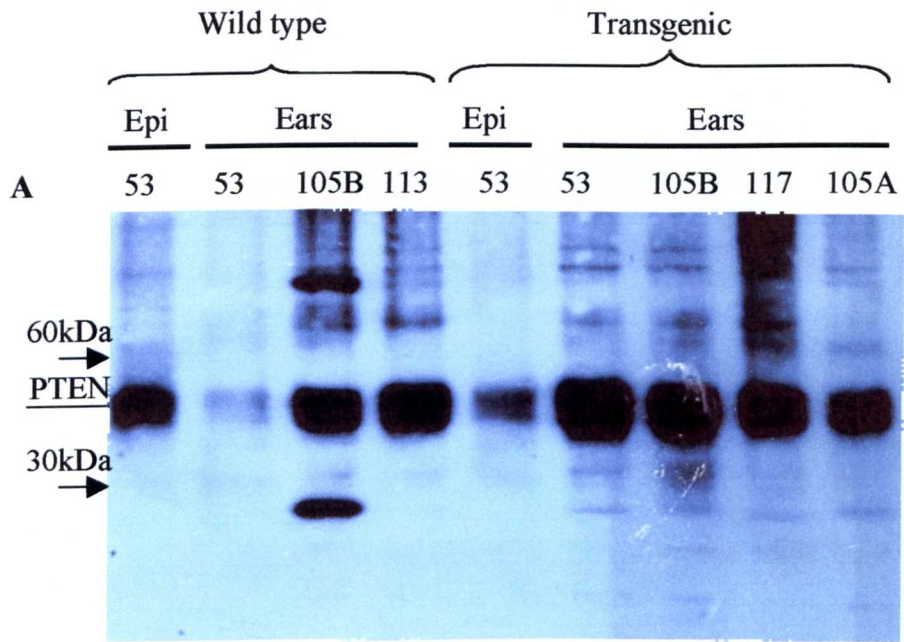
Figure 4.16: Phospho-Akt (ser) and (thr) expression in the ears of lines 105A , 105B and 117 mice.

Protein was extracted from ears of both wild type and transgenic mice. 100 μ g of protein extract/track was separated by 10% SDS-PAGE and the gel was blotted. The blot was probed with a rabbit anti-mouse phospho-Akt (ser for A and thr for B) primary antibody (1:1000) and a goat anti-rabbit secondary antibody (1:4000) and visualised with ECL+. The 60kDa band corresponding to phospho-Akt is indicated. Molecular weights as per marker track are shown.

Figure 4.17: PTEN and phospho-GSK3 β expression in skin and ears of lines 53, 105A, 105B, 113 and 117 mice.

Protein was extracted from 5 day old pup epidermis (line 53) and ears both wild type and transgenic (lines 105A, 105B, 113 and 117). 100 μ g of protein extract/track was separated by 10% SDS-PAGE and the gel was blotted. The blot was probed initially with a rabbit anti-mouse phospho-PTEN primary antibody (1:1000) and a goat anti-rabbit secondary antibody (1:4000) and visualised with ECL+ (A). The blot was stripped and reprobed with a rabbit anti-mouse phospho-GSK3 β primary antibody (1:1000) and a goat anti-rabbit secondary antibody (1:4000) and visualised with ECL+ (B). The 54kDa PTEN and 46kDa band corresponding to GSK3 β are indicated. Molecular weights according to the marker track are shown. The blot was stripped and reprobed with a goat anti-mouse actin primary antibody (1:1000) and a donkey anti-goat secondary antibody (1:4000) and visualised with ECL+ in order to determine loading levels (C).

Note that the wild type line 53 ear track and the transgenic line 53 epidermis samples are underloaded as seen by the actin blot.



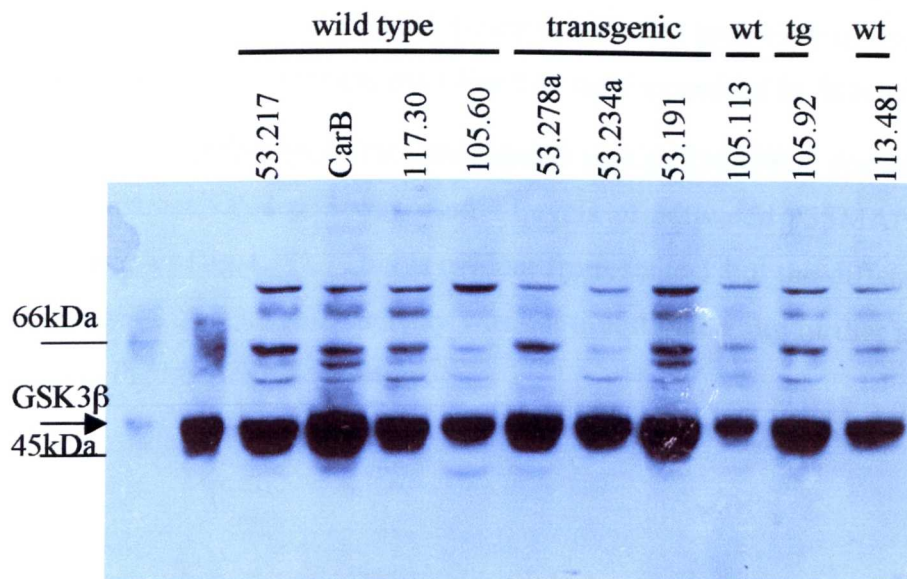


Figure 4.18: Phospho-GSK3 β expression in LMP1 and control carcinoma derived cell lines.

Protein was extracted from cell pellets derived from carcinomas of both wild type (wt) and transgenic (tg) mice of lines 53, 105B, 113 and 117. 100 μ g of protein extract/track was separated by 10% SDS-PAGE and the gel was blotted. The blot was probed with a rabbit anti-mouse phospho-GSK3 β primary antibody (1:1000) and a goat anti-rabbit secondary antibody (1:4000) and visualised with ECL+. The 46kDa band corresponding to GSK3 β is indicated. Molecular weights according to the marker track are shown.

4.4 LMP1^{CAO} and the p38 MAPK pathway

Several other pathways apart from MAPK and PI3K/Akt have been shown to be activated by LMP1 in epithelial cells, B cells and rat fibroblasts in culture. These include the p38MAPK pathway, the JNK/AP1, the NF- κ B pathway and the JAK/STAT pathway. In order to investigate whether LMP1^{CAO} could activate these other pathways in the epithelium *in vivo*, control and transgenic ear extracts from line 117 were examined by Western blotting.

The first of these pathways to be investigated was p38MAPK. An antibody specifically directed against activated p38 was used. Levels of activated p38MAPK are increased in transgenic samples (fig.4.19). This is evident from stage 1 but the difference becomes more intense in stages 2 and 3. This pathway was not investigated any further as the main focus of the thesis was the MEK/ERK pathway.

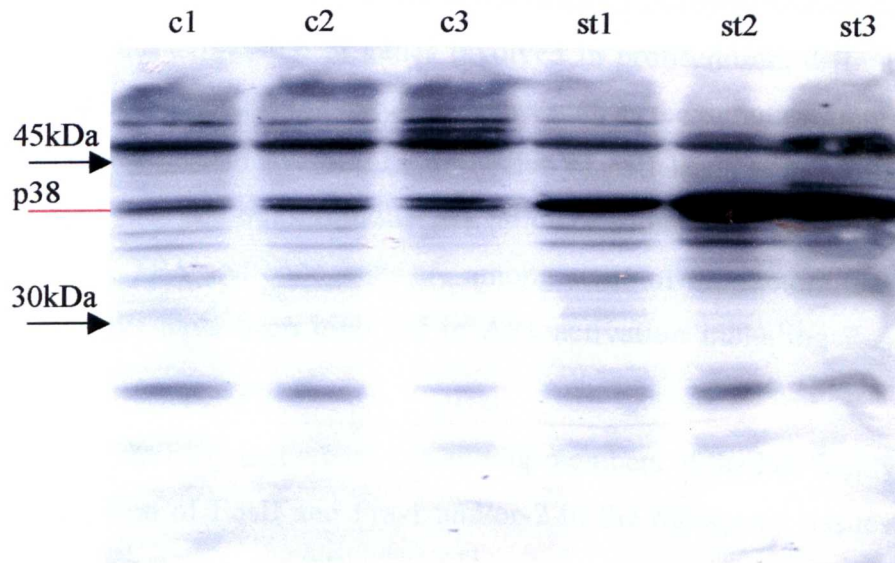


Figure 4.19: p38 activation in ears of line 117 ($L2LMP1^{CAO}$) mice.

Protein extracts were produced from ears of line 117 mice of increasing phenotypic stage, stages 1-3 (st1-3) alongside age matched stage 1-3 controls (c1-3). 100 μ g of protein extract/track was analysed on a 10% SDS-PAGE and the gel blotted. The blot was probed with a rabbit anti-mouse phospho p38 primary antibody (1:1000) and a goat anti-rabbit IgG-HRP secondary antibody (1:4000) and visualised with ECL+. The 38kDa band corresponding to phospho-p38 is indicated. Molecular weights according to the marker track are shown.

4.5 LMP1^{CAO} and the AP1 family

AP1 is a transcription factor complex, composed of Jun family homodimers or heterodimers between Jun and Fos family proteins or heterodimers between Fos or Jun and ATF/CREB proteins. The Jun family consists of c-Jun, JunB and JunD. The Fos family consists of c-Fos, FosB, Fra-1 and Fra-2. AP1 can become activated by phosphorylation of these components. AP1 regulates the expression of genes involved in proliferation, differentiation, apoptosis, immunity and inflammation and regulates genes such as the tumour suppressors p16, p19, p53, p21 and cell cycle protein Cyclin D1. Activation of AP1 leads to its binding at TPA response element (TRE) sites and transcriptional activation or sometimes repression of its target genes. Growth factors, TPA and oncogenes are among some of the factors that can activate AP1. Several pathways have been involved in AP1 activation including Ras/MAPK, JNK and p38MAPK.

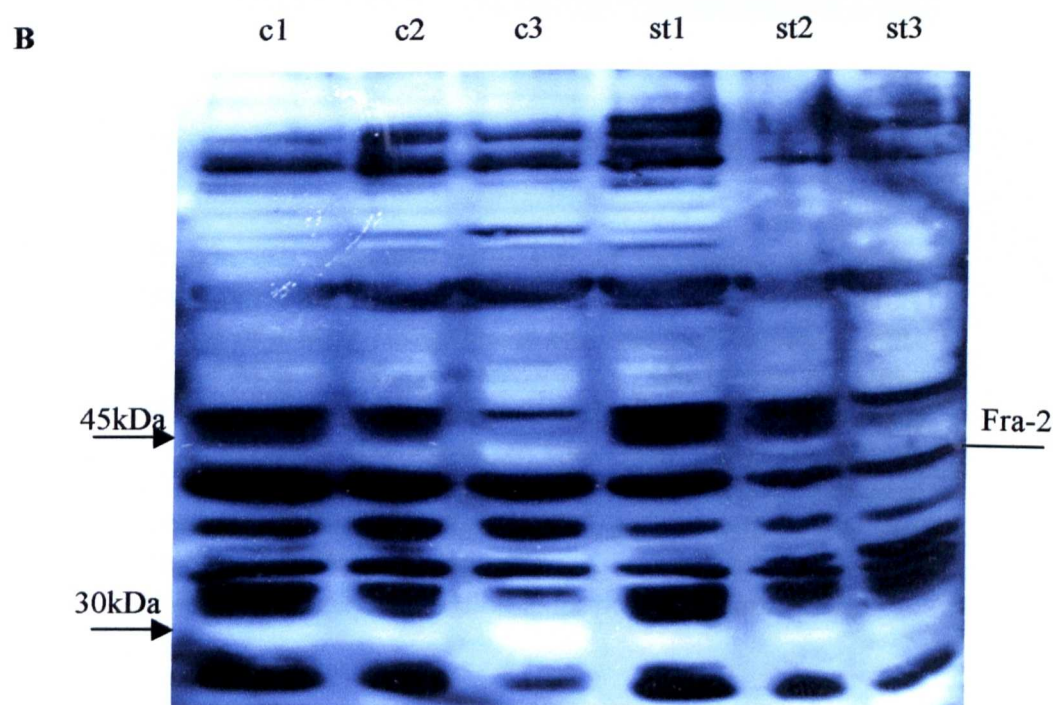
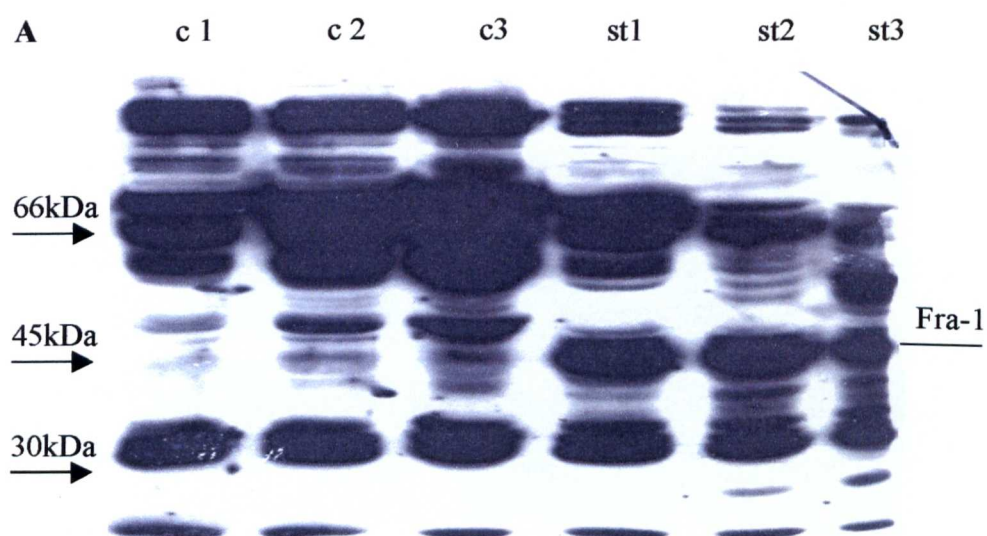
Using a pan-fos antibody that recognises all four members of the Fos family, it was possible to detect upregulation of FosB and Fra-1 and/or-2 in the transgenic tissues of line 117 when compared to their wild type sibling controls in contrast to c-fos with equivalent expression levels across the samples (fig.4.20a). Line 53 epidermal tissues do not show any difference in the low level of the Fos family proteins between control and transgenic samples. When levels of Fra-1 and Fra-2 were specifically examined, it was found that Fra-1 is upregulated in line 117 transgenic tissues whereas Fra-2 levels are unchanged (fig.4.21.a, b). Examining levels of c-Jun, it was found that there is no apparent difference between transgenic and wild type samples of lines 53 and 117 (fig.4.20b). On the other hand, JunB is strongly upregulated in transgenic samples from line 117 at all three stages examined (fig.4.22) (stage 1: 1.98 fold, stage 2: 2.44 fold, stage 3: 1.43 fold compared to controls).

Figure 4.20: Pan Fos and c-Jun expression in the skin and ears of lines 53 (PyLMP1^{B95-8}) and 117(L2LMP1^{CAO}) mice.

Protein extracts were produced from epidermis of 5 day old pups of line 53 both transgenic (+) and wild type siblings (-) and ears of mice of line 117. The protein extracts from ears were produced from increasing phenotypic ears of stages 1-3 (st1-3) and age matched sibling controls (c1-3). Extracts from NIH3T3 and A431 cell pellets were used as positive controls for fos family members and c-Jun. 100µg of protein extract/track was separated by 10% SDS-PAGE and the gel was blotted. The blot (A) was probed initially with a rabbit anti-mouse pan fos primary antibody (1:1000) and a goat anti-rabbit IgG-HRP secondary antibody (1:4000) and visualised with ECL+. The blot was then stripped and reprobed with a rabbit anti-mouse c-Jun primary antibody (1:1000) and a goat anti-rabbit IgG-HRP secondary antibody (1:4000) and visualised with ECL+ (B). Molecular weights according to the marker track are shown. The 62kDa band corresponding to c-fos, the 42kDa and 43kDa bands corresponding to fra-1 and -2 and the 36kDa band corresponding to fos B are indicated in A. The 39kDa band corresponding to c-Jun is indicated in B. The bottom picture (C) is a Ponceau's staining that was used to show loading.

Figure 4.21: Fra-1 and -2 expression in ears of line 117 (L2LMP1^{CAO}) mice.

Protein was extracted from ears of increasing phenotypic stages; stages 1-3 (st1-3) alongside age matched controls (c1-3). 100µg of protein extract/track was separated through a 10% SDS-PAGE and the gel was blotted. The blot (A) was probed with a rabbit anti-mouse Fra-1 primary antibody (1:1000) and a goat anti-rabbit IgG-HRP secondary antibody (1:4000) and visualised with ECL+. B was probed with a rabbit anti-mouse Fra-2 primary antibody (1:1000) and a goat anti-rabbit IgG-HRP secondary antibody (1:4000) and visualised with ECL+. The bands corresponding to Fra-1 (43kDa) or Fra-2 (42kDa) are indicated. Molecular weights according to the marker track are shown.



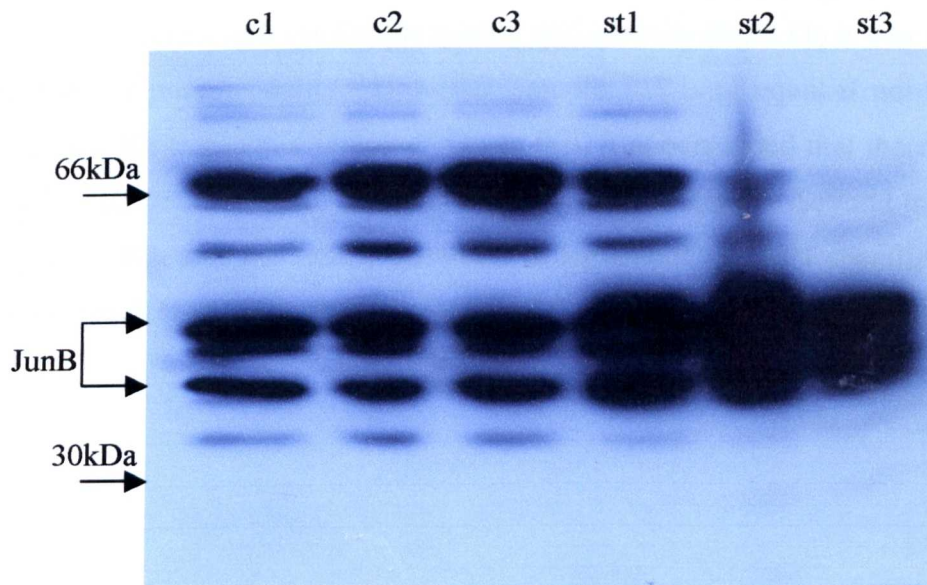


Figure 4.22: JunB expression in ears of line 117 (L2LMP1^{CAO}) mice.

Protein was extracted from ears of increasing phenotypic stage (st1-3) and their aged matched sibling controls (c1-3). 100µg of protein extract/track was separated through a 10% SDS-PAGE and the gel was blotted. The blot is a reprobe of the Fra-2 probed blot shown in fig.4.21. In this case it has been stripped and reprobbed with goat anti-mouse JunB primary antibody (1:1000) and a donkey anti-goat secondary antibody (1:4000) and visualised with ECL+. The doublet (45kDa) corresponding to JunB is indicated. Molecular weights according to marker track are shown.

In order to assess the DNA binding activity of AP1 factor in line 117 ear tissues an EMSA was performed using the oligo containing the TRE binding site (fig.4.23). The control A431 cell extract showed a specific band A that was competed with excess (200x) unlabelled oligo. Transgenic samples 347, 349 and 359 showed enhanced specific binding compared to wild type tissues 367 and 375 that show little or no binding. When an Sp1 EMSA was performed on these samples to check for sample quality and quantity (fig.4.11) it was shown that sample 367 may be of poorer quality. However, sample 375 is of equal if not better quality and quantity than the transgenic samples. Given this, it is concluded that there is enhanced AP1 activity in transgenic samples as compared to control samples. Several trials using specific antibodies to Fos and Jun family members to supershift the AP1 specific band in order to determine which components of each family make up the AP1 factor have failed.

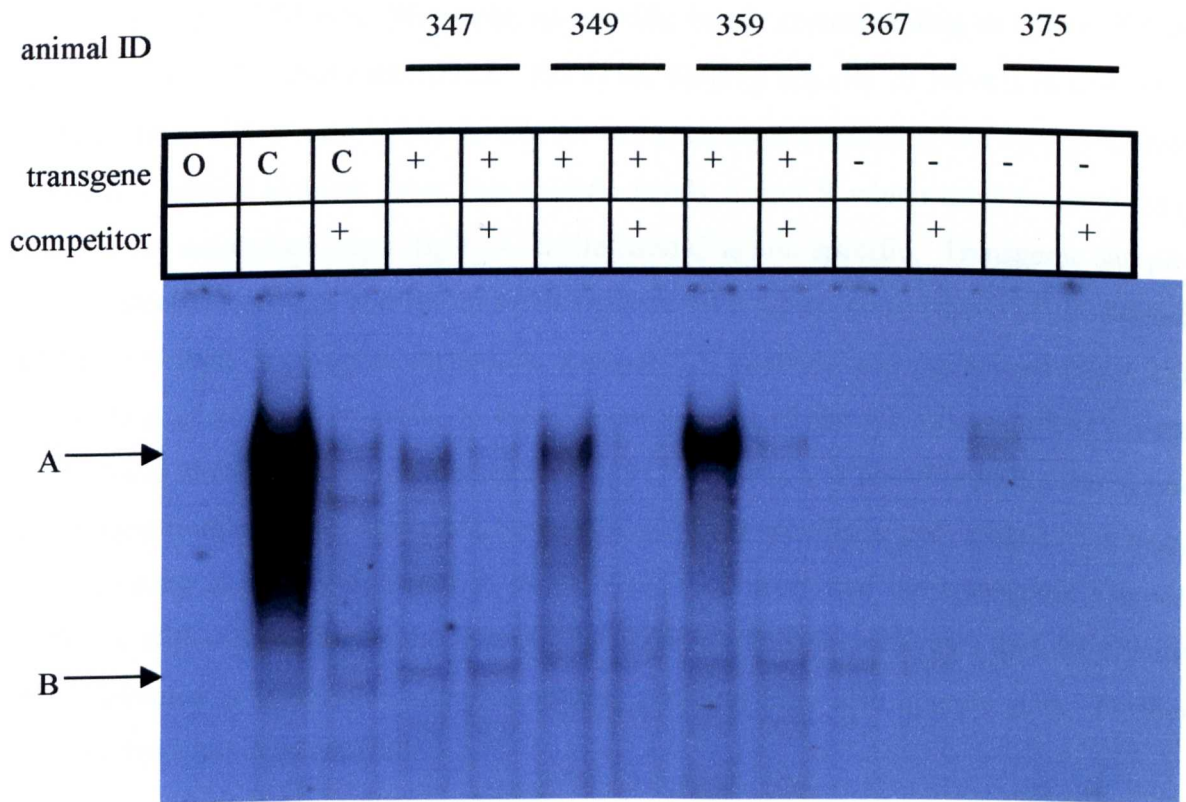


Figure 4.23: An EMSA showing specific binding of ear extracts of line 117 (L2LMP1^{CAO}) to TRE binding oligo.

Protein was extracted from transgenic (+) and wild type ears (-) and 5µg/track were separated by 5% PAGE. 5µg of A431 cell extracts were used as positive control (c). Labelled oligo without extract (O) was added as an extra control. 200x competitor (unlabelled oligo) was added to the samples indicated (+). The transgenic samples (mouse numbers: 347, 349 and 359) show specific binding to the TRE sequence while the wild type samples (mouse numbers: 367 and 375) show comparatively little binding activity (see band A). The specific TRE binding band is indicated with an arrow (A) and non specific indicated by B. Sp1 binding by these extracts was shown in fig.4.11. Sample 367 showed weak binding while sample 375 showed as strong binding as 359, which was stronger than 347 and 349.

4.6 LMP1^{CAO} and NF- κ B

The final pathway that was investigated, in this study was the NF- κ B pathway. Levels of NF- κ B were initially investigated using Western blotting and antibodies against p50 or p65; two of the components of NF- κ B. However, no specific bands corresponding to either of these components could be clearly identified. The DNA binding activity of NF- κ B in transgenic and control samples was assayed by an EMSA using an oligo containing the NF- κ B binding site. NIH3T3 control extracts show two specific bands A and B which are competed away using excess of unlabelled oligo (fig.4.24) while band C is non specific. Transgenic samples also show specific bands A and B. In order to determine which components of the NF- κ B family are involved in complex formation, a supershift analysis was performed (fig.4.25). Upon addition of antibody specific to the p50 component of the NF- κ B complex, a band migrating more slowly is readily detected in NIH3T3 controls and possibly in the transgenic sample (mouse number 347). Upon addition of the antibody specific to p65, a band even more slowly migrating is readily detected in both NIH3T3 controls and the transgenic sample, concomitant with a reduction in the intensity of band A. This demonstrates that the NF- κ B complex activated in transgenic samples contain p65 and may also contain p50. Further components have not been assayed.

The above studies show that LMP1^{CAO} can activate at least p38MAPK and NF- κ B in the epithelium *in vivo*. It probably can activate the JNK pathway but this has not been specifically shown in these sets of experiments although members of the AP1 family are upregulated and AP1 is activated.

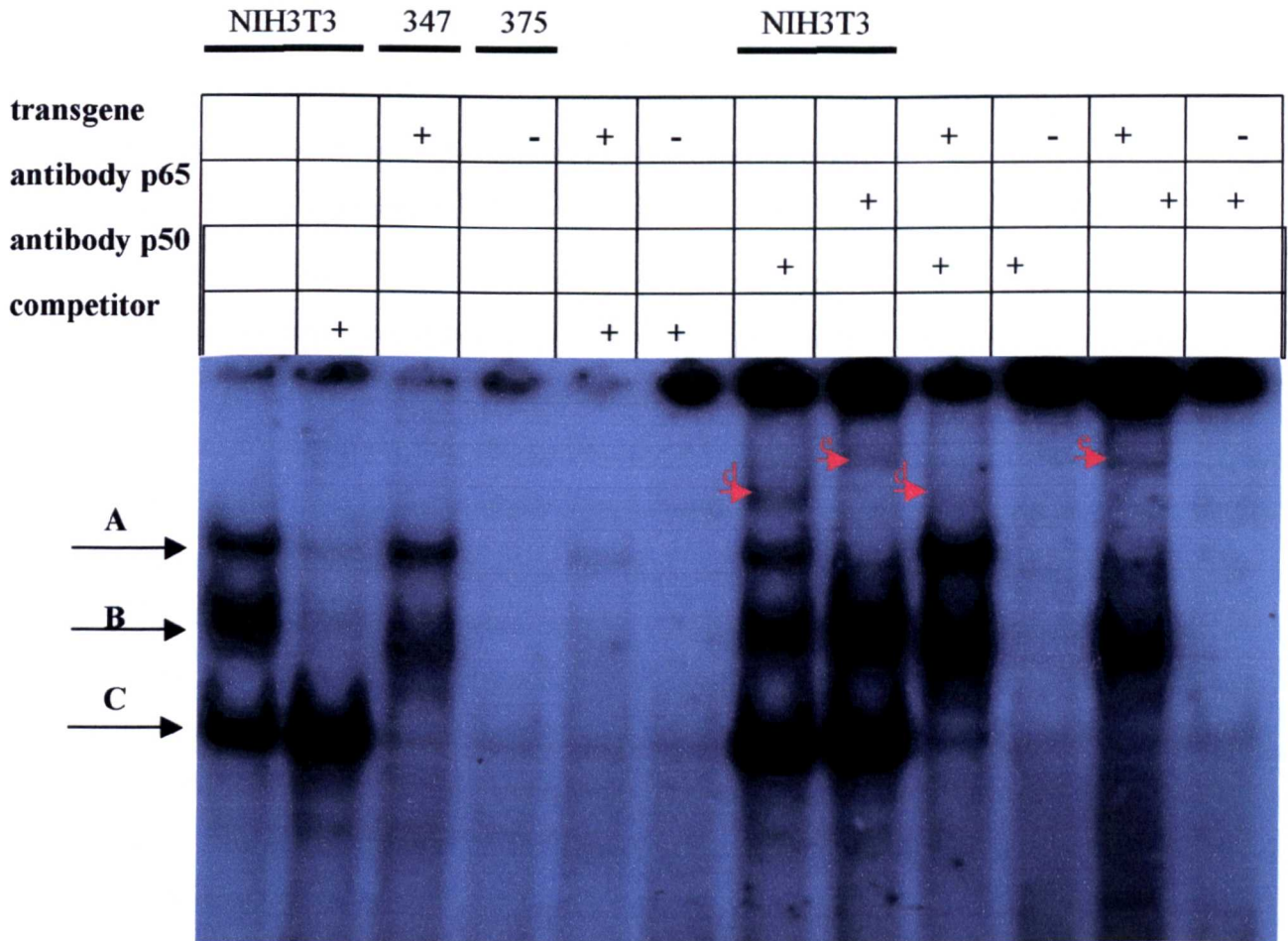


Figure 4.25: An EMSA showing supershifting in ear extracts of line 117 (L2LMP1^{CAO}) to NF- κ B binding oligo.

Protein was extracted from transgenic (+) and wild type ears (-) and 10 μ g/track were separated on a 6% PAGE. 10 μ g of NIH3T3 cell extracts were used as positive control (c). 50x competitor (unlabelled oligo) was added to the samples indicated (+). The control and transgenic sample (mouse number:347) show specific binding to NF- κ B sequence while the wild type sample (mouse number: 375) shows no binding activity (bands A and B). Non specific band C is seen in all samples. Upon addition of 0.6 μ g of p50 antibody, a slower migrating band (d) appears in the control and transgenic sample. Upon addition of 0.6 μ g of p65 antibody an even slower migrating band (e) appears in the control and transgenic sample. There is no evidence of bands d and e in the wild type sample.

4.7 Conclusion and Discussion (summary in table 4.4)

The phenotypic similarity between LMP1^{CAO} and TGF α transgenic mice prompted an investigation of the levels of TGF α in the affected tissues of LMP1^{CAO} mice. Indeed as shown, TGF α levels are upregulated in affected tissues. This upregulation in TGF α expression appears to be a direct effect of LMP1 as it is observed early in the phenotype and is consistent at all stages and in line 53 expression was limited to phenotypic epidermis.

EGFR is activated as a response to its ligand upregulation. Initially levels of total full length EGFR are increased in comparison to the wild type control but the levels decrease as the phenotype progresses. This is consistent with what has been previously observed in TGF α transgenic animals that showed decreased levels of total EGFR (Shibata et al., 1997). This reflects the tight homeostatic control at work in the skin and as a response to increased ligand binding, the tissue is recycling the receptor and downregulating its expression. This is partially in agreement with previous studies that have shown upregulation of EGFR (in C33A cells) as a response to LMP1 expression (Miller et al., 1998a; Miller et al., 1997). NPC tissue also shows upregulation in the expression of EGFR (Zheng et al., 1994a). The difference that is observed with these studies is that as the phenotype worsens levels of full length EGFR decrease. This is possibly due to the loss of homeostatic controls or negative feedback loops that exist in a preneoplastic tissue, upon carcinogenic progression. In agreement with these studies, cells obtained from carcinomas that developed on LMP1 transgenic mice, were shown to have equal if not higher EGFR expression to transgenic negative cell lines.

Levels of phosphorylated smaller EGFR products increase as the phenotype worsens, suggesting that EGFR is activated and recycled. It is possible that these smaller products represent EGFR that has translocated to the nucleus. In a recent study using breast cancer cells, it was shown that the intracellular part of ErbB4 – a member of the EGFR family – could get cleaved and translocate to the nucleus where it controlled activation of its transcriptional target STAT5 (Williams et al., 2004). It is not yet known if EGFR can go through a similar procedure.

Two of the downstream pathways that can be activated by EGFR are the Ras/MAPK cascade and PI3K/Akt pathway. Previous reports have shown that LMP1 in rodent fibroblasts leads to ERK1/2 activation. In our system, there is initial activation of MEK1/2 which decreases as the phenotype worsens, while there is constant activation of ERK2 in transgenic positive samples. There may be a negative feedback loop in place, downregulating aberrant MEK1/2

activation, with an as yet unidentified kinase activating ERK2 in a MEK1/2 independent fashion. Direction of activated MEK1 to the suprabasal layers of transgenic mice led to increased proliferation and disruption of proper terminal differentiation leading to a hyperplastic epidermal phenotype along with skin inflammation and spontaneous papilloma formation on older animals (Hobbs et al., 2004). This phenotype greatly resembles what has been seen in the LMP1^{CAO} mice consistent with the finding that MEK1 is active in the transgenic LMP1^{CAO} system.

It is interesting that no activation of c-Raf was observed in these tissues when MEK1/2 activation was observed. It could be that other homologs of c-Raf are activated in this system, for example BRaf or Araf. When a variant of E6 of the human papilloma virus (HPV) was studied, it was shown that it preferentially led to BRaf activation (Chakrabarti et al., 2004). It could be that this is true in the LMP1^{CAO} system and this needs further investigation.

Akt is deactivated as a consequence of LMP1 expression in transgenic tissues. Others (Dawson et al., 2003) have shown that LMP1 leads to activation of Akt in epithelial cells again highlighting possible differences between a precancerous tissue and carcinoma cells. Other groups have concluded that there is a cross talk between the Ras/MAPK and the PI3K/Akt pathways. For example, in HEK293 epithelial cells, Akt can downregulate ERK1/2 activity thus leading to a decrease in the activity of the MAPK pathway (Galetic et al., 2003). It is not known if ERK1/2 similarly affects Akt activation. In fact when Ras inducible mice were generated, it was found that the MAPK pathway was activated whereas the PI3K/Akt was not (Tarutani et al., 2003). The lack of change in PTEN levels when there is an Akt deactivation, implies the presence of other Akt effectors. A downstream effector of Akt, GSK3 β , showed no change in phosphorylation levels. Akt has many other downstream targets and it is possible that in this system, deactivation of Akt impacts other targets. Further study is needed to clarify this.

NF- κ B components p65 and possibly p50, were found to form the NF- κ B complex that shows increased binding in the transgenic samples compared to controls. This is consistent with previous studies that identified increased activation of NF- κ B as a direct LMP1 consequence and identified p50 and p65 as the members of the NF- κ B complex (Thornburg et al., 2003). Also the AP1 complex showed increased DNA binding in the transgenic samples compared to controls, consistent with previous studies that have demonstrated activation of AP1 as an effect of LMP1 expression (Eliopoulos and Young, 1998). Even though the supershift analysis, was not successful, Western blot analysis showed that there were higher levels of

JunB, Fra-1 and FosB in transgenic samples compared to controls making these possible candidates for being the components of the active AP1 complex. A recent study has described a new heterodimer formation between JunB and c-Jun induced by LMP1 (Song et al., 2004b). In these tissues, increased expression of JunB, Fra-1 and FosB results from LMP1 expression and not a consequence of the phenotypic progression as their upregulation is evident from the youngest samples studied (phenotypic stage 1). Similarly, p38MAPK activation is also observed from stage 1, but increasing phenotypic stages show further increase in p38MAPK activation levels, implying that progression of the phenotype increases the effect. Activation of both NF- κ B and AP1 is consistent with TGF α upregulation, as the TGF α promoter contains AP1 and NF- κ B binding sites.

In conclusion, LMP1 leads to TGF α upregulation possibly via activation of NF- κ B and AP1. TGF α upregulation leads to activation of EGFR and its faster turnover. Activated EGFR *in vivo*, probably leads to activation of the MAPK pathway, however it is not clear what leads to deactivation of the PI3K/Akt pathway. The apparent opposing effects that LMP1 has on these two pathways may reflect mechanisms within the epidermis to control aberrant proliferation.

Table 4.4: Summary of the proteins examined in line 117 mice (LMP1^{CA0})

The effect of LMP1^{CA0} on the following is shown. Yellow colour represents activation/upregulation that increased with respect to phenotypic progression. Orange represents deactivation which increases with increasing phenotypic progression. Green colour represents a constant difference from wild type across the phenotypic stages. In *italics>* and non bold lettering are the proteins for which the change is not strongly supported by the current data.

Activated	Not Activated	Deactivated	Upregulated	Not Upregulated	Upregulated then downregulated
					Activated then deactivated

Chapter 5: Does LMP1 induce hyperplasia by upregulating TGF α ?

As described in the introduction, several transgenic models overexpressing TGF α showed a phenotype of epidermal hyperplasia, ear thickening and spontaneous papilloma formation that resembles the phenotype observed in PyLMP1^{B95-8} and L2LMP1^{CAO} transgenic lines. Given the results described in Chapter 4, where TGF α upregulation and activation of the Ras/MAPK pathway was shown in tissues from line 117, it was hypothesised that LMP1^{CAO} may exert its proliferative effects via upregulation of TGF α . In order to test this hypothesis it was decided to entirely remove TGF α from the system by crossing LMP1 expressing animals to TGF α null animals and examine the resulting phenotype and the signalling pathways involved.

Testing of this hypothesis will extend the understanding of the role of LMP1 in tumourigenesis and could contribute to the design of targeted interventions.

5.1 Outline of approach

Mice of lines 53 (PyLMP1^{B95-8}) and 117 (L2LMP1^{CAO}) were separately crossbred with TGF α null animals. A detailed description of the TGF α null animals used can be found in section 1.7. These animals are referred to in this work as line 125. Line 125 mice were crossed with lines 53 or 117 to produce mice heterozygous for TGF α . These progeny were crossed together to generate TGF α null, heterozygous or wild type. The TGF α genotype was tested by PCR as described in figure.5.1 and section 2.2.3M.

Subsequently the animals produced were monitored for any phenotypic changes. Affected tissues from animals that expressed the LMP1^{CAO} transgene in a TGF α null background were examined by Western blotting to determine if absence of TGF α affects any of the pathways already analysed in Chapter 4.

Further analyses included examination by histopathological staining of affected tissues from both LMP1^{CAO} transgenic animals in wild type and null TGF α background with markers of proliferation and apoptosis.

These studies were aimed at answering the following questions:

1. Does LMP1 induce hyperplasia primarily by upregulating TGF α ?

2. What effect does absence of TGF α have on the signalling pathways deregulated by LMP1?
3. Does LMP1 in a TGF α null background play a role in proliferation or apoptosis of epithelial cells?

Results

5.2 Phenotypic examination of LMP1/TGF α null mice

The first cross conducted was between line 53 (PyLMP1^{B95-8}) and line 125 (TGF α null). In total 84 pups were produced from the 53/125 cross. All pups were euthanased between days 3–5 and the skin and whisker phenotype was observed and noted (fig.5.2A and 5.3). Genomic DNA extracted from the tissues was used to confirm their genotype compared to the observed phenotypes. 7 LMP1^{B95-8}/TGF α null, 34 LMP1^{B95-8}/TGF α heterozygous, 3 LMP1^{B95-8}/TGF α wild type, 26 LMP1^{B95-8} negative/ TGF α null and 14 LMP1^{B95-8} negative/TGF α heterozygous mice were produced and observed. It is observed that the expected Mendelian inheritance pattern is not followed with respect to the number of LMP1^{B95-8} positive mice in a TGF α null background. Whereas the expected number of LMP1 transgenic offspring that are TGF α heterozygous or null is 18.5 respectively, 30 of the offspring are TGF α heterozygous and only 7 are TGF α null. Conducting a χ^2 test on these data shows that the numbers deviate from the expected ratios with statistical significance (P=0.0005). This might suggest that LMP1 in a TGF α null background leads to reduced embryonic fitness (table 5.1).

Out of the 7 LMP1^{B95-8}/TGF α null animals produced, 4 showed the scaly skin phenotype (57.14%) (table 5.2). Although this is less than LMP1 in a heterozygous TGF α background (29/34)(85.29%) the numbers are too few to be able to conduct a meaningful statistical analysis. In the LMP1 negative mice, a few mice are noted on having a scaly skin irrespective of TGF α status (table5.2). While this study was subjective and too few mice used for a meaningful statistical comparison, it did reveal that absence of TGF α did not abolish the LMP1 induced scaly pup skin phenotype, or increase it in a marked way.

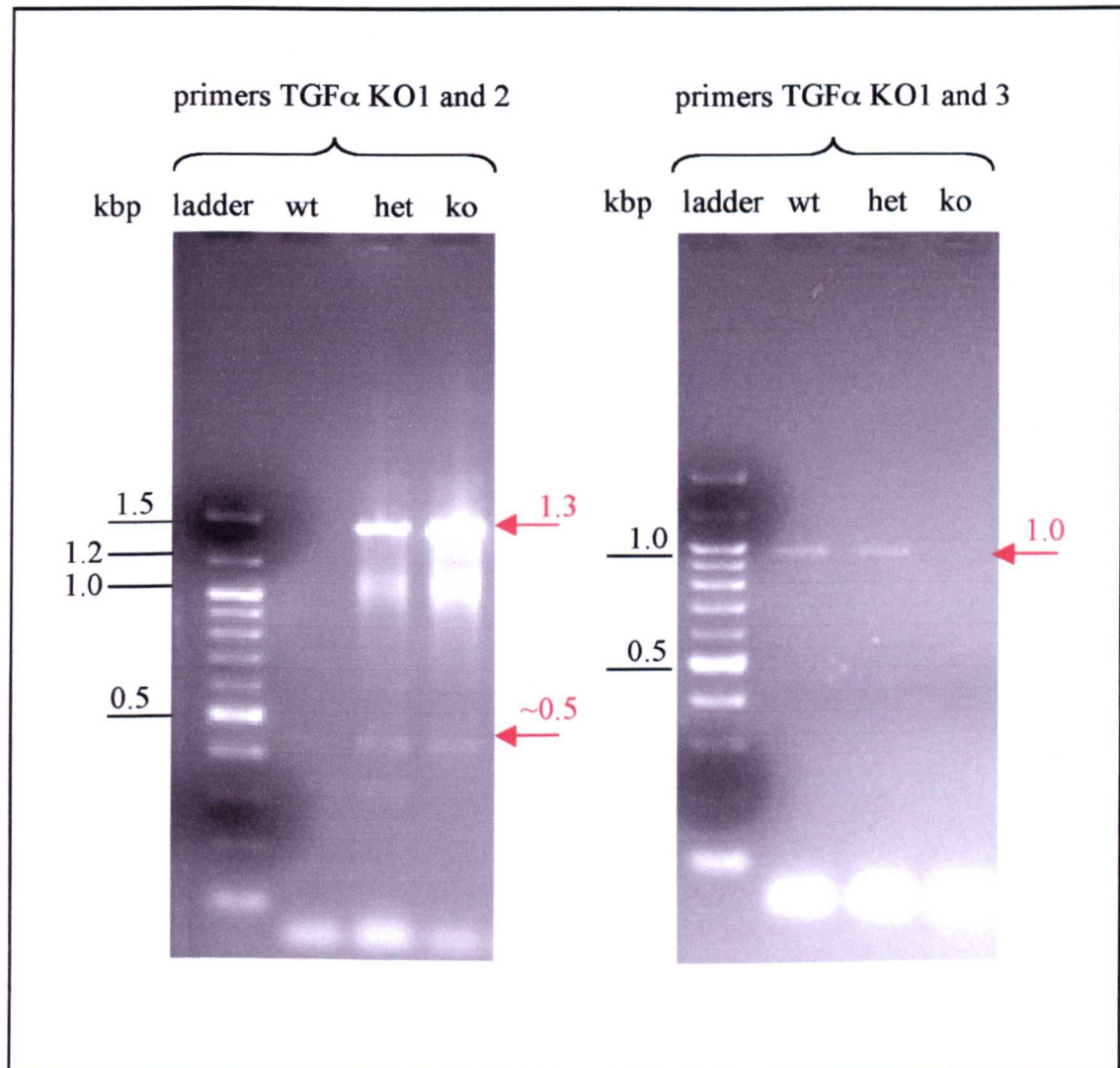


Figure 5. 1: Genotyping of line 125 by PCR

Primers TGF α KO1 and 2 were used to detect the 1300bp band corresponding to TGF α disrupted by the neomycin cassette. A control band at 500bp is routinely observed, whereas a non specific band of 1000bp is also observed in some of the reactions. Use of the primer pair TGF α KO1 and 2 leads to identification of mice that are either heterozygous (het) or null (ko) for TGF α .

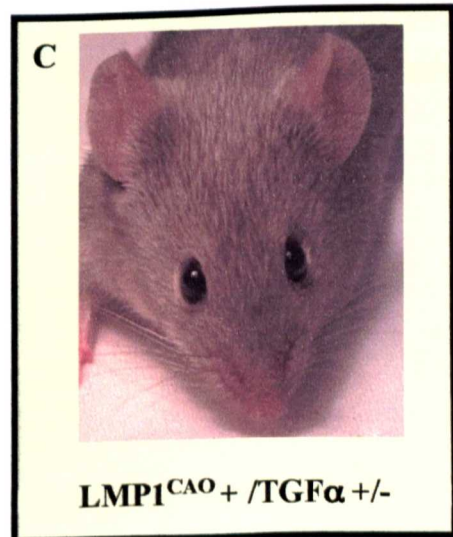
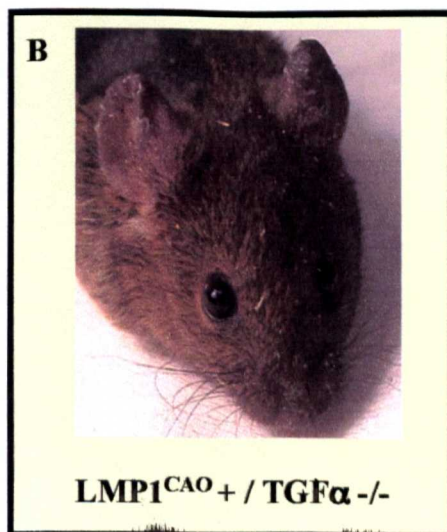
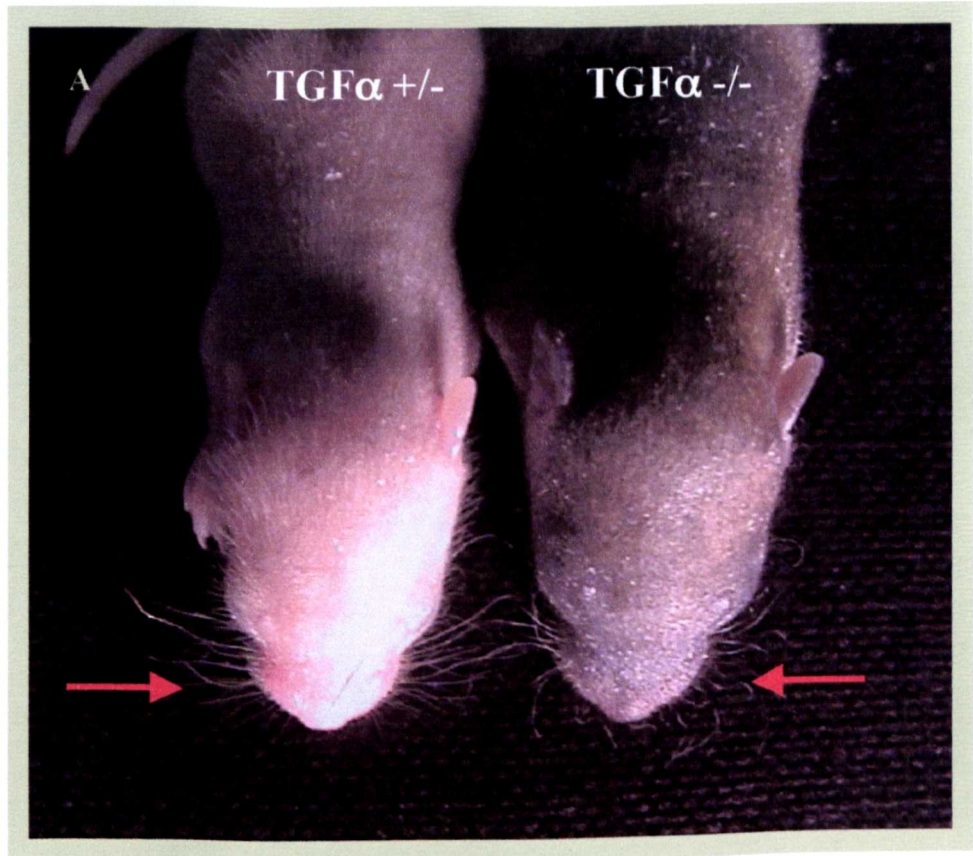
Primers TGF α KO1 and 3 are used to detect a 1000bp band corresponding to exon 3 of the TGF α gene which is disrupted by the neomycin cassette. This pair of primers leads to identification of mice that are wild type (wt) or het for TGF α .

Simultaneous use of these two primer pairs leads to identification of all three genotypes of mice for the TGF α gene.

Figure 5.2: Whisker phenotype of 53/125 pups (A) and 117/125 adult (B and C) mice.

A shows two 53/125 pups. The one on the left is heterozygous for $TGF\alpha$ (+/-) and the one on the right is $TGF\alpha$ null (-/-). As indicated by the red arrows, the $TGF\alpha$ -/- pup has markedly curly whiskers, whereas the $TGF\alpha$ +/- has relatively straight whiskers indistinguishable from wild type. Note that the coat colour (albino on the left and agouti on the right) is independent of $TGF\alpha$ status reflecting the FVB/C57/129 mixed strain background.

B and C show the ear and whisker phenotype of 117/125 adult mice that are $LMP1^{CAO}$ transgenic and $TGF\alpha$ null (B) or heterozygous (C). B has curly whiskers whereas C has straight whiskers.



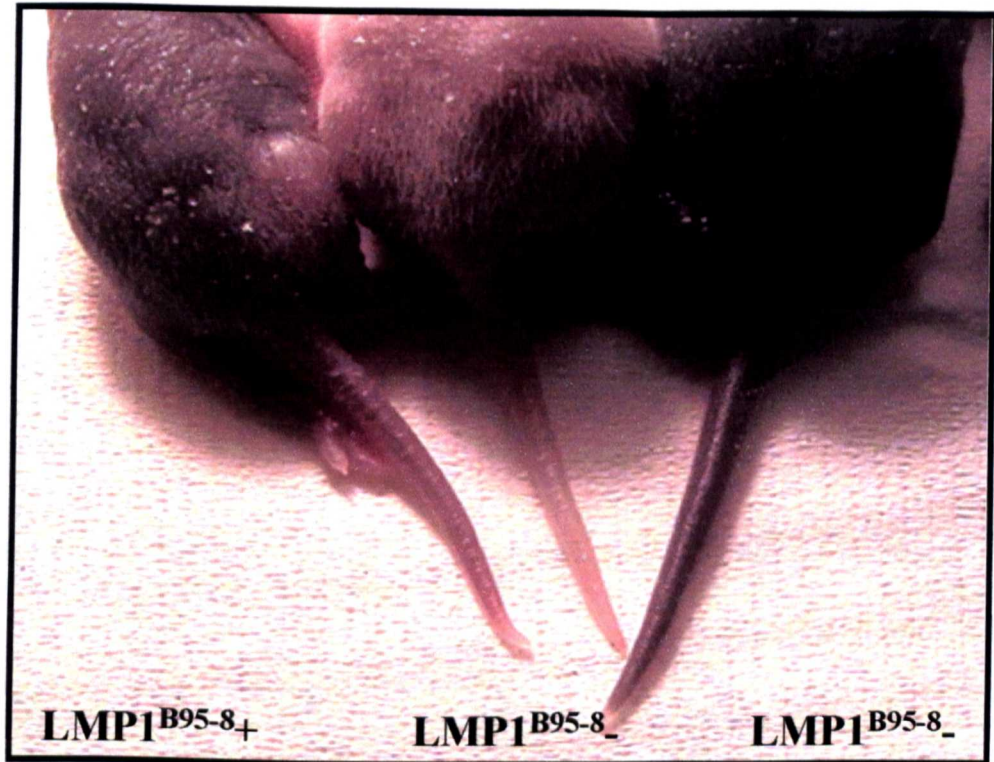


Figure 5.3: Skin and tail phenotype of 53/125 pups

The three pups shown above come from the 53/125 cross. The one on the left is $LMP1^{B95-8}$ transgenic (+) and the two on the right are $LMP1^{B95-8}$ negative (-). Wrinkly tail and scaly skin is observed on the transgenic pups and not the wild type pups.

Parental genotype (LMP1 / TGF α)	Litter Size	No of pups LMP1 +	No of pups TGF α +/+	No of pups TGF α +/-	No of pups TGF α -/-	No of pups LMP1 + and TGF α +/-	No of pups LMP1 + and TGF α -/-
- / -/- x + / +/-	10	5	0	6	4	5	0
- / -/- x + / +/-	12	4	0	6	6	4	0
- / -/- x + / +/-	12	8	0	8	4	7	1
+ / +/- x - / +/-	11	7	3	6	2	4	0
- / -/- x + / +/-	2	1	0	1	1	1	0
- / -/- x + / +/-	13	10	0	9	4	7	3
- / -/- x + / +/-	10	4	0	5	5	3	1
- / -/- x + / +/-	14	5	0	7	7	3	2

Cross - / -/- x + / +/-					
Total no of pups born: 73	No of LMP1 +	No of TGF α +/-	No of TGF α -/-	No of LMP1+ and TGF α +/-	No of LMP1+ and TGF α -/-
Observed	37	42	31	30	7
Expected	36.5	36.5	36.5	18.5	18.5
df	1	1	1	2	2
χ^2	0.01	1.658	1.658	14.43	14.43
P value	>0.25	>0.25	>0.25	0.0005	0.0005

Cross + / +/- x - / +/-							
Total no of pups born: 11	No of LMP1 +	No of TGF α +/+	No of TGF α +/-	No of TGF α -/-	No of LMP1+ and TGF α +/+	No of LMP1+ and TGF α +/-	No of LMP1+ and TGF α -/-
Observed	7	3	6	2	3	4	0
Expected	5.5	2.75	5.5	2.75	1.75	3.5	1.75
df	1	1	1	1	2	2	2
χ^2	0.82	0.273	0.273	0.273	2.71	2.71	2.71
P value	>0.25	>0.25	>0.25	>0.25	>0.25	>0.25	>0.25

Table 5.1: 53/125 litter genotyping and Mendelian inheritance

The top table shows the various litters produced and the pup genotype along with the totals of the different genotypes from two genotypic crosses: TGF α null x TGF α heterozygous cross (black) and a TGF α heterozygous x TGF α heterozygous cross (blue). The following two tables show the totals observed and expected proportions of each genotype and the chi squared analyses for the specific crosses shown.

	LMP1^{B95-8} + /TGFα -/-	LMP1^{B95-8} + /TGFα +/-	LMP1^{B95-8} + /TGFα +/+
Total number of pups	7	34	3
Number of pups with scaly skin	4 (57.14%)	29 (85.29%)	2 (66.66%)
Number of pups without a scaly skin	3 (42.86%)	4 (11.76%)	1 (33.33%)
No phenotype Dead at birth	0	1 (2.94%)	0

	LMP1^{B95-8} - /TGFα -/-	LMP1^{B95-8} - /TGFα +/-	LMP1^{B95-8} - /TGFα +/+
Total number of pups	26	14	0
Number of pups with scaly skin	2 (7.69%)	4 (28.6%)	0
Number of pups without a scaly skin	23(88.46%)	10 (71.43%)	0
No phenotype Dead at birth	1 (3.85%)	0	0

Table 5.2: Correlation of genotype and observed phenotype of cross 53/125 pups

The above tables show the number of LMP1^{CAO} transgenic positive (top) and transgenic negative (bottom) in each TGFα genotypic group. The number of animals in each group showing a specific phenotype is given. The percentage values (%) shown are out of the total number of animals in each specific genotypic group.

A more informative experiment was provided by the second cross between line 117 (L2LMP1^{CAO}) and line 125 (TGF α null). In total 60 animals were monitored from 4 weeks of age to about 30 weeks. Of these, 8 were LMP1^{CAO}/TGF α null, 9 LMP1^{CAO}/TGF α heterozygous, 7 LMP1^{CAO}/TGF α wild type and 36 mice were negative for LMP1^{CAO}, the latter did not show any ear phenotype. These ratios do not suggest any loss of LMP1^{CAO}/TGF α null genotype group. The animals were monitored once a week and the ear phenotype was visually categorised according to the ear stages figure (fig.1.14). The dorsal skin of these mice was also monitored for spontaneous papilloma formation. No papilloma formation was detected in any of the animals. However, it should be noted that the strain background of these mice differs from the 117 line under study in chapter 3 which was largely FVB. The introduction of the TGF α null strain also introduced a 129/C57 mouse strain component and papilloma formation is strain sensitive. In monitoring the ear phenotype it was observed that the LMP1^{CAO}/TGF α null mice developed an ear phenotype that was more progressed than the LMP1^{CAO}/TGF α heterozygous or wild type ear phenotype (fig.5.2B and C).

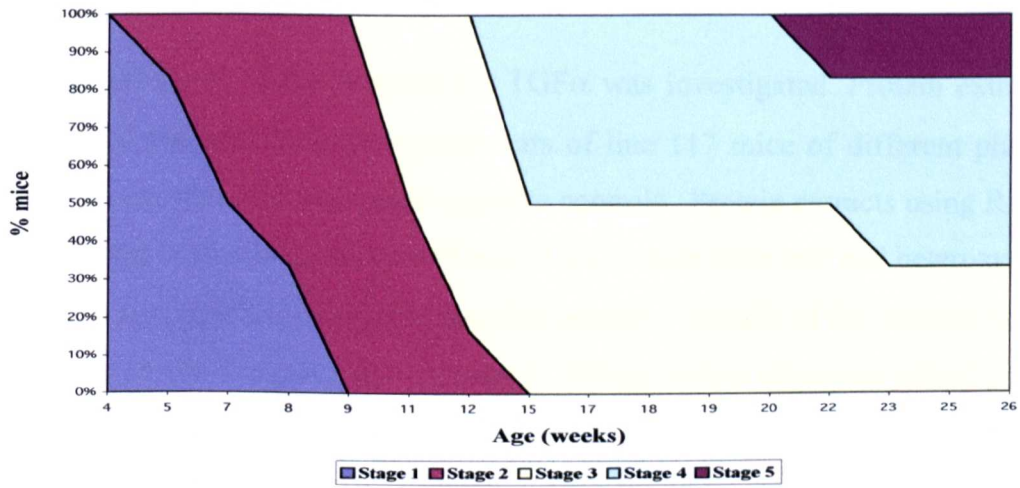
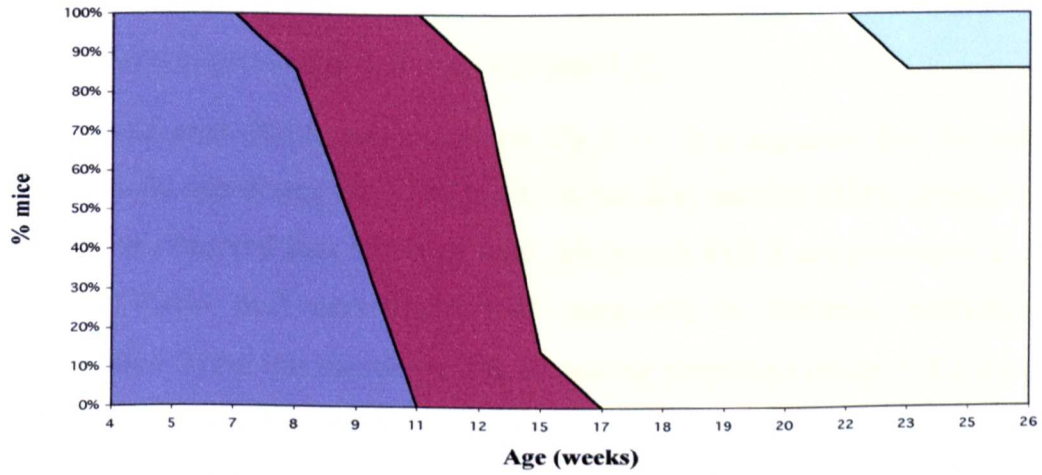
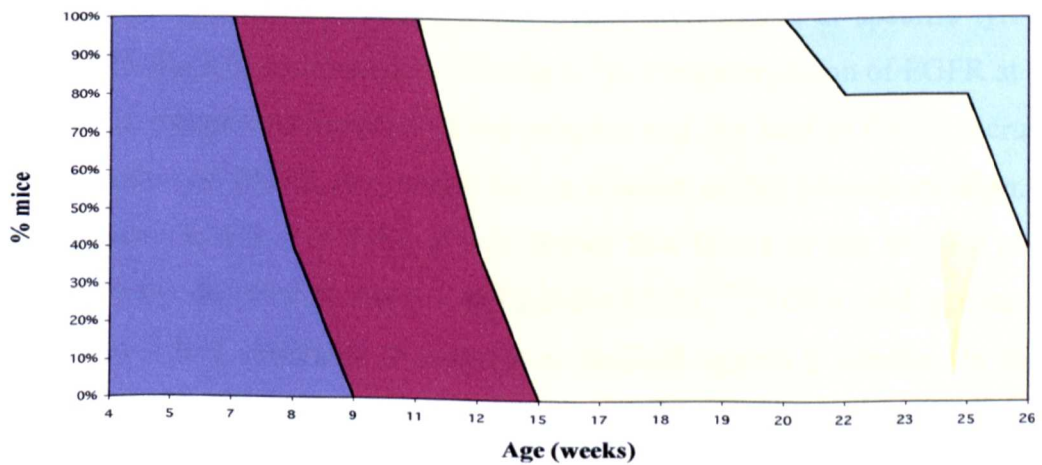
In order to quantify this, the proportion of mice with ears at the phenotypic stages have been plotted against age (fig.5.4). As seen from the graphs (fig. 5.4), at about 5 weeks of age all the TGF α heterozygous or wild type animals show a stage 1 ear phenotype whereas 80% of the TGF α null mice show stage 1 ear phenotype and 20% exhibit a progressed ear phenotype of stage 2. At 7 weeks of age, 100% of the TGF α heterozygous and wild type mice show stage 1 ear phenotype whereas only 50% of TGF α null mice show stage 1 ear phenotype. By 9 weeks all null and wild type ears show a stage 2 phenotype, while 50% of the heterozygous ears show stage 2. A more consistent difference between TGF α null and the heterozygous or wild type groups becomes apparent at the later stages, 4 and 5 of the phenotype. By 15 weeks 50% of the null mice developed a stage 4 phenotype and by 20 weeks some mice began to develop a stage 5 phenotype. By contrast, the TGF α heterozygote and wild type mice did not start to develop the stage 4 phenotype until 22 and 20 weeks respectively and in the time frame of this study this phenotype did not progress to stage 5. The phenotype progression in heterozygous and wild type mice follows largely the same pattern.

There is a general trend apparent that the null mice ear phenotype progresses faster than the heterozygous and wild type mice. This is contrary to what would be expected if the hypothesis was correct in that the LMP1 induced ear phenotype is mediated via upregulation of TGF α alone. While the data is subjective in nature it was absolutely clear that loss of TGF α did not negate the LMP1 induced phenotype. However, upregulation of other EGFR

ligands has not been examined in this system and it is possible that upon withdrawal of TGF α , other EGFR ligands can compensate.

Figure 5.4: Graphs showing the phenotypic progression of ears of mice from line 117/125.

Ears from LMP1^{CAO} transgenic animals that were null (A), heterozygous (B) or wild type (C) for TGF α were observed once every two weeks for 22 weeks and categorised into phenotypic stages. Phenotypic stage 1 ears are represented by purple colour, stage 2 are magenta, stage 3 are yellow, stage 4 are light blue and stage 5 are dark purple. The percentage of mice from each genotypic group that showed the particular ear phenotype stage is indicated on the Y-axis of each graph. Note that a mouse was categorised according to the ear of worse (higher number) stage if its ears were different.

A**Percentage of LMP1 + / TGFA -/- mice in each phenotypic stage****B****Percentage of LMP1 + / TGFA +/- mice in each phenotypic stage****C****Percentage of LMP1 + / TGFA ++ mice in each phenotypic stage**

5.3 Analysis of signalling pathways activation in LMP1^{CAO}/TGF α null mice

A. TGF α /EGFR/Ras/MAPK pathway

Initially, the status of the receptor for TGF α was investigated. Protein extracts using RIPA buffer were prepared from transgenic ears of line 117 mice of different phenotypic stages along with age matched transgenic negative controls. Protein extracts using RIPA buffer, were also prepared from transgenic ears of line 117/125 mice both null and heterozygous for TGF α along with age matched transgenic negative controls. Details of the animals used in these and subsequent studies are given in Appendix 3. 100 μ g (unless otherwise stated) of protein extract per track was separated by SDS-PAGE, the gel was blotted and the appropriate antibodies were used to detect the desired proteins. Densitometric analysis was routinely performed where needed, to compare levels of the detected protein under study to its non-phosphorylated form or to β tubulin, which was used to indicate loading levels. These analyses were performed as was previously described (chapter 4.2).

Expression of total EGFR was examined (fig.5.5). It is apparent that the antibody to total EGFR not only can detect the 170kDa EGFR but also smaller EGFR products at 75, 65 and 50kDa. It is observed that levels of total full length EGFR are increased at stage 1 in the LMP1^{CAO} /TGF α null ears (1.36 fold compared to controls, normalised against β tubulin)(table 5.3) but this decreases with advancing phenotype (stage 2: 1.1 fold, stage 3: 0.91 fold) and this is concomitant with the appearance of smaller EGFR products (as reported in chapter 4). This decrease in the 170kDa EGFR and the increase in the smaller EGFR products appears to be independent of TGF α loss. Some of these smaller products react with two antibodies that specifically recognise phosphorylated EGFR at specific tyrosine residues (tyrosine 845 (fig.5.6) and tyrosine 1068 (fig.5.7)). Phosphorylation of EGFR at tyrosine 1068 is a result of autophosphorylation of the receptor and can lead to GRB2 recruitment whilst phosphorylation of EGFR at tyrosine 845 is a result of Src phosphorylation. Using anti-phosphorylated EGFR (tyr 845), it was shown that levels of the smaller phosphorylated products initially decrease at stages 1 and 2 in the LMP1^{CAO}/TGF α wild type ears but increase at stage 3 by 3 fold compared to controls normalised against β tubulin. In the LMP1^{CAO} / TGF α null ears, levels increase from stages 2 to 4 (stage 2: 1.23 fold, stage 3: 2.32 fold, stage 4: 4.36 fold when compared to controls) (table 5.4). The increase in phosphorylated products detected with the antibodies to tyr1068 EGFR mirrors the results

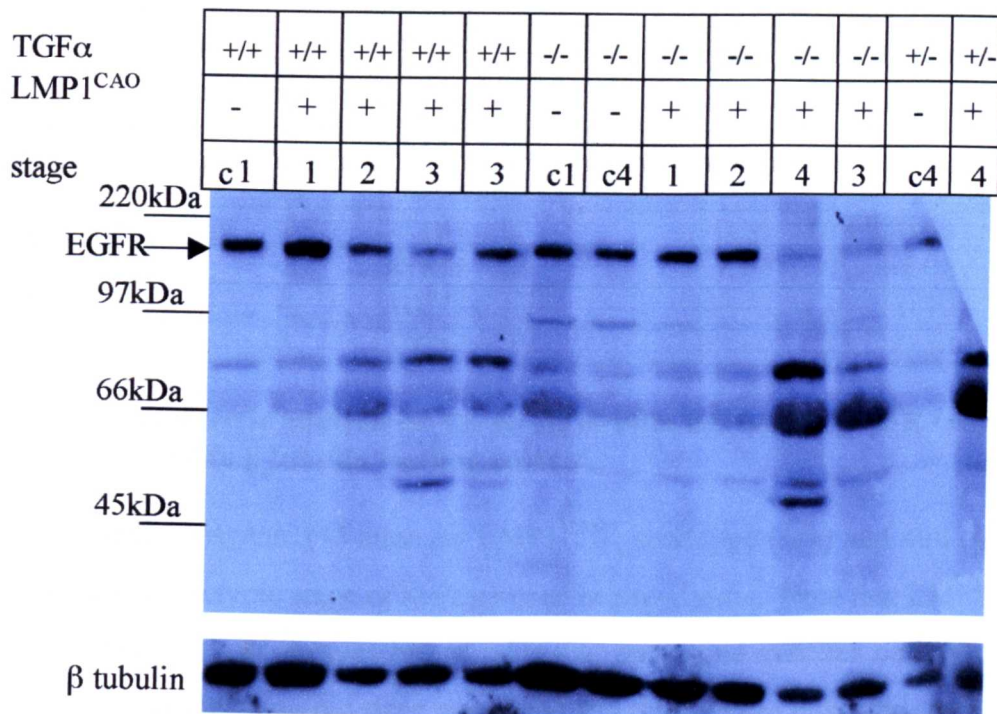


Figure 5.5: Total EGFR western blot of protein extracts from ears of mice of lines 117 and 117/125.

Protein extracts were prepared from phenotypic ears, stages 1-3 (st1-3) from mice that were transgenic for LMP1(+) and wild type (+/+), heterozygous (+/-) or null (-/-) for TGF α . Age matched control extracts from ears of LMP1^{CAO} transgenic negative siblings (-) were also prepared. 100 μ g of protein extract/track was separated by 7.5% SDS-PAGE and the gel was blotted. The blot was probed with a rabbit anti-mouse total EGFR primary antibody (1:1000) and a goat anti-rabbit IgG-HRP secondary antibody (1:4000) and visualised with ECL+. The 170kDa corresponding to total EGFR is indicated. Molecular weights according to marker track are shown. The bottom picture shows the β tubulin reprobing of the blot to show relative loading levels.

Genotype			A	B	C
LMP1	TGF α	Phenotypic stage	EGFR (170kDa): β tubulin EGFR smaller bands: β tubulin	LMP1 ^{CAO} : wild type	Null to wild type in respect of TGF α
-	+/+	C1	0.11 / 0.02	1	
+	+/+	1	0.15 / 0.02	1.36 / 1.13	
+	+/+	2	0.12 / 0.04	1.10 / 1.60	
+	+/+	3	0.10 / 0.06	0.85 / 3	
+	+/+	3	(average)		
-	-/-	C1	0.11 / 0.03		
-	-/-	C4	(average)		
+	-/-	1	0.10 / 0.03	0.96 / 0.98	0.68 / 1.23
+	-/-	2	0.13 / 0.03	1.17 / 1.01	1.02 / 0.80
+	-/-	4	0.07 / 0.13	0.68 / 4.34	0.70 / 2.17
+	-/-	3	0.05 / 0.05	0.44 / 1.72	0.50 / 0.83

Table 5.3: Densitometric analysis on the levels of total full length EGFR / smaller EGFR products respective to β tubulin loading control.

Wild type (-) and transgenic (+) mice for LMP1^{CAO}, wild type (+/+) and null (-/-) for TGF α are shown. The phenotypic stage of the ears used is also shown. Note that LMP1^{CAO} negative mice do not have an ear phenotype but animals that were aged matched controls of LMP1^{CAO} + mice of a particular phenotypic stage were used and that stage is indicated.

Values given are after the deduction of the background intensity.

Column A : Total EGFR: β tubulin (black), smaller EGFR products : β tubulin (blue)

Column B: LMP1^{CAO} : control (TGF α wild type are black for full length EGFR, blue for smaller products, TGF α null are pink for full length EGFR, green for smaller products)

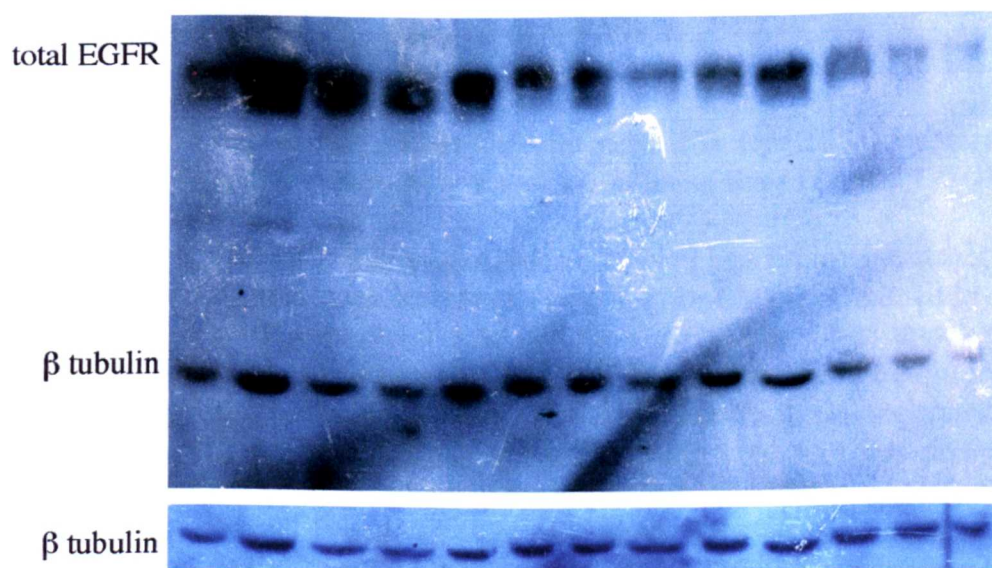
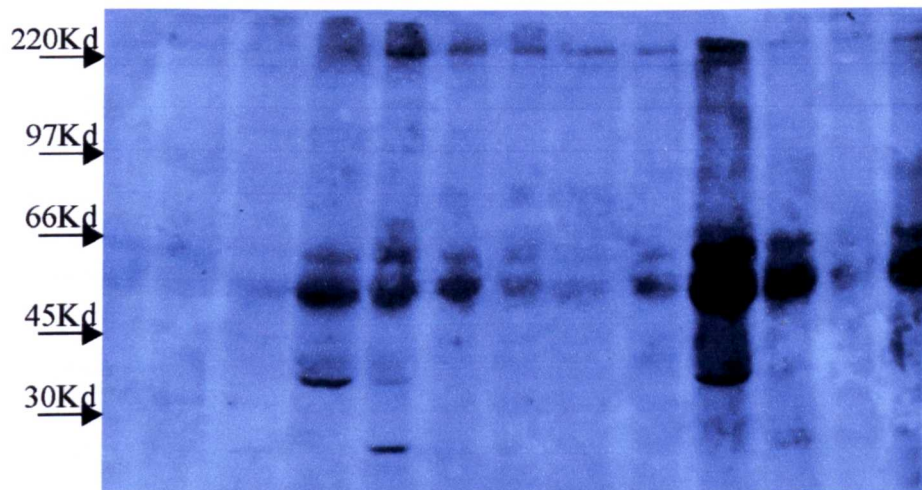
Column C: LMP1^{CAO} / TGF α null : LMP1^{CAO} / TGF α wild type (black for full length EGFR, blue for smaller EGFR products).

Note that LMP1^{CAO} negative in a TGF α null or wild type background give some reading.

Figure 5.6: Phosphorylated EGFR (tyr 845) western blot of protein extracts from ears of mice of lines 117 and 117/125.

Protein extracts were prepared from phenotypic ears, stages 1-3 (st1-3) from mice that were transgenic for LMP1(+) and wild type (+/+), heterozygous (+/-) or null (-/-) for TGF α . Age matched control extracts from ears of LMP1^{CAO} transgenic negative siblings (-) were also prepared. 100 μ g of protein extract/track was separated by 7.5% SDS-PAGE and the gel was blotted. The blot was probed with a rabbit anti-mouse phospho-EGFR (tyr845) primary antibody (1:1000) and a goat anti-rabbit IgG-HRP secondary antibody (1:4000) and visualised with ECL+. Molecular weights according to marker track are shown. The blot was stripped and reprobed with total EGFR and β tubulin to show relative loading levels.

TGF α	+/+	+/+	+/+	+/+	+/+	-/-	-/-	-/-	-/-	-/-	-/-	+/-	+/-
LMP1 ^{CAO}	-	+	+	+	+	-	-	+	+	+	+	-	+
stage	c1	1	2	3	3	c1	c4	1	2	4	3	c4	4



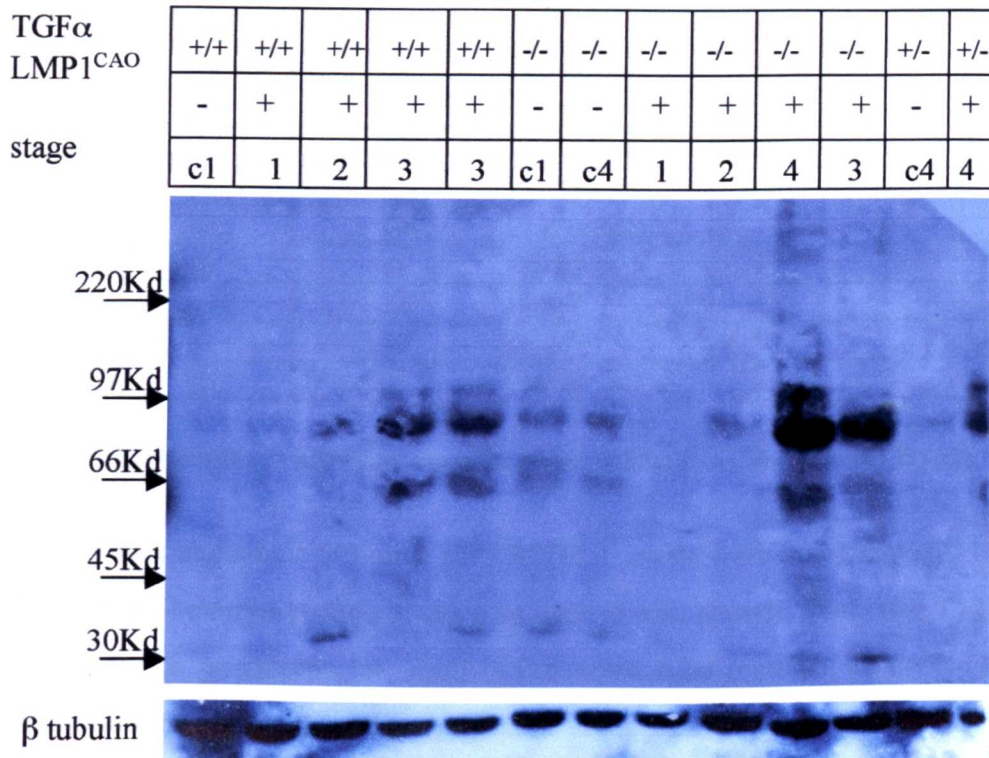


Figure 5.7: Phosphorylated EGFR (tyr 1068) western blot of protein extracts from ears of mice of lines 117 and 117/125.

Protein extracts were prepared from phenotypic ears, stages 1-3 (st1-3) from mice that were transgenic for LMP1(+) and wild type (+/+), heterozygous (+/-) or null (-/-) for TGF α . Age matched control extracts from ears of LMP1^{CAO} transgenic negative siblings (-) were also prepared. 100 μ g of protein extract/track was separated by 7.5% SDS-PAGE and the gel was blotted. The blot was probed with a rabbit anti-mouse phospho-EGFR (tyr1068) primary antibody (1:1000) and a goat anti-rabbit IgG-HRP secondary antibody (1:4000) and visualised with ECL+. Molecular weights according to marker track are shown. The blot was stripped and reprobed with β tubulin to show relative loading levels.

Genotype			A	B	C
LMP1	TGF α	Phenotypic stage	pEGFR (tyr845) : β tubulin	LMP1 ^{CAO} : wild type	Null or het to wild type in respect of TGF α
-	+/+	C1	0.16	1	
+	+/+	1	0.11	0.66	
+	+/+	2	0.07	0.45	
+	+/+	3	0.48	3.00	
+	+/+	3	(average)		
-	-/-	C1	0.22		
-	-/-	C4	(average)		
+	-/-	1	0.16	0.73	1.45
+	-/-	2	0.27	1.23	3.59
+	-/-	4	0.96	4.36	2
+	-/-	3	0.51	2.32	1.06

Table 5.4: Densitometric analysis on phosphorylated EGFR (tyr845) levels

Wild type (-) and transgenic (+) mice for LMP1^{CAO}, wild type (+/+) and null (-/-) for TGF α are shown. The phenotypic stage of the ears used is also shown. Note that LMP1^{CAO} - mice do not have an ear phenotype but animals that were aged matched controls of LMP1^{CAO} + mice of a particular phenotypic stage were used and that stage is indicated.

Values given are after the deduction of the background intensity.

Column A: Phosphorylated EGFR (tyr845): β tubulin

Column B: LMP1^{CAO} : control (TGF α wild type are black, TGF α null are pink)

Column C: LMP1^{CAO} / TGF α null : LMP1^{CAO} / TGF α wild type

Note that LMP1^{CAO} negative in a TGF α null or wild type background give some reading.

obtained with tyr845 EGFR. This indicates that removal of TGF α does not lead to reduced signalling through EGFR and suggests instead that it may lead to over-compensation by other EGFR ligands thus leading to increased EGFR activation.

In order to examine whether other EGFR family members are involved in LMP1 signalling, a HER2/ErbB2 antibody that recognises phosphorylated HER2/ErbB2 (tyr 1112) was used to probe a western blot of lines 117 and 117/125 ear extracts (fig.5.8). As with EGFR, there is increase in the levels of phosphorylated smaller HER2/ErbB2 products in the LMP^{CAO} / TGF α wild type ears when compared to the LMP^{CAO} negative / TGF α wild type ears and this increase seems to be even higher in the LMP^{CAO} transgenic ears in a TGF α null background. The blot could not be reprobed for β tubulin in order to ascertain loading levels. Note that a smaller product at about 66kDa, recognised by the phosphorylated HER2/ErbB2 antibody, is observed only in LMP^{CAO} transgenic ears of phenotypic stages 3 in the TGF α wild type background and at stages 4 in the TGF α null background. The identity of this protein is unknown.

In order to investigate whether TGF α upregulation and faster EGFR cycling play a role in Ras/MAPK signalling, the levels of total c-Raf, BRaf, MEK1/2, ERK1/2 and their phosphorylated forms were examined by probing Western blots, with the appropriate antibody. Levels of total and phosphorylated c-Raf could not be clearly detected from the experiments as the specific antibodies did not show any bands of the appropriate size corresponding to c-Raf (data not shown). Total BRaf was used to probe a western blot (fig.5.9). Levels of BRaf are equivalent in LMP^{CAO} / TGF α wild type stage 1 and stage 3 ears compared to wild type controls (stage 1: 1.03 fold compared to controls normalised against β tubulin, stage 3: 1.02 fold) but are slightly reduced in stage 2 ears (stage 2: 0.74 fold). This slight decrease observed in BRaf levels is also observed in LMP^{CAO}/TGF α null ears. This effect seems to be an LMP1 effect and not an effect of the absence of TGF α . However, the values obtained are not markedly different from the LMP^{CAO} negative / TGF α wild type control ears so it is not clear if this observed decrease is artifactual or not (table 5.5).

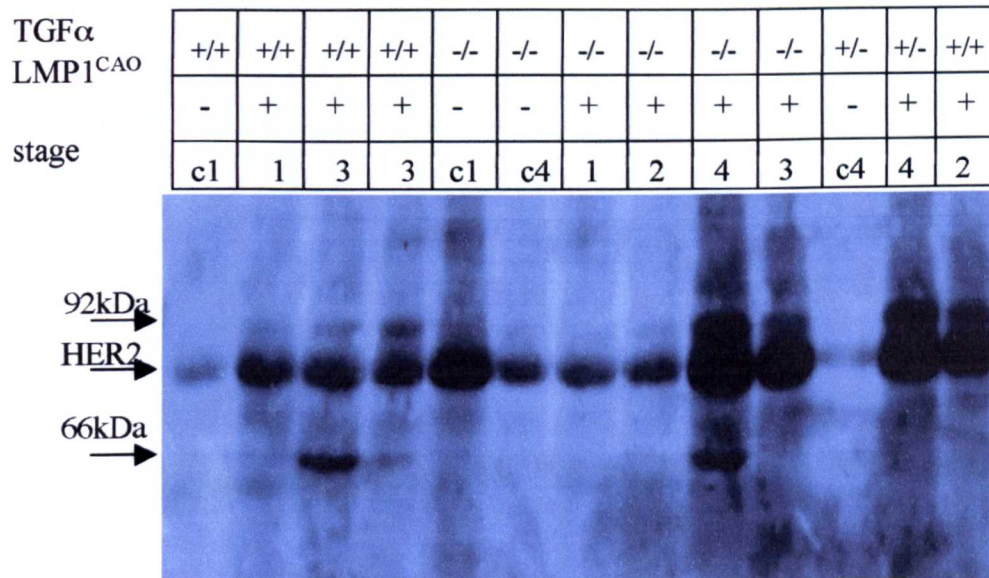


Figure 5.8: Phosphorylated HER2/ErbB2 western blot of protein extracts from ears of mice of lines 117 and 117/125.

This is a reprobe of the blot shown in figure 5.18. The blot was stripped and reprobbed with rabbit anti-mouse phosphorylated HER2 primary antibody (1:1000), a goat anti-rabbit IgG-HRP secondary antibody (1:4000) and visualised with ECL⁺. The 80kDa band corresponding to phosphorylated smaller HER2 product is indicated. Molecular weights according to the marker track are shown.

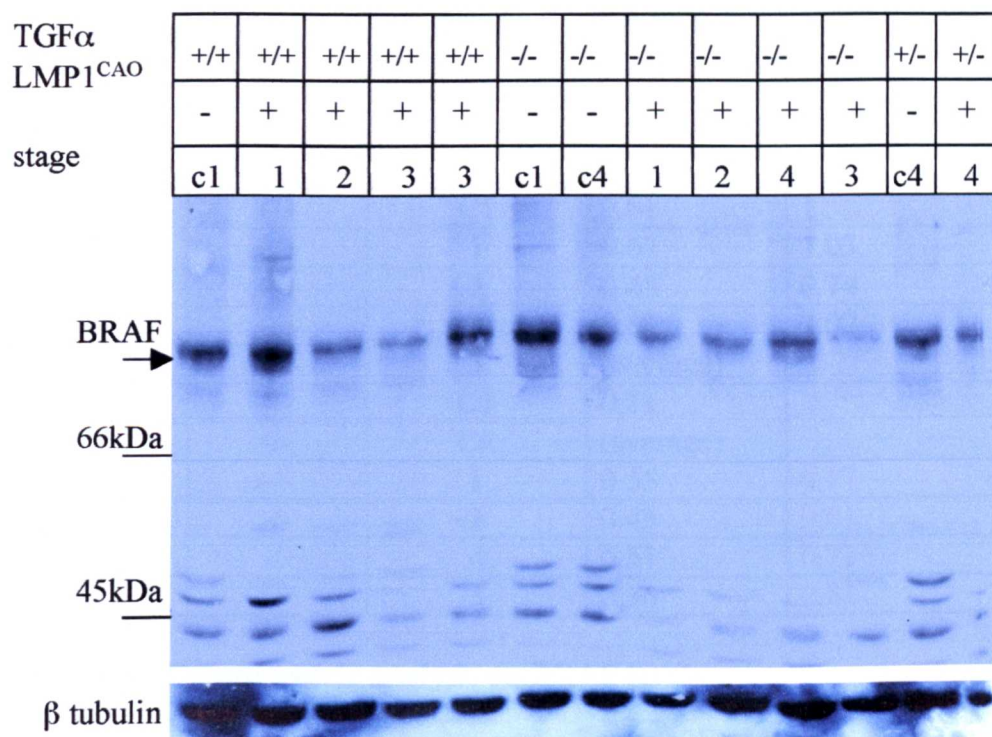


Figure 5.9: BRAF western blot of protein extracts from ears of mice of lines 117 and 117/125.

Protein extracts were prepared from phenotypic ears, stages 1-3 (st1-3) from mice that were transgenic for LMP1(+) and wild type (+/+), heterozygous (+/-) or null (-/-) for TGF α . Age matched control extracts from ears of LMP1^{CAO} transgenic negative siblings (-) were also prepared. 100 μ g of protein extract/track was separated by 7.5% SDS-PAGE and the gel was blotted. The blot was probed with a rabbit anti-mouse BRAF primary antibody (1:1000) and a goat anti-rabbit IgG-HRP secondary antibody (1:4000) and visualised with ECL+. The 95kDa band corresponding to BRAF is indicated. Molecular weights according to marker track are shown. The bottom blot shows β tubulin probing used as a loading control. This blot is a reprobe of the blot probed with phospho-EGFR (tyr 1068) shown in figure 5.7.

Genotype			A	B	C
LMP1	TGF α	Phenotypic stage	BRAF: β tubulin	LMP1 ^{CAO} : wild type	Null or het to wild type in respect of TGF α
-	+/+	C1	0.61	1	
+	+/+	1	0.67	1.03	
+	+/+	2	0.45	0.74	
+	+/+	3	0.62	1.02	
+	+/+	3	(average)		
-	-/-	C1	0.71		
-	-/-	C4	(average)		
+	-/-	1	0.55	0.77	0.82
+	-/-	2	0.43	0.61	0.96
+	-/-	4	0.51	0.72	0.82
+	-/-	3	0.36	0.51	0.58

Table 5.5: Densitometric analysis on BRAF levels

Wild type (-) and transgenic (+) mice for LMP1^{CAO}, wild type (+/+) and null (-/-) for TGF α are shown. The phenotypic stage of the ears used is also shown. Note that LMP1^{CAO} - mice do not have an ear phenotype but animals that were aged matched controls of LMP1^{CAO} + mice of a particular phenotypic stage were used and that stage is indicated.

Values given are after the deduction of the background intensity.

Column A: BRAF: β tubulin

Column B: LMP1^{CAO} : control (TGF α wild type are black, TGF α null are pink)

Column C: LMP1^{CAO} / TGF α null : LMP1^{CAO} / TGF α wild type

Note that LMP1^{CAO} negative in a TGF α null or wild type background give some reading.

Confirming the observations in chapter 4, levels of total MEK1/2 were equivalent throughout the sample panel (fig.5.10B). Once again, levels of the phosphorylated form of MEK1/2 show differences according to phenotypic stage (fig.5.10A). As the densitometric analysis shows (table 5.6), there is an initial increase in activated MEK1/2 in LMP1^{CAO} transgenic ears stages 1 and 2 (stage 1: 8.19 fold compared to controls normalised against total MEK1/2, stage 2: 4.67 fold). As the ear phenotype progresses to stage 3, this activation is decreased (stage 3: 2.57 fold) returning to control levels. A similar pattern is observed in the LMP1^{CAO} / TGF α null ears (stage 1: 3.28 fold, stage 2: 2.83 fold, stage 3: 1.43 fold, stage 4: 1.57 fold). It is evident that MEK1/2 is activated to a lesser extent in the TGF α null LMP1^{CAO} transgenic ears. Note that stage 4 ears in LMP1^{CAO} / TGF α wild type were not examined.

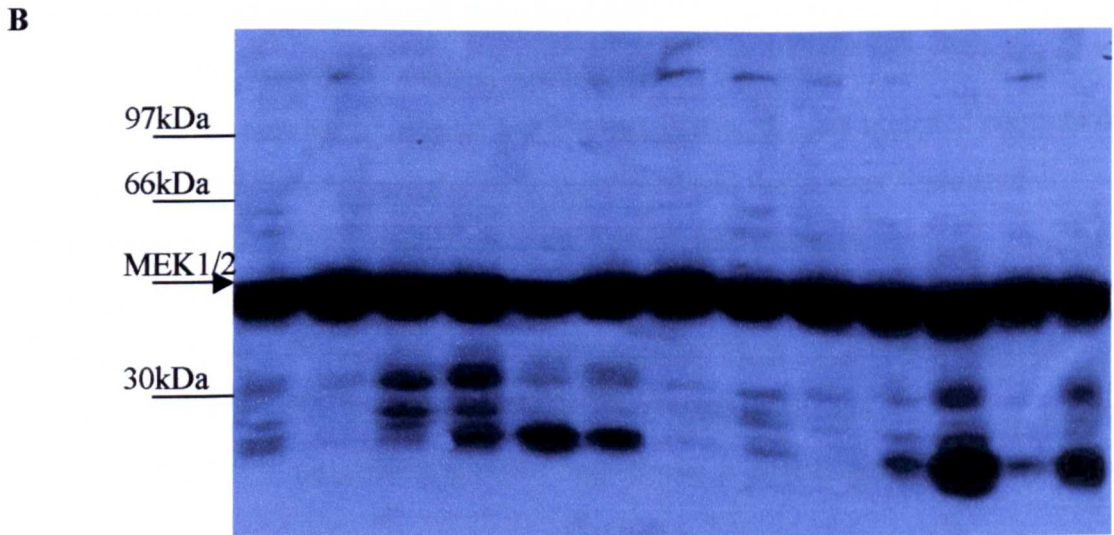
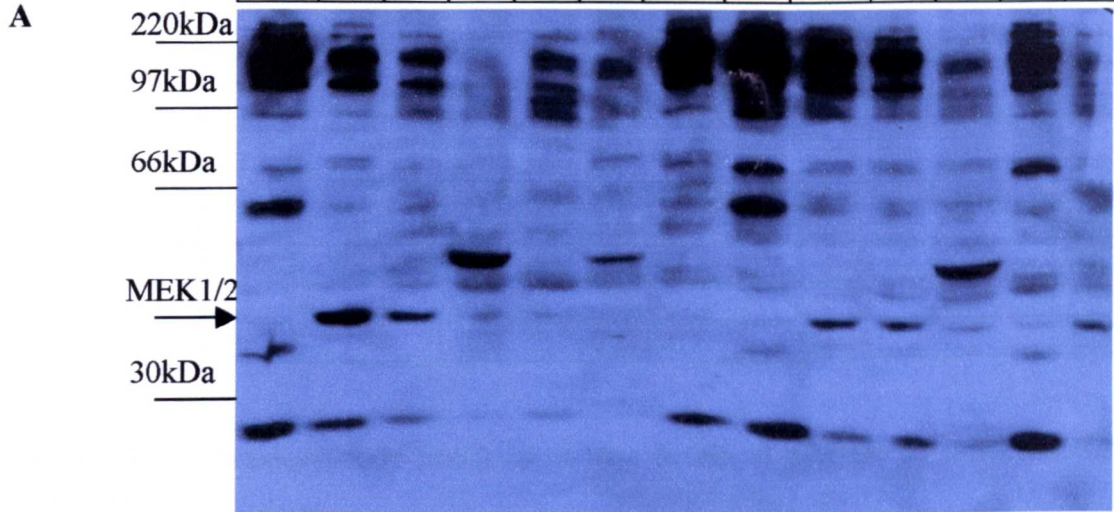
It can also be seen from this western blot (fig.5.10) that there are a number of proteins cross reactive to this phospho-specific antiserum that show expression or activation changes in respect to phenotypic stage. Note a band at approximately 60kDa present only in non transgenic samples, a series of bands in the 100-200kDa range that are strong in controls at stage 1, decreasing though at stages 2-4. A band at approximately 25kDa similarly strong in controls and decreasing with increasing phenotypic stage. The bands may represent phospho-proteins that are activated or deactivated in response to LMP1 signalling, effectors or targets. What is clear from these studies is that only a small fraction of the changes induced by LMP1 can be examined in this approach.

Levels of total ERK1/2 were equivalent in all samples (fig.5.11B). Levels of phosphorylated ERK1/2 show a modest increase in LMP1^{CAO} transgenic ears that is more evident as the ear phenotype worsens (stage 1: 1.59 fold, stage 2: 1.26 fold, stage 3: 2.18 fold compared to controls normalised against total ERK1/2) (table5.7). This increase is not observed in the LMP1^{CAO} / TGF α null ears. This might suggest that the increase in activated ERK1/2 is mediated by TGF α . However as the increase noted in the wild type background is modest the consistency of this result should be tested in further samples of both wild type and null background. Note that cross reactive bands at 66kDa and at 35kDa are observed in LMP1^{CAO} irrespective of TGF α status in stage 2, 3 and 4 ears.

Figure 5.10: Phosphorylated MEK1/2 (A) and total MEK1/2 (B) western blot of protein extracts from ears of mice of line 117 and 117/125.

Protein extracts were prepared from phenotypic ears, stages 1-3 (st1-3) from mice that were transgenic for LMP1(+) and wild type (+/+), heterozygous (+/-) or null (-/-) for TGF α . Age matched control extracts from ears of siblings (-) were also prepared. 100 μ g of protein extract/track was separated by 10% SDS-PAGE and the gel was blotted. The blot was probed with a rabbit anti-mouse phospho-MEK1/2 (A) and a goat anti-rabbit IgG-HRP secondary antibody (1:4000) and visualised with ECL+. The blot was stripped and reprobed with rabbit anti-mouse total MEK1/2 (B) primary antibody (1:1000) and a goat anti-rabbit IgG-HRP secondary antibody (1:4000) and visualised with ECL+. The 45kDa band corresponding to MEK1/2 is indicated. Molecular weights according to marker track are shown.

TGF α	+/+	+/+	+/+	+/+	-/-	+/+	-/-	-/-	-/-	-/-	-/-	+/-	+/-
LMP1 ^{CAO}	-	+	+	+	+	+	-	-	+	+	+	-	+
stage	c1	1	2	3	4	3	c1	c4	1	2	3	c4	4



Genotype			A	B	C
LMP1	TGF α	Phenotypic stage	PMEK: total MEK	LMP1 ^{CAO} : wild type	Null or het to wild type in respect of TGF α
-	+/+	C1	0.05	1	
+	+/+	1	0.42	8.19	
+	+/+	2	0.24	4.67	
+	+/+	3	0.10	2.57	
+	+/+	3	(average)		
-	-/-	C1	0.07		
-	-/-	C4	(average)		
+	-/-	1	0.23	3.28	0.55
+	-/-	2	0.20	2.83	0.83
+	-/-	4	0.11	1.57	1.10
+	-/-	3	0.10	1.43	1.00

Table 5.6: Densitometric analysis on the levels of pMEK to total MEK1/2 loading control.

Wild type (-) and transgenic (+) mice for LMP1^{CAO}, wild type (+/+) and null (-/-) for TGF α are shown. The phenotypic stage of the ears used is also shown. Note that LMP1^{CAO} negative mice do not have an ear phenotype but animals that were aged matched controls of LMP1^{CAO} + mice of a particular phenotypic stage were used and that stage is indicated.

Values given are after the deduction of the background intensity.

Column A: Phosphorylated MEK1/2 : total MEK1/2

Column B: LMP1^{CAO} : control (TGF α wild type are black, TGF α null are pink)

Column C: LMP1^{CAO} / TGF α null : LMP1^{CAO} / TGF α wild type

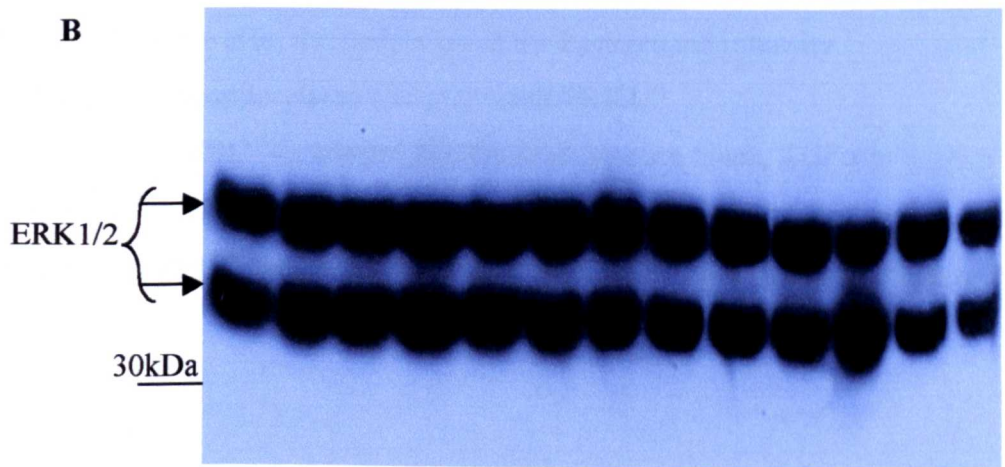
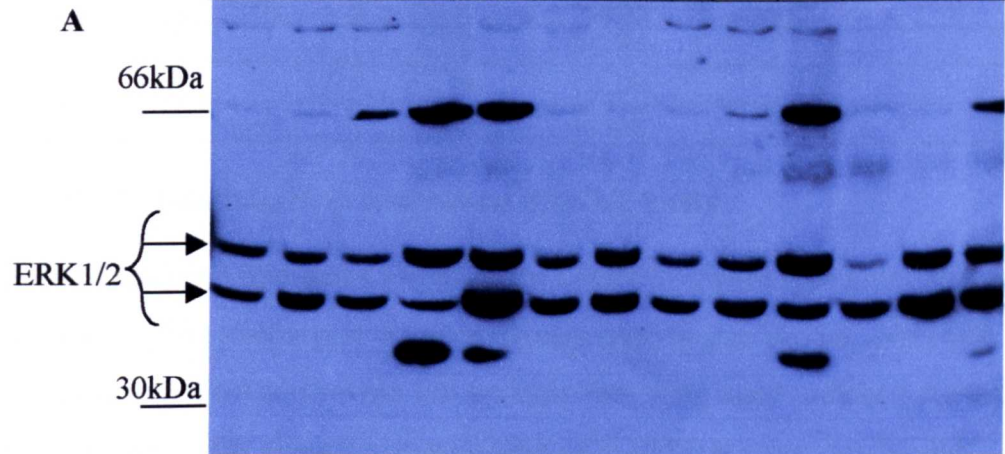
Note that LMP1^{CAO} negative in a TGF α null or wild type background give some reading.

Figure 5.11: Phospho-ERK1/2 and total ERK1/2 western blot of protein extracts from ears of mice of line 117 and 117/125.

Protein extracts were prepared from phenotypic ears, stages 1-3 (st1-3) from mice that were transgenic for LMP1(+) and wild type (+/+), heterozygous (+/-) or null (-/-) for TGF α . Age matched control extracts from ears of LMP1^{CAO} transgenic negative siblings (-) were also prepared. 100 μ g of protein extract/track was separated by 10% SDS-PAGE and the gel was blotted. The blot was probed with a rabbit anti-mouse phospho-ERK1/2 (A) and a goat anti-rabbit IgG-HRP secondary antibody (1:4000) and visualised with ECL+. The blot was stripped and reprobed with rabbit anti-mouse total ERK1/2 (B) primary antibody (1:1000) and a goat anti-rabbit IgG-HRP secondary antibody (1:4000) and visualised with ECL+. The 44 and 42kDa bands corresponding to ERK1/2 are indicated. Molecular weights according to the marker track are shown.

Note cross reacting bands at approximately 66kDa and 35kDa are detected strongly in stage 3/4 LMP1^{CAO} transgenic samples in wild type, heterozygous and null TGF α background. The identity of these proteins is not known.

TGF α	+/+	+/+	+/+	+/+	+/+	-/-	-/-	-/-	-/-	-/-	-/-	+/-	+/-
LMP1 ^{CAO}	-	+	+	+	+	-	-	+	+	+	+	-	+
stage	c1	1	2	3	3	c1	c4	1	2	4	3	c4	4



Genotype			A	B	C
LMP1	TGF α	Phenotypic stage	pERK: total ERK	LMP1 ^{CAO} : wild type	Null or het to wild type in respect of TGF α
-	+/+	C1	0.50	1	
+	+/+	1	0.79	1.59	
+	+/+	2	0.63	1.26	
+	+/+	3	1.09	2.18	
+	+/+	3	(average)		
-	-/-	C1	0.87		
-	-/-	C4	(average)		
+	-/-	1	0.63	0.73	0.80
+	-/-	2	0.85	0.98	1.35
+	-/-	4	1.09	1.25	1
+	-/-	3	0.62	0.71	0.57

Table 5.7: Densitometric analysis on ERK1/2 levels

Wild type (-) and transgenic (+) mice for LMP1^{CAO}, wild type (+/+) and null (-/-) for TGF α are shown. The phenotypic stage of the ears used is also shown. Note that LMP1^{CAO} - mice do not have an ear phenotype but animals that were aged matched controls of LMP1^{CAO} + mice of a particular phenotypic stage were used and that stage is indicated.

Values given are after the deduction of the background intensity.

Column A: Phosphorylated ERK1/2: total ERK1/2

Column B: LMP1^{CAO}: control (TGF α wild type are black, TGF α null are pink)

Column C: LMP1^{CAO} / TGF α null : LMP1^{CAO} / TGF α wild type

Note that LMP1^{CAO} negative in a TGF α null or wild type background give some reading.

Other MAPKs that were investigated was the phosphorylated forms of SEK/MKK4 and SAPK/JNK. The western blot for phosphorylated SEK/MKK4 is not very clear and even though the 46kDa band corresponding to phosphorylated SEK/MKK4 is observed, no reliable comparison can be made to the β tubulin reprobe to determine if there is a difference in activation levels or not (fig.5.12). For the SAPK/JNK, there may seem to be an initial upregulation of the 54kDa phosphorylated JNK2/3 at stage 1 of the LMP1^{CAO} transgenic ears (fig.5.13). What is apparent is that the levels of phosphorylated JNK2/3 decrease as the ear phenotype progresses. However, levels of the 46kDa band corresponding to phosphorylated JNK1 seem to be constant throughout irrespective of LMP1 or TGF α background. It was not possible to reprobe this blot with β tubulin to allow an accurate comparison to be made, however, a cross reacting band at about 40kDa just below the phosphorylated JNK1 complex, seems to be equivalent in all tracks suggesting equal loading.

B. Apoptotic and Progression proteins

The ear phenotype progression in LMP1^{CAO}/TGF α null animals appeared faster than in LMP1^{CAO} transgenic animals that are in the heterozygous or wild type TGF α background as presented in section 5.1. This progression in phenotype is accompanied by increased ulceration and necrosis. In order to investigate this phenotype and to determine whether apoptotic proteins play a role, levels of caspase-3 and anti-apoptotic protein Akt were investigated. Levels of MMP9, a progression marker were also investigated.

Levels of full length and cleaved caspase-3 were examined using the respective antibodies (fig.5.14A, B). Full length caspase-3 (35kDa) levels increase in LMP^{CAO} transgenic ears as the phenotype progresses (stage 1: 2.23 fold, stage 2: 4.80 fold, stage 3: 4.50 fold compared to controls, normalised against β tubulin) and this is irrespective of TGF α background as the levels in LMP1^{CAO}/TGF α null ears show (stage 1: 1.90 fold, stage 2: 4.27 fold, stage 3: 1.16 fold, stage 4: 4.63 fold) (table5.8). The 17 and 19kDa corresponding to cleaved caspase-3 can be seen in LMP1^{CAO} / TGF α wild type stage 3 ears and in LMP1^{CAO} / TGF α null stage 3 and 4 ears when the blots are probed with either the full length caspase-3 antibody (fig.5.14A) or the antibody to cleaved caspase-3 (fig.5.14B). Note that there are bands at about 60 and 40kDa recognised by the full length and the cleaved caspase-3 antibodies that are evident only in the

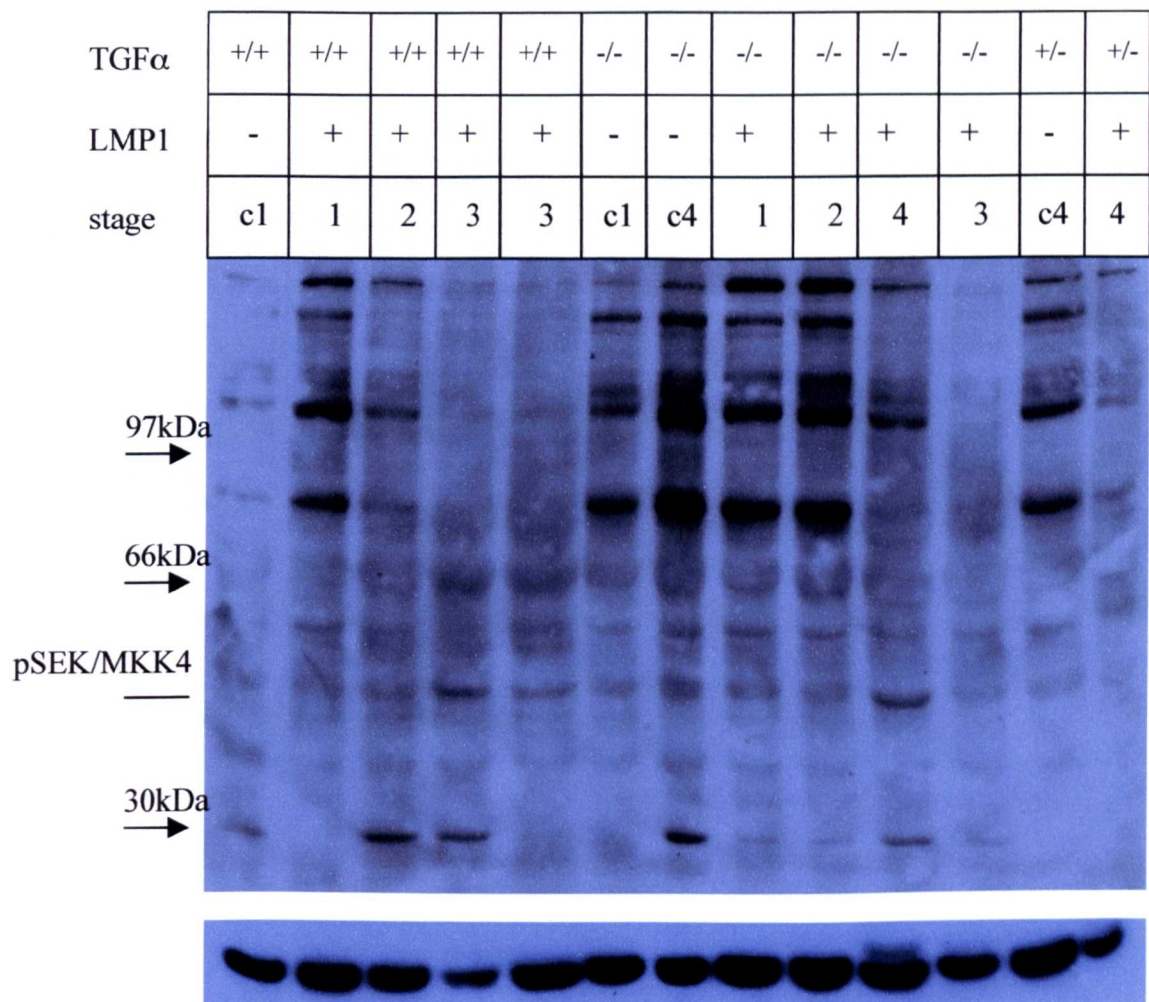


Figure 5.12: Phosphorylated SEK/MKK4 western blot of protein extracts from ears of mice of lines 117 and 117/125.

Protein extracts were prepared from phenotypic ears, stages 1-3 (st1-3) from mice that were transgenic for LMP1(+) and wild type (+/+), heterozygous (+/-) or null (-/-) for TGF α . Age matched control extracts from ears of LMP1^{CAO} transgenic negative siblings (-) were also prepared. 100 μ g of protein extract/track was separated by 10% SDS-PAGE and the gel was blotted. The blot was probed with a rabbit anti-mouse phospho-SEK/MKK4 primary antibody (1:1000) and a goat anti-rabbit IgG-HRP secondary antibody (1:4000) and visualised with ECL+. The 46kDa corresponding to pSEK/MKK4 is indicated. Molecular weights according to marker track are shown. The bottom picture shows the β tubulin reprobing of the blot to show relative loading levels.

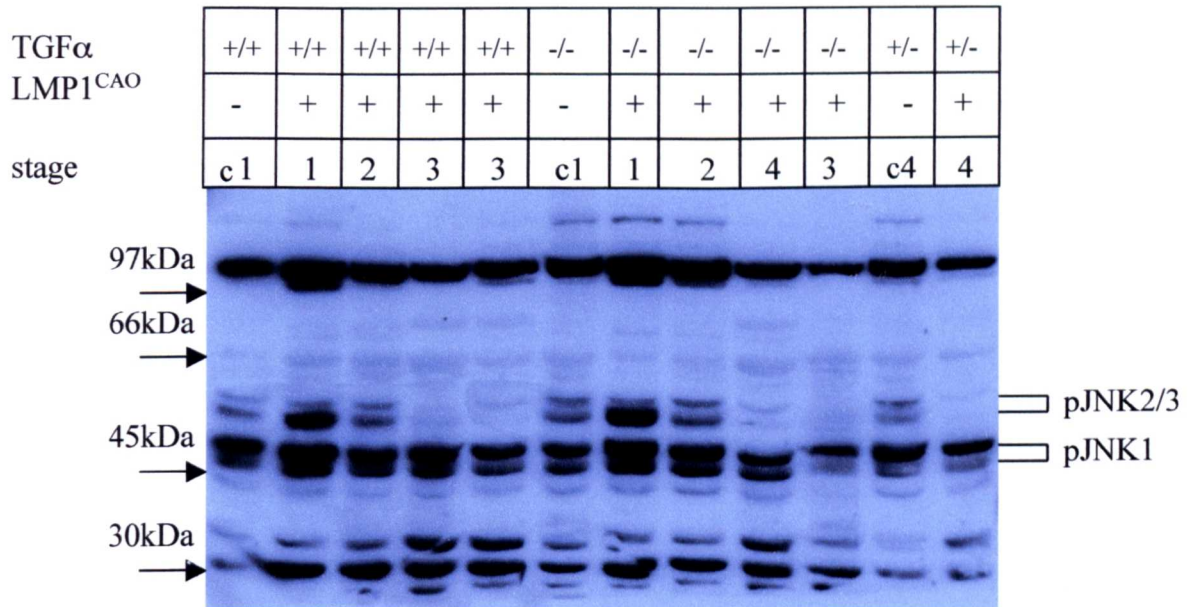


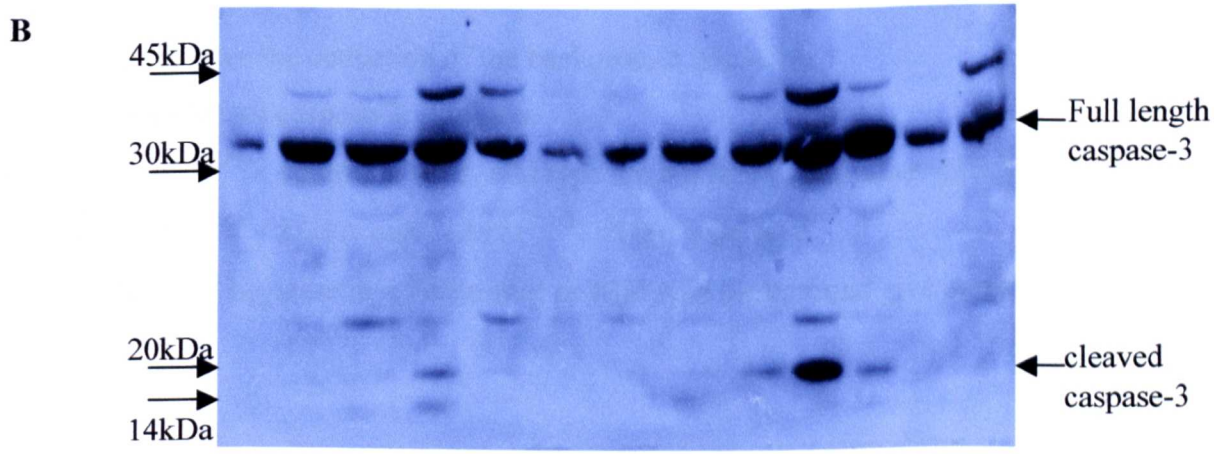
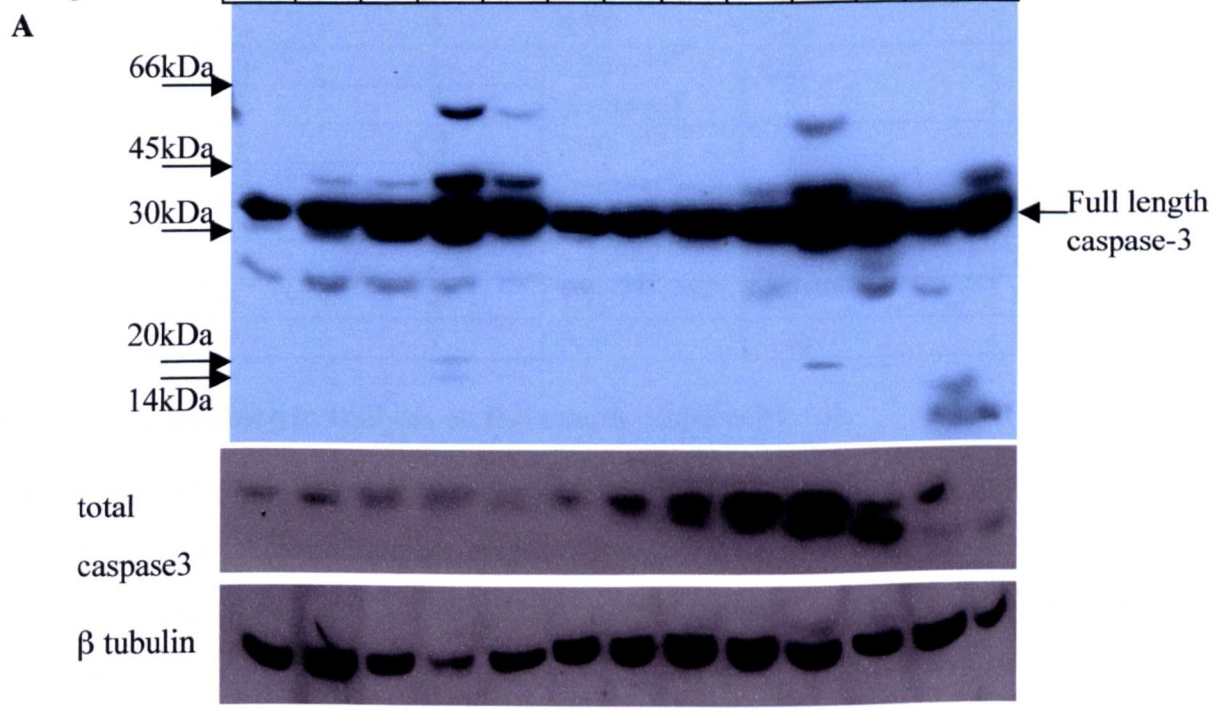
Figure 5.13: SAPK/JNK western blot of protein extracts from ears of mice of lines 117 and 117/125.

Protein extracts were prepared from phenotypic ears, stages 1-3 (st1-3) from mice that were transgenic for LMP1(+) and wild type (+/+), heterozygous (+/-) or null (-/-) for TGF α . Age matched control extracts from ears of siblings (-) were also prepared. 100 μ g of protein extract/track was separated by 10% SDS-PAGE. The blot was probed with a rabbit anti-mouse total SAPK/JNK (Thr183/Tyr185) primary antibody (1:1000) and a goat anti-rabbit secondary antibody (1:4000) and visualised with ECL+. The 46kDa doublet corresponding to phosphorylated JNK1 and the 54kDa doublet corresponding to phosphorylated JNK2/3 are indicated. Molecular weights as per marker track are shown.

Figure 5.14: Total and activated caspase-3 western blots of protein extracts from ears of mice of lines 117 and 117/125.

Protein extracts were prepared from phenotypic ears, stages 1-3 (st1-3) from mice that were transgenic for LMP1(+) and wild type (+/+), heterozygous (+/-) or null (-/-) for TGF α . Age matched control extracts from ears of siblings (-) were also prepared. 100 μ g of protein extract/track was analysed on a 10% SDS-PAGE. The blot was probed with a rabbit anti-mouse total caspase-3 (1:1000) and a goat anti-rabbit secondary antibody (1:4000) and visualised with ECL+. The activated caspase-3 blot is a reprobe of the p53 blot shown in figure 5.21. After stripping, it was reprobbed with a rabbit anti-mouse activated caspase-3 (1:1000) primary antibody and a goat anti-rabbit secondary antibody (1:4000) and visualised with ECL+. Molecular weights according to the marker track are shown.

TGF α	+/+	+/+	+/+	+/+	+/+	-/-	-/-	-/-	-/-	-/-	-/-	+/-	+/-
LMP1 ^{CAO}	-	+	+	+	+	-	-	+	+	+	+	-	+
stage	c1	1	2	3	3	c1	c4	1	2	4	3	c4	4



Genotype			A	B	C
LMP1	TGF α	Phenotypic stage	Total caspase-3: β tubulin	Transgenic: Wild type in respect to LMP1	Null to wild type in respect of TGF α
-	+/+	C1	0.11	1	
+	+/+	1	0.24	2.23	
+	+/+	2	0.53	4.80	
+	+/+	3	0.50 (average)	4.50	
+	+/+	3			
-	-/-	C1	0.40		
-	-/-	C4	(average)		
+	-/-	1	0.50	1.90	2.06
+	-/-	2	1.13	4.27	2.14
+	-/-	4	1.22	4.63	1.67
+	-/-	3	0.31	1.16	1.24

Table 5.8: Densitometric analysis on full length caspase-3 levels

Wild type (-) and transgenic (+) mice for LMP1^{CAO}, wild type (+/+) and null (-/-) for TGF α are shown. The phenotypic stage of the ears used is also shown. Note that LMP1^{CAO} - mice do not have an ear phenotype but animals that were aged matched controls of LMP1^{CAO} + mice of a particular phenotypic stage were used and that stage is indicated.

Values given are after the deduction of the background intensity.

Column A: Full length caspase-3: β tubulin

Column B: LMP1^{CAO}: control (TGF α wild type are black, TGF α null are pink)

Column C: LMP1^{CAO} / TGF α null : LMP1^{CAO} / TGF α wild type

Note that LMP1^{CAO} negative in a TGF α null or wild type background give some reading.

LMP1^{CAO}/ TGF α wild type samples stage 3 and in the LMP1^{CAO}/ TGF α null samples stage 4 only. The identity of these proteins is unknown.

It is obvious that both levels and activation of caspase-3 is affected by the increase in the severity of the ear phenotype and correlates with the observed necrosis and ulceration at stages 3 and 4.

In order to further examine this ear phenotype and whether TGF α plays a role in proliferation or apoptosis, ears of LMP1^{CAO}/ TGF α wild type or null and LMP1^{CAO} negative / TGF α wild type or null were collected, fixed in 10% neutral buffered formalin, paraffin embedded, sectioned (2 μ m) and stained with PCNA to assess for proliferation levels or full length caspase-3 antibody to assess for apoptosis. Sectioning of the tissues and antibody staining was performed by Mr. Colin Nixon, a trained histotechnologist. A number of other staining trials using the antibodies to cleaved caspase-3, total and phosphorylated EGFR were not successful.

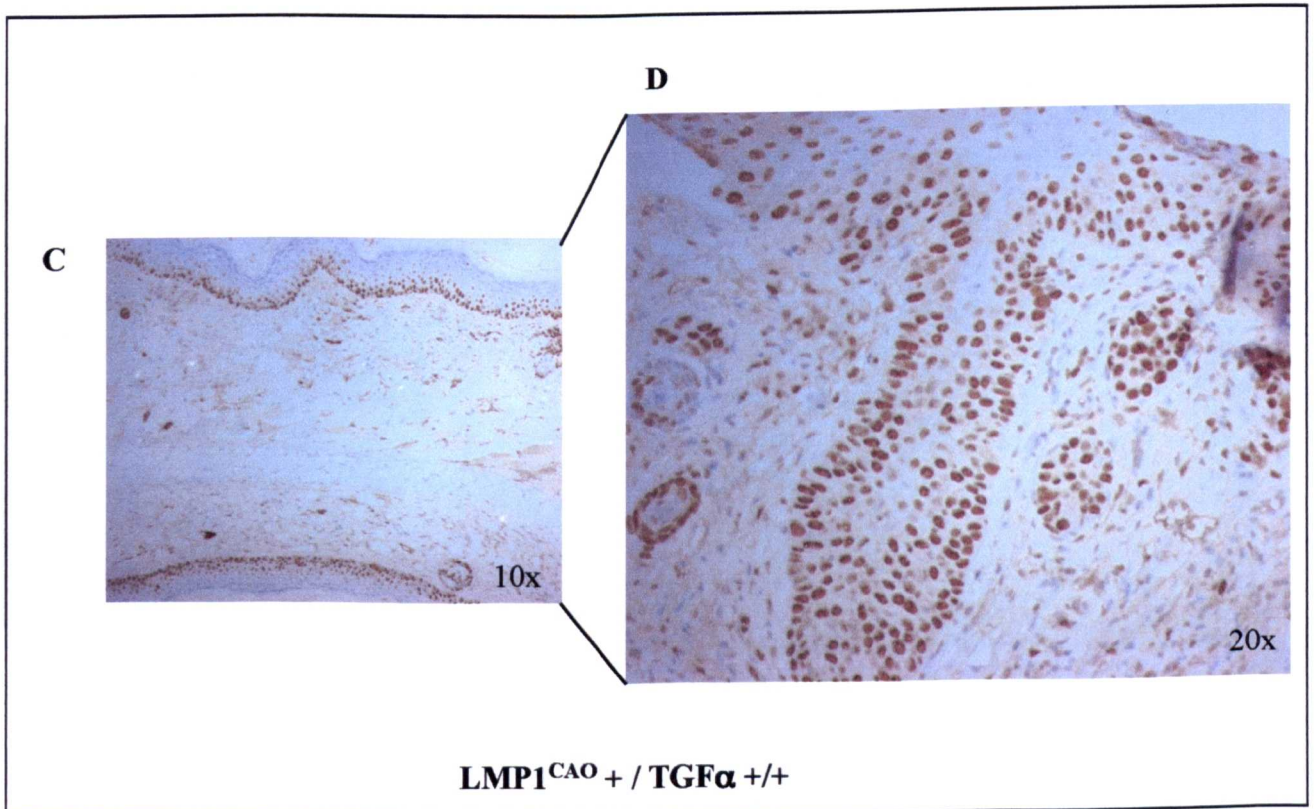
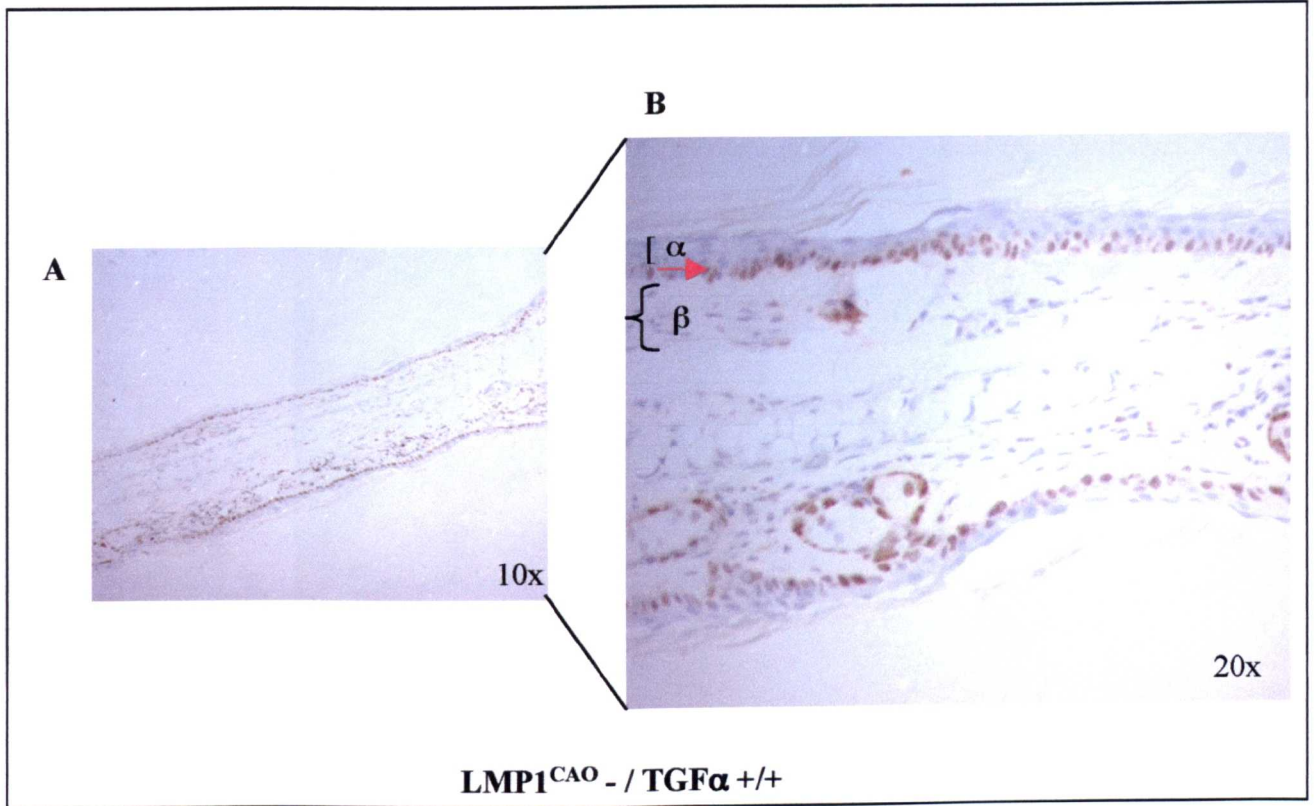
From the PCNA staining, it can be seen that LMP1^{CAO} transgenic ears irrespective of TGF α background show an extensive proliferation that takes place in the basal layer of the epidermis and extends into the thickened suprabasal layers (fig.5.15). Normal epidermis has a one cell thick basal layer (as indicated by a red arrow on fig.5.15.B) to which proliferation is confined. It was not possible to accurately quantify the degree of proliferation and deduce whether the presence or absence of TGF α , in an LMP1^{CAO} transgenic animal leads to an increase in proliferation or not.

Staining the sections with an antibody to full length caspase-3, gave similar results as PCNA staining. Whereas little or no staining, was observed on wild type ear sections irrespective of TGF α background, the basal layer of both TGF α wild type and null LMP1^{CAO} transgenic ears was stained. This staining was not limited to individual cells but to the whole of the basal layer (fig.5.16). It was not possible to quantify whether TGF α leads to increased apoptosis or not although the staining does appear stronger in the wild type background.

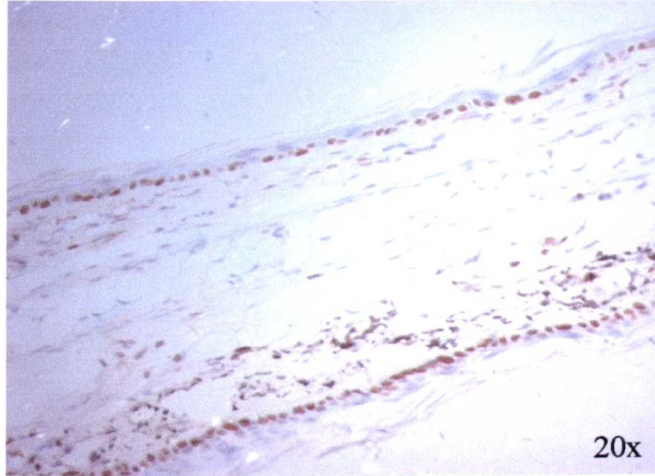
Total levels of Akt may show some decrease, with increasing phenotypic stage as was seen in fig. 4.14 but this is not clear (fig.5.17B). However, levels of phosphorylated Akt (Thr) in LMP1^{CAO} transgenic samples show a dramatic reduction with increasing phenotype (stage 1: 0.76 fold, stage 2: 0.09 fold, stage 3: 0 (equals the background level), when compared to controls, normalised to total Akt)(table 5.9) confirming the observation made previously in chapter 4.

Figure 5.15: PCNA staining on ears from line 117 and 117/125

Ears from LMP1 negative (-) / TGF α wild type (+/+) (A,B), LMP1 transgenic (+) / TGF α +/+ (C,D), LMP1 negative /TGF α null (-/-) (E) and LMP1 transgenic / TGF α null (F, G) stage 3 ears were collected, fixed in 10% neutral buffered formalin and paraffin embedded. Sections of 2 μ m thickness were cut and stained with PCNA primary antibody (1:50). The secondary antibody of the DakoCytomation EnVision kit was used and visualised with DAB which stains specific antibody recognition sites brown. The lens magnification used to take the pictures is indicated on the right bottom corner. On picture B, the red arrow indicates the one cell thick basal layer, α indicates the other layers of the epidermis and β the dermis layer.

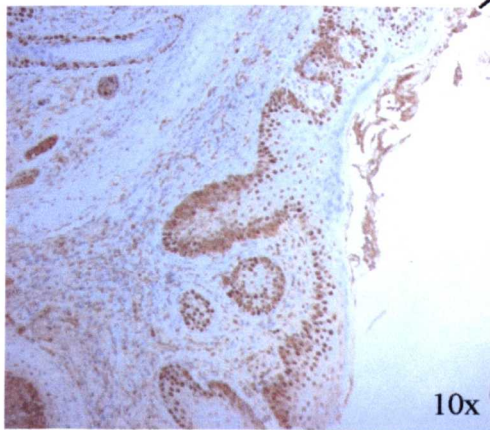


E

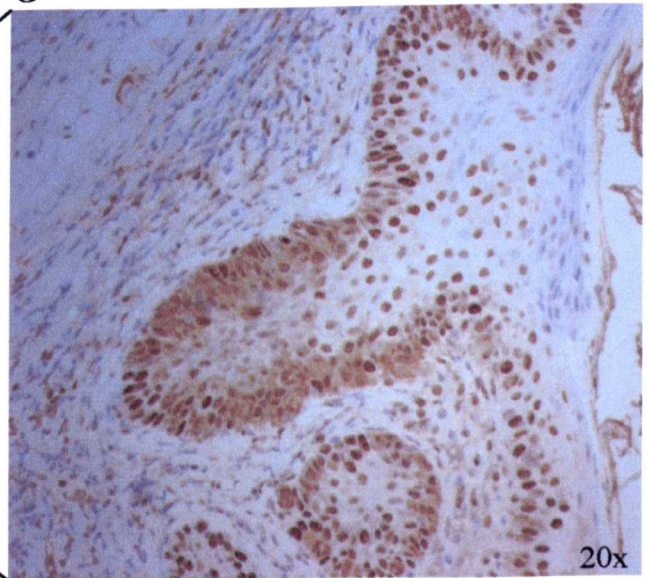


LMP1^{CAO}- / TGFα^{-/-}

F



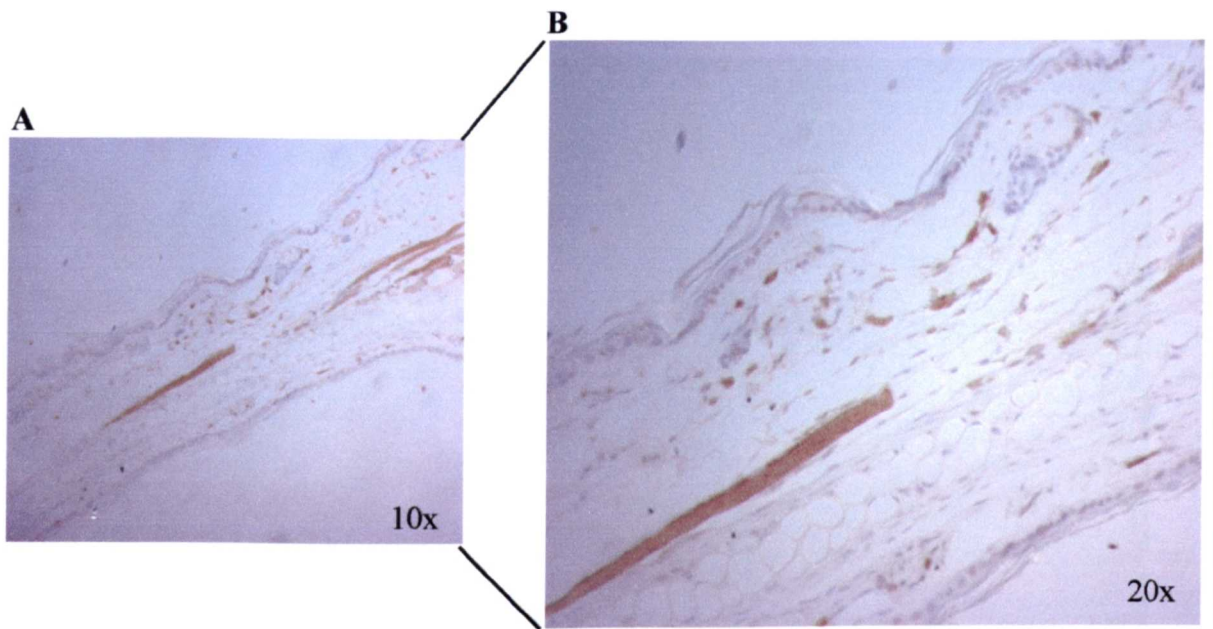
G



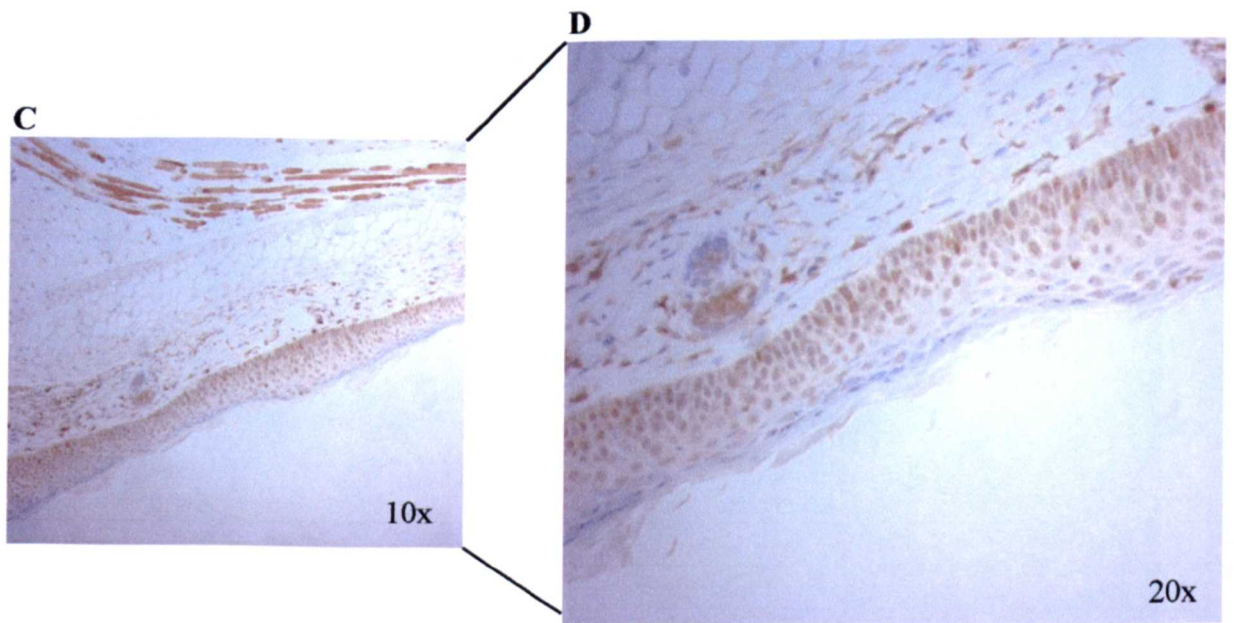
LMP1^{CAO}+ / TGFα^{-/-}

Figure 5.16: Full length caspase-3 staining on ears from line 117 and 117/125

Ears from LMP1 negative (-) / TGF α wild type (+/+) (A,B), LMP1 transgenic (+) / TGF α +/+ (C,D), LMP1 - / TGF α null (-/-) (E,F) and LMP1+ / TGF α -/- (G,H) were collected, fixed in 10% neutral buffered formalin and paraffin embedded. Sections of 2 μ m thickness were cut and stained with total caspase 3 primary antibody (1:50). The secondary antibody of the DakoCytomation EnVision kit was used and visualised with DAB which stains specific antibody recognition sites brown. The lens magnification used to take the pictures is indicated on the right bottom corner.

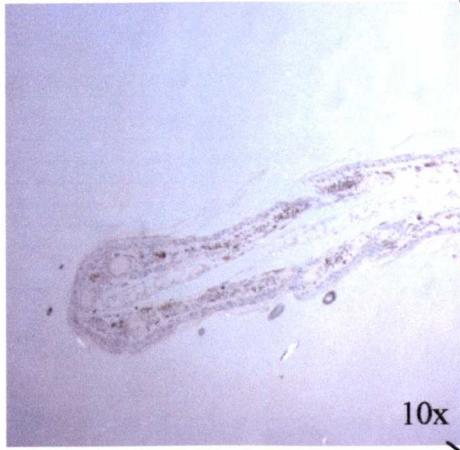


$LMP1^{CAO-} / TGF\alpha^{+/+}$



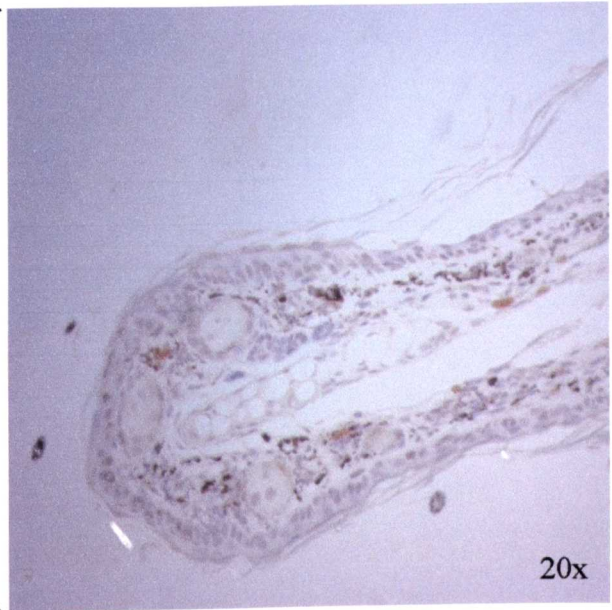
$LMP1^{CAO+} / TGF\alpha^{+/+}$

E



10x

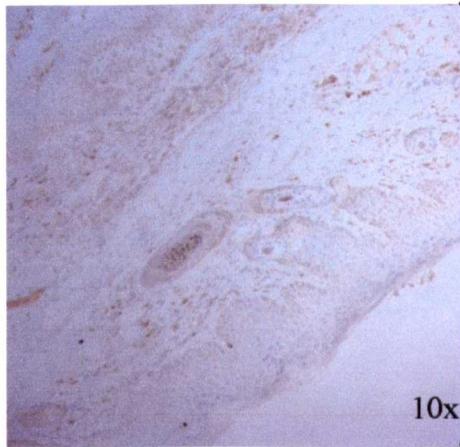
F



20x

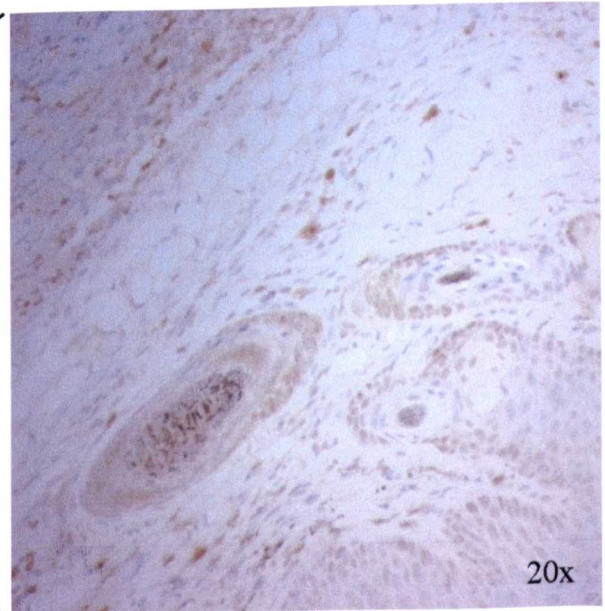
LMP1^{CAO} - / TGF α -/-

G



10x

H

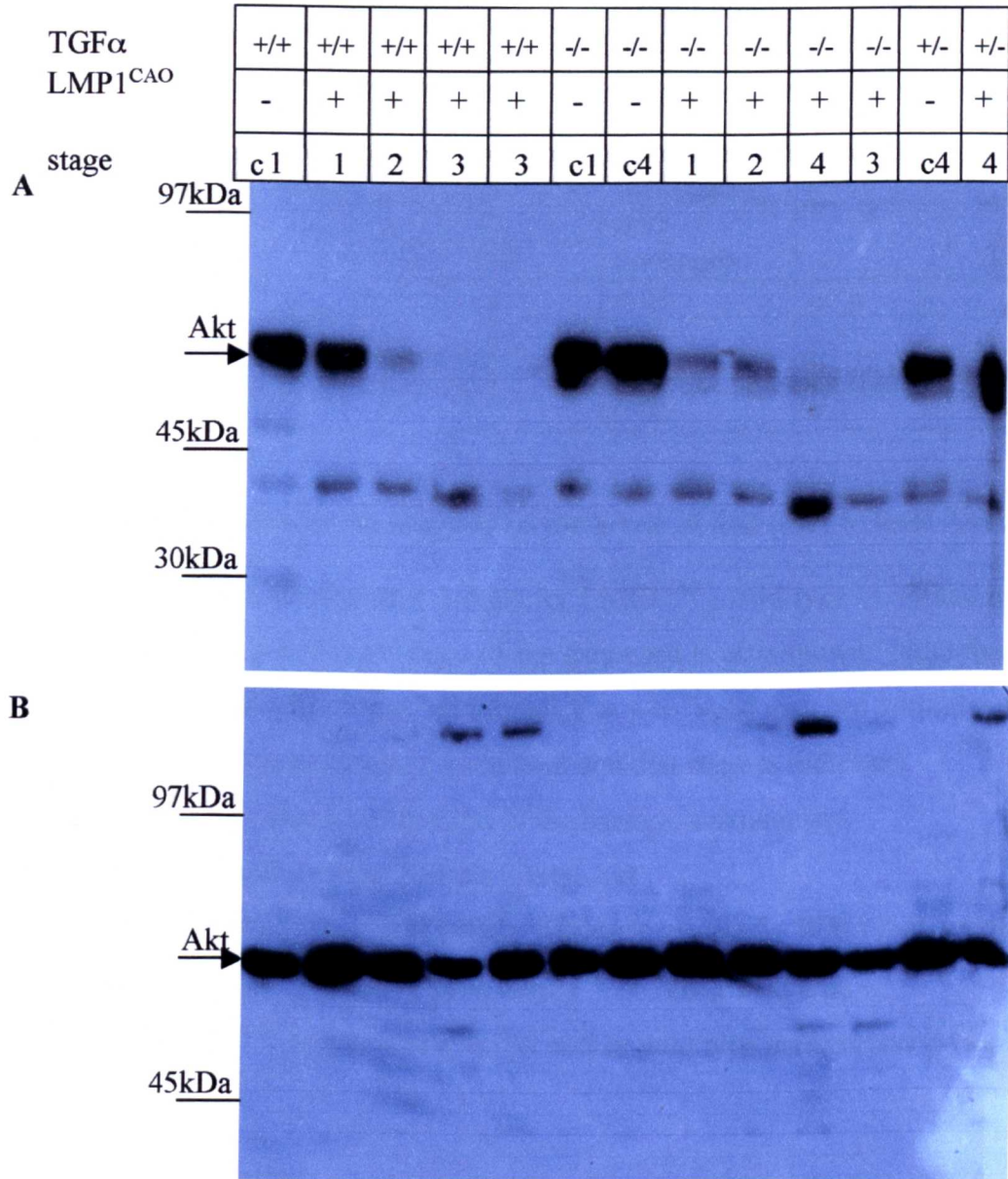


20x

LMP1^{CAO} + / TGF α -/-

Figure 5.17: Phosphorylated Akt (thr) and total Akt western blot of protein extracts from ears of mice of line 117 and 117/125.

Protein extracts were prepared from phenotypic ears, stages 1-3 (st1-3) from mice that were transgenic for LMP1(+) and wild type (+/+), heterozygous (+/-) or null (-/-) for TGF α . Age matched control extracts from ears of LMP1^{CAO} transgenic negative siblings (-) were also prepared. 100 μ g of protein extract/track was separated by 10% SDS-PAGE and the gel was blotted. The blot was probed with a rabbit anti-mouse phospho Akt (thr) (A) primary antibody or a rabbit anti-mouse total Akt (B) (1:1000) and a goat anti-rabbit IgG-HRP secondary antibody (1:4000) and visualised with ECL+. The 60kDa corresponding to Akt is indicated. Molecular weights according to marker track are shown.



Genotype			A	B	C
LMP1	TGF α	Phenotypic stage	Akt (thr): total Akt	Transgenic: Wild type in respect to LMP1	Null or het to wild type in respect of TGF α
-	+/+	C1	0.87	1	
+	+/+	1	0.67	0.76	
+	+/+	2	0.09	0.09	
+	+/+	3	0	0	
+	+/+	3	(average)		
-	-/-	C1	0.93		
-	-/-	C4	(average)		
+	-/-	1	0.24	0.26	0.36
+	-/-	2	0.28	0.31	3.32
+	-/-	3	0.14	0.15	0
+	-/-	3	0.06	0.07	0

Table 5.9: Densitometric analysis on the levels of Akt (thr) to total Akt .

Wild type (-) and transgenic (+) mice for LMP1^{CAO} , wild type (+/+) and null (-/-) for TGF α are shown. The phenotypic stage of the ears used is also shown. Note that LMP1^{CAO} - mice do not have an ear phenotype but animals that were aged matched controls of LMP1^{CAO} + mice of a particular phenotypic stage were used and that stage is indicated.

Values given are after the deduction of the background intensity.

Column A: Phosphorylated Akt (thr): total Akt

Column B: LMP1^{CAO} : control (TGF α wild type are black, TGF α null are pink)

Column C: LMP1^{CAO} / TGF α null : LMP1^{CAO} / TGF α wild type

Note that LMP1^{CAO} negative in a TGF α null or wild type background give some reading.

This decrease in Akt activation, implies that there is less protection against apoptosis in the LMP1^{CAO} transgenic ears.

Levels of uncleaved MMP9 (92kDa) are higher in LMP1^{CAO} transgenic ears irrespective of TGF α background (fig.5.18). This increase is more evident as the ear phenotype worsens comparable with MMP9 being a marker of progression. The cleaved MMP9 (84kDa) is seen in LMP1^{CAO}/ TGF α null ears stages 1 and 2 but is less apparent in the more progressed phenotypic stages. MMP9 is a matrix metalloprotease, an enzyme that can degrade the extracellular matrix allowing angiogenesis and tumour progression.

TNF α converting enzyme (TACE) levels, a metalloprotease that cleaves the membrane bound form of TNF α (and TGF α) to release soluble TNF α (and TGF α) was also investigated (Borrell-Pages et al., 2003). Repeated probing proved unsuccessful to detect the 74kDa product expected in the ear tissue.

C. Proliferation and Cell cycle suppression

In order to investigate how LMP1^{CAO} affects cell cycle progression in the presence or absence of TGF α , several cell cycle related proteins were examined.

Jun B (and not c-Jun) was seen to be upregulated in LMP1^{CAO} transgenic ear tissue (fig.4.22). The larger band (approximately 46kDa) was detected in control samples while both the larger and the smaller (approximately 44kDa) JunB bands were detected in LMP1 transgenic samples upregulated compared to control, but relatively consistent across the phenotypic stages. Comparison in a TGF α null background revealed that this strong upregulation is independent of TGF α (fig.5.19). Also the upregulation observed in both the 44 and 46kDa bands is constant across the stages (not increasing), suggesting that this is an early response of the tissue to LMP1^{CAO}.

JunB regulates the expression of the cell cycle suppressor p16^{INK4a}, as the latter has upstream AP1 promoter elements (Passegue and Wagner, 2000). When p16^{INK4a} protein expression was examined this did not correlate with the consistently high levels of JunB observed in LMP1^{CAO} transgenic samples (fig.5.20). p16^{INK4a} expression was detected in LMP1^{CAO}/ TGF α null ears that are stage 3 or 4 only. Previous experiments in the laboratory by another investigator, showed that LMP1^{CAO}/ TGF α wild type ears of phenotypic stage 4/5 did show p16^{INK4a} expression, confirming that p16^{INK4a} expression is induced at later phenotypic stages in both TGF α wild type and null samples (Stevenson *et. al.* in press). The levels of p19^{ARF}

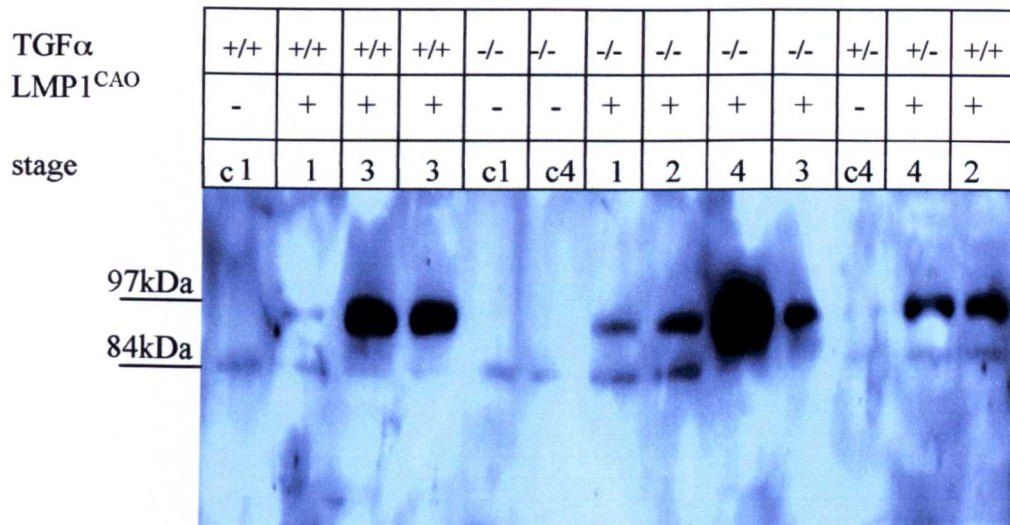


Figure 5.18: MMP9 western blot of protein extracts from ears of mice of lines 117 and 117/125.

Protein extracts were prepared from phenotypic ears, stages 1-3 (st1-3) from mice that were transgenic for LMP1(+) and wild type (+/+), heterozygous (+/-) or null (-/-) for TGF α . Age matched control extracts from ears of LMP1^{CAO} transgenic negative siblings (-) were also prepared. 100 μ g of protein extract/track was separated by 10% SDS-PAGE and the gel was blotted. The blot was probed with a goat anti-mouse MMP9 primary antibody (1:1000) and a donkey anti-goat IgG-HRP secondary antibody (1:4000) and visualised with ECL+. The 92kDa corresponding to MMP9 is indicated. The cleaved 84kDa MMP9 band is also shown.

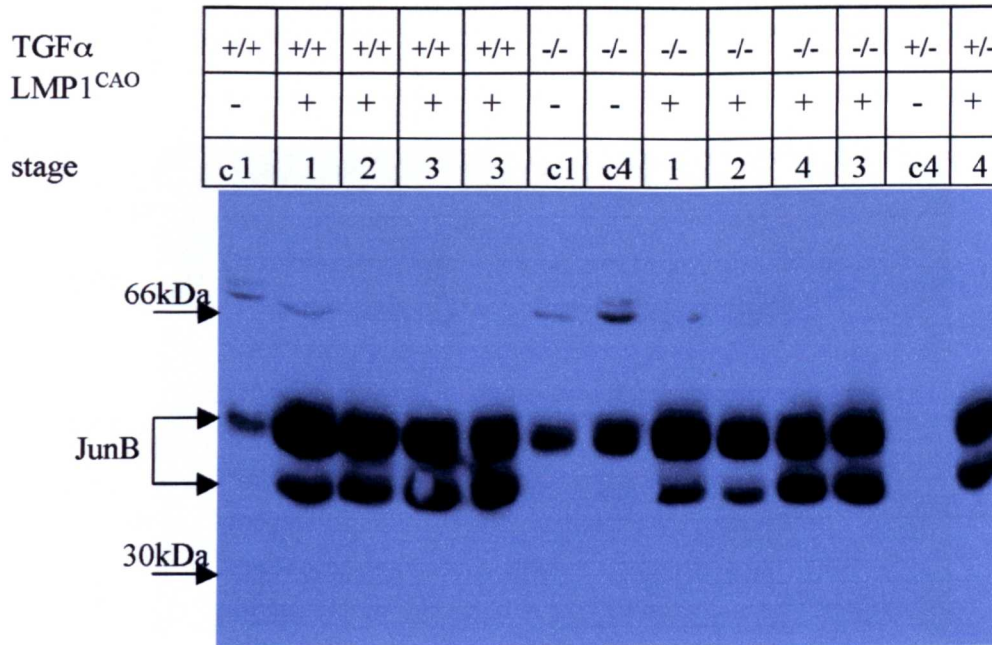


Figure 5.19: Jun B western blot of protein extracts from ears of mice of lines 117 and 117/125.

Protein extracts were prepared from phenotypic ears, stages 1-3 (st1-3) from mice that were transgenic for LMP1(+) and wild type (+/+), heterozygous (+/-) or null (-/-) for TGF α . Age matched control extracts from ears of LMP1^{CAO} transgenic negative siblings (-) were also prepared. 100 μ g of protein extract/track was separated on 10% SDS-PAGE. The blot was probed with a rabbit anti-mouse Jun B primary antibody (1:1000) and a goat anti-rabbit secondary antibody (1:4000) and visualised with ECL+. The bands (46 and 44kDa) corresponding to Jun B are indicated. Molecular weights according to the marker track are shown.

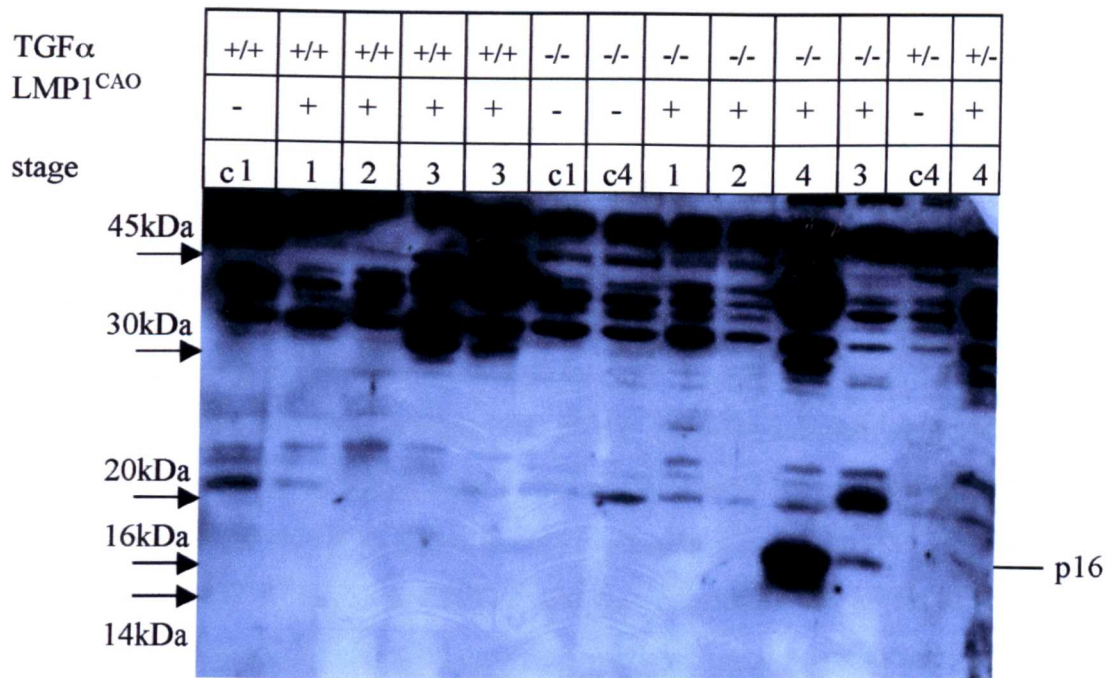


Figure 5.20: p16^{INK4a} western blot of protein extracts from ears of mice of lines 117 and 117/125.

Protein extracts were prepared from phenotypic ears, stages 1-3 (st1-3) from mice that were transgenic for LMP1(+) and wild type (+/+), heterozygous (+/-) or null (-/-) for TGF α . Age matched control extracts from ears of LMP1^{CAO} transgenic negative siblings (-) were also prepared. 100 μ g of protein extract/track was separated on 10% SDS-PAGE and the gel was blotted. The blot was probed with a rabbit anti-mouse p16^{INK4a} primary antibody (1:1000) and a goat anti-rabbit secondary antibody (1:4000) and visualised with ECL+. The 16kDa band corresponding to p16^{INK4a} is indicated. Molecular weights according to the marker track are shown.

protein were also investigated but the 19kDa band corresponding to p19^{ARF} could not be detected by Western analysis of those tissues, despite repeated efforts and using 0.05%SDS in the transfer buffer to aid transfer of p19^{ARF} due to its neutral charge.

The cell cycle protein p53 was also investigated. Levels of p53 are upregulated in LMP1^{CAO} transgenic ears irrespective of TGF α background (fig.5.21). Note that there is a cross reacting band at approximately 30kDa that is detected strongly in the stages 2, 3 and 4 of LMP1^{CAO} transgenic ears irrespective of TGF α background. The identity of this protein is unknown. Also the band at 45kDa is relatively constant by comparison suggesting that the increase observed is not due to a loading error.

Levels of total Rb and phosphorylated Rb were examined (fig.5.22, 5.23). There is a group of reactive bands at the 110kDa region (fig.5.22). Without a definitive positive control for Rb it is difficult to determine which band corresponds to total Rb and therefore no conclusions can be drawn. However, using an antibody to phosphorylated Rb, the 110kDa product is clear (fig.5.23). LMP1^{CAO} negative / TGF α wild type ears show low levels of phospho-Rb. Stage 1 LMP1^{CAO} transgenic / TGF α wild type ears show an initial increase but stage 2 and 3 levels are lower. The phospho-Rb band is apparent in all the TGF α null samples, whether LMP1^{CAO} transgenic or not. Maybe Rb phosphorylation is independent of LMP1, or TGF α loss may cause the phosphorylation of Rb consistent with the increased severity in the phenotype of 117/125 mice. However, two samples (stage 4 LMP1^{CAO}/ TGF α null and stage 3 LMP1^{CAO}/TGF α wild type) contradict the above hypothesis. It could be that the two samples have been mixed up or that the above hypothesis is wrong and a larger number of samples needs to be examined. Note that there is a cross reacting band at approximately 220kDa that parallels the phosphorylated Rb levels and it could possibly be an Rb complex (fig5.23). Also another cross reacting band at about 50kDa is observed predominantly in stages 3 and 4 of LMP1^{CAO} transgenic ears irrespective of TGF α background. The identity of this protein is not known.

Rassf1 is a mediator of apoptosis from Ras signalling and has been observed to be downregulated by promoter methylation or deletion in NPC lesions. In order to investigate the Rassf1 levels in the LMP1 transgenic tissues, a specific antibody detecting Rassf1 protein was used to probe a Western blot of lines 117 and 117/125 ear extracts (fig.5.24). Rassf1 levels are higher in all the LMP1^{CAO} / TGF α wild type samples (stage 1: 6.59 fold, stage 2: 12.53 fold, stage 3: 4.33 fold compared to controls, normalised against β tubulin)(table5.10). However, in the absence of TGF α in LMP1^{CAO} transgenic ears, Rassf1 remains at the level

detected in control samples suggesting that LMP1^{CAO} upregulates Rassf1 via TGF α . Note that a stage 3 LMP1^{CAO}/ TGF α wild type sample does not show this increase. It is possible that this sample is not of the best quality. Also a TGF α heterozygous sample shows low level expression. Further samples need to be examined in order to confirm the observation.

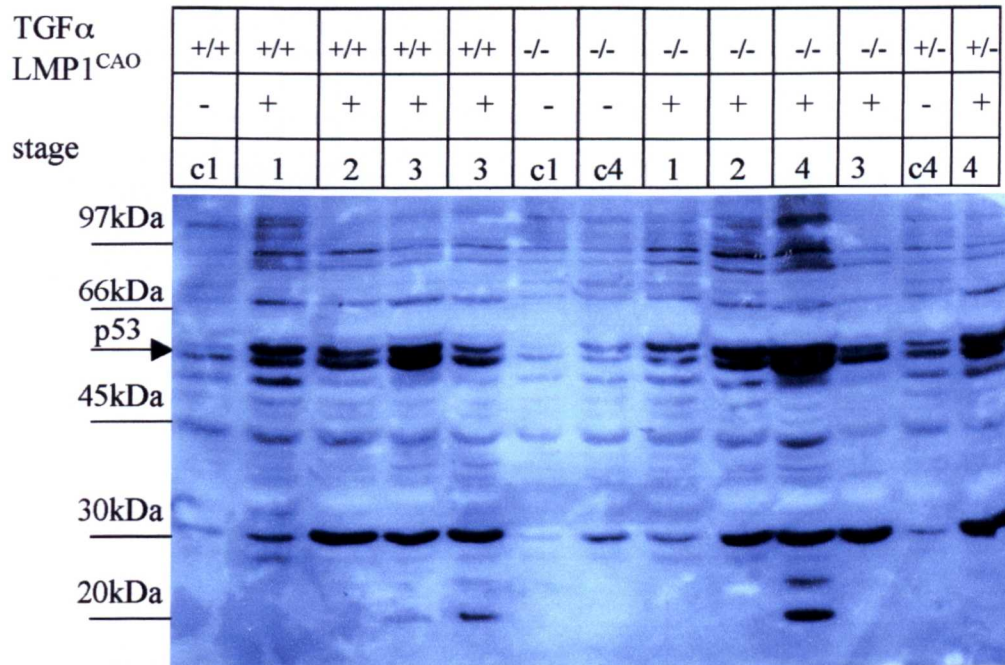


Figure 5.21: p53 western blot of protein extracts from ears of mice of line 117 and 117/125.

Protein extracts were prepared from phenotypic ears, stages 1-3 (st1-3) from mice that were transgenic for LMP1(+) and wild type (+/+), heterozygous (+/-) or null (-/-) for TGF α . Age matched control extracts from ears of siblings (-) were also prepared. 100 μ g of protein extract/track was separated through a 10% SDS-PAGE and the gel was blotted. The blot was probed with a goat anti-mouse p53 primary antibody (1:1000) and a donkey anti-goat IgG-HRP secondary antibody (1:4000) and visualised with ECL+. The doublet corresponding to p53 is indicated. Molecular weights according to markers track are shown. Note that there is a cross reacting band at 30kDa which is more prominent in the stages 2,3 and 4 of LMP1^{CAO} + ears irrespective of TGF α background. The identity of this protein is not known.

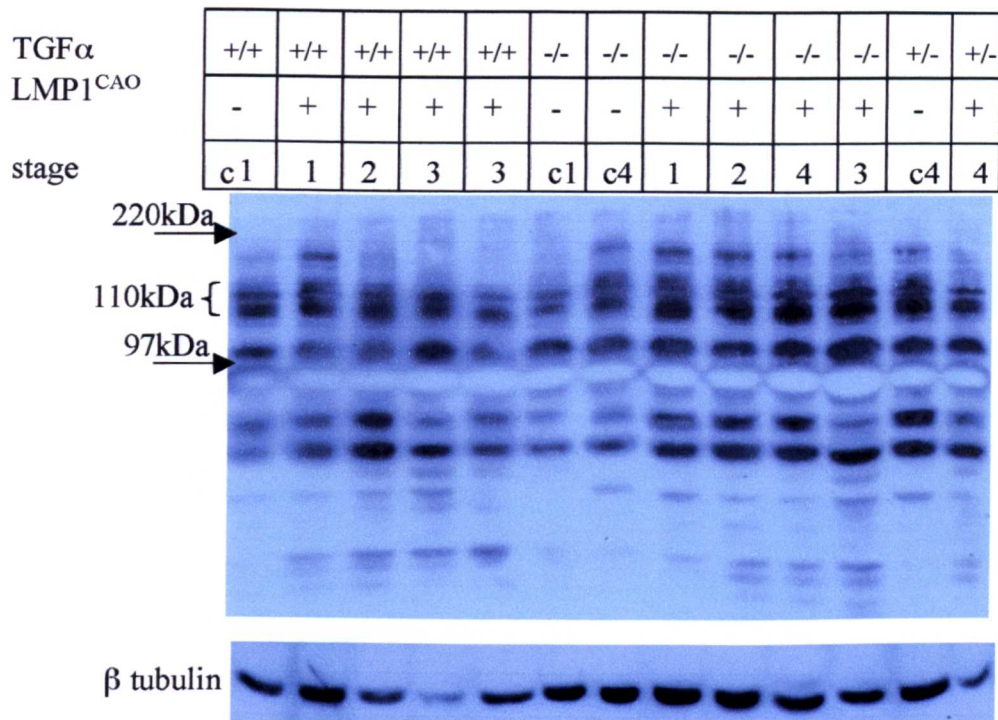


Figure 5.22: Total Rb western blot of protein extracts from ears of mice of lines 117 and 117/125.

Protein extracts were prepared from phenotypic ears, stages 1-3 (st1-3) from mice that were transgenic for LMP1(+) and wild type (+/+), heterozygous (+/-) or null (-/-) for TGF α . Age matched control extracts from ears of siblings (-) were also prepared. 100 μ g of protein extract/track was analysed on a 10% SDS-PAGE. The blot was probed with a rabbit anti-mouse total Rb (1:1000) primary antibody and a goat anti-rabbit secondary antibody and visualised with ECL⁺. The 110kDa doublet corresponding to total Rb is indicated. Molecular weights according to the markers track are shown.

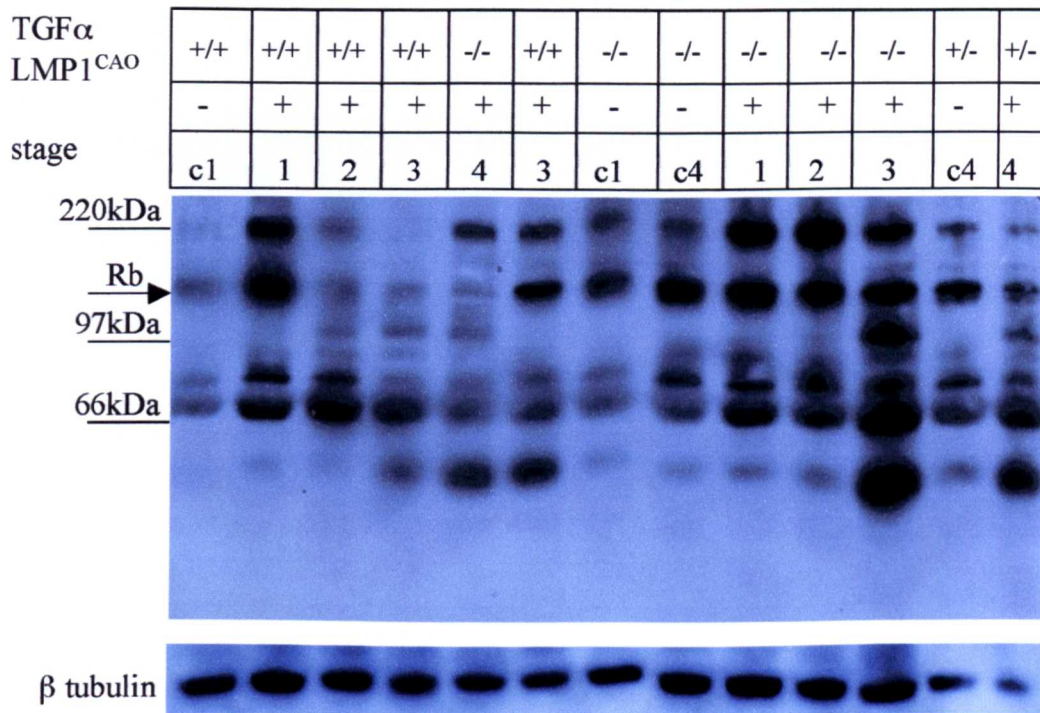


Figure 5.23: Phosphorylated Rb Western blot of protein extracts from ears of mice of line 117 and 117/125.

Protein extracts were prepared from phenotypic ears, stages 1-3 (st1-3) from mice that were transgenic for LMP1(+) and wild type (+/+), heterozygous (+/-) or null (-/-) for TGF α . Age matched control extracts from ears of siblings (-) were also prepared. 100 μ g of protein extract/track was separated through a 10% SDS-PAGE and the gel was blotted. The blot was probed with a rabbit anti-mouse phospho-Rb primary antibody (1:1000) and a goat anti-rabbit IgG-HRP secondary antibody (1:4000) and visualised with ECL+. The 110kDa corresponding to pRb is indicated. Molecular weights according to markers track are shown. This blot is a reprobe of the blot probed with phospho- and total MEK shown on figure 5.10. Note that there is a cross reacting band at about 220kDa that mirrors the phosphorylated Rb expression levels and it could possibly be an Rb complex. Also a cross reacting band at about 50kDa is detected strongly in the stages 3 and 4 of LMP1^{CAO}+ ears irrespective of TGF α background.

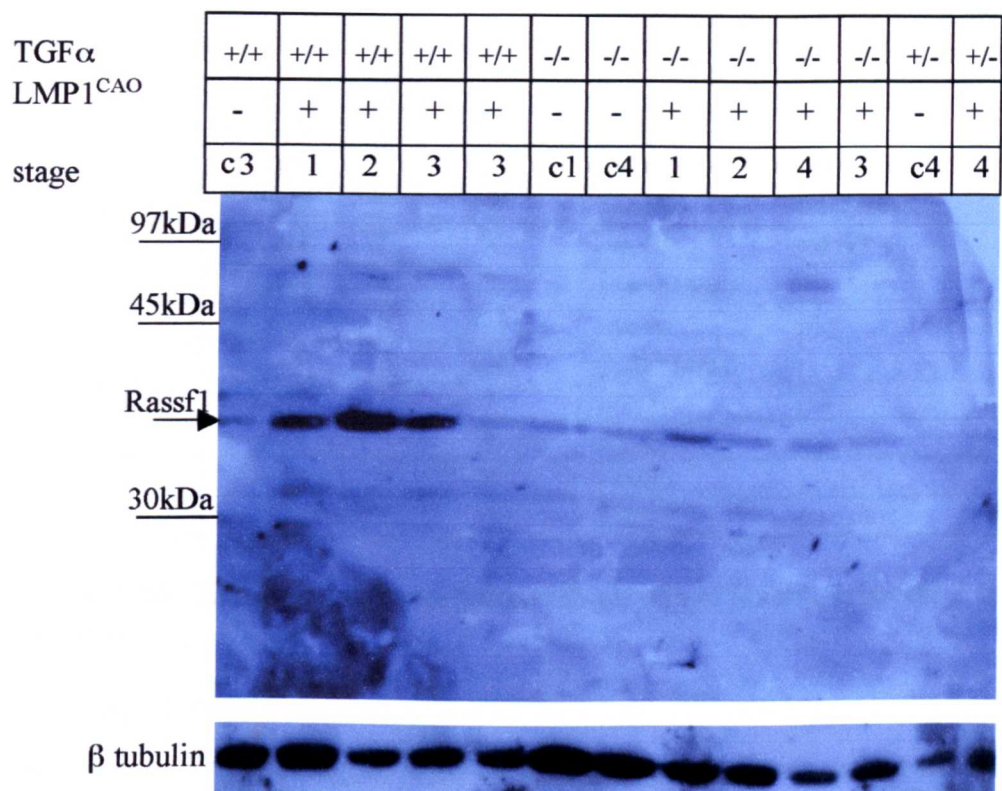


Figure 5.24: Rassf1 western blot of protein extracts from ears of mice of lines 117 and 117/125.

Protein extracts were prepared from phenotypic ears, stages 1-3 (st1-3) from mice that were transgenic for LMP1(+) and wild type (+/+), heterozygous (+/-) or null (-/-) for TGF α . Age matched control extracts from ears of LMP1^{CAO} transgenic negative siblings (-) were also prepared. 100 μ g of protein extract/track was separated by 7.5% SDS-PAGE and the gel was blotted. The blot was probed with a goat anti-mouse Rassf1 primary antibody (1:1000) and a donkey anti-goat IgG-HRP secondary antibody (1:4000) and visualised with ECL+. The 43kDa corresponding to Rassf1 is indicated. Molecular weights according to markers track are shown. The bottom picture shows the β tubulin reprobing of the blot to show relative loading levels. This blot is a reprobe of the total EGFR blot shown in figure 5.5.

Genotype			A	B	C
LMP1	TGF α	Phenotypic stage	Rassf1 (A): β tubulin	Transgenic: Wild type in respect to LMP1	Null or het to wild type in respect of TGF α
-	+/+	C1	0.03	1	
+	+/+	1	0.18	6.59	
+	+/+	2	0.34	12.53	
+	+/+	3	0.13	4.33	
+	+/+	3	(average)		
-	-/-	C1	0.07		
-	-/-	C4	(average)		
+	-/-	1	0.01	0.16	0.06
+	-/-	2	0.12	1.67	0.35
+	-/-	4	0.06	0.83	0.46
+	-/-	3	0.07	1.00	0.54

Table 5.10: Densitometric analysis on the levels of Rassf1 relative to β tubulin loading control.

Wild type (-) and transgenic (+) mice for LMP1^{CAO}, wild type (+/+) and null (-/-) for TGF α are shown. The phenotypic stage of the ears used is also shown. Note that LMP1^{CAO} - mice do not have an ear phenotype but animals that were aged matched controls of LMP1^{CAO} + mice of a particular phenotypic stage were used and that stage is indicated.

Values given are after the deduction of the background intensity.

Column A: Rassf1: β tubulin

Column B: LMP1^{CAO}: control (TGF α wild type are black, TGF α null are pink)

Column C: LMP1^{CAO} / TGF α null : LMP1^{CAO} / TGF α wild type

Note that LMP1^{CAO} negative in a TGF α null or wild type background give some reading.

In order to investigate the cell cycle arrest hypothesis further the levels of expression of cyclins A, B and D1 were investigated in these tissues (fig.5.25, 5.26, 5.27). Cyclins are proteins that play a role in the progression of the cell cycle. Analysis of the expression levels of Cyclin A (fig.5.25), cyclin B (fig.5.26) and cyclin D1 (fig.5.27) did not reveal an obvious or consistent pattern with respect to LMP1 transgenic status or TGF α null status. Interpreting the steady state levels in a whole tissue is complicated by the fact that higher levels may indicate increased proliferation but might also be evidence of a block at a certain cell cycle stage. It is therefore difficult to interpret these data. However, a cross reactive band with the antibody to cyclin B at approximately 66kDa is observed in phenotypic stages 2, 3 and 4 of LMP1^{CAO} transgenic ears in both wild type and null TGF α background. The identity of this protein is not known.

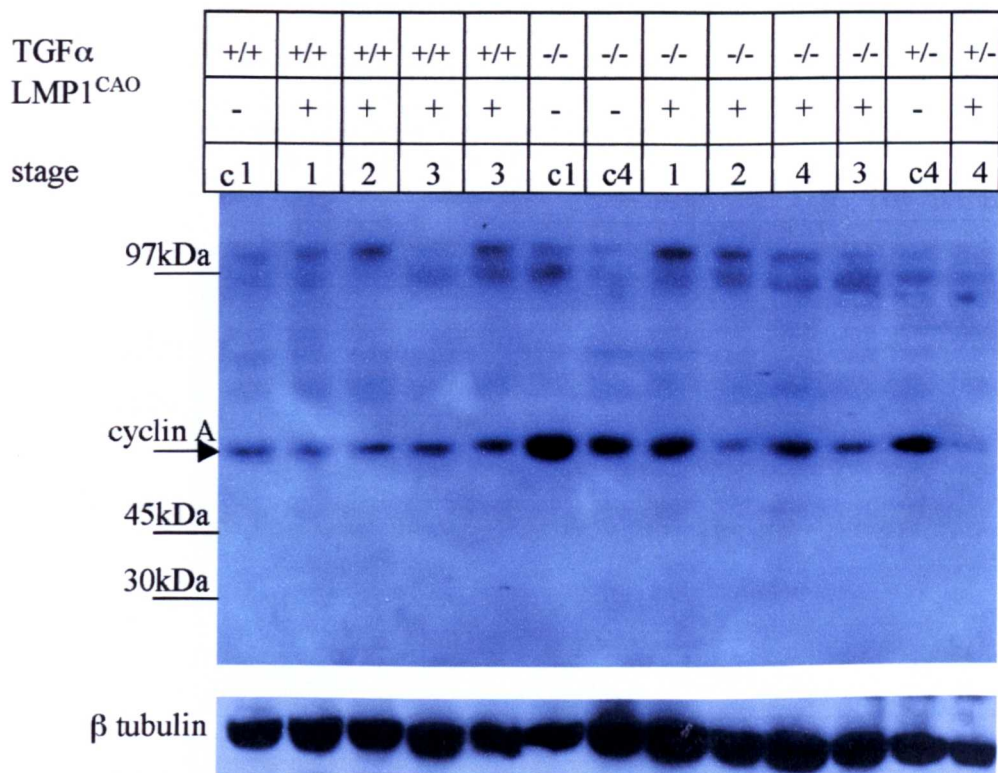


Figure 5.25: Cyclin A western blot of protein extracts from ears of mice of line 117 and 117/125.

Protein extracts were prepared from phenotypic ears, stages 1-3 (st1-3) from mice that were transgenic for LMP1(+) and wild type (+/+), heterozygous (+/-) or null (-/-) for TGF α . Age matched control extracts from ears of siblings (-) were also prepared. 100 μ g of protein extract/track was separated through a 10% SDS-PAGE and the gel was blotted. The blot was probed with a rabbit anti-mouse Cyclin A primary antibody (1:1000) and a goat anti-rabbit IgG-HRP secondary antibody (1:4000) and visualised with ECL+. The 50-55kDa corresponding to Cyclin A is indicated. Molecular weights according to markers track are shown. The bottom picture shows the β tubulin probing of the blot used as a loading control.

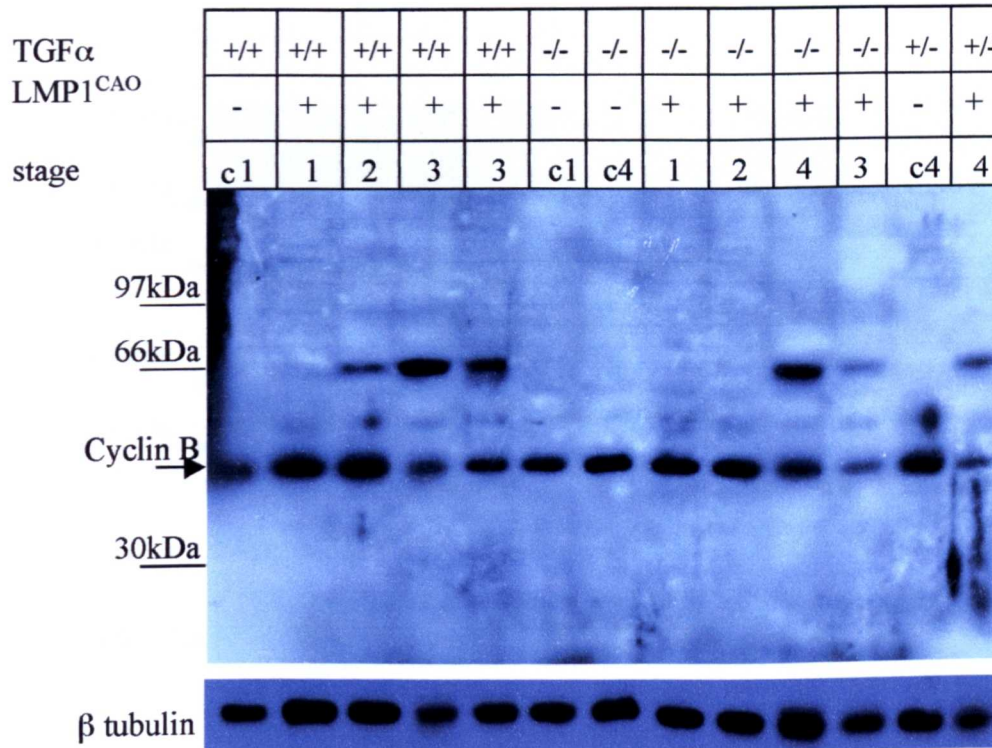


Figure 5.26: Cyclin B western blot of protein extracts from ears of mice of line 117 and 117/125.

Protein extracts were prepared from phenotypic ears, stages 1-3 (st1-3) from mice that were transgenic for LMP1(+) and wild type (+/+), heterozygous (+/-) or null (-/-) for TGF α . Age matched control extracts from ears of siblings (-) were also prepared. 100 μ g of protein extract/track was separated through a 10% SDS-PAGE and the gel was blotted. The blot was probed with a rabbit anti-mouse Cyclin B primary antibody (1:1000) and a goat anti-rabbit IgG-HRP secondary antibody (1:4000) and visualised with ECL+. The 50kDa corresponding to Cyclin B is indicated. Molecular weights according to markers track are shown. The bottom picture shows the β tubulin probing of the blot used as a loading control. Note cross reacting band at approximately 66kDa is detected in stages 2, 3 and 4 of LMP1^{CAO} transgenic samples in both wild type and null TGF α background. The identity of this protein is not known.

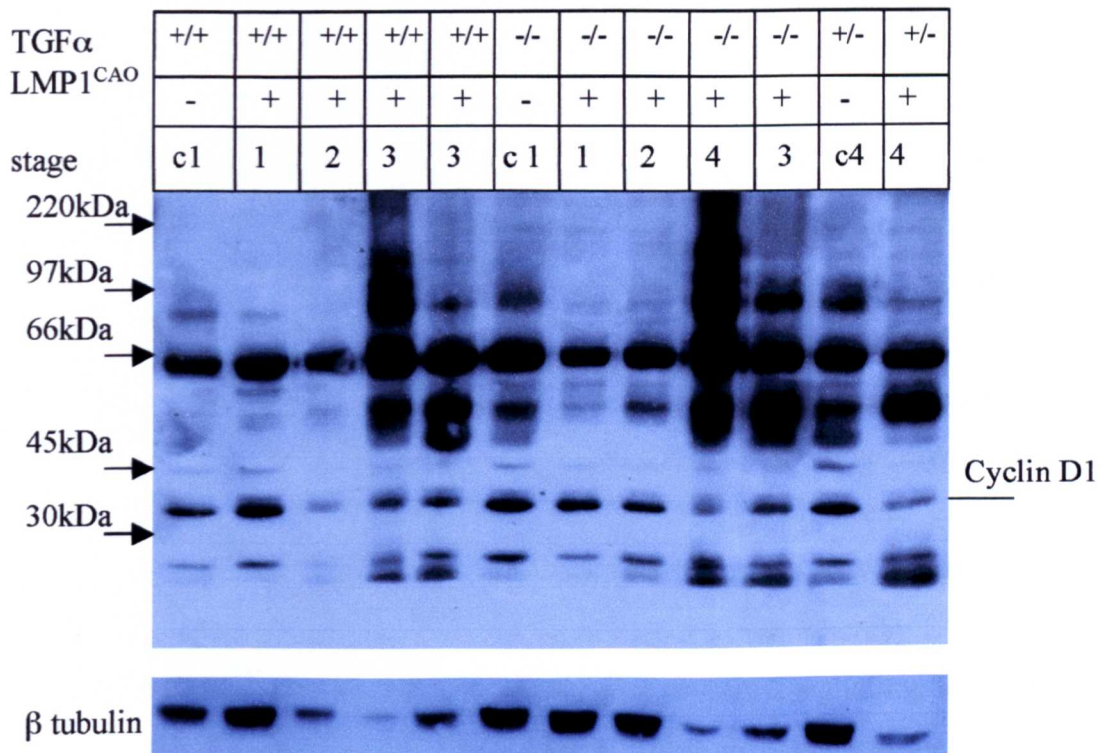


Figure 5.27: Cyclin D1 western blot of protein extracts from ears of mice of lines 117 and 117/125.

Protein extracts were prepared from phenotypic ears, stages 1-3 (st1-3) from mice that were transgenic for LMP1(+) and wild type (+/+), heterozygous (+/-) or null (-/-) for TGF α . Age matched control extracts from ears of LMP1^{CAO} transgenic negative siblings (-) were also prepared. 100 μ g of protein extract/track was analysed on a 10% SDS-PAGE. The blot was probed with a rabbit anti-mouse cyclin D1 primary antibody (1:1000) and a goat anti-rabbit secondary antibody (1:4000) and visualised with ECL⁺. The 36 kDa band corresponding to cyclin D1 is indicated. Molecular weights according to markers track are shown.

5.4 Conclusions and Discussion (summary in table 5.11)

Results presented in this chapter explore the impact of removal of a known oncogene (TGF α) from the system on the phenotype and signalling pathways known to be affected by LMP1 and its downstream targets. The results presented show that this removal of TGF α did not lead to alleviation of the observed phenotype. For example, 53/125 mice that were LMP1^{B95-8} / TGF α null mice still exhibited the scaly skin phenotype and 117/125 mice that were LMP1^{CAO} transgenic in a TGF α null background still exhibited the hyperplastic ear phenotype. Both phenotypes are LMP1 induced. Contrary to the initial hypothesis that LMP1^{CAO} may exert its proliferative effects via TGF α , it was shown that complete removal of TGF α did not alleviate the phenotype but instead led to its worsening in cross 117/125. Phenotypic examination of the ears of 117/125 mice, revealed that the LMP1^{CAO} / TGF α null ears show a faster phenotypic progression than the LMP1^{CAO} / TGF α heterozygous or wild type ears. This study therefore suggests that if TGF α upregulation is a mechanism whereby LMP1^{CAO} exerts its proliferative effects it is clearly not the only route since EGFR signalling is still active in the transgenic tissue. Moreover, removal of TGF α seems to potentiate the EGFR signalling further rather than reduce it.

When the EGFR signalling pathway was analysed using Western blotting, it was shown that in LMP1^{CAO} transgenic ears there is an increase in total EGFR levels when compared to transgenic negative ears at an early phenotypic stage. However, this increase in levels of total EGFR decreases as the phenotypic stage progresses. There was an increase in smaller –EGFR related products- observed in LMP1^{CAO} transgenic ears. These smaller products were shown to be phosphorylated when phospho-specific EGFR antibodies were used. When activation of a second receptor of the EGFR family was examined, it was shown that phosphorylated HER2/ErbB2 levels were increased in the LMP1^{CAO} transgenic ears, more so in TGF α null ears. These results collectively show that LMP1 induction of EGFR is not TGF α dependent. It is possible that other ligands such as EGF are compensating for TGF α loss by upregulating their action. In an experiment using keratinocytes null for TGF α , other factors such as amphiregulin, betacellulin and HB-EGF were found to be upregulated in squamous tumours produced from grafting those keratinocytes onto nude mice (Dlugosz et al., 1995). It is possible that these other EGFR ligands are also upregulated by LMP1^{CAO} in these transgenic ears and possibly upregulated to a greater extent in the absence of TGF α . This needs to be

explored in order to fully understand the route of EGFR activation along with an examination of the status of HER3 and 4.

The MAPK pathway was examined in this system as an EGFR target. Expression of c-Raf-1 was not detected and this could be either due to failure of the particular antibody to detect the murine c-Raf-1 or that c-Raf-1 levels in these tissues are too low for reasonable detection. A recent publication (Chakrabarti et al., 2004) showed that a variant of the E6 protein of HPV preferentially led to BRaf and not c-Raf-1 activation via Rap. When levels of BRaf were investigated in 117 and 117/125 tissues the results were not conclusive.

MEK1/2 showed marked activation at the phenotypic stage 1, which was possibly reduced in the TGF α null background. However, this activation decreased with increasing age and phenotype of the mice. These results show that in order for the tissue to exert homeostatic control on this aberrant MAPK signalling due to activated EGFR a negative feedback loop acting directly on MEK1/2 is in place. This suggests that TGF α contributes to MEK1/2 activation.

In contrast to MEK1/2 activation, levels of activated ERK1/2 increase slightly in LMP1^{CAO} transgenic tissues independent of TGF α background throughout all the phenotypic stages and therefore ERK1/2 must be activated via another route and not only via MEK1/2 directly.

Conversely a decrease in phosphorylated JNK2/3 is observed in the later phenotypic stage of LMP1^{CAO} transgenic ears compared to controls independent of TGF α background. Since previous studies have shown that JNK3 expression is specific to the brain, heart and testicles, it might be that the observed products are due to JNK2 alone (for review see (Bogoyevitch et al., 2004). Knock out mice studies have revealed considerable information about the roles of JNKs as have the studies concerned with mouse chemical carcinogenesis. It was shown that mice that were JNK1 null had an increased load of tumours when they had undergone a chemical carcinogenesis regime whilst JNK2 null mice showed an inhibition of tumourigenesis in a similar setting (Chen et al., 2001; She et al., 2002). This would imply that the loss of JNK2 activation would have a tumour inhibitory effect on these tissues and may result from a tissue homeostatic response to the increase in proliferation. It is clearly not a direct effect of LMP1 as it is not seen in stage 1 tissue samples. Why JNK2 seems to be decreasing in LMP1 transgenic tissues when other studies have reported upregulation of JNK by LMP1 and in these tissues there is AP1 activation is not clear. Possibly this decrease is due to the tissue homeostatic control. It is possible that the AP1 activation observed is solely due to the upregulation of Fra-1 and JunB that is observed in these tissues or due to activation of

other pathways that lead to AP1 activation such as p38. Another explanation for the reduced JNK activation observed in the LMP1 transgenic tissues is that maybe there is cross talk between activated ERK and JNK. For example, a study using MDCK cells showed that scatter factor/hepatocyte growth factor led to activation of ERK and inhibition of JNK. AP1 was still activated in those cells (Paumelle et al., 2000). Also a second study using human microvascular endothelial cells showed that VEGF led to activation of ERK 1/2 and inhibition of JNK leading to apoptosis (Gupta K, 1999). It has been shown that VEGF is upregulated in LMP1 transgenic ear samples and this may be a potential route via which JNK activation is reduced (Stevenson *et. al.*, in press). Further investigation of this hypothesis is needed in order to ascertain which protein plays a role in this JNK deactivation.

Examination of pro- and anti-apoptotic proteins in line 117 and 117/125 tissues, has shown that LMP1 enhances apoptosis. Levels of full length caspase-3 were increased in LMP1^{CAO} transgenic ears and this increase was proportional to the phenotypic stage. The cleaved caspase-3 was observed only in the more progressed ears consistent with the phenotype. Furthermore, p53 – another mediator of apoptosis- levels in LMP1^{CAO} transgenic ears are increased. Levels of activated Akt (thr) are significantly decreased in LMP1^{CAO} transgenic ears in a way proportional to the phenotypic stage. The decrease in activated Akt (thr) and possibly total Akt levels is consistent with an increase in caspase-3 levels and activation of apoptosis in the transgenic tissues. Why activated EGFR does not lead to increased Akt activation as would be expected is not clear. It could be that EGFR is translocated to the nucleus and is therefore unavailable to activate the PI3K/Akt effectors. However, this is not consistent as MEK1/2 activation is observed. Alternative since the p85 subunit of PI3K preferably associates with ErbB3 and not EGFR it is possible that in the LMP1 transgenic mouse model ErbB3 is at reduced levels. Examination of the status of ErbB3 is needed. Also even though EGFR phosphorylation at Tyr1068 can activate the PI3K/Akt pathway, it is phosphorylation at Tyr1086 that preferentially leads to Akt activation. The phosphorylation status of Tyr1086 has not been studied in the LMP1 transgenic tissues. It could be that this specific tyrosine is not phosphorylated in these tissues. Also other phosphatases leading to Akt deactivation could be involved but this is not known.

The effect the phenotype has on the expression of proteins is more clearly demonstrated with MMP9. Whereas uncleaved MMP9 accumulates at the more severe phenotypic stages of LMP1^{CAO} transgenic ears irrespective of TGF α , the low level cleaved MMP9 form is observed

at stages 1 and 2 only. Enhanced vascularisation is apparent from the early stages and the activation of MMP9 may facilitate this process.

Levels of JunB are upregulated in LMP1^{CAO} transgenic ears irrespective of TGF α . However, p16^{INK4a} levels do not correlate with this upregulation, implying that in this system p16^{INK4a} is either activated by another protein or is inhibited (overriding JunB) at the early stages. Upregulation of p16^{INK4a} is observed in the later phenotypic stages and even though in this study it is observed in stage 3/4 LMP1^{CAO} / TGF α null ears only, it has been also observed in LMP1^{CAO} / TGF α wild type stage 4/5 ears as well (Stevenson *et. al.*, in press). This effect therefore results from the phenotypic progression and is not the direct consequence of LMP1 expression. Even though this result contradicts other studies that have shown that LMP1 inhibits p16^{INK4a} expression, it is consistent with what is observed in NPC progression and chemical carcinogenesis studies. If LMP1 did inhibit p16^{INK4a} expression, there would be no selective pressure to silence p16^{INK4a} in NPC development or cooperative effect in expression of LMP1 and loss of INK4a. It is important to examine levels of p19^{ARF}, the other product of the INK4a locus, to determine its role in the LMP1 expressing mice and in NPC development.

Another tumour suppressor gene that is often found silenced or deleted in NPC is Rassf1a. In this study, Rassf1 expression was examined and it was observed that LMP1 led to increased Rassf1 levels. It did so in both a wild type and null TGF α background, however, removal of TGF α greatly decreased this LMP1 induced Rassf1 expression, implying that LMP1 mediates the increase in Rassf1 expression via TGF α . This observation discriminates between the action of TGF α and EGFR and the other receptors or ligands. Somehow TGF α activates a pathway that very specifically leads to Rassf1 activation. It is still not known how Rassf1a becomes activated. A recent study has revealed more about its role in mediating apoptosis. It was shown that NORE1/RASSF1 complexes can associate with the pro-apoptotic protein MST1 and inhibit its activation, but can also localise it close to activated Ras and increase its activity thus selectively inducing apoptosis (Praskova *et al.*, 2004). This would be consistent with the apparent decrease in caspase-3 levels that is observed in TGF α null ears. These ears show reduced levels of Rassf1. This could possibly lead to a decrease in MST1 activation and a decrease in apoptosis and this is confirmed by the reduced levels of total caspase-3 observed in TGF α null ears when compared to TGF α wild type ears. Investigation of the status of MST1/2 is needed.

LMP1 led to the activation of Rb and this activation seems to be increased in the absence of TGF α from the tissues. This increase in Rb activation is not consistent with the increased

p16^{INK4a} levels observed in the LMP1 transgenic ears. It could be that the p16^{INK4a} is not functional in these tissues, or that the spatial expression of p16^{INK4a} and Rb differ, or it could be that Rb gets suppressed in the presence of TGF α . How TGF α could induce this is not known. The effect that Rassf1 may have on p16^{INK4a} and Rb is still not known.

It can be concluded from the above that LMP1 expression leads to activation of the MAPK pathway. It also leads to increased apoptosis and induction of several tumour suppressors such as Rassf1 and p53. However, their expression is not enough to overcome the observed proliferative effects. It could be that the aberrant proliferation signal is too strong for the tumour suppressors to control or that spatial expression of the tumour suppressors is different from the spatial expression of the aberrant signal. For example, in this study, whole skin was examined. It could be that tumour suppressors were induced not directly via LMP1 but due to the phenotypic effect and it is possible that they were expressed in the dermis, for example or in an epidermal compartment different from the proliferative pathway.

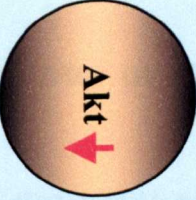
It is not clear from this study why TGF α loss does not seem to have any major effect on the pathways activated by LMP1. It may be that in this system upon withdrawal of one of the EGFR ligands, the other five EGFR ligands can compensate. Indeed, a recent study where amphiregulin (one of the EGFR specific ligands) was overexpressed in the basal layer of murine epidermis, showed that the transgenic mice generated had a hyperplastic epidermis with thickened tail and ears (Cook et al., 2004). The phenotype of these animals greatly resembles the phenotype of the L2LMP1^{CAO}, PyLMP1^{B95-8} animals and of transgenic TGF α animals. When EGF transgenic animals were created EGF was not targeted towards an epithelial compartment and so direct comparison with the LMP1 mouse model or other EGFR ligand transgenic animals cannot be made (Chan and Wong, 2000; Erwin et al., 1999; Krakowski et al., 1999; Wong et al., 2000). No other transgenic mouse models have been described overexpressing epiregulin, betacellulin or HB-EGF, the other ligands of EGFR. However, from what is seen upon targeted overexpression of specific EGFR ligands to the epithelium, one can conclude that the overexpression of EGFR specific ligands leads to similar phenotypes. Given the similarity between the LMP1 mouse model described here and the EGFR ligand transgenic models a preferable therapeutic route would be to target inhibition of the actual receptor and not its ligands. An approach to analyse this would be to cross breed LMP1^{CAO} mice to EGFR knock out animals however, EGFR knock out animals show either embryonic or perinatal lethality (Miettinen et al., 1995; Sibilias and Wagner, 1995; Threadgill et al., 1995). Another approach would be to cross breed mice harbouring dominant negative

EGFR in the basal layer (these mice are viable and fertile), given that LMP1^{CAO} expression in line 117 is confirmed to be in the basal layer (Murillas et al., 1995). Indeed, a previous study in which mice overexpressing TGF α in type II cells under the control of the human lung-specific surfactant protein C (SP-C) were crossed to mice expressing dominant negative EGFR under the human SP-C promoter, showed an improvement of the lung phenotype (Hardie et al., 1996). A different approach would be topical application of chemical EGFR inhibitors or even topical application of MEK and/or ERK inhibitors on the LMP1 expressing mice as a first step towards developing a therapeutic approach relevant to LMP1 expressing NPC.

The results presented in this chapter suggest that LMP1 via TGF α may be signalling to the tumour suppressor Rassf1 possibly via the MAPK pathway. Further work is needed to unravel the exact mechanism of action of TGF α on Rassf1. If in this system Rassf1 acts as a tumour suppressor, then its decrease in the TGF α null ears could explain the observed worsening in the ear phenotype.

To summarise, in this system TGF α may act as a control for some of the LMP1 mediated signalling pathways. However, its withdrawal does not lead to any phenotypic alleviation, instead it has quite opposite effects.

Table 5.11: Summary of the proteins examined in lines 117 and 117/125 mice
 The effect of LMP1^{CAO} on the following proteins is shown. Red arrows indicate the effect loss of TGF α had. Yellow colour represents activation/upregulation that increased with respect to phenotypic progression. Orange colour represents deactivation with respect to phenotype. Green colour represents a constant difference from wild type across the phenotypic stages. In *italics* and non bold lettering are the proteins for which the change is not strongly supported by the data.

Activated	Not Activated	Deactivated	Upregulated	Not Upregulated	Upregulated then downregulated
 EGFR	 <i>c-Raf-1</i>	 Akt	 p16	 <i>c-fos</i>	 Total EGFR
 HER2	 BRAF	 pJNK2/3	 JunB	 <i>Fra-2</i>	
 <i>pEGFR</i>	 p-JNK1		 Fos B	 c-Jun	 MEK1/2
 <i>ERK1/2</i>			 p53		
 Rb			 Total caspase-3		
			 Rassf1		
			 MMP9		
					Activated then deactivated

Chapter 6: Final Discussion

The aim of this project was to investigate the role LMP1^{CAO} plays in the genesis and development of epithelial tumours such as NPC using transgenic mice as a model. A considerable amount of information is known about the functions of LMP1, mostly from B cell studies, whereas very little is known about its role in disease in the epithelium *in vivo*. A series of transgenic mice that were generated in the laboratory expressing LMP1^{CAO} in the epithelium, under the direction of the viral ED-L2 promoter were used for this study (Stevenson *et. al.*, in press). The expression pattern of the transgene and the occurring phenotype was investigated. Signalling pathways activated by LMP1^{CAO}, in the epithelium *in vivo*, were examined with an emphasis on the Ras/MAPK pathway. In order to deduce whether LMP1^{CAO} exerts its action via TGF α upregulation, a TGF α null mouse strain was used.

6.1 LMP1^{CAO} as a tumour promoter or initiator?

It has been shown in rat fibroblasts that LMP1 acts as a classical oncogene inducing a transformed phenotype. It has also been shown that LMP1 expression in the murine epithelium under the Py promoter leads to epidermal hyperplasia (Wilson et al., 1990). Using the ED-L2 promoter to direct expression of LMP1^{CAO} to the murine epithelium leads to a hyperplastic ear phenotype which progresses from benign keratoacanthoma to squamous cell carcinoma in some cases and leads to spontaneous formation of benign lesions in susceptible mouse strains as described in this thesis (Stevenson *et. al.*, in press). Genetic susceptibility is thought to be a risk factor of NPC development. Certain ethnic backgrounds such as S.Chinese, Alaskan and African Mediterranean populations show an increased risk for NPC. In the transgenic mouse, the fact that LMP1^{CAO} led to spontaneous lesions only in a genetically susceptible mouse strain demonstrates the importance of genetic background to the action of the primary oncogene of EBV. A previous study in which PyLMP1^{B95-8} mice were chemically treated showed that LMP1^{B95-8} acts to augment the action of TPA but cannot replace DMBA in this model of carcinogenesis thus showing that LMP1^{B95-8} is acting as a tumour promoter (to induce proliferation) and not as an initiator (Curran et al., 2001). Given the above, it was of interest to explore if LMP1^{CAO} acts differently to LMP1^{B95-8} in this respect. If LMP1^{CAO} could replace chemical initiation in this approach, supply of LMP1 in the

form of a transgene would make use of a chemical initiator such as DMBA in the process of chemical carcinogenesis redundant.

The results obtained from this thesis, confirmed that LMP1^{CAO} is acting as a tumour promoter and not as an initiator in the epithelium *in vivo*, just as LMP1^{B95-8}. However, the fact that lesions appear at all on untreated mice, implies that LMP1^{CAO} is supplying a weak initiation signal. Whether LMP1^{CAO} is more tumourigenic than LMP1^{B95-8} is still not clear from these studies. When L2LMP1^{B95-8} mice were created, only two founders were born and those had a severe phenotype and died early before establishing a line. However, the small number of L2LMP1^{B95-8} mice generated does not allow for a formative comparison to be made. Furthermore the fact that no spontaneous papillomas form on PyLMP1^{B95-8} mice does not necessarily show that LMP1^{CAO} is more tumourigenic. Since the epidermal compartment where the L2 and the Py transgenes are expressed is unknown, this could be a site specific effect and not an LMP1 effect. Creating PyLMP1^{CAO} or further L2LMP1^{B95-8} mice would be a way to directly compare these two LMP1 strains *in vivo*.

6.2 LMP1^{CAO} and INK4a locus

It has been shown in this study using 117/113 mice and in a previous study using 53/113 mice (Macdiarmid et al., 2003) that loss of the INK4a locus in conjunction with LMP1 expression leads to increased lesion load, with larger lesions and progression to malignancy. These results imply that there is cooperation between LMP1 and loss of either p16^{INK4a} and/or p19^{ARF} leading to both lesion expansion and conversion. In NPC and EBV associated gastric carcinoma, loss of heterozygosity on chromosome 9 (a region encoding INK4a, INK4b and ARF), is an early event that is thought to precede EBV infection. EBV infection has not yet been identified in pre-malignant lesions of the nasopharynx or the gastric mucosa. This suggests that loss of heterozygosity of INK4a and/or ARF is predisposing the affected area, following EBV infection to malignant progression. Consistent with this, the above studies using 53/113 and 117/113 mice have demonstrated a cooperation between EBV LMP1 and INK4a loss.

Other studies have shown using murine and human fibroblasts that LMP1 leads to the inhibition of p16^{INK4a} expression and action (Ohtani et al., 2003; Yang et al., 2000a). However, in the LMP1^{CAO} transgenic epithelium p16^{INK4a} expression is upregulated at the later phenotypic stages of the affected tissue. This would suggest that this is not a direct LMP1^{CAO} effect but rather a subsequent response to the developing phenotype. The apparent

contradictory results described above, may be due to the nature of the studies. For example, it is possible that *in vivo* the LMP1 induced phenotype leads to p16^{INK4a} upregulation and thus loss of p16^{INK4a} is advantageous in carcinogenic progression whereas in an established fibroblast cell line *in vitro*, the growth status of the cell is very different and several checkpoints have already been overcome by mutation.

In support of this premise, whereby the cellular environment determines the effect LMP1 may have on p16, it has been recently reported that LMP1 is not sufficient to inhibit p16^{INK4a} expression in LCLs (Hayes et al., 2004).

6.3 LMP1^{CAO} and the Ras/MAPK pathway

Activating *ras* mutations are a common feature of many human cancers (Bos, 1989). In NPC *ras* mutations have not been found. One hypothesis for this observation is that LMP1 can lead to activation of *ras* therefore, there would be no selective advantage for constitutive *ras* mutation during tumour development or another hypothesis is that LMP1 activation may lead to *ras* pathway inhibition. The signalling pathways that were investigated in this thesis showed that LMP1^{CAO} leads to TGF α upregulation, EGFR activation and subsequent initial activation of MEK1/2 that is then deactivated, and a continuous activation of ERK1/2 and several downstream transcription factors. These results have confirmed a previous observation showing that LMP1 led to ERK activation in rat fibroblasts *in vitro* (Roberts and Cooper, 1998) and is the first report to show that LMP1 activates the EGFR/MAPK pathway in the epithelium *in vivo*. It supports previous studies demonstrating that LMP1 induced upregulation of EGFR, correlated with EGFR expression in NPC biopsies and a study that showed that LMP1 regulates EGFR nuclear translocation and therefore its function in HNE2 epithelial cells (Tao et al., 2005; Zheng et al., 1994a). As can be deduced from the above, even though the status of *ras* in this system has not been specifically investigated, one of its upstream activators (EGFR) and one of its downstream pathways (MAPK) are activated by LMP1^{CAO}, possibly suggesting that *ras* or related protein (eg. Rap) can be activated by LMP1 signalling and thus activating mutations are not selected for in tumourigenesis. In order to test this, papillomas that spontaneously develop on line 117 transgenic mice could be assayed in order to identify any *ras* activating mutations by sequencing. Similar assays could be performed using lesions that developed on LMP1 transgenic mice after chemical carcinogen treatment. Absence of *ras* mutations in the spontaneous lesions, would imply that LMP1^{CAO}

overrides or inhibits any selection for activating *ras* mutations in the development of these lesions.

Incidental evidence comes from the observation that LMP1^{CAO} expression leads to spontaneous papillomas in line 117 mice. Appearance of these lesions suggests that LMP1^{CAO} could be activating *ras* or a parallel pathway to a degree even if this activation is not strong enough to completely replace activated *ras*. However, not all lesions develop as a result of *ras* activation so this is unequivocal. Also when line 53 mice were crossed with transgenic *ras* mice the bitransgenic mice developed fewer lesions than the monotransgenic *ras* mice. Since LMP1 activates the MAPK pathway, supplying an extra proliferating signal by transgenic *ras*, could lead to anti-proliferative responses such as upregulation of p16^{INK4a}. For example, this has been seen in line 117 ears where as the phenotype becomes worse, there is upregulation in the expression of p16^{INK4a} and this is mediated possibly via activation of *ras*. Also another tumour suppressor that is found to be upregulated as the phenotype worsens is *Rassf1*. In both NPC and EBV associated gastric carcinomas, loss of heterozygosity on chromosome 3 that contains the gene that encodes *Rassf1* is an early event, prior to EBV infection. Extensive hypermethylation of *Rassf1a* and its subsequent silencing is also observed. Studies have shown that activated *ras* can lead to upregulation of *Rassf1*. In this study, it was shown that LMP1 leads to *Rassf1* upregulation via TGF α . Taken together, these data suggest that LMP1 in the murine epithelium *in vivo*, is activating a key *ras* signalling pathway and that removal of growth inhibitors activated by this pathway, such as p16 and *Rassf1* are critical in LMP1 (and thus EBV) associated carcinogenesis.

6.4 LMP1^{CAO} and Other Signalling pathways

Other MAPKs such as p38 were found to be activated by LMP1^{CAO}, this being consistent with the observation that LMP1 leads to p38 activation in epithelial cells *in vitro* (Eliopoulos et al., 1999). In contrast, even though EGFR was activated, Akt was found to be deactivated by LMP1^{CAO}, giving the opposite result from what was observed in epithelial cells in culture (Dawson et al., 2003). It is possible that the PI3K/Akt pathway is not activated by EGFR as the status of the specific tyrosine needed for Akt activation has not been studied and it may be possible that activation of the MAPK pathway has opposing effects on PI3K/Akt activation. It is possible that in these tissues, EGFR may be sequestered away in a different compartment and therefore not even basal level Akt activation is observed. Also the fact that Dawson *et*.

al., are using carcinoma cells that have already surpassed all the control mechanisms that are in place in a live, responsive tissue may explain this apparent contradictory observation.

AP1 and NF- κ B were found to be activated in the transgenic tissues and it was shown that LMP1^{CAO} leads to activation of apoptosis (increased caspase-3), activation of tumour suppressors (p53, Rb and Rassf1) and activation of the invasion pathway (increased MMP9 levels). Activation of Rb by phosphorylation leads to release of E2F that can increase p19 expression that leads to stabilisation of p53. Both stabilised p53 and Rassf1 activation can lead to an increase in apoptosis.

A novel effect of LMP1 on the tumour suppressor Rassf1 has been observed, showing that one of the actions of LMP1 may be to keep the proliferation under control. Whereas at the same time LMP1 is activating proliferative pathways such as MAPK, it also leads to increased expression of Rassf1 that has been shown to inhibit proliferation by promoting apoptosis and cell cycle arrest. This observation is consistent with the smaller size of lesions observed in mice of line 53 compared to wild type that were chemically treated (Macdiarmid et al., 2003). This is the first study that examines the action of LMP1^{CAO} in the epithelium *in vivo*, and as noted above some opposing results have been obtained highlighting the differences between a carcinoma cell line that harbours multiple mutations in cellular oncogenes and tumour suppressor genes and has lost several of its growth control mechanisms and a pre-cancerous tissue that still has most of the negative feedback loops intact.

When TGF α is removed from this system, an increase in severity of the phenotype is observed. However, this does not negate any significant changes in the signalling pathways studied. For example, there is still LMP1^{CAO} induced EGFR/HER2 and MEK1/2 activation, although the latter is to a lower degree. It is possible that TGF α loss is compensated for by upregulation of other EGFR ligands. For example in a study using murine keratinocytes, activation of *ras* was not affected by TGF α loss and other ligands were found to be upregulated (Dlugosz et al., 1995). In the transgenic tissue it is possible that TGF α is acting as a regulator of LMP1 action, since its removal leads to a worsening of phenotype. By overexpression of an oncogene such as TGF α , it is possible that cell cycle arrest or apoptotic pathways are activated. Alternatively removal of TGF α may lead to overcompensation of other EGFR ligands leading to a stronger proliferative signal. In either scenario TGF α appears to dampen the consequences of LMP1 action indicating that as well as its known oncogenic role in proliferation it may also serve as a regulator of this activity.

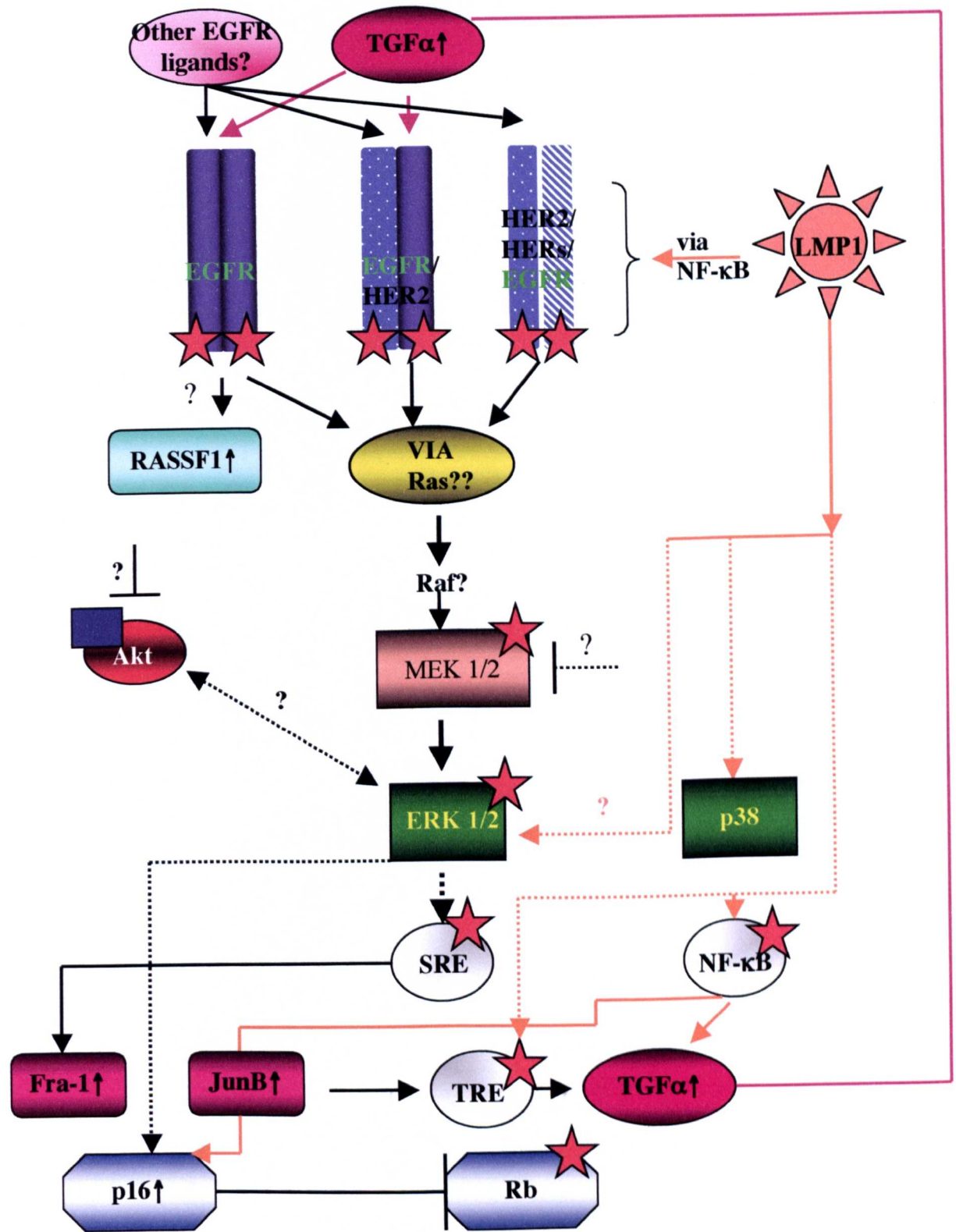
The exact role EGFR activation plays in murine carcinogenesis is still not very clear. A recent study has suggested that its role is more important in tumour invasion than in cellular proliferation (Scott et al., 2004). This would be consistent with the observed upregulation of MMP9, VEGF (Stevenson *et al.* in press) and Fra-1 (which was shown to enhance invasiveness in mammary epithelial cells) (Kustikova et al., 1998) in the LMP1 transgenic tissues.

The signalling mechanism that we propose is summarised in figure 6.1. LMP1, activates NF- κ B and AP1 complexes that lead to TGF α upregulation which in turn activates EGFR. Moreover, EGFR contains NF- κ B binding sites in its promoter and it has been shown that LMP1 directly upregulates EGFR via NF- κ B (Tao et al., 2004c). EGFR signalling leads to activation of the MAPK cascade. A possible consequence of this is the observed induction of JunB, p16^{INK4a} and Fra-1. How this precisely impacts proliferation, apoptosis and invasion is not clear. TGF α upregulation seems to play a role in controlling LMP1 induced EGFR action.

In the viral context, it is possible that LMP1 may promote growth pathways and differentiation of cells in order to support viral production and release. Under normal circumstances, EBV infected peripheral B cells express only LMP2 and possibly EBNA1 but upon a cellular trigger such as differentiation, EBV may switch into the lytic cycle and produce virions. LMP1 is the only latent protein to be expressed in the lytic cycle, so it may play a role in viral reproduction in B cells. EBV epithelial infection is a rare event. It is possible that in an epithelial cell context, LMP1 activation of the EGFR/MAPK pathway leading to excessive proliferation of the epithelium may be an inadvertent consequence of the signalling pathways activated by LMP1 designed to promote the viral life cycle in a B cell.

Figure 6.1: Possible pathway of LMP1^{CAO} action in line 117 ears.

In the line 117 ear tissue, LMP1^{CAO} activates both NF- κ B and AP1 to increase factor binding to NF- κ B and TRE sites (respectively). Binding elements for both exist in the promoter of the TGF α gene. LMP1^{CAO} leads to TGF α upregulation probably via activation of the promoter. NF- κ B binding elements also exist in the EGFR promoter possibly leading to direct upregulation of EGFR expression by LMP1. In conjunction with TGF α upregulation (and possibly other EGFR ligands) this leads to an increase in EGFR and HER2 activation. EGFR and HER2 can form homo/heterodimers with each other to activate downstream pathways. (Other heterodimers with other receptors of the EGFR family have not been investigated.) One of the pathways examined was the MEK/ERK pathway, where initial activation of MEK1/2 followed by deactivation in the later phenotypic stage ears was observed. This suggests that there is a negative feedback loop acting on MEK1/2 (represented by a dotted line). ERK1/2 is activated by LMP1 and increased binding at SRE containing sites is observed. ERK1/2 activation can upregulate fra-1 and p16^{INK4a}. p16^{INK4a} can block Rb activation. Therefore it is not clear how Rb remains active when p16^{INK4a} is expressed. It is not known if LMP1 can directly activate Rb at this stage. Rassf1 is upregulated via TGF α but whether this is a Ras mediated effect is not known. LMP1 can activate other MAPKs such as p38. Another pathway affected by EGFR signalling is the PI3K/Akt pathway. In ear tissues deactivation of Akt is observed. Note that the red star implies activation, the blue box deactivation and where the pathway is not direct from one molecule to the next a dotted line was used.



6.5 Future Directions

It has not yet been clarified in exactly which epidermal layer the LMP1^{CAO} and the LMP1^{B95-8} transgenes are expressed. It is important to determine this either by IHC or by RNA *in situ*, in order to allow a direct comparison of the effect of the two strains to be made. When L2LMP1^{B95-8} mice were created, the 2 transgenic pups born died due to a severe phenotype before a line could be established. This could imply that either the LMP1^{B95-8} variant is more potent in hyperplasia and apoptosis or that its expression in the specific epidermal layer alters its effects. This would not be surprising since other oncogenes for example, *ras* and TGF α when expressed in different epidermal layers have quite different effects. The small number of pups created does not allow for a definitive comparison to be made.

It is also important to find out where (epidermal layer or dermis) the different upregulated and activated products are expressed/present by IHC. For example, an increase in p16 expression and activation of Rb may not be taking place in the same cells but in different cells of the tissue. Also MMPs are typically expressed in mesenteric tissues such as dermis and the observed MMP9 upregulation may not be occurring in the same cells as LMP1 is expressed but upregulated in a responsive tissue (eg. TGF α can affect neighbouring cells and tissues). Such a finding, could significantly impact the interpretation of these data.

Further investigation of pathways that could be activated by LMP1^{CAO} is still pending. For example, the JAK/STAT pathway has not been investigated in this study and is one of the pathways known to be activated by LMP1 in fibroblasts. During the preparation of this thesis, Chan and co-workers reported that EGFR activation during murine skin chemical carcinogenesis led to STAT activation, particularly STAT3 (Chan et al., 2004). Since the STAT pathway is activated by both EGFR and LMP1 it would be very interesting to examine STAT3 levels and activation in the transgenic tissues.

The hypothesis that TGF α loss may be compensated for by the action of the other EGFR specific ligands needs to be tested by Western blot analysis.

However, even if the other ligands are compensating, their functions are not completely overlapping as some observations (such as Rassf1 levels and Rb phosphorylation) are different in the absence of TGF α , so it would be interesting to determine what effect the loss of TGF α will have in spontaneous papilloma formation and how TGF α specifically causes these effects. So far, the analysis of the effects of TGF α loss in cooperation with LMP1^{CAO} expression, was performed in tissues that came from mice of mixed strain C57BL/6/FVB and 129 background.

It has been highlighted extensively in this thesis the effect that strain background can have on the phenotype. It would therefore be interesting to bring the 117/125 mice into the FVB strain and observe whether loss of TGF α leads to any changes in the spontaneous lesion formation. It is predicted that possibly there would be an increase in the number of papillomas observed compared to 117 mice.

Examining the activity of *ras* and related proteins such as Rap in the 117 mice is important. This could be done by sequencing of spontaneous papillomas as described before or by assays measuring the ratio between Ras-GTP and Ras-GDP. For example, use of the Ras binding domain of Raf-1 preferentially binds Ras-GTP precipitating it from cell suspension (de Rooij and Bos, 1997). Determining whether Raf-1, Braf or Araf is involved in MEK activation is also of interest and this can be done by further controlled Western blots using the appropriate antibodies. Mutated forms of Braf have been shown to lead to increased ERK activation from Rap. It would be interesting to determine whether Braf in the transgenic tissues is activated.

Further examination of the PI3K/Akt pathway would be informative. For example only GSK3 β has been examined so far whereas other downstream targets such as Bad have not been examined. Examining the status of the specific tyrosine of EGFR responsible for activation of PI3K/Akt by Western blot would clarify whether the Akt deactivation observed is due to the tyrosine not being activated. It would also be interesting to deduce in which cellular compartment activated EGFR goes.

So far, the most striking difference observed between LMP1 transgenic TGF α wild type and null ears lies in the decreased levels of Rassf1 observed in the TGF α null ears. It is known that Rassf1a expression is silenced not only in NPC but in a variety of other human tumours. The mechanism of action of Rassf1a is not entirely clear and it would be important to investigate the relationship between TGF α expression and Rassf1. It has been recently suggested that Rassf1 is involved in the TGF β /Smad signalling pathway and so investigation of the status of this pathway in line 117 and 117/125 tissues would be informative. When exogenous Rassf1a was transfected into epithelial nasopharyngeal carcinoma cells lacking Rassf1a and an oligonucleotide array was performed, it was shown that expression of Rassf1a led to an increase in arrestin beta E – a TGF β /Smad pathway effector, and downregulation of inhibitor of differentiator (Id) 2 – a TGF β /Smad downstream target (Lo KW Oral presentation). Ids (1-4) bind to E proteins and prevent them from binding to DNA thus inhibiting regulation of expression by E proteins. Ids are downstream targets of the MAPK pathway as well and it will be very interesting to investigate Id levels in the transgenic tissues

to see if these observations correlate in the epithelium *in vivo* (reviewed in (Ruzinova and Benezra, 2003). One might predict that Id2 may well be downregulated in the transgenic tissues as they show overexpression of Rassf1. It has been shown by two groups that LMP1 leads to upregulation of Id1 and Id3 in epithelial cells in culture (Everly et al., 2004; Li et al., 2004). It is possible that LMP1 in the transgenic tissues, leads to Id1 and 3 upregulation thus preventing E2A binding to transcription factors and activating p16. Inhibition of p16 allows Rb phosphorylation.

With respect to potential therapeutic approaches the future plan is to treat mice of lines 117 and 117/125 with EGFR chemical inhibitors either by topical application or in drinking water in order to assess the therapeutic potential in targeting inhibition of the receptor.

Clearly, TGF α removal alone does not lead to an alleviation of the observed phenotype. On the contrary it seems to accelerate the phenotype. It is therefore, important not to target ligands with therapies without this kind of *in vivo* analysis. Moreover, targeting receptors should be fully investigated before taken to clinical trials. For example, IressaTM (an EGFR inhibitor developed by AstraZeneca) is not increasing survival rate in non-small cell lung cancer and its action *in vivo* models may not have been fully explored. However, it does show some benefit such as tumour shrinkage and its efficacy in other types of cancer is still under investigation. Therefore, caution needs to be taken before inhibiting a pathway as the opposite results may be obtained.

In conclusion, the above study has highlighted the critical role that examination of an *in vivo* model plays in order to correctly target a factor for therapy. As was concluded, complete withdrawal of the ligand that was proposed to cause or contribute to the phenotypic effect not only did not alleviate the phenotype but led to its worsening highlighting the fine tuning of the homeostatic controls that are in place in a living tissue. As such, before any potential therapies are taken to human trials, a thorough examination in suitable *in vivo* models would be highly advisable.

References

- Abbot, S. D., Rowe, M., Cadwallader, K., Ricksten, A., Gordon, J., Wang, F., Rymo, L., and Rickinson, A. B. (1990). Epstein-Barr virus nuclear antigen 2 induces expression of the virus-encoded latent membrane protein. *J Virol* *64*, 2126-2134.
- Addinger, H. K., Delius, H., Freese, U. K., Clarke, J., and Bornkamm, G. W. (1985). A putative transforming gene of Jijoye virus differs from that of Epstein-Barr virus prototypes. *Virology* *141*, 221-234.
- Adler, B., Schaadt, E., Kempkes, B., Zimmer-Strobl, U., Baier, B., and Bornkamm, G. W. (2002). Control of Epstein-Barr virus reactivation by activated CD40 and viral latent membrane protein 1. *Proc Natl Acad Sci U S A* *99*, 437-442.
- Agathangelou, A., Dallol, A., Zochbauer-Muller, S., Morrissey, C., Honorio, S., Hesson, L., Martinsson, T., Fong, K. M., Kuo, M. J., Yuen, P. W., *et al.* (2003). Epigenetic inactivation of the candidate 3p21.3 suppressor gene BLU in human cancers. *Oncogene* *22*, 1580-1588.
- Allan, G. J., Inman, G. J., Parker, B. D., Rowe, D. T., and Farrell, P. J. (1992). Cell growth effects of Epstein-Barr virus leader protein. *J Gen Virol* *73* (Pt 6), 1547-1551.
- Allday, M. J., Crawford, D. H., and Griffin, B. E. (1989). Epstein-Barr virus latent gene expression during the initiation of B cell immortalization. *J Gen Virol* *70* (Pt 7), 1755-1764.
- Allday, M. J., Crawford, D. H., and Thomas, J. A. (1993). Epstein-Barr virus (EBV) nuclear antigen 6 induces expression of the EBV latent membrane protein and an activated phenotype in Raji cells. *J Gen Virol* *74* (Pt 3), 361-369.
- Allday, M. J., and Farrell, P. J. (1994). Epstein-Barr virus nuclear antigen EBNA3C/6 expression maintains the level of latent membrane protein 1 in G1-arrested cells. *J Virol* *68*, 3491-3498.
- Ambinder, R. F., Lambe, B. C., Mann, R. B., Hayward, S. D., Zehnauer, B. A., Burns, W. S., and Charache, P. (1990). Oligonucleotides for polymerase chain reaction amplification and hybridization detection of Epstein-Barr virus DNA in clinical specimens. *Mol Cell Probes* *4*, 397-407.
- Anagnostopoulos, I., Hummel, M., Kreschel, C., and Stein, H. (1995). Morphology, immunophenotype, and distribution of latently and/or productively Epstein-Barr virus-infected cells in acute infectious mononucleosis: implications for the interindividual infection route of Epstein-Barr virus. *Blood* *85*, 744-750.
- Anklesaria, P., Teixido, J., Laiho, M., Pierce, J. H., Greenberger, J. S., and Massague, J. (1990). Cell-cell adhesion mediated by binding of membrane-anchored transforming growth factor alpha to epidermal growth factor receptors promotes cell proliferation. *Proc Natl Acad Sci U S A* *87*, 3289-3293.

- Arrand, J. R., Rymo, L., Walsh, J. E., Bjorck, E., Lindahl, T., and Griffin, B. E. (1981). Molecular cloning of the complete Epstein-Barr virus genome as a set of overlapping restriction endonuclease fragments. *Nucleic Acids Res* 9, 2999-3014.
- Arrand, J. R., Young, L. S., and Tugwood, J. D. (1989). Two families of sequences in the small RNA-encoding region of Epstein-Barr virus (EBV) correlate with EBV types A and B. *J Virol* 63, 983-986.
- Aslanian, A., Iaquinta, P. J., Verona, R., and Lees, J. A. (2004). Repression of the Arf tumor suppressor by E2F3 is required for normal cell cycle kinetics. *Genes Dev* 18, 1413-1422.
- Aviel, S., Winberg, G., Massucci, M., and Ciechanover, A. (2000). Degradation of the Epstein-Barr virus latent membrane protein 1 (LMP1) by the ubiquitin-proteasome pathway. Targeting via ubiquitination of the N-terminal residue. *J Biol Chem* 275, 23491-23499.
- Babcock, G. J., Hochberg, D., and Thorley-Lawson, A. D. (2000). The expression pattern of Epstein-Barr virus latent genes in vivo is dependent upon the differentiation stage of the infected B cell. *Immunity* 13, 497-506.
- Babcock, G. J., and Thorley-Lawson, D. A. (2000). Tonsillar memory B cells, latently infected with Epstein-Barr virus, express the restricted pattern of latent genes previously found only in Epstein-Barr virus-associated tumors. *Proc Natl Acad Sci U S A* 97, 12250-12255.
- Baer, R., Bankier, A. T., Biggin, M. D., Deininger, P. L., Farrell, P. J., Gibson, T. J., Hatfull, G., Hudson, G. S., Satchwell, S. C., and Seguin, C. (1984). DNA sequence and expression of the B95-8 Epstein-Barr virus genome. *Nature* 310, 207-211.
- Baichwal, V. R., and Sugden, B. (1987). Posttranslational processing of an Epstein-Barr virus-encoded membrane protein expressed in cells transformed by Epstein-Barr virus. *J Virol* 61, 866-875.
- Baichwal, V. R., and Sugden, B. (1988). Transformation of Balb 3T3 cells by the BNLF-1 gene of Epstein-Barr virus. *Oncogene* 2, 461-467.
- Baichwal, V. R., and Sugden, B. (1989). The multiple membrane-spanning segments of the BNLF-1 oncogene from Epstein-Barr virus are required for transformation. *Oncogene* 4, 67-74.
- Bailleul, B., Surani, M. A., White, S., Barton, S. C., Brown, K., Blessing, M., Jorcano, J., and Balmain, A. (1990). Skin hyperkeratosis and papilloma formation in transgenic mice expressing a ras oncogene from a suprabasal keratin promoter. *Cell* 62, 697-708.
- Ballerini, P., Gaidano, G., Gong, J. Z., Tassi, V., Saglio, G., Knowles, D. M., and Dalla-Favera, R. (1993). Multiple genetic lesions in acquired immunodeficiency syndrome-related non-Hodgkin's lymphoma. *Blood* 81, 166-176.

- Balmain, A., Brown, K., Akhurst, R. J., and Fee, F. M. (1988). Molecular analysis of chemical carcinogenesis in the skin. *Br J Cancer Suppl* 9, 72-75.
- Balmain, A., Ramsden, M., Bowden, G. T., and Smith, J. (1984). Activation of the mouse cellular Harvey-ras gene in chemically induced benign skin papillomas. *Nature* 307, 658-660.
- Bar-Sagi, D., and Feramisco, J. R. (1985). Microinjection of the ras oncogene protein into PC12 cells induces morphological differentiation. *Cell* 42, 841-848.
- Barbacid, M. (1987). ras genes. *Annu Rev Biochem* 56, 779-827.
- Bates, S., Phillips, A. C., Clark, P. A., Stott, F., Peters, G., Ludwig, R. L., and Vousden, K. H. (1998). p14ARF links the tumour suppressors RB and p53. *Nature* 395, 124-125.
- Birnboim, H. C., and Doly, J. (1979). A rapid alkaline extraction procedure for screening recombinant plasmid DNA. *Nucleic Acids Res* 7, 1513-1523.
- Bizub, D., Wood, A. W., and Skalka, A. M. (1986). Mutagenesis of the Ha-ras oncogene in mouse skin tumors induced by polycyclic aromatic hydrocarbons. *Proc Natl Acad Sci U S A* 83, 6048-6052.
- Blake, S. M., Eliopoulos, A. G., Dawson, C. W., and Young, L. S. (2001). The transmembrane domains of the EBV-encoded latent membrane protein 1 (LMP1) variant CAO regulate enhanced signalling activity. *Virology* 282, 278-287.
- Bogoyevitch, M. A., Boehm, I., Oakley, A., Ketterman, A. J., and Barr, R. K. (2004). Targeting the JNK MAPK cascade for inhibition: basic science and therapeutic potential. *Biochim Biophys Acta* 1697, 89-101.
- Bonnet, M., Guinebretiere, J. M., Kremmer, E., Grunewald, V., Benhamou, E., Contesso, G., and Joab, I. (1999). Detection of Epstein-Barr virus in invasive breast cancers. *J Natl Cancer Inst* 91, 1376-1381.
- Borrell-Pages, M., Rojo, F., Albanell, J., Baselga, J., and Arribas, J. (2003). TACE is required for the activation of the EGFR by TGF-alpha in tumors. *Embo J* 22, 1114-1124.
- Bos, J. L. (1989). ras oncogenes in human cancer: a review. *Cancer Res* 49, 4682-4689.
- Brachmann, R., Lindquist, P. B., Nagashima, M., Kohr, W., Lipari, T., Napier, M., and Derynck, R. (1989). Transmembrane TGF-alpha precursors activate EGF/TGF-alpha receptors. *Cell* 56, 691-700.
- Brennan, P., Floettmann, J. E., Mehl, A., Jones, M., and Rowe, M. (2001). Mechanism of action of a novel latent membrane protein-1 dominant negative. *J Biol Chem* 276, 1195-1203.

- Brodeur, S. R., Cheng, G., Baltimore, D., and Thorley-Lawson, D. A. (1997). Localization of the major NF- κ B-activating site and the sole TRAF3 binding site of LMP-1 defines two distinct signaling motifs. *J Biol Chem* 272, 19777-19784.
- Brooks, L., Yao, Q. Y., Rickinson, A. B., and Young, L. S. (1992). Epstein-Barr virus latent gene transcription in nasopharyngeal carcinoma cells: coexpression of EBNA1, LMP1, and LMP2 transcripts. *J Virol* 66, 2689-2697.
- Brousset, P., Drouet, E., Schlaifer, D., Icart, J., Payen, C., Meggetto, F., Marchou, B., Massip, P., and Delsol, G. (1994). Epstein-Barr virus (EBV) replicative gene expression in tumour cells of AIDS-related non-Hodgkin's lymphoma in relation to CD4 cell number and antibody titres to EBV. *Aids* 8, 583-590.
- Brown, K., Buchmann, A., and Balmain, A. (1990). Carcinogen-induced mutations in the mouse c-Ha-ras gene provide evidence of multiple pathways for tumor progression. *Proc Natl Acad Sci U S A* 87, 538-542.
- Brown, K., Strathdee, D., Bryson, S., Lambie, W., and Balmain, A. (1998). The malignant capacity of skin tumours induced by expression of a mutant H-ras transgene depends on the cell type targeted [In Process Citation]. *Curr Biol* 8, 516-524.
- Buday, L., and Downward, J. (1993). Epidermal growth factor regulates p21ras through the formation of a complex of receptor, Grb2 adapter protein, and Sos nucleotide exchange factor. *Cell* 73, 611-620.
- Buell, P. (1974). The effect of migration on the risk of nasopharyngeal cancer among Chinese. *Cancer Res* 34, 1189-1191.
- Burbee, D. G., Forgacs, E., Zochbauer-Muller, S., Shivakumar, L., Fong, K., Gao, B., Randle, D., Kondo, M., Virmani, A., Bader, S., *et al.* (2001). Epigenetic inactivation of RASSF1A in lung and breast cancers and malignant phenotype suppression. *J Natl Cancer Inst* 93, 691-699.
- Burgstahler, R., Kempkes, B., Steube, K., and Lipp, M. (1995). Expression of the chemokine receptor BLR2/EBI1 is specifically transactivated by Epstein-Barr virus nuclear antigen 2. *Biochem Biophys Res Commun* 215, 737-743.
- Caldwell, R. G., Wilson, J. B., Anderson, S. J., and Longnecker, R. (1998). Epstein-Barr virus LMP2A drives B cell development and survival in the absence of normal B cell receptor signals. *Immunity* 9, 405-411.
- Calender, A., Billaud, M., Aubry, J. P., Banchereau, J., Vuillaume, M., and Lenoir, G. M. (1987). Epstein-Barr virus (EBV) induces expression of B-cell activation markers on in vitro infection of EBV-negative B-lymphoma cells. *Proc Natl Acad Sci U S A* 84, 8060-8064.
- Carpenter, G. (1999). Employment of the epidermal growth factor receptor in growth factor-independent signaling pathways. *J Cell Biol* 146, 697-702.

- Carpenter, G., and Cohen, S. (1990). Epidermal growth factor. *J Biol Chem* 265, 7709-7712.
- Chakrabarti, O., Veeraraghavalu, K., Tergaonkar, V., Liu, Y., Androphy, E. J., Stanley, M. A., and Krishna, S. (2004). Human papillomavirus type 16 E6 amino acid 83 variants enhance E6-mediated MAPK signaling and differentially regulate tumorigenesis by notch signaling and oncogenic Ras. *J Virol* 78, 5934-5945.
- Chan, K. S., Carbajal, S., Kiguchi, K., Clifford, J., Sano, S., and DiGiovanni, J. (2004). Epidermal growth factor receptor-mediated activation of Stat3 during multistage skin carcinogenesis. *Cancer Res* 64, 2382-2389.
- Chan, S. Y., and Wong, R. W. (2000). Expression of epidermal growth factor in transgenic mice causes growth retardation. *J Biol Chem* 275, 38693-38698.
- Chang, M. H., Ng, C. K., Lin, Y. J., Liang, C. L., Chung, P. J., Chen, M. L., Tyan, Y. S., Hsu, C. Y., Shu, C. H., and Chang, Y. S. (1997). Identification of a promoter for the latent membrane protein 1 gene of Epstein-Barr virus that is specifically activated in human epithelial cells. *DNA Cell Biol* 16, 829-837.
- Chen, H., Hutt-Fletcher, L., Cao, L., and Hayward, S. D. (2003). A positive autoregulatory loop of LMP1 expression and STAT activation in epithelial cells latently infected with Epstein-Barr virus. *J Virol* 77, 4139-4148.
- Chen, H., Smith, P., Ambinder, R. F., and Hayward, S. D. (1999). Expression of Epstein-Barr virus BamHI-A rightward transcripts in latently infected B cells from peripheral blood. *Blood* 93, 3026-3032.
- Chen, M. L., Hsu, N. C., Liu, S. T., and Chang, Y. S. (1995). Identification of an internal promoter of the latent membrane protein 1 gene of Epstein-Barr virus. *DNA Cell Biol* 14, 205-211.
- Chen, M. L., Tsai, C. N., Liang, C. L., Shu, C. H., Huang, C. R., Sulitzeanu, D., Liu, S. T., and Chang, Y. S. (1992). Cloning and characterization of the latent membrane protein (LMP) of a specific Epstein-Barr virus variant derived from the nasopharyngeal carcinoma in the Taiwanese population. *Oncogene* 7, 2131-2140.
- Chen, N., Nomura, M., She, Q. B., Ma, W. Y., Bode, A. M., Wang, L., Flavell, R. A., and Dong, Z. (2001). Suppression of skin tumorigenesis in c-Jun NH(2)-terminal kinase-2-deficient mice. *Cancer Res* 61, 3908-3912.
- Chomczynski, P., and Sacchi, N. (1987). Single-step method of RNA isolation by acid guanidinium thiocyanate-phenol-chloroform extraction. *Anal Biochem* 162, 156-159.
- Chow LS, L. K., Kwong J, To KF, Tsang KS, Lam CW, Dammann R, Huang DP. (2004). RASSF1A is a target tumor suppressor from 3p21.3 in nasopharyngeal carcinoma. *Int J Cancer* 2004 May 10;109(6):839-47.

- Chow, L. S., Lo, K. W., Kwong, J., Wong, A. Y., and Huang, D. P. (2004). Aberrant methylation of RASSF4/AD037 in nasopharyngeal carcinoma. *Oncol Rep* 12, 781-787.
- Chu, J. S., Chen, C. C., and Chang, K. J. (1998). In situ detection of Epstein-Barr virus in breast cancer. *Cancer Lett* 124, 53-57.
- Chung, P. J., Chang, Y. S., Liang, C. L., and Meng, C. L. (2002). Negative regulation of Epstein-Barr virus latent membrane protein 1-mediated functions by the bone morphogenetic protein receptor IA-binding protein, BRAM1. *J Biol Chem* 277, 39850-39857.
- Clarke, P. A., Schwemmler, M., Schickinger, J., Hilse, K., and Clemens, M. J. (1991). Binding of Epstein-Barr virus small RNA EBER-1 to the double-stranded RNA-activated protein kinase DAI. *Nucleic Acids Res* 19, 243-248.
- Clarke, P. A., Sharp, N. A., and Clemens, M. J. (1992). Expression of genes for the Epstein-Barr virus small RNAs EBER-1 and EBER-2 in Daudi Burkitt's lymphoma cells: effects of interferon treatment. *J Gen Virol* 73 (Pt 12), 3169-3175.
- Cochet, C., Martel-Renoir, D., Grunewald, V., Bosq, J., Cochet, G., Schwaab, G., Bernaudin, J. F., and Joab, I. (1993). Expression of the Epstein-Barr virus immediate early gene, BZLF1, in nasopharyngeal carcinoma tumor cells. *Virology* 197, 358-365.
- Coffin, W. F., 3rd, Erickson, K. D., Hoedt-Miller, M., and Martin, J. M. (2001). The cytoplasmic amino-terminus of the Latent Membrane Protein-1 of Epstein-Barr Virus: relationship between transmembrane orientation and effector functions of the carboxy-terminus and transmembrane domain. *Oncogene* 20, 5313-5330.
- Coffin, W. F., 3rd, Geiger, T. R., and Martin, J. M. (2003). Transmembrane domains 1 and 2 of the latent membrane protein 1 of Epstein-Barr virus contain a lipid raft targeting signal and play a critical role in cytotaxis. *J Virol* 77, 3749-3758.
- Cohen, J. I., and Kieff, E. (1991). An Epstein-Barr virus nuclear protein 2 domain essential for transformation is a direct transcriptional activator. *J Virol* 65, 5880-5885.
- Cohen, J. I., Wang, F., and Kieff, E. (1991). Epstein-Barr virus nuclear protein 2 mutations define essential domains for transformation and transactivation. *J Virol* 65, 2545-2554.
- Cohen, S., Ushiro, H., Stoscheck, C., and Chinkers, M. (1982). A native 170,000 epidermal growth factor receptor-kinase complex from shed plasma membrane vesicles. *J Biol Chem* 257, 1523-1531.
- Cook, P. W., Brown, J. R., Cornell, K. A., and Pittelkow, M. R. (2004). Suprabasal expression of human amphiregulin in the epidermis of transgenic mice induces a severe, early-onset, psoriasis-like skin pathology: expression of amphiregulin in the basal epidermis is also associated with synovitis. *Exp Dermatol* 13, 347-356.

- Cook, P. W., Piepkorn, M., Clegg, C. H., Plowman, G. D., DeMay, J. M., Brown, J. R., and Pittelkow, M. R. (1997). Transgenic expression of the human amphiregulin gene induces a psoriasis-like phenotype. *J Clin Invest* *100*, 2286-2294.
- Cordier, M., Calender, A., Billaud, M., Zimmer, U., Rousselet, G., Pavlish, O., Banchereau, J., Tursz, T., Bornkamm, G., and Lenoir, G. M. (1990). Stable transfection of Epstein-Barr virus (EBV) nuclear antigen 2 in lymphoma cells containing the EBV P3HR1 genome induces expression of B-cell activation molecules CD21 and CD23. *J Virol* *64*, 1002-1013.
- Coutinho, C. M., Bassini, A. S., Gutierrez, L. G., Butugan, O., Kowalski, L. P., Brentani, M. M., and Nagai, M. A. (1999). Genetic alterations in Ki-ras and Ha-ras genes in juvenile nasopharyngeal angiofibromas and head and neck cancer. *Sao Paulo Med J* *117*, 113-120.
- Crook, T., Nicholls, J. M., Brooks, L., O'Nions, J., and Allday, M. J. (2000). High level expression of deltaN-p63: a mechanism for the inactivation of p53 in undifferentiated nasopharyngeal carcinoma (NPC)? *Oncogene* *19*, 3439-3444.
- Curran, J. A., Lavery, F. S., Campbell, D., Macdiarmid, J., and Wilson, J. B. (2001). Epstein-Barr virus encoded latent membrane protein-1 induces epithelial cell proliferation and sensitizes transgenic mice to chemical carcinogenesis. *Cancer Res* *61*, 6730-6738.
- D'Souza, B., Rowe, M., and Walls, D. (2000). The bfl-1 gene is transcriptionally upregulated by the Epstein-Barr virus LMP1, and its expression promotes the survival of a Burkitt's lymphoma cell line. *J Virol* *74*, 6652-6658.
- D'Souza, B. N., Edelstein, L. C., Pegman, P. M., Smith, S. M., Loughran, S. T., Clarke, A., Mehl, A., Rowe, M., Gelinas, C., and Walls, D. (2004). Nuclear factor kappa B-dependent activation of the antiapoptotic bfl-1 gene by the Epstein-Barr virus latent membrane protein 1 and activated CD40 receptor. *J Virol* *78*, 1800-1816.
- Dadmanesh, F., Peterse, J. L., Sapino, A., Fonelli, A., and Eusebi, V. (2001). Lymphoepithelioma-like carcinoma of the breast: lack of evidence of Epstein-Barr virus infection. *Histopathology* *38*, 54-61.
- Dajee, M., Tarutani, M., Deng, H., Cai, T., and Khavari, P. A. (2002). Epidermal Ras blockade demonstrates spatially localized Ras promotion of proliferation and inhibition of differentiation. *Oncogene* *21*, 1527-1538.
- Dambaugh, T., Hennessy, K., Chamnankit, L., and Kieff, E. (1984). U2 region of Epstein-Barr virus DNA may encode Epstein-Barr nuclear antigen 2. *Proc Natl Acad Sci U S A* *81*, 7632-7636.
- Dammann, R., Li, C., Yoon, J. H., Chin, P. L., Bates, S., and Pfeifer, G. P. (2000). Epigenetic inactivation of a RAS association domain family protein from the lung tumour suppressor locus 3p21.3. *Nat Genet* *25*, 315-319.

- Dammann, R., Schagdarsurengin, U., Liu, L., Otto, N., Gimm, O., Dralle, H., Boehm, B. O., Pfeifer, G. P., and Hoang-Vu, C. (2003). Frequent RASSF1A promoter hypermethylation and K-ras mutations in pancreatic carcinoma. *Oncogene* 22, 3806-3812.
- Dawson, C. W., Eliopoulos, A. G., Blake, S. M., Barker, R., and Young, L. S. (2000). Identification of functional differences between prototype Epstein-Barr virus-encoded LMP1 and a nasopharyngeal carcinoma-derived LMP1 in human epithelial cells. *Virology* 272, 204-217.
- Dawson, C. W., Rickinson, A. B., and Young, L. S. (1990). Epstein-Barr virus latent membrane protein inhibits human epithelial cell differentiation. *Nature* 344, 777-780.
- Dawson, C. W., Tramontanis, G., Eliopoulos, A. G., and Young, L. S. (2003). Epstein-Barr Virus Latent Membrane Protein 1 (LMP1) Activates the Phosphatidylinositol 3-Kinase/Akt Pathway to Promote Cell Survival and Induce Actin Filament Remodeling. *J Biol Chem* 278, 3694-3704.
- de Rooij, J., and Bos, J. L. (1997). Minimal Ras-binding domain of Raf1 can be used as an activation-specific probe for Ras. *Oncogene* 14, 623-625.
- de Stanchina, E., McCurrach, M. E., Zindy, F., Shieh, S. Y., Ferbeyre, G., Samuelson, A. V., Prives, C., Roussel, M. F., Sherr, C. J., and Lowe, S. W. (1998). E1A signaling to p53 involves the p19(ARF) tumor suppressor. *Genes Dev* 12, 2434-2442.
- de-The, G., Geser, A., Day, N. E., Tukei, P. M., Williams, E. H., Beri, D. P., Smith, P. G., Dean, A. G., Bronkamm, G. W., Feorino, P., and Henle, W. (1978). Epidemiological evidence for causal relationship between Epstein-Barr virus and Burkitt's lymphoma from Ugandan prospective study. *Nature* 274, 756-761.
- Deacon, E. M., Pallesen, G., Niedobitek, G., Crocker, J., Brooks, L., Rickinson, A. B., and Young, L. S. (1993). Epstein-Barr virus and Hodgkin's disease: transcriptional analysis of virus latency in the malignant cells. *J Exp Med* 177, 339-349.
- Decaussin, G., Sbih-Lammali, F., de Turenne-Tessier, M., Bouguermouh, A., and Ooka, T. (2000). Expression of BARF1 gene encoded by Epstein-Barr virus in nasopharyngeal carcinoma biopsies. *Cancer Res* 60, 5584-5588.
- Derynck, R. (1988). Transforming growth factor alpha. *Cell* 54, 593-595.
- Derynck, R. (1992). The physiology of transforming growth factor-alpha. *Adv Cancer Res* 58, 27-52.
- Devergne, O., Birkenbach, M., and Kieff, E. (1997). Epstein-Barr virus-induced gene 3 and the p35 subunit of interleukin 12 form a novel heterodimeric hematopoietin. *Proc Natl Acad Sci U S A* 94, 12041-12046.

Devergne, O., Hatzivassiliou, E., Izumi, K. M., Kaye, K. M., Kleijnen, M. F., Kieff, E., and Mosialos, G. (1996). Association of TRAF1, TRAF2, and TRAF3 with an Epstein-Barr virus LMP1 domain important for B-lymphocyte transformation: role in NF- κ B activation. *Mol Cell Biol* 16, 7098-7108.

Devergne, O., McFarland, E. C., Mosialos, G., Izumi, K. M., Ware, C. F., and Kieff, E. (1998). Role of the TRAF binding site and NF- κ B activation in Epstein-Barr virus latent membrane protein 1-induced cell gene expression. *J Virol* 72, 7900-7908.

DiGiovanni, J., Walker, S. C., Beltran, L., Naito, M., and Eastin, W. C., Jr. (1991). Evidence for a common genetic pathway controlling susceptibility to mouse skin tumor promotion by diverse classes of promoting agents. *Cancer Res* 51, 1398-1405.

Dimri, G. P., Itahana, K., Acosta, M., and Campisi, J. (2000). Regulation of a senescence checkpoint response by the E2F1 transcription factor and p14(ARF) tumor suppressor. *Mol Cell Biol* 20, 273-285.

Dipple, A., Pigott, M. A., Bigger, C. A., and Blake, D. M. (1984). 7,12-dimethylbenz[a]anthracene--DNA binding in mouse skin: response of different mouse strains and effects of various modifiers of carcinogenesis. *Carcinogenesis* 5, 1087-1090.

Dlugosz, A. A., Cheng, C., Williams, E. K., Darwiche, N., Dempsey, P. J., Mann, B., Dunn, A. R., Coffey, R. J., Jr., and Yuspa, S. H. (1995). Autocrine transforming growth factor alpha is dispensible for v-rasHa-induced epidermal neoplasia: potential involvement of alternate epidermal growth factor receptor ligands. *Cancer Res* 55, 1883-1893.

Dolcetti, R., and Boiocchi, M. (1998). Epstein-Barr virus in the pathogenesis of Hodgkin's disease. *Biomed Pharmacother* 52, 13-25.

Dominey, A. M., Wang, X. J., King, L. E., Jr., Nanney, L. B., Gagne, T. A., Sellheyer, K., Bundman, D. S., Longley, M. A., Rothnagel, J. A., Greenhalgh, D. A., and et al. (1993). Targeted overexpression of transforming growth factor- α in the epidermis of transgenic mice elicits hyperplasia, hyperkeratosis, and spontaneous, squamous papillomas. *Cell Growth Differ* 4, 1071-1082.

Downward, J. (2003). Targeting RAS signalling pathways in cancer therapy. *Nat Rev Cancer* 3, 11-22.

Effert, P., McCoy, R., Abdel-Hamid, M., Flynn, K., Zhang, Q., Busson, P., Tursz, T., Liu, E., and Raab-Traub, N. (1992). Alterations of the p53 gene in nasopharyngeal carcinoma. *J Virol* 66, 3768-3775.

Eliopoulos, A. G., Gallagher, N. J., Blake, S. M., Dawson, C. W., and Young, L. S. (1999). Activation of the p38 mitogen-activated protein kinase pathway by Epstein-Barr virus-encoded latent membrane protein 1 coregulates interleukin-6 and interleukin-8 production. *J Biol Chem* 274, 16085-16096.

- Eliopoulos, A. G., and Young, L. S. (1998). Activation of the cJun N-terminal kinase (JNK) pathway by the Epstein-Barr virus-encoded latent membrane protein 1 (LMP1). *Oncogene* 16, 1731-1742.
- Erwin, C. R., Helmrath, M. A., Shin, C. E., Falcone, R. A., Jr., Stern, L. E., and Warner, B. W. (1999). Intestinal overexpression of EGF in transgenic mice enhances adaptation after small bowel resection. *Am J Physiol* 277, G533-540.
- Esteban, L. M., Vicario-Abejon, C., Fernandez-Salguero, P., Fernandez-Medarde, A., Swaminathan, N., Yienger, K., Lopez, E., Malumbres, M., McKay, R., Ward, J. M., *et al.* (2001). Targeted genomic disruption of H-ras and N-ras, individually or in combination, reveals the dispensability of both loci for mouse growth and development. *Mol Cell Biol* 21, 1444-1452.
- Everly, D. N., Jr., Mainou, B. A., and Raab-Traub, N. (2004). Induction of Id1 and Id3 by Latent Membrane Protein 1 of Epstein-Barr Virus and Regulation of p27/Kip and Cyclin-Dependent Kinase 2 in Rodent Fibroblast Transformation. *J Virol* 78, 13470-13478.
- Fåhraeus, R., Rymo, L., Rhim, J. S., and Klein, G. (1990). Morphological transformation of human keratinocytes expressing the LMP gene of Epstein-Barr virus. *Nature* 345, 447-449.
- Faulkner, G. C., Burrows, S. R., Khanna, R., Moss, D. J., Bird, A. G., and Crawford, D. H. (1999). X-Linked agammaglobulinemia patients are not infected with Epstein-Barr virus: implications for the biology of the virus. *J Virol* 73, 1555-1564.
- Feig, L. A., and Buchsbaum, R. J. (2002). Cell signaling: life or death decisions of ras proteins. *Curr Biol* 12, R259-261.
- Fennewald, S., van Santen, V., and Kieff, E. (1984). Nucleotide sequence of an mRNA transcribed in latent growth-transforming virus infection indicates that it may encode a membrane protein. *J Virol* 51, 411-419.
- Fenton, S. L., Dallol, A., Agathangelou, A., Hesson, L., Ahmed-Choudhury, J., Baksh, S., Sardet, C., Dammann, R., Minna, J. D., Downward, J., *et al.* (2004). Identification of the E1A-regulated transcription factor p120 E4F as an interacting partner of the RASSF1A candidate tumor suppressor gene. *Cancer Res* 64, 102-107.
- Fielding, C. A., Sandvej, K., Mehl, A., Brennan, P., Jones, M., and Rowe, M. (2001). Epstein-Barr virus LMP-1 natural sequence variants differ in their potential to activate cellular signaling pathways. *J Virol* 75, 9129-9141.
- Fingerroth, J. D., Diamond, M. E., Sage, D. R., Hayman, J., and Yates, J. L. (1999). CD21-Dependent infection of an epithelial cell line, 293, by Epstein-Barr virus. *J Virol* 73, 2115-2125.

- Floettmann, J. E., and Rowe, M. (1997). Epstein-Barr virus latent membrane protein-1 (LMP1) C-terminus activation region 2 (CTAR2) maps to the far C-terminus and requires oligomerisation for NF- κ B activation. *Oncogene* 15, 1851-1858.
- Fries, K. L., Miller, W. E., and Raab-Traub, N. (1996). Epstein-Barr virus latent membrane protein 1 blocks p53-mediated apoptosis through the induction of the A20 gene. *J Virol* 70, 8653-8659.
- Fries, K. L., Miller, W. E., and Raab-Traub, N. (1999). The A20 protein interacts with the Epstein-Barr virus latent membrane protein 1 (LMP1) and alters the LMP1/TRAF1/TRADD complex. *Virology* 264, 159-166.
- Fries, K. L., Sculley, T. B., Webster-Cyriaque, J., Rajadurai, P., Sadler, R. H., and Raab-Traub, N. (1997). Identification of a novel protein encoded by the BamHI A region of the Epstein-Barr virus. *J Virol* 71, 2765-2771.
- Fruehling, S., and Longnecker, R. (1997). The immunoreceptor tyrosine-based activation motif of Epstein-Barr virus LMP2A is essential for blocking BCR-mediated signal transduction. *Virology* 235, 241-251.
- Fruehling, S., Swart, R., Dolwick, K. M., Kremmer, E., and Longnecker, R. (1998). Tyrosine 112 of latent membrane protein 2A is essential for protein tyrosine kinase loading and regulation of Epstein-Barr virus latency. *J Virol* 72, 7796-7806.
- Fuchs, E. (1995). Keratins and the skin. *Annu Rev Cell Dev Biol* 11, 123-153.
- Fuchs, E., and Byrne, C. (1994). The epidermis: rising to the surface. *Curr Opin Genet Dev* 4, 725-736.
- Fuchs, E., and Raghavan, S. (2002). Getting under the skin of epidermal morphogenesis. *Nat Rev Genet* 3, 199-209.
- Fukayama, M., Hayashi, Y., Iwasaki, Y., Chong, J., Ooba, T., Takizawa, T., Koike, M., Mizutani, S., Miyaki, M., and Hirai, K. (1994). Epstein-Barr virus-associated gastric carcinoma and Epstein-Barr virus infection of the stomach. *Lab Invest* 71, 73-81.
- Fukuda, M., Kurosaki, W., Yanagihara, K., Kuratsune, H., and Sairenji, T. (2002). A mechanism in Epstein-Barr virus oncogenesis: inhibition of transforming growth factor-beta 1-mediated induction of MAPK/p21 by LMP1. *Virology* 302, 310-320.
- Fukuda, M., and Longnecker, R. (2004). Latent membrane protein 2A inhibits transforming growth factor-beta 1-induced apoptosis through the phosphatidylinositol 3-kinase/Akt pathway. *J Virol* 78, 1697-1705.
- Galetic, I., Maira, S. M., Andjelkovic, M., and Hemmings, B. A. (2003). Negative regulation of ERK and Elk by protein kinase B modulates c-Fos transcription. *J Biol Chem* 278, 4416-4423.

- Gee, J. M., and Knowlden, J. M. (2003). ADAM metalloproteases and EGFR signalling. *Breast Cancer Res* 5, 223-224.
- Getchell, T. V., Narla, R. K., Little, S., Hyde, J. F., and Getchell, M. L. (2000). Horizontal basal cell proliferation in the olfactory epithelium of transforming growth factor-alpha transgenic mice. *Cell Tissue Res* 299, 185-192.
- Gilligan, K. J., Rajadurai, P., Lin, J. C., Busson, P., Abdel-Hamid, M., Prasad, U., Tursz, T., and Raab-Traub, N. (1991). Expression of the Epstein-Barr virus BamHI A fragment in nasopharyngeal carcinoma: evidence for a viral protein expressed in vivo. *J Virol* 65, 6252-6259.
- Gires, O., Kohlhuber, F., Kilger, E., Baumann, M., Kieser, A., Kaiser, C., Zeidler, R., Scheffer, B., Ueffing, M., and Hammerschmidt, W. (1999). Latent membrane protein 1 of Epstein-Barr virus interacts with JAK3 and activates STAT proteins. *EMBO J* 18, 3064-3073.
- Gires, O., Zimmer-Strobl, U., Gonnella, R., Ueffing, M., Marschall, G., Zeidler, R., Pich, D., and Hammerschmidt, W. (1997). Latent membrane protein 1 of Epstein-Barr virus mimics a constitutively active receptor molecule. *EMBO J* 16, 6131-6140.
- Glaser, S. L., Ambinder, R. F., DiGiuseppe, J. A., Horn-Ross, P. L., and Hsu, J. L. (1998). Absence of Epstein-Barr virus EBER-1 transcripts in an epidemiologically diverse group of breast cancers. *Int J Cancer* 75, 555-558.
- Glickman, J. N., Howe, J. G., and Steitz, J. A. (1988). Structural analyses of EBER1 and EBER2 ribonucleoprotein particles present in Epstein-Barr virus-infected cells. *J Virol* 62, 902-911.
- Goldsmith, K., Bendell, L., and Frappier, L. (1993). Identification of EBNA1 amino acid sequences required for the interaction of the functional elements of the Epstein-Barr virus latent origin of DNA replication. *J Virol* 67, 3418-3426.
- Greenhalgh, D. A., Rothnagel, J. A., Quintanilla, M. I., Orengo, C. C., Gagne, T. A., Bundman, D. S., Longley, M. A., and Roop, D. R. (1993a). Induction of epidermal hyperplasia, hyperkeratosis, and papillomas in transgenic mice by a targeted v-Ha-ras oncogene. *Mol Carcinog* 7, 99-110.
- Greenhalgh, D. A., Rothnagel, J. A., Wang, X. J., Quintanilla, M. I., Orengo, C. C., Gagne, T. A., Bundman, D. S., Longley, M. A., Fisher, C., and Roop, D. R. (1993b). Hyperplasia, hyperkeratosis and benign tumor production in transgenic mice by a targeted v-fos oncogene suggest a role for fos in epidermal differentiation and neoplasia. *Oncogene* 8, 2145-2157.
- Greifenegger, N., Jager, M., Kunz-Schughart, L. A., Wolf, H., and Schwarzmann, F. (1998). Epstein-Barr virus small RNA (EBER) genes: differential regulation during lytic viral replication. *J Virol* 72, 9323-9328.

Gupta K, K. S., Li W, Gui L, Ramakrishnan S, Gupta P, Law PY, Hebbel RP. (1999). VEGF prevents apoptosis of human microvascular endothelial cells via opposing effects on MAPK/ERK and SAPK/JNK signaling. *Exp Cell Res* 247, 495-504.

Gutierrez, M. I., Bhatia, K., Barriga, F., Diez, B., Muriel, F. S., de Andreas, M. L., Epelman, S., Risueno, C., and Magrath, I. T. (1992). Molecular epidemiology of Burkitt's lymphoma from South America: differences in breakpoint location and Epstein-Barr virus association from tumors in other world regions. *Blood* 79, 3261-3266.

Hammerschmidt, W., and Sugden, B. (1989). Genetic analysis of immortalizing functions of Epstein-Barr virus in human B lymphocytes. *Nature* 340, 393-397.

Hammerschmidt, W., Sugden, B., and Baichwal, V. R. (1989). The transforming domain alone of the latent membrane protein of Epstein-Barr virus is toxic to cells when expressed at high levels. *J Virol* 63, 2469-2475.

Han, I., Harada, S., Weaver, D., Xue, Y., Lane, W., Orstavik, S., Skalhegg, B., and Kieff, E. (2001). EBNA-LP associates with cellular proteins including DNA-PK and HA95. *J Virol* 75, 2475-2481.

Harada, S., and Kieff, E. (1997). Epstein-Barr virus nuclear protein LP stimulates EBNA-2 acidic domain-mediated transcriptional activation. *J Virol* 71, 6611-6618.

Hardie, W. D., Kerlakian, C. B., Bruno, M. D., Huelsman, K. M., Wert, S. E., Glasser, S. W., Whitsett, J. A., and Korfhagen, T. R. (1996). Reversal of lung lesions in transgenic transforming growth factor alpha mice by expression of mutant epidermal growth factor receptor. *Am J Respir Cell Mol Biol* 15, 499-508.

Hatfull, G., Bankier, A. T., Barrell, B. G., and Farrell, P. J. (1988). Sequence analysis of Raji Epstein-Barr virus DNA. *Virology* 164, 334-340.

Hatzivassiliou, E., Miller, W. E., Raab-Traub, N., Kieff, E., and Mosialos, G. (1998). A fusion of the EBV latent membrane protein-1 (LMP1) transmembrane domains to the CD40 cytoplasmic domain is similar to LMP1 in constitutive activation of epidermal growth factor receptor expression, NF- κ B, and stress-activated protein kinase. *J Immunol* 160, 1116-1121.

Hayes, M. J., Koundouris, A., Gruis, N., Bergman, W., Peters, G. G., and Sinclair, A. J. (2004). p16(INK4A)-independence of Epstein-Barr virus-induced cell proliferation and virus latency. *J Gen Virol* 85, 1381-1386.

Hearing, J. C., and Levine, A. J. (1985). The Epstein-Barr virus nuclear antigen (BamHI K antigen) is a single-stranded DNA binding phosphoprotein. *Virology* 145, 105-116.

Henderson, S., Rowe, M., Gregory, C., Croom-Carter, D., Wang, F., Longnecker, R., Kieff, E., and Rickinson, A. (1991). Induction of bcl-2 expression by Epstein-Barr virus latent membrane protein 1 protects infected B cells from programmed cell death. *Cell* 65, 1107-1115.

- Henle, G., and Henle, W. (1967). Immunofluorescence, interference, and complement fixation techniques in the detection of the herpes-type virus in Burkitt tumor cell lines. *Cancer Res* 27, 2442-2446.
- Hennessy, K., Fennewald, S., Hummel, M., Cole, T., and Kieff, E. (1984). A membrane protein encoded by Epstein-Barr virus in latent growth-transforming infection. *Proc Natl Acad Sci U S A* 81, 7207-7211.
- Hennings, H., Glick, A. B., Lowry, D. T., Krsmanovic, L. S., Sly, L. M., and Yuspa, S. H. (1993). FVB/N mice: an inbred strain sensitive to the chemical induction of squamous cell carcinomas in the skin. *Carcinogenesis* 14, 2353-2358.
- Herrmann, K., and Niedobitek, G. (2003). Lack of evidence for an association of Epstein-Barr virus infection with breast carcinoma. *Breast Cancer Res* 5, R13-17.
- Hesson, L., Bieche, I., Krex, D., Criniere, E., Hoang-Xuan, K., Maher, E. R., and Latif, F. (2004). Frequent epigenetic inactivation of RASSF1A and BLU genes located within the critical 3p21.3 region in gliomas. *Oncogene* 23, 2408-2419.
- Hesson, L., Dallol, A., Minna, J. D., Maher, E. R., and Latif, F. (2003). NORE1A, a homologue of RASSF1A tumour suppressor gene is inactivated in human cancers. *Oncogene* 22, 947-954.
- Heussinger, N., Buttner, M., Ott, G., Brachtel, E., Pilch, B. Z., Kremmer, E., and Niedobitek, G. (2004). Expression of the Epstein-Barr virus (EBV)-encoded latent membrane protein 2A (LMP2A) in EBV-associated nasopharyngeal carcinoma. *J Pathol* 203, 696-699.
- Hildesheim, A., Anderson, L. M., Chen, C. J., Cheng, Y. J., Brinton, L. A., Daly, A. K., Reed, C. D., Chen, I. H., Caporaso, N. E., Hsu, M. M., *et al.* (1997). CYP2E1 genetic polymorphisms and risk of nasopharyngeal carcinoma in Taiwan. *J Natl Cancer Inst* 89, 1207-1212.
- Hildesheim, A., and Levine, P. H. (1993). Etiology of nasopharyngeal carcinoma: a review. *Epidemiol Rev* 15, 466-485.
- Hill, M. M., Feng, J., and Hemmings, B. A. (2002). Identification of a plasma membrane Raft-associated PKB Ser473 kinase activity that is distinct from ILK and PDK1. *Curr Biol* 12, 1251-1255.
- Hitt, M. M., Allday, M. J., Hara, T., Karran, L., Jones, M. D., Busson, P., Tursz, T., Ernberg, I., and Griffin, B. E. (1989). EBV gene expression in an NPC-related tumour. *EMBO J* 8, 2639-2651.
- Hobbs, R. M., Silva-Vargas, V., Groves, R., and Watt, F. M. (2004). Expression of activated MEK1 in differentiating epidermal cells is sufficient to generate hyperproliferative and inflammatory skin lesions. *J Invest Dermatol* 123, 503-515.

- Hopwood, P., and Crawford, D. H. (2000). The role of EBV in post-transplant malignancies: a review. *J Clin Pathol* 53, 248-254.
- Hording, U., Nielsen, H. W., Albeck, H., and Daugaard, S. (1993). Nasopharyngeal carcinoma: histopathological types and association with Epstein-Barr Virus. *Eur J Cancer B Oral Oncol* 29B, 137-139.
- Horiguchi, K., Tomizawa, Y., Tosaka, M., Ishiuchi, S., Kurihara, H., Mori, M., and Saito, N. (2003). Epigenetic inactivation of RASSF1A candidate tumor suppressor gene at 3p21.3 in brain tumors. *Oncogene* 22, 7862-7865.
- Horikawa, T., Sheen, T. S., Takeshita, H., Sato, H., Furukawa, M., and Yoshizaki, T. (2001). Induction of c-Met proto-oncogene by Epstein-Barr virus latent membrane protein-1 and the correlation with cervical lymph node metastasis of nasopharyngeal carcinoma. *Am J Pathol* 159, 27-33.
- Horiuchi, K., Mishima, K., Ohsawa, M., and Aozasa, K. (1994). Carcinoma of stomach and breast with lymphoid stroma: localisation of Epstein-Barr virus. *J Clin Pathol* 47, 538-540.
- Hsu, J. L., and Glaser, S. L. (2000). Epstein-barr virus-associated malignancies: epidemiologic patterns and etiologic implications. *Crit Rev Oncol Hematol* 34, 27-53.
- Hu, L., Troyanovsky, B., Zhang, X., Trivedi, P., Ernberg, I., and Klein, G. (2000). Differences in the immunogenicity of latent membrane protein 1 (LMP1) encoded by Epstein-Barr virus genomes derived from LMP1-positive and -negative nasopharyngeal carcinoma. *Cancer Res* 60, 5589-5593.
- Hu, L.-F. (1991). Isolation and Sequencing of the Epstein-Barr virus BNLF-1 gene (LMP1) from a Chinese nasopharyngeal carcinoma. *Journal of General Virology* 72, 2399-2409.
- Hu, L. F., Chen, F., Zhen, Q. F., Zhang, Y. W., Luo, Y., Zheng, X., Winberg, G., Ernberg, I., and Klein, G. (1995). Differences in the growth pattern and clinical course of EBV-LMP1 expressing and non-expressing nasopharyngeal carcinomas. *Eur J Cancer* 5, 658-660.
- Hu, L. F., Li, X. L., Jiang, J. Q., Yao, J., Yu, Y., Cao, S. L., Huang, K. M., Shen, D. T., Wang, L. P., and Gu, J. R. (1986). Transforming activity of human nasopharyngeal carcinoma DNA. *J Cell Physiol Suppl* 4, 21-26.
- Huang, D. P., Ho, J. H., Saw, D., and Teoh, T. B. (1978). Carcinoma of the nasal and paranasal regions in rats fed Cantonese salted marine fish. *IARC Sci Publ*, 315-328.
- Hudson, G. S., Farrell, P. J., and Barrell, B. G. (1985). Two related but differentially expressed potential membrane proteins encoded by the EcoRI Dhet region of Epstein-Barr virus B95-8. *J Virol* 53, 528-535.

- Huen, D. S., Fox, A., Kumar, P., and Searle, P. F. (1993). Dilated heart failure in transgenic mice expressing the Epstein-Barr virus nuclear antigen-leader protein. *J Gen Virol* 74 (Pt 7), 1381-1391.
- Huen, D. S., Henderson, S. A., Croom-Carter, D., and Rowe, M. (1995). The Epstein-Barr virus latent membrane protein-1 (LMP1) mediates activation of NF- κ B and cell surface phenotype via two effector regions in its carboxy-terminal cytoplasmic domain. *Oncogene* 10, 549-560.
- Humme, S., Reisbach, G., Feederle, R., Delecluse, H. J., Bousset, K., Hammerschmidt, W., and Schepers, A. (2003). The EBV nuclear antigen 1 (EBNA1) enhances B cell immortalization several thousandfold. *Proc Natl Acad Sci U S A* 100, 10989-10994.
- Imai, S., Nishikawa, J., and Takada, K. (1998). Cell-to-cell contact as an efficient mode of Epstein-Barr virus infection of diverse human epithelial cells. *J Virol* 72, 4371-4378.
- Ise, K., Nakamura, K., Nakao, K., Shimizu, S., Harada, H., Ichise, T., Miyoshi, J., Gondo, Y., Ishikawa, T., Aiba, A., and Katsuki, M. (2000). Targeted deletion of the H-ras gene decreases tumor formation in mouse skin carcinogenesis. *Oncogene* 19, 2951-2956.
- Izumi, K. M., Kaye, K. M., and Kieff, E. D. (1994). Epstein-Barr virus recombinant molecular genetic analysis of the LMP1 amino-terminal cytoplasmic domain reveals a probable structural role, with no component essential for primary B-lymphocyte growth transformation. *J Virol* 68, 4369-4376.
- Izumi, K. M., Kaye, K. M., and Kieff, E. D. (1997). The Epstein-Barr virus LMP1 amino acid sequence that engages tumor necrosis factor receptor associated factors is critical for primary B lymphocyte growth transformation. *Proc Natl Acad Sci U S A* 94, 1447-1452.
- Izumi, K. M., and Kieff, E. D. (1997). The Epstein-Barr virus oncogene product latent membrane protein 1 engages the tumor necrosis factor receptor-associated death domain protein to mediate B lymphocyte growth transformation and activate NF- κ B. *Proc Natl Acad Sci U S A* 94, 12592-12597.
- Izumi, K. M., McFarland, E. C., Ting, A. T., Riley, E. A., Seed, B., and Kieff, E. D. (1999). The Epstein-Barr virus oncoprotein latent membrane protein 1 engages the tumor necrosis factor receptor-associated proteins TRADD and receptor-interacting protein (RIP) but does not induce apoptosis or require RIP for NF- κ B activation. *Mol Cell Biol* 19, 5759-5767.
- Jankelevich, S., Kolman, J. L., Bodnar, J. W., and Miller, G. (1992). A nuclear matrix attachment region organizes the Epstein-Barr viral plasmid in Raji cells into a single DNA domain. *Embo J* 11, 1165-1176.
- Jayasurya, A., Bay, B. H., Yap, W. M., and Tan, N. G. (2000). Correlation of metallothionein expression with apoptosis in nasopharyngeal carcinoma. *Br J Cancer* 82, 1198-1203.

- Jiang, W. Q., Szekely, L., Wendel-Hansen, V., Ringertz, N., Klein, G., and Rosen, A. (1991). Co-localization of the retinoblastoma protein and the Epstein-Barr virus-encoded nuclear antigen EBNA-5. *Exp Cell Res* 197, 314-318.
- Jochner, N., Eick, D., Zimmer-Strobl, U., Pawlita, M., Bornkamm, G. W., and Kempkes, B. (1996). Epstein-Barr virus nuclear antigen 2 is a transcriptional suppressor of the immunoglobulin mu gene: implications for the expression of the translocated c-myc gene in Burkitt's lymphoma cells. *Embo J* 15, 375-382.
- Johannsen, E., Miller, C. L., Grossman, S. R., and Kieff, E. (1996). EBNA-2 and EBNA-3C extensively and mutually exclusively associate with RBPJK in Epstein-Barr virus-transformed B lymphocytes. *J Virol* 70, 4179-4183.
- Johnson, L., Greenbaum, D., Cichowski, K., Mercer, K., Murphy, E., Schmitt, E., Bronson, R. T., Umanoff, H., Edelmann, W., Kucherlapati, R., and Jacks, T. (1997). K-ras is an essential gene in the mouse with partial functional overlap with N-ras. *Genes Dev* 11, 2468-2481.
- Johnson, R. J., Stack, M., Hazlewood, S. A., Jones, M., Blackmore, C. G., Hu, L. F., and Rowe, M. (1998). The 30-base-pair deletion in Chinese variants of the Epstein-Barr virus LMP1 gene is not the major effector of functional differences between variant LMP1 genes in human lymphocytes. *J Virol* 72, 4038-4048.
- Jones, E. H., Biggar, R. J., Nkrumah, F. K., and Lawler, S. D. (1985). HLA-DR7 association with African Burkitt's lymphoma. *Hum Immunol* 13, 211-217.
- Joneson, T., and Bar-Sagi, D. (1999). Suppression of Ras-induced apoptosis by the Rac GTPase. *Mol Cell Biol* 19, 5892-5901.
- Joseph, A. M., Babcock, G. J., and Thorley-Lawson, D. A. (2000). Cells expressing the Epstein-Barr virus growth program are present in and restricted to the naive B-cell subset of healthy tonsils. *J Virol* 74, 9964-9971.
- Kaiser, C., Laux, G., Eick, D., Jochner, N., Bornkamm, G. W., and Kempkes, B. (1999). The proto-oncogene c-myc is a direct target gene of Epstein-Barr virus nuclear antigen 2. *J Virol* 73, 4481-4484.
- Kamijo, T., Weber, J. D., Zambetti, G., Zindy, F., Roussel, M. F., and Sherr, C. J. (1998). Functional and physical interactions of the ARF tumor suppressor with p53 and Mdm2. *Proc Natl Acad Sci U S A* 95, 8292-8297.
- Kamijo, T., Zindy, F., Roussel, M. F., Quelle, D. E., Downing, J. R., Ashmun, R. A., Grosveld, G., and Sherr, C. J. (1997). Tumor suppression at the mouse INK4a locus mediated by the alternative reading frame product p19ARF. *Cell* 91, 649-659.
- Kapoor, P., and Frappier, L. (2003). EBNA1 partitions Epstein-Barr virus plasmids in yeast cells by attaching to human EBNA1-binding protein 2 on mitotic chromosomes. *J Virol* 77, 6946-6956.

Katze, M. G., Wambach, M., Wong, M. L., Garfinkel, M., Meurs, E., Chong, K., Williams, B. R., Hovanessian, A. G., and Barber, G. N. (1991). Functional expression and RNA binding analysis of the interferon-induced, double-stranded RNA-activated, 68,000-Mr protein kinase in a cell-free system. *Mol Cell Biol* *11*, 5497-5505.

Kawanishi, M. (2000). The Epstein-Barr virus latent membrane protein 1 (LMP1) enhances TNF alpha-induced apoptosis of intestine 407 epithelial cells: the role of LMP1 C-terminal activation regions 1 and 2. *Virology* *270*, 258-266.

Kaye, K. M., Devergne, O., Harada, J. N., Izumi, K. M., Yalamanchili, R., Kieff, E., and Mosialos, G. (1996). Tumor necrosis factor receptor associated factor 2 is a mediator of NF- κ B activation by latent infection membrane protein 1, the Epstein-Barr virus transforming protein. *Proc Natl Acad Sci U S A* *93*, 11085-11090.

Kaye, K. M., Izumi, K. M., and Kieff, E. (1993). Epstein-Barr virus latent membrane protein 1 is essential for B-lymphocyte growth transformation. *Proc Natl Acad Sci U S A* *90*, 9150-9154.

Kaye, K. M., Izumi, K. M., Mosialos, G., and Kieff, E. (1995). The Epstein-Barr virus LMP1 cytoplasmic carboxy terminus is essential for B-lymphocyte transformation; fibroblast cocultivation complements a critical function within the terminal 155 residues. *J Virol* *69*, 675-683.

Kaykas, A., and Sugden, B. (2000). The amino-terminus and membrane-spanning domains of LMP-1 inhibit cell proliferation. *Oncogene* *19*, 1400-1410.

Kaykas, A., Worringer, K., and Sugden, B. (2001). CD40 and LMP-1 both signal from lipid rafts but LMP-1 assembles a distinct, more efficient signaling complex. *Embo J* *20*, 2641-2654.

Kempkes, B., Spitkovsky, D., Jansen-Durr, P., Ellwart, J. W., Kremmer, E., Delecluse, H. J., Rottenberger, C., Bornkamm, G. W., and Hammerschmidt, W. (1995). B-cell proliferation and induction of early G1-regulating proteins by Epstein-Barr virus mutants conditional for EBNA2. *EMBO J* *14*, 88-96.

Kennedy, G., Komano, J., and Sugden, B. (2003). Epstein-Barr virus provides a survival factor to Burkitt's lymphomas. *Proc Natl Acad Sci U S A* *100*, 14269-14274.

Khan, G., Coates, P. J., Kangro, H. O., and Slavin, G. (1992). Epstein Barr virus (EBV) encoded small RNAs: targets for detection by in situ hybridisation with oligonucleotide probes. *J Clin Pathol* *45*, 616-620.

Khanna, R., and Burrows, S. R. (2000). Role of cytotoxic T lymphocytes in Epstein-Barr virus-associated diseases. *Annu Rev Microbiol* *54*, 19-48.

- Khokhlatchev, A., Rabizadeh, S., Xavier, R., Nedwidek, M., Chen, T., Zhang, X. F., Seed, B., and Avruch, J. (2002). Identification of a novel Ras-regulated proapoptotic pathway. *Curr Biol* 12, 253-265.
- Kieser, A., Kilger, E., Gires, O., Ueffing, M., Kolch, W., and Hammerschmidt, W. (1997). Epstein-Barr virus latent membrane protein-1 triggers AP-1 activity via the c-Jun N-terminal kinase cascade. *EMBO J* 16, 6478-6485.
- Kilger, E., Kieser, A., Baumann, M., and Hammerschmidt, W. (1998). Epstein-Barr virus-mediated B-cell proliferation is dependent upon latent membrane protein 1, which simulates an activated CD40 receptor. *EMBO J* 17, 1700-1709.
- Kloth, M. T., Laughlin, K. K., Biscardi, J. S., Boerner, J. L., Parsons, S. J., and Silva, C. M. (2003). STAT5b, a Mediator of Synergism between c-Src and the Epidermal Growth Factor Receptor. *J Biol Chem* 278, 1671-1679.
- Knecht, H., Bachmann, E., Brousset, P., Rothenberger, S., Einsele, H., Lestou, V. S., Delsol, G., Bachmann, F., Ambros, P. F., and Odermatt, B. F. (1995). Mutational hot spots within the carboxy terminal region of the LMP1 oncogene of Epstein-Barr virus are frequent in lymphoproliferative disorders. *Oncogene* 10, 523-528.
- Knight, J. S., and Robertson, E. S. (2004). Epstein-Barr virus nuclear antigen 3C regulates cyclin A/p27 complexes and enhances cyclin A-dependent kinase activity. *J Virol* 78, 1981-1991.
- Knox, P. G., and Young, L. S. (1995). Epstein-Barr virus infection of CR2-transfected epithelial cells reveals the presence of MHC class II on the virion. *Virology* 213, 147-157.
- Knutson, J. C. (1990). The level of c-fgr RNA is increased by EBNA-2, an Epstein-Barr virus gene required for B-cell immortalization. *J Virol* 64, 2530-2536.
- Koh, J., Enders, G. H., Dynlacht, B. D., and Harlow, E. (1995). Tumour-derived p16 alleles encoding proteins defective in cell-cycle inhibition. *Nature* 375, 506-510.
- Komano, J., Maruo, S., Kurozumi, K., Oda, T., and Takada, K. (1999). Oncogenic role of Epstein-Barr virus-encoded RNAs in Burkitt's lymphoma cell line Akata. *J Virol* 73, 9827-9831.
- Komano, J., Sugiura, M., and Takada, K. (1998). Epstein-Barr virus contributes to the malignant phenotype and to apoptosis resistance in Burkitt's lymphoma cell line Akata. *J Virol* 72, 9150-9156.
- Kouvidou, C., Stefanaki, K., Dai, Y., Tzardi, M., Koutsoubi, K., Darivianaki, K., Karidi, E., Rontogianni, D., Zois, E., Kakolyris, S., *et al.* (1997). P21/waf1 protein expression in nasopharyngeal carcinoma. Comparative study with PCNA, p53 and MDM-2 protein expression. *Anticancer Res* 17, 2615-2619.

- Krakowski, M. L., Kritzik, M. R., Jones, E. M., Krahl, T., Lee, J., Arnush, M., Gu, D., Mroczkowski, B., and Sarvetnick, N. (1999). Transgenic expression of epidermal growth factor and keratinocyte growth factor in beta-cells results in substantial morphological changes. *J Endocrinol* *162*, 167-175.
- Krimpenfort, P., Quon, K. C., Mooi, W. J., Loonstra, A., and Berns, A. (2001). Loss of p16Ink4a confers susceptibility to metastatic melanoma in mice. *Nature* *413*, 83-86.
- Krueger, G. R., Kottaridis, S. D., Wolf, H., Ablashi, D. V., Sesterhenn, K., and Bertram, G. (1981). Histological types of nasopharyngeal carcinoma as compared to EBV serology. *Anticancer Res* *1*, 187-194.
- Kulwichit, W., Edwards, R. H., Davenport, E. M., Baskar, J. F., Godfrey, V., and Raab-Traub, N. (1998). Expression of the Epstein-Barr virus latent membrane protein 1 induces B cell lymphoma in transgenic mice. *Proc Natl Acad Sci U S A* *95*, 11963-11968.
- Kuroki, T., Trapasso, F., Yendamuri, S., Matsuyama, A., Alder, H., Mori, M., and Croce, C. M. (2003). Allele loss and promoter hypermethylation of VHL, RAR-beta, RASSF1A, and FHIT tumor suppressor genes on chromosome 3p in esophageal squamous cell carcinoma. *Cancer Res* *63*, 3724-3728.
- Kustikova, O., Kramerov, D., Grigorian, M., Berezin, V., Bock, E., Lukanidin, E., and Tulchinsky, E. (1998). Fra-1 induces morphological transformation and increases in vitro invasiveness and motility of epithelioid adenocarcinoma cells. *Mol Cell Biol* *18*, 7095-7105.
- Kwong, J., Lo, K. W., To, K. F., Teo, P. M., Johnson, P. J., and Huang, D. P. (2002). Promoter hypermethylation of multiple genes in nasopharyngeal carcinoma. *Clin Cancer Res* *8*, 131-137.
- Labrecque, L. G., Barnes, D. M., Fentiman, I. S., and Griffin, B. E. (1995). Epstein-Barr virus in epithelial cell tumors: a breast cancer study. *Cancer Res* *55*, 39-45.
- Laing, K. G., Matys, V., and Clemens, M. J. (1995). Effects of expression of the Epstein-Barr virus small RNA EBER-1 in heterologous cells on protein synthesis and cell growth. *Biochem Soc Trans* *23*, 311S.
- Lam, N., Sandberg, M. L., and Sugden, B. (2004). High physiological levels of LMP1 result in phosphorylation of eIF2 alpha in Epstein-Barr virus-infected cells. *J Virol* *78*, 1657-1664.
- Lam, N., and Sugden, B. (2003). LMP1, a viral relative of the TNF receptor family, signals principally from intracellular compartments. *Embo J* *22*, 3027-3038.
- Laux, G., Dugrillon, F., Eckert, C., Adam, B., Zimmer-Strobl, U., and Bornkamm, G. W. (1994). Identification and characterization of an Epstein-Barr virus nuclear antigen 2-responsive cis element in the bidirectional promoter region of latent membrane protein and terminal protein 2 genes. *J Virol* *68*, 6947-6958.

- Le Roux, A., Kerdiles, B., Walls, D., Dedieu, J. F., and Perricaudet, M. (1994). The Epstein-Barr virus determined nuclear antigens EBNA-3A, -3B, and -3C repress EBNA-2-mediated transactivation of the viral terminal protein 1 gene promoter. *Virology* 205, 596-602.
- Leder, A., Kuo, A., Cardiff, R. D., Sinn, E., and Leder, P. (1990). v-Ha-ras transgene abrogates the initiation step in mouse skin tumorigenesis: effects of phorbol esters and retinoic acid. *Proc Natl Acad Sci U S A* 87, 9178-9182.
- Lee AW, F. W., Mang O, Sze WM, Chappell R, Lau WH, Ko WM. (2003). Changing epidemiology of nasopharyngeal carcinoma in Hong Kong over a 20-year period (1980-99): an encouraging reduction in both incidence and mortality. *Int J Cancer* 103, 680-685.
- Lee, M. A., Diamond, M. E., and Yates, J. L. (1999). Genetic evidence that EBNA-1 is needed for efficient, stable latent infection by Epstein-Barr virus. *J Virol* 73, 2974-2982.
- Lerner, M. R., Andrews, N. C., Miller, G., and Steitz, J. A. (1981). Two small RNAs encoded by Epstein-Barr virus and complexed with protein are precipitated by antibodies from patients with systemic lupus erythematosus. *Proc Natl Acad Sci U S A* 78, 805-809.
- Lespagnard, L., Cochaux, P., Larsimont, D., Degeyter, M., Velu, T., and Heimann, R. (1995). Absence of Epstein-Barr virus in medullary carcinoma of the breast as demonstrated by immunophenotyping, in situ hybridization and polymerase chain reaction. *Am J Clin Pathol* 103, 449-452.
- Levitskaya, J., Coram, M., Levitsky, V., Imreh, S., Steigerwald-Mullen, P. M., Klein, G., Kurilla, M. G., and Masucci, M. G. (1995). Inhibition of antigen processing by the internal repeat region of the Epstein-Barr virus nuclear antigen-1. *Nature* 375, 685-688.
- Levitskaya, J., Sharipo, A., Leonchiks, A., Ciechanover, A., and Masucci, M. G. (1997). Inhibition of ubiquitin/proteasome-dependent protein degradation by the Gly-Ala repeat domain of the Epstein-Barr virus nuclear antigen 1. *Proc Natl Acad Sci U S A* 94, 12616-12621.
- Li, H. M., Zhuang, Z. H., Wang, Q., Pang, J. C., Wang, X. H., Wong, H. L., Feng, H. C., Jin, D. Y., Ling, M. T., Wong, Y. C., *et al.* (2004). Epstein-Barr virus latent membrane protein 1 (LMP1) upregulates Id1 expression in nasopharyngeal epithelial cells. *Oncogene* 23, 4488-4494.
- Li, Q. X., Young, L. S., Niedobitek, G., Dawson, C. W., Birkenbach, M., Wang, F., and Rickinson, A. B. (1992). Epstein-Barr virus infection and replication in a human epithelial cell system. *Nature* 356, 347-350.
- Li, S. N., Chang, Y. S., and Liu, S. T. (1996). Effect of a 10-amino acid deletion on the oncogenic activity of latent membrane protein 1 of Epstein-Barr virus. *Oncogene* 12, 2129-2135.

- Libermann, T. A., Nusbaum, H. R., Razon, N., Kris, R., Lax, I., Soreq, H., Whittle, N., Waterfield, M. D., Ullrich, A., and Schlessinger, J. (1985). Amplification and overexpression of the EGF receptor gene in primary human glioblastomas. *J Cell Sci Suppl* 3, 161-172.
- Liebowitz, D., Kopan, R., Fuchs, E., Sample, J., and Kieff, E. (1987). An Epstein-Barr virus transforming protein associates with vimentin in lymphocytes. *Mol Cell Biol* 7, 2299-2308.
- Liebowitz, D., Mannick, J., Takada, K., and Kieff, E. (1992). Phenotypes of Epstein-Barr virus LMP1 deletion mutants indicate transmembrane and amino-terminal cytoplasmic domains necessary for effects in B-lymphoma cells. *J Virol* 66, 4612-4616.
- Lin, A. W., Barradas, M., Stone, J. C., van Aelst, L., Serrano, M., and Lowe, S. W. (1998). Premature senescence involving p53 and p16 is activated in response to constitutive MEK/MAPK mitogenic signaling. *Genes Dev* 12, 3008-3019.
- Lin, A. W., and Lowe, S. W. (2001). Oncogenic ras activates the ARF-p53 pathway to suppress epithelial cell transformation. *Proc Natl Acad Sci U S A* 98, 5025-5030.
- Lin, J., Johannsen, E., Robertson, E., and Kieff, E. (2002). Epstein-Barr virus nuclear antigen 3C putative repression domain mediates coactivation of the LMP1 promoter with EBNA-2. *J Virol* 76, 232-242.
- Ling, P. D., Hsieh, J. J., Ruf, I. K., Rawlins, D. R., and Hayward, S. D. (1994). EBNA-2 upregulation of Epstein-Barr virus latency promoters and the cellular CD23 promoter utilizes a common targeting intermediate, CBF1. *J Virol* 68, 5375-5383.
- Ling, P. D., Rawlins, D. R., and Hayward, S. D. (1993). The Epstein-Barr virus immortalizing protein EBNA-2 is targeted to DNA by a cellular enhancer-binding protein. *Proc Natl Acad Sci U S A* 90, 9237-9241.
- Liu, L. T., Peng, J. P., Chang, H. C., and Hung, W. C. (2003). RECK is a target of Epstein-Barr virus latent membrane protein 1. *Oncogene* 22, 8263-8270.
- Lo, K. W., Cheung, S. T., Leung, S. F., van Hasselt, A., Tsang, Y. S., Mak, K. F., Chung, Y. F., Woo, J. K., Lee, J. C., and Huang, D. P. (1996). Hypermethylation of the p16 gene in nasopharyngeal carcinoma. *Cancer Res* 56, 2721-2725.
- Lo, K. W., Huang, D. P., and Lau, K. M. (1995). p16 gene alterations in nasopharyngeal carcinoma. *Cancer Res* 55, 2039-2043.
- Longnecker, R. (2000). Epstein-Barr virus latency: LMP2, a regulator or means for Epstein-Barr virus persistence? *Adv Cancer Res* 79, 175-200.
- Longnecker, R., Druker, B., Roberts, T. M., and Kieff, E. (1991). An Epstein-Barr virus protein associated with cell growth transformation interacts with a tyrosine kinase. *J Virol* 65, 3681-3692.

- Luetke, N. C., Qiu, T. H., Peiffer, R. L., Oliver, P., Smithies, O., and Lee, D. C. (1993). TGF alpha deficiency results in hair follicle and eye abnormalities in targeted and waved-1 mice. *Cell* 73, 263-278.
- Luftig, M., Prinarakis, E., Yasui, T., Tschritzis, T., Cahir-McFarland, E., Inoue, J., Nakano, H., Mak, T. W., Yeh, W. C., Li, X., *et al.* (2003). Epstein-Barr virus latent membrane protein 1 activation of NF-kappaB through IRAK1 and TRAF6. *Proc Natl Acad Sci U S A* 100, 15595-15600.
- Luftig, M., Yasui, T., Soni, V., Kang, M. S., Jacobson, N., Cahir-McFarland, E., Seed, B., and Kieff, E. (2004). Epstein-Barr virus latent infection membrane protein 1 TRAF-binding site induces NIK/IKK alpha-dependent noncanonical NF-kappaB activation. *Proc Natl Acad Sci U S A* 101, 141-146.
- Lung, M. L., and Chang, G. C. (1992). Detection of distinct Epstein-Barr virus genotypes in NPC biopsies from southern Chinese and Caucasians. *Int J Cancer* 52, 34-37.
- Lung, M. L., Chang, G. C., Miller, T. R., Wara, W. M., and Phillips, T. L. (1994). Genotypic analysis of Epstein-Barr virus isolates associated with nasopharyngeal carcinoma in Chinese immigrants to the United States. *Int J Cancer* 59, 743-746.
- Luo, B., Wang, Y., Wang, X. F., Liang, H., Yan, L. P., Huang, B. H., and Zhao, P. (2005). Expression of Epstein-Barr virus genes in EBV-associated gastric carcinomas. *World J Gastroenterol* 11, 629-633.
- Macdiarmid, J., Stevenson, D., Campbell, D. H., and Wilson, J. B. (2003). The latent membrane protein 1 of Epstein-Barr virus and loss of the INK4a locus: paradoxes resolve to cooperation in carcinogenesis in vivo. *Carcinogenesis* 24, 1209-1218.
- Macdiarmid, J., and Wilson, J. B. (2001). Separation of epidermal tissue from underlying dermis and primary keratinocyte culture. *Epstein-Barr Virus Protocols* Ed JB Wilson and GHW May *Methods in Molecular Biology* 174, The Humana Press Inc. 401-410.
- Mackey, D., Middleton, T., and Sugden, B. (1995). Multiple regions within EBNA1 can link DNAs. *J Virol* 69, 6199-6208.
- Magrath, I., and Bhatia, K. (1999). Breast cancer: a new Epstein-Barr virus-associated disease? *J Natl Cancer Inst* 91, 1349-1350.
- Magrath, I. T. (1991). African Burkitt's lymphoma. History, biology, clinical features, and treatment. *Am J Pediatr Hematol Oncol* 13, 222-246.
- Mann, G. B., Fowler, K. J., Gabriel, A., Nice, E. C., Williams, R. L., and Dunn, A. R. (1993). Mice with a null mutation of the TGF alpha gene have abnormal skin architecture, wavy hair, and curly whiskers and often develop corneal inflammation. *Cell* 73, 249-261.

- Mann, K. P., Staunton, D., and Thorley-Lawson, D. A. (1985). Epstein-Barr virus-encoded protein found in plasma membranes of transformed cells. *J Virol* 55, 710-720.
- Mannick, J. B., Cohen, J. I., Birkenbach, M., Marchini, A., and Kieff, E. (1991). The Epstein-Barr virus nuclear protein encoded by the leader of the EBNA RNAs is important in B-lymphocyte transformation. *J Virol* 65, 6826-6837.
- Mannick, J. B., Tong, X., Hemnes, A., and Kieff, E. (1995). The Epstein-Barr virus nuclear antigen leader protein associates with hsp72/hsc73. *J Virol* 69, 8169-8172.
- Marshall, D., and Sample, C. (1995). Epstein-Barr virus nuclear antigen 3C is a transcriptional regulator. *J Virol* 69, 3624-3630.
- Massague, J. (1990). Transforming growth factor-alpha. A model for membrane-anchored growth factors. *J Biol Chem* 265, 21393-21396.
- May, M. J., and Ghosh, S. (1998). Signal transduction through NF-kappa B. *Immunol Today* 19, 80-88.
- McKay, J. A., Murray, L. J., Curran, S., Ross, V. G., Clark, C., Murray, G. I., Cassidy, J., and McLeod, H. L. (2002). Evaluation of the epidermal growth factor receptor (EGFR) in colorectal tumours and lymph node metastases. *Eur J Cancer* 38, 2258-2264.
- McKeller, R. N., Fowler, J. L., Cunningham, J. J., Warner, N., Smeyne, R. J., Zindy, F., and Skapek, S. X. (2002). The Arf tumor suppressor gene promotes hyaloid vascular regression during mouse eye development. *Proc Natl Acad Sci U S A* 99, 3848-3853.
- Miettinen, P. J., Berger, J. E., Meneses, J., Phung, Y., Pedersen, R. A., Werb, Z., and Derynck, R. (1995). Epithelial immaturity and multiorgan failure in mice lacking epidermal growth factor receptor. *Nature* 376, 337-341.
- Miller, C. L., Lee, J. H., Kieff, E., and Longnecker, R. (1994a). An integral membrane protein (LMP2) blocks reactivation of Epstein-Barr virus from latency following surface immunoglobulin crosslinking. *Proc Natl Acad Sci U S A* 91, 772-776.
- Miller, C. L., Longnecker, R., and Kieff, E. (1993). Epstein-Barr virus latent membrane protein 2A blocks calcium mobilization in B lymphocytes. *J Virol* 67, 3087-3094.
- Miller, G., and Heston, L. (1974). Expression of Epstein-Barr viral capsid, complement fixing, and nuclear antigens in stationary and exponential phase cultures. *Yale J Biol Med* 47, 123-135.
- Miller, W. E., Cheshire, J. L., Baldwin, A. S., Jr., and Raab-Traub, N. (1998a). The NPC derived C15 LMP1 protein confers enhanced activation of NF- κ B and induction of the EGFR in epithelial cells. *Oncogene* 16, 1869-1877.

- Miller, W. E., Cheshire, J. L., and Raab-Traub, N. (1998b). Interaction of tumor necrosis factor receptor-associated factor signaling proteins with the latent membrane protein 1 PXXXT motif is essential for induction of epidermal growth factor receptor expression. *Mol Cell Biol* 18, 2835-2844.
- Miller, W. E., Earp, H. S., and Raab-Traub, N. (1995). The Epstein-Barr virus latent membrane protein 1 induces expression of the epidermal growth factor receptor. *J Virol* 69, 4390-4398.
- Miller, W. E., Edwards, R. H., Walling, D. M., and Raab-Traub, N. (1994b). Sequence variation in the Epstein-Barr virus latent membrane protein 1. *J Gen Virol* 75 (Pt 10), 2729-2740.
- Miller, W. E., Mosialos, G., Kieff, E., and Raab-Traub, N. (1997). Epstein-Barr virus LMP1 induction of the epidermal growth factor receptor is mediated through a TRAF signaling pathway distinct from NF- κ B activation. *J Virol* 71, 586-594.
- Mitchell, T., and Sugden, B. (1995). Stimulation of NF- κ B-mediated transcription by mutant derivatives of the latent membrane protein of Epstein-Barr virus. *J Virol* 69, 2968-2976.
- Molesworth, S. J., Lake, C. M., Borza, C. M., Turk, S. M., and Hutt-Fletcher, L. M. (2000). Epstein-Barr virus gH is essential for penetration of B cells but also plays a role in attachment of virus to epithelial cells. *J Virol* 74, 6324-6332.
- Moorthy, R., and Thorley-Lawson, D. A. (1990). Processing of the Epstein-Barr virus-encoded latent membrane protein p63/LMP. *J Virol* 64, 829-837.
- Moorthy, R. K., and Thorley-Lawson, D. A. (1993). All three domains of the Epstein-Barr virus-encoded latent membrane protein LMP-1 are required for transformation of rat-1 fibroblasts. *J Virol* 67, 1638-1646.
- Mosialos, G., Birkenbach, M., Yalamanchili, R., VanArsdale, T., Ware, C., and Kieff, E. (1995). The Epstein-Barr virus transforming protein LMP1 engages signaling proteins for the tumor necrosis factor receptor family. *Cell* 80, 389-399.
- Murillas, R., Larcher, F., Conti, C. J., Santos, M., Ullrich, A., and Jorcano, J. L. (1995). Expression of a dominant negative mutant of epidermal growth factor receptor in the epidermis of transgenic mice elicits striking alterations in hair follicle development and skin structure. *EMBO J* 14, 5216-5223.
- Murono, S., Inoue, H., Tanabe, T., Joab, I., Yoshizaki, T., Furukawa, M., and Pagano, J. S. (2001). Induction of cyclooxygenase-2 by Epstein-Barr virus latent membrane protein 1 is involved in vascular endothelial growth factor production in nasopharyngeal carcinoma cells. *Proc Natl Acad Sci U S A* 98, 6905-6910.

- Murono, S., Yoshizaki, T., Park, C. S., and Furukawa, M. (1999). Association of Epstein-Barr virus infection with p53 protein accumulation but not bcl-2 protein in nasopharyngeal carcinoma. *Histopathology* 34, 432-438.
- Murray, P. G., Lissauer, D., Junying, J., Davies, G., Moore, S., Bell, A., Timms, J., Rowlands, D., McConkey, C., Reynolds, G. M., *et al.* (2003). Reactivity with A monoclonal antibody to Epstein-Barr virus (EBV) nuclear antigen 1 defines a subset of aggressive breast cancers in the absence of the EBV genome. *Cancer Res* 63, 2338-2343.
- Nakagawa, H., Wang, T. C., Zukerberg, L., Odze, R., Togawa, K., May, G. H., Wilson, J., and Rustgi, A. K. (1997). The targeting of the cyclin D1 oncogene by an Epstein-Barr virus promoter in transgenic mice causes dysplasia in the tongue, esophagus and forestomach. *Oncogene* 14, 1185-1190.
- Nakagomi, H., Dolcetti, R., Bejarano, M. T., Pisa, P., Kiessling, R., and Masucci, M. G. (1994). The Epstein-Barr virus latent membrane protein-1 (LMP1) induces interleukin-10 production in Burkitt lymphoma lines. *Int J Cancer* 57, 240-244.
- Nakamura, A., Arimoto, M., Takeuchi, K., and Fujii, T. (2002). A rapid extraction procedure of human hair proteins and identification of phosphorylated species. *Biol Pharm Bull* 25, 569-572.
- Nanbo, A., Inoue, K., Adachi-Takasawa, K., and Takada, K. (2002). Epstein-Barr virus RNA confers resistance to interferon-alpha-induced apoptosis in Burkitt's lymphoma. *Embo J* 21, 954-965.
- Nazar-Stewart, V., Vaughan, T. L., Burt, R. D., Chen, C., Berwick, M., and Swanson, G. M. (1999). Glutathione S-transferase M1 and susceptibility to nasopharyngeal carcinoma. *Cancer Epidemiol Biomarkers Prev* 8, 547-551.
- Nicholls, J., Hahn, P., Kremmer, E., Frohlich, T., Arnold, G. J., Sham, J., Kwong, D., and Grasser, F. A. (2004). Detection of wild type and deleted latent membrane protein 1 (LMP1) of Epstein-Barr virus in clinical biopsy material. *J Virol Methods* 116, 79-88.
- Nicholson, L. J., Hopwood, P., Johannessen, I., Salisbury, J. R., Codd, J., Thorley-Lawson, D., and Crawford, D. H. (1997). Epstein-Barr virus latent membrane protein does not inhibit differentiation and induces tumorigenicity of human epithelial cells. *Oncogene* 15, 275-283.
- Niedobitek, G., Agathangelou, A., Barber, P., Smallman, L. A., Jones, E. L., and Young, L. S. (1993). P53 overexpression and Epstein-Barr virus infection in undifferentiated and squamous cell nasopharyngeal carcinomas [see comments]. *J Pathol* 170, 457-461.
- Niedobitek, G., Hansmann, M. L., Herbst, H., Young, L. S., Dienemann, D., Hartmann, C. A., Finn, T., Pitteroff, S., Welt, A., Anagnostopoulos, I., and *et al.* (1991). Epstein-Barr virus and carcinomas: undifferentiated carcinomas but not squamous cell carcinomas of the nasopharynx are regularly associated with the virus. *J Pathol* 165, 17-24.

- Niedobitek, G., Young, L. S., and Herbst, H. (1997). Epstein-Barr virus infection and the pathogenesis of malignant lymphomas. *Cancer Surv* 30, 143-162.
- Niedobitek, G., Young, L. S., Sam, C. K., Brooks, L., Prasad, U., and Rickinson, A. B. (1992). Expression of Epstein-Barr virus genes and of lymphocyte activation molecules in undifferentiated nasopharyngeal carcinomas. *Am J Pathol* 140, 879-887.
- Niller, H. H., Salamon, D., Ilg, K., Koroknai, A., Banati, F., Bauml, G., Rucker, O., Schwarzmann, F., Wolf, H., and Minarovits, J. (2003). The in vivo binding site for oncoprotein c-Myc in the promoter for Epstein-Barr virus (EBV) encoding RNA (EBER) 1 suggests a specific role for EBV in lymphomagenesis. *Med Sci Monit* 9, HY1-9.
- Nishizuka, Y. (1984). The role of protein kinase C in cell surface signal transduction and tumour promotion. *Nature* 308, 693-698.
- Nitsche, F., Bell, A., and Rickinson, A. (1997). Epstein-Barr virus leader protein enhances EBNA-2-mediated transactivation of latent membrane protein 1 expression: a role for the W1W2 repeat domain. *J Virol* 71, 6619-6628.
- Nitta, T., Chiba, A., Yamamoto, N., and Yamaoka, S. (2004). Lack of cytotoxic property in a variant of Epstein-Barr virus latent membrane protein-1 isolated from nasopharyngeal carcinoma. *Cell Signal* 16, 1071-1081.
- Nitta, T., Chiba, A., Yamashita, A., Rowe, M., Israel, A., Reth, M., Yamamoto, N., and Yamaoka, S. (2003). NF-kappaB is required for cell death induction by latent membrane protein 1 of Epstein-Barr virus. *Cell Signal* 15, 423-433.
- Noh, S. J., Li, Y., Xiong, Y., and Guan, K. L. (1999). Identification of functional elements of p18INK4C essential for binding and inhibition of cyclin-dependent kinase (CDK) 4 and CDK6. *Cancer Res* 59, 558-564.
- Ohtani, N., Brennan, P., Gaubatz, S., Sanij, E., Hertzog, P., Wolvetang, E., Ghysdael, J., Rowe, M., and Hara, E. (2003). Epstein-Barr virus LMP1 blocks p16INK4a-RB pathway by promoting nuclear export of E2F4/5. *J Cell Biol* 162, 173-183.
- Olayioye, M. A., Neve, R. M., Lane, H. A., and Hynes, N. E. (2000). The ErbB signaling network: receptor heterodimerization in development and cancer. *Embo J* 19, 3159-3167.
- Ortiz-Vega, S., Khokhlatchev, A., Nedwidek, M., Zhang, X. F., Dammann, R., Pfeifer, G. P., and Avruch, J. (2002). The putative tumor suppressor RASSF1A homodimerizes and heterodimerizes with the Ras-GTP binding protein Nore1. *Oncogene* 21, 1381-1390.
- Paine, E., Scheinman, R. I., Baldwin, A. S., Jr., and Raab-Traub, N. (1995). Expression of LMP1 in epithelial cells leads to the activation of a select subset of NF- κ B/Rel family proteins. *J Virol* 69, 4572-4576.

- Palmero, I., Pantoja, C., and Serrano, M. (1998). p19ARF links the tumour suppressor p53 to Ras. *Nature* 395, 125-126.
- Pandya, J., and Walling, D. M. (2004). Epstein-Barr virus latent membrane protein 1 (LMP-1) half-life in epithelial cells is down-regulated by lytic LMP-1. *J Virol* 78, 8404-8410.
- Papesch, M., and Watkins, R. (2001). Epstein-Barr virus infectious mononucleosis. *Clin Otolaryngol* 26, 3-8.
- Parker, B. D., Bankier, A., Satchwell, S., Barrell, B., and Farrell, P. J. (1990). Sequence and transcription of Raji Epstein-Barr virus DNA spanning the B95-8 deletion region. *Virology* 179, 339-346.
- Parker, G. A., Crook, T., Bain, M., Sara, E. A., Farrell, P. J., and Allday, M. J. (1996). Epstein-Barr virus nuclear antigen (EBNA)3C is an immortalizing oncoprotein with similar properties to adenovirus E1A and papillomavirus E7. *Oncogene* 13, 2541-2549.
- Parker, G. A., Touitou, R., and Allday, M. J. (2000). Epstein-Barr virus EBNA3C can disrupt multiple cell cycle checkpoints and induce nuclear division divorced from cytokinesis. *Oncogene* 19, 700-709.
- Passegue, E., and Wagner, E. F. (2000). JunB suppresses cell proliferation by transcriptional activation of p16(INK4a) expression. *Embo J* 19, 2969-2979.
- Pathmanathan, R., Prasad, U., Sadler, R., Flynn, K., and Raab-Traub, N. (1995). Clonal proliferations of cells infected with Epstein-Barr virus in preinvasive lesions related to nasopharyngeal carcinoma. *N Engl J Med* 333, 693-698.
- Paumelle, R., Tulasne, D., Leroy, C., Coll, J., Vandebunder, B., and Fafeur, V. (2000). Sequential activation of ERK and repression of JNK by scatter factor/hepatocyte growth factor in madin-darby canine kidney epithelial cells. *Mol Biol Cell* 11, 3751-3763.
- Pearson, G. R., Weiland, L. H., Neel, H. B., 3rd, Taylor, W., Earle, J., Mulrone, S. E., Goepfert, H., Lanier, A., Talvot, M. L., Pilch, B., *et al.* (1983). Application of Epstein-Barr virus (EBV) serology to the diagnosis of North American nasopharyngeal carcinoma. *Cancer* 51, 260-268.
- Peng-Pilon, M., Ruuth, K., Lundgren, E., and Brodin, P. (1995). The cytoplasmic C-terminal domain but not the N-terminal domain of latent membrane protein 1 of Epstein-Barr virus is essential for B cell activation. *J Gen Virol* 76 (Pt 4), 767-777.
- Polvino-Bodnar, M., Kiso, J., and Schaffer, P. A. (1988). Mutational analysis of Epstein-Barr virus nuclear antigen 1 (EBNA 1). *Nucleic Acids Res* 16, 3415-3435.
- Pope, J. H., Achong, B. G., and Epstein, M. A. (1968). Cultivation and fine structure of virus-bearing lymphoblasts from a second New Guinea Burkitt lymphoma: establishment of sublines with unusual cultural properties. *Int J Cancer* 3, 171-182.

- Porter, M. J., Field, J. K., Leung, S. F., Lo, D., Lee, J. C., Spandidos, D. A., and van Hasselt, C. A. (1994a). The detection of the c-myc and ras oncogenes in nasopharyngeal carcinoma by immunohistochemistry. *Acta Otolaryngol (Stockh)* 114, 105-109.
- Porter, M. J., Field, J. K., Leung, S. F., Lo, D., Lee, J. C., Spandidos, D. A., and van Hasselt, C. A. (1994b). The detection of the c-myc and ras oncogenes in nasopharyngeal carcinoma by immunohistochemistry. *Acta Otolaryngol* 114, 105-109.
- Praskova, M., Khokhlatchev, A., Ortiz-Vega, S., and Avruch, J. (2004). Regulation of the MST1 kinase by autophosphorylation, by the growth inhibitory proteins, RASSF1 and NORE1, and by Ras. *Biochem J* 381, 453-462.
- Prokova, V., Mosialos, G., and Kardassis, D. (2002). Inhibition of transforming growth factor beta signaling and Smad-dependent activation of transcription by the Latent Membrane Protein 1 of Epstein-Barr virus. *J Biol Chem* 277, 9342-9350.
- Puls, A., Eliopoulos, A. G., Nobes, C. D., Bridges, T., Young, L. S., and Hall, A. (1999). Activation of the small GTPase Cdc42 by the inflammatory cytokines TNF α and IL-1, and by the Epstein-Barr virus transforming protein LMP1. *J Cell Sci* 112, 2983-2992.
- Quelle, D. E., Zindy, F., Ashmun, R. A., and Sherr, C. J. (1995). Alternative reading frames of the INK4a tumor suppressor gene encode two unrelated proteins capable of inducing cell cycle arrest. *Cell* 83, 993-1000.
- Quintanilla, M., Brown, K., Ramsden, M., and Balmain, A. (1986). Carcinogen-specific mutation and amplification of Ha-ras during mouse skin carcinogenesis. *Nature* 322, 78-80.
- Raab-Traub, N. (2002). Epstein-Barr virus in the pathogenesis of NPC. *Semin Cancer Biol* 12, 431-441.
- Raab-Traub, N., and Flynn, K. (1986). The structure of the termini of the Epstein-Barr virus as a marker of clonal cellular proliferation. *Cell* 47, 883-889.
- Raab-Traub, N., Flynn, K., Pearson, G., Huang, A., Levine, P., Lanier, A., and Pagano, J. (1987). The differentiated form of nasopharyngeal carcinoma contains Epstein-Barr virus DNA. *Int J Cancer* 39, 25-29.
- Rabizadeh, S., Xavier, R. J., Ishiguro, K., Bernabeortiz, J., Lopez-Illasaca, M., Khokhlatchev, A., Mollahan, P., Pfeifer, G. P., Avruch, J., and Seed, B. (2004). The scaffold protein CNK1 interacts with the tumor suppressor RASSF1A and augments RASSF1A-induced cell death. *J Biol Chem* 279, 29247-29254.
- Radfar, A., Unnikrishnan, I., Lee, H. W., DePinho, R. A., and Rosenberg, N. (1998). p19(Arf) induces p53-dependent apoptosis during abelson virus-mediated pre-B cell transformation. *Proc Natl Acad Sci U S A* 95, 13194-13199.

- Radkov, S. A., Touitou, R., Brehm, A., Rowe, M., West, M., Kouzarides, T., and Allday, M. J. (1999). Epstein-Barr virus nuclear antigen 3C interacts with histone deacetylase to repress transcription. *J Virol* 73, 5688-5697.
- Razzouk, B. I., Srinivas, S., Sample, C. E., Singh, V., and Sixbey, J. W. (1996). Epstein-Barr Virus DNA recombination and loss in sporadic Burkitt's lymphoma. *J Infect Dis* 173, 529-535.
- Reisman, D., and Sugden, B. (1986). trans activation of an Epstein-Barr viral transcriptional enhancer by the Epstein-Barr viral nuclear antigen 1. *Mol Cell Biol* 6, 3838-3846.
- Rickinson, A. B., and Kieff, E. (1996). Epstein-Barr Virus. Fields Virology, 3rd ed Fields, BN, Knipe, PM and Howley, PM, Lippincott-Raven Publishers, Philadelphia.
- Rickinson, A. B., and Moss, D. J. (1997). Human cytotoxic T lymphocyte responses to Epstein-Barr virus infection. *Annu Rev Immunol* 15, 405-431.
- Rickinson, A. B., Young, L. S., and Rowe, M. (1987). Influence of the Epstein-Barr virus nuclear antigen EBNA 2 on the growth phenotype of virus-transformed B cells. *J Virol* 61, 1310-1317.
- Rizos, H., Diefenbach, E., Badhwar, P., Woodruff, S., Becker, T. M., Rooney, R. J., and Kefford, R. F. (2003). Association of p14ARF with the p120E4F transcriptional repressor enhances cell cycle inhibition. *J Biol Chem* 278, 4981-4989.
- Roberts, M. L., and Cooper, N. R. (1998). Activation of a ras-MAPK-dependent pathway by Epstein-Barr virus latent membrane protein 1 is essential for cellular transformation. *Virology* 240, 93-99.
- Robertson, E. S., Grossman, S., Johannsen, E., Miller, C., Lin, J., Tomkinson, B., and Kieff, E. (1995). Epstein-Barr virus nuclear protein 3C modulates transcription through interaction with the sequence-specific DNA-binding protein J κ . *J Virol* 69, 3108-3116.
- Robertson, E. S., Lin, J., and Kieff, E. (1996). The amino-terminal domains of Epstein-Barr virus nuclear proteins 3A, 3B, and 3C interact with RBPJ(κ). *J Virol* 70, 3068-3074.
- Robertson, E. S., Tomkinson, B., and Kieff, E. (1994). An Epstein-Barr virus with a 58-kilobase-pair deletion that includes BARF0 transforms B lymphocytes in vitro. *J Virol* 68, 1449-1458.
- Rooney, C., Howe, J. G., Speck, S. H., and Miller, G. (1989). Influence of Burkitt's lymphoma and primary B cells on latent gene expression by the nonimmortalizing P3J-HR-1 strain of Epstein-Barr virus. *J Virol* 63, 1531-1539.
- Rothenberger, S., Bachmann, E., and Knecht, H. (1997). Molecular and functional analysis of the Epstein-Barr virus LMP1 oncogene promoter in lymphoproliferative diseases. *Exp Hematol* 25, 1326-1332.

- Rowe, M., Peng-Pilon, M., Huen, D. S., Hardy, R., Croom-Carter, D., Lundgren, E., and Rickinson, A. B. (1994). Upregulation of bcl-2 by the Epstein-Barr virus latent membrane protein LMP1: a B-cell-specific response that is delayed relative to NF- κ B activation and to induction of cell surface markers. *J Virol* 68, 5602-5612.
- Rowe, M., Young, L. S., Cadwallader, K., Petti, L., Kieff, E., and Rickinson, A. B. (1989). Distinction between Epstein-Barr virus type A (EBNA 2A) and type B (EBNA 2B) isolates extends to the EBNA 3 family of nuclear proteins. *J Virol* 63, 1031-1039.
- Ruas, M., and Peters, G. (1998). The p16INK4a/CDKN2A tumor suppressor and its relatives. *Biochim Biophys Acta* 1378, F115-177.
- Ruf, I. K., Rhyne, P. W., Yang, C., Cleveland, J. L., and Sample, J. T. (2000). Epstein-Barr virus small RNAs potentiate tumorigenicity of Burkitt lymphoma cells independently of an effect on apoptosis. *J Virol* 74, 10223-10228.
- Ruzinova, M. B., and Benezra, R. (2003). Id proteins in development, cell cycle and cancer. *Trends Cell Biol* 13, 410-418.
- Sadler, R. H., and Raab-Traub, N. (1995). The Epstein-Barr virus 3.5-kilobase latent membrane protein 1 mRNA initiates from a TATA-Less promoter within the first terminal repeat. *J Virol* 69, 4577-4581.
- Saitoh, A., Kimura, M., Takahashi, R., Yokoyama, M., Nomura, T., Izawa, M., Sekiya, T., Nishimura, S., and Katsuki, M. (1990). Most tumors in transgenic mice with human c-Ha-ras gene contained somatically activated transgenes. *Oncogene* 5, 1195-1200.
- Sall, A., Caserta, S., Jolicoeur, P., Franqueville, L., de Turenne-Tessier, M., and Ooka, T. (2004). Mitogenic activity of Epstein-Barr virus-encoded BARTF1 protein. *Oncogene* 23, 4938-4944.
- Sam, C. K., Prasad, U., and Pathmanathan, R. (1989). Serological markers in the diagnosis of histopathological types of nasopharyngeal carcinoma. *Eur J Surg Oncol* 15, 357-360.
- Sample, J., Liebowitz, D., and Kieff, E. (1989). Two related Epstein-Barr virus membrane proteins are encoded by separate genes. *J Virol* 63, 933-937.
- Sample, J., Young, L., Martin, B., Chatman, T., Kieff, E., and Rickinson, A. (1990). Epstein-Barr virus types 1 and 2 differ in their EBNA-3A, EBNA-3B, and EBNA-3C genes. *J Virol* 64, 4084-4092.
- Sandberg, M., Hammerschmidt, W., and Sugden, B. (1997). Characterization of LMP-1's association with TRAF1, TRAF2, and TRAF3. *J Virol* 71, 4649-4656.
- Sandberg, M. L., Kaykas, A., and Sugden, B. (2000). Latent membrane protein 1 of Epstein-Barr virus inhibits as well as stimulates gene expression. *J Virol* 74, 9755-9761.

- Sasaoka, T., Langlois, W. J., Leitner, J. W., Draznin, B., and Olefsky, J. M. (1994a). The signaling pathway coupling epidermal growth factor receptors to activation of p21ras. *J Biol Chem* *269*, 32621-32625.
- Sasaoka, T., Rose, D. W., Jhun, B. H., Saltiel, A. R., Draznin, B., and Olefsky, J. M. (1994b). Evidence for a functional role of Shc proteins in mitogenic signaling induced by insulin, insulin-like growth factor-1, and epidermal growth factor. *J Biol Chem* *269*, 13689-13694.
- Scholle, F., Bendt, K. M., and Raab-Traub, N. (2000). Epstein-Barr virus LMP2A transforms epithelial cells, inhibits cell differentiation, and activates Akt. *J Virol* *74*, 10681-10689.
- Schroder, W., Kienzle, N., Bushell, G., and Sculley, T. (2002). Antiserum raised against the Epstein-Barr virus BARF0 protein reacts to HLA-DR beta chain. *Arch Virol* *147*, 723-729.
- Schwemmle, M., Clemens, M. J., Hilse, K., Pfeifer, K., Troster, H., Muller, W. E., and Bachmann, M. (1992). Localization of Epstein-Barr virus-encoded RNAs EBER-1 and EBER-2 in interphase and mitotic Burkitt lymphoma cells. *Proc Natl Acad Sci U S A* *89*, 10292-10296.
- Scott, L. A., Vass, J. K., Parkinson, E. K., Gillespie, D. A., Winnie, J. N., and Ozanne, B. W. (2004). Invasion of normal human fibroblasts induced by v-Fos is independent of proliferation, immortalization, and the tumor suppressors p16INK4a and p53. *Mol Cell Biol* *24*, 1540-1559.
- Serrano, M., Lee, H., Chin, L., Cordon-Cardo, C., Beach, D., and DePinho, R. A. (1996). Role of the INK4a locus in tumor suppression and cell mortality. *Cell* *85*, 27-37.
- Serrano, M., Lin, A. W., McCurrach, M. E., Beach, D., and Lowe, S. W. (1997). Oncogenic ras provokes premature cell senescence associated with accumulation of p53 and p16INK4a. *Cell* *88*, 593-602.
- Sewing, A., Wiseman, B., Lloyd, A. C., and Land, H. (1997). High-intensity Raf signal causes cell cycle arrest mediated by p21Cip1. *Mol Cell Biol* *17*, 5588-5597.
- Sharpless, N. E., Bardeesy, N., Lee, K. H., Carrasco, D., Castrillon, D. H., Aguirre, A. J., Wu, E. A., Horner, J. W., and DePinho, R. A. (2001). Loss of p16Ink4a with retention of p19Arf predisposes mice to tumorigenesis. *Nature* *413*, 86-91.
- Sharpless, N. E., Ramsey, M. R., Balasubramanian, P., Castrillon, D. H., and DePinho, R. A. (2004). The differential impact of p16(INK4a) or p19(ARF) deficiency on cell growth and tumorigenesis. *Oncogene* *23*, 379-385.
- She, Q. B., Chen, N., Bode, A. M., Flavell, R. A., and Dong, Z. (2002). Deficiency of c-Jun-NH(2)-terminal kinase-1 in mice enhances skin tumor development by 12-O-tetradecanoylphorbol-13-acetate. *Cancer Res* *62*, 1343-1348.

- Sheen, T. S., Huang, Y. T., Chang, Y. L., Ko, J. Y., Wu, C. S., Yu, Y. C., Tsai, C. H., and Hsu, M. M. (1999). Epstein-Barr virus-encoded latent membrane protein 1 co-expresses with epidermal growth factor receptor in nasopharyngeal carcinoma. *Jpn J Cancer Res* 90, 1285-1292.
- Sheng, W., Decaussin, G., Ligout, A., Takada, K., and Ooka, T. (2003). Malignant transformation of Epstein-Barr virus-negative Akata cells by introduction of the BART1 gene carried by Epstein-Barr virus. *J Virol* 77, 3859-3865.
- Sheng, Z. M., Barrois, M., Klijanienko, J., Micheau, C., Richard, J. M., and Riou, G. (1990). Analysis of the c-Ha-ras-1 gene for deletion, mutation, amplification and expression in lymph node metastases of human head and neck carcinomas. *Br J Cancer* 62, 398-404.
- Sheu LF, C. A., Lee HS, Hsu HY, Yu DS. (1998). Cooperative interactions among p53, bcl-2 and Epstein-Barr virus latent membrane protein 1 in nasopharyngeal carcinoma cells. *Pathol Int* 2004 Jul;54(7):475-85.
- Shibata, M. A., Ward, J. M., Green, J. E., and Merlino, G. (1997). Enhanced sensitivity to tumor growth and development in multistage skin carcinogenesis by transforming growth factor- α -induced epidermal growth factor receptor activation but not p53 inactivation. *Mol Carcinog* 18, 160-170.
- Shivakumar, L., Minna, J., Sakamaki, T., Pestell, R., and White, M. A. (2002). The RASSF1A tumor suppressor blocks cell cycle progression and inhibits cyclin D1 accumulation. *Mol Cell Biol* 22, 4309-4318.
- Sibilia, M., and Wagner, E. F. (1995). Strain-dependent epithelial defects in mice lacking the EGF receptor [published erratum appears in *Science* 1995 Aug 18;269(5226):909]. *Science* 269, 234-238.
- Sinclair, A. J., Palmero, I., Peters, G., and Farrell, P. J. (1994). EBNA-2 and EBNA-LP cooperate to cause G0 to G1 transition during immortalization of resting human B lymphocytes by Epstein-Barr virus. *Embo J* 13, 3321-3328.
- Sixbey, J. W., and Yao, Q. Y. (1992). Immunoglobulin A-induced shift of Epstein-Barr virus tissue tropism. *Science* 255, 1578-1580.
- Slieker, L. J., Martensen, T. M., and Lane, M. D. (1986). Synthesis of epidermal growth factor receptor in human A431 cells. Glycosylation-dependent acquisition of ligand binding activity occurs post-translationally in the endoplasmic reticulum. *J Biol Chem* 261, 15233-15241.
- Smith, P. R., de Jesus, O., Turner, D., Hollyoake, M., Karstegl, C. E., Griffin, B. E., Karran, L., Wang, Y., Hayward, S. D., and Farrell, P. J. (2000). Structure and coding content of CST (BART) family RNAs of Epstein-Barr virus. *J Virol* 74, 3082-3092.

- Snudden, D. K., Hearing, J., Smith, P. R., Grasser, F. A., and Griffin, B. E. (1994). EBNA-1, the major nuclear antigen of Epstein-Barr virus, resembles 'RGG' RNA binding proteins. *EMBO J* 13, 4840-4847.
- Song, M. S., Song, S. J., Ayad, N. G., Chang, J. S., Lee, J. H., Hong, H. K., Lee, H., Choi, N., Kim, J., Kim, H., *et al.* (2004a). The tumour suppressor RASSF1A regulates mitosis by inhibiting the APC-Cdc20 complex. *Nat Cell Biol* 6, 129-137.
- Song, X., Tao, Y. G., Deng, X. Y., Jin, X., Tan, Y. N., Tang, M., Wu, Q., Lee, L. M., and Cao, Y. (2004b). Heterodimer formation between c-Jun and Jun B proteins mediated by Epstein-Barr virus encoded latent membrane protein 1. *Cell Signal* 16, 1153-1162.
- Speck, P., Haan, K. M., and Longnecker, R. (2000). Epstein-Barr virus entry into cells. *Virology* 277, 1-5.
- Spruck, C. H., 3rd, Tsai, Y. C., Huang, D. P., Yang, A. S., Rideout, W. M., 3rd, Gonzalez-Zulueta, M., Choi, P., Lo, K. W., Yu, M. C., and Jones, P. A. (1992). Absence of p53 gene mutations in primary nasopharyngeal carcinomas. *Cancer Res* 52, 4787-4790.
- Spugnardi, M., Tommasi, S., Dammann, R., Pfeifer, G. P., and Hoon, D. S. (2003). Epigenetic inactivation of RAS association domain family protein 1 (RASSF1A) in malignant cutaneous melanoma. *Cancer Res* 63, 1639-1643.
- Stewart, J. P., and Arrand, J. R. (1993). Expression of the Epstein-Barr virus latent membrane protein in nasopharyngeal carcinoma biopsy specimens. *Hum Pathol* 24, 239-242.
- Strockbine, L. D., Cohen, J. I., Farrah, T., Lyman, S. D., Wagener, F., DuBose, R. F., Armitage, R. J., and Spriggs, M. K. (1998). The Epstein-Barr virus BARF1 gene encodes a novel, soluble colony-stimulating factor-1 receptor. *J Virol* 72, 4015-4021.
- Su, W., Middleton, T., Sugden, B., and Echols, H. (1991). DNA looping between the origin of replication of Epstein-Barr virus and its enhancer site: stabilization of an origin complex with Epstein-Barr nuclear antigen 1. *Proc Natl Acad Sci U S A* 88, 10870-10874.
- Subramanian, C., and Robertson, E. S. (2002). The metastatic suppressor Nm23-H1 interacts with EBNA3C at sequences located between the glutamine- and proline-rich domains and can cooperate in activation of transcription. *J Virol* 76, 8702-8709.
- Sugawara, Y., Mizugaki, Y., Uchida, T., Torii, T., Imai, S., Makuuchi, M., and Takada, K. (1999). Detection of Epstein-Barr virus (EBV) in hepatocellular carcinoma tissue: a novel EBV latency characterized by the absence of EBV-encoded small RNA expression. *Virology* 256, 196-202.
- Sung, N. S., Kenney, S., Gutsch, D., and Pagano, J. S. (1991). EBNA-2 transactivates a lymphoid-specific enhancer in the BamHI C promoter of Epstein-Barr virus. *J Virol* 65, 2164-2169.

- Swaminathan, S., Tomkinson, B., and Kieff, E. (1991). Recombinant Epstein-Barr virus with small RNA (EBER) genes deleted transforms lymphocytes and replicates in vitro. *Proc Natl Acad Sci U S A* *88*, 1546-1550.
- Sylla, B. S., Hung, S. C., Davidson, D. M., Hatzivassiliou, E., Malinin, N. L., Wallach, D., Gilmore, T. D., Kieff, E., and Mosialos, G. (1998). Epstein-Barr virus-transforming protein latent infection membrane protein 1 activates transcription factor NF- κ B through a pathway that includes the NF- κ B-inducing kinase and the I κ B kinases IKK α and IKK β . *Proc Natl Acad Sci U S A* *95*, 10106-10111.
- Szekely, L., Selivanova, G., Magnusson, K. P., Klein, G., and Wiman, K. G. (1993). EBNA-5, an Epstein-Barr virus-encoded nuclear antigen, binds to the retinoblastoma and p53 proteins. *Proc Natl Acad Sci U S A* *90*, 5455-5459.
- Tao, Y., Song, X., Deng, X., Xie, D., Lee, L. M., Liu, Y., Li, W., Li, L., Deng, L., Wu, Q., *et al.* (2005). Nuclear accumulation of epidermal growth factor receptor and acceleration of G1/S stage by Epstein-Barr-encoded oncoprotein latent membrane protein 1. *Exp Cell Res* *303*, 240-251.
- Tao, Y., Song, X., Tan, Y., Lin, X., Zhao, Y., Zeng, L., Tang, M., Li, W., Wu, Q., and Cao, Y. (2004a). Nuclear translocation of EGF receptor regulated by Epstein-Barr virus encoded latent membrane protein 1. *Sci China C Life Sci* *47*, 258-267.
- Tao, Y. G., Tan, Y. N., Liu, Y. P., Song, X., Zeng, L., Gu, H. H., Tang, M., Li, W., Yi, W., and Cao, Y. (2004b). Epstein-Barr virus latent membrane protein 1 modulates epidermal growth factor receptor promoter activity in a nuclear factor kappa B-dependent manner. *Cell Signal* *16*, 781-790.
- Tao, Y. G., Tan, Y. N., Liu, Y. P., Song, X., Zeng, L., Gu, H. H., Tang, M., Li, W., Yi, W., and Cao, Y. (2004c). Nuclear factor kappa B (NFkappaB) dependent modulation of Epstein-Barr virus latent membrane protein 1 (LMP1) in epidermal growth factor receptor (EGFR) promoter activity. *Virus Res* *104*, 61-70.
- Tarutani, M., Cai, T., Dajee, M., and Khavari, P. A. (2003). Inducible activation of Ras and Raf in adult epidermis. *Cancer Res* *63*, 319-323.
- Thornburg, N. J., Pathmanathan, R., and Raab-Traub, N. (2003). Activation of nuclear factor-kappaB p50 homodimer/Bcl-3 complexes in nasopharyngeal carcinoma. *Cancer Res* *63*, 8293-8301.
- Threadgill, D. W., Dlugosz, A. A., Hansen, L. A., Tennenbaum, T., Lichti, U., Yee, D., LaMantia, C., Mourton, T., Herrup, K., Harris, R. C., and *et al.* (1995). Targeted disruption of mouse EGF receptor: effect of genetic background on mutant phenotype. *Science* *269*, 230-234.
- Tomkinson, B., Robertson, E., and Kieff, E. (1993). Epstein-Barr virus nuclear proteins EBNA-3A and EBNA-3C are essential for B-lymphocyte growth transformation. *J Virol* *67*, 2014-2025.

- Tommasi, S., Dammann, R., Jin, S. G., Zhang Xf, X. F., Avruch, J., and Pfeifer, G. P. (2002). RASSF3 and NORE1: identification and cloning of two human homologues of the putative tumor suppressor gene RASSF1. *Oncogene 21*, 2713-2720.
- Trivedi, P., Hu, L. F., Chen, F., Christensson, B., Masucci, M. G., Klein, G., and Winberg, G. (1994). Epstein-Barr virus (EBV)-encoded membrane protein LMP1 from a nasopharyngeal carcinoma is non-immunogenic in a murine model system, in contrast to a B cell-derived homologue. *Eur J Cancer 30A*, 84-88.
- Tsimbouri, P., Drotar, M. E., Coy, J. L., and Wilson, J. B. (2002). bcl-xL and RAG genes are induced and the response to IL-2 enhanced in EμEBNA-1 transgenic mouse lymphocytes. *Oncogene 21*, 5182-5187.
- Umanoff, H., Edelmann, W., Pellicer, A., and Kucherlapati, R. (1995). The murine N-ras gene is not essential for growth and development. *Proc Natl Acad Sci U S A 92*, 1709-1713.
- Varmus, H. E. (1984). The molecular genetics of cellular oncogenes. *Annu Rev Genet 18*, 553-612.
- Vasef, M. A., Ferlito, A., and Weiss, L. M. (1997). Nasopharyngeal carcinoma, with emphasis on its relationship to Epstein-Barr virus. *Ann Otol Rhinol Laryngol 106*, 348-356.
- Vassar, R., and Fuchs, E. (1991). Transgenic mice provide new insights into the role of TGF- α during epidermal development and differentiation. *Genes Dev 5*, 714-727.
- Vassar, R., Hutton, M. E., and Fuchs, E. (1992). Transgenic overexpression of transforming growth factor- α bypasses the need for c-Ha-ras mutations in mouse skin tumorigenesis. *Mol Cell Biol 12*, 4643-4653.
- Vavvas, D., Li, X., Avruch, J., and Zhang, X. F. (1998). Identification of Nore1 as a potential Ras effector. *J Biol Chem 273*, 5439-5442.
- Voorhoeve, P. M., and Agami, R. (2003). The tumor-suppressive functions of the human INK4A locus. *Cancer Cell 4*, 311-319.
- Vos, M. D., Ellis, C. A., Bell, A., Birrer, M. J., and Clark, G. J. (2000). Ras uses the novel tumor suppressor RASSF1 as an effector to mediate apoptosis. *J Biol Chem 275*, 35669-35672.
- Wakisaka, N., Kondo, S., Yoshizaki, T., Murono, S., Furukawa, M., and Pagano, J. S. (2004). Epstein-Barr virus latent membrane protein 1 induces synthesis of hypoxia-inducible factor 1 alpha. *Mol Cell Biol 24*, 5223-5234.
- Waltzer, L., Perricaudet, M., Sergeant, A., and Manet, E. (1996). Epstein-Barr virus EBNA3A and EBNA3C proteins both repress RBP-J κ -EBNA2-activated transcription by inhibiting the binding of RBP-J κ to DNA. *J Virol 70*, 5909-5915.

- Wan, J., Sun, L., Mendoza, J. W., Chui, Y. L., Huang, D. P., Chen, Z. J., Suzuki, N., Suzuki, S., Yeh, W. C., Akira, S., *et al.* (2004). Elucidation of the c-Jun N-terminal kinase pathway mediated by Epstein-Barr virus-encoded latent membrane protein 1. *Mol Cell Biol* *24*, 192-199.
- Wang, D., Liebowitz, D., and Kieff, E. (1985). An EBV membrane protein expressed in immortalized lymphocytes transforms established rodent cells. *Cell* *43*, 831-840.
- Wang, D., Liebowitz, D., and Kieff, E. (1988). The truncated form of the Epstein-Barr virus latent-infection membrane protein expressed in virus replication does not transform rodent fibroblasts. *J Virol* *62*, 2337-2346.
- Wang, F., Gregory, C., Sample, C., Rowe, M., Liebowitz, D., Murray, R., Rickinson, A., and Kieff, E. (1990). Epstein-Barr virus latent membrane protein (LMP1) and nuclear proteins 2 and 3C are effectors of phenotypic changes in B lymphocytes: EBNA-2 and LMP1 cooperatively induce CD23. *J Virol* *64*, 2309-2318.
- Wang, F., Gregory, C. D., Rowe, M., Rickinson, A. B., Wang, D., Birkenbach, M., Kikutani, H., Kishimoto, T., and Kieff, E. (1987). Epstein-Barr virus nuclear antigen 2 specifically induces expression of the B-cell activation antigen CD23. *Proc Natl Acad Sci U S A* *84*, 3452-3456.
- Wang, X. J., Greenhalgh, D. A., Donehower, L. A., and Roop, D. R. (2000). Cooperation between Ha-ras and fos or transforming growth factor alpha overcomes a paradoxical tumor-inhibitory effect of p53 loss in transgenic mouse epidermis. *Mol Carcinog* *29*, 67-75.
- Wang, X. J., Greenhalgh, D. A., Eckhardt, J. N., Rothnagel, J. A., and Roop, D. R. (1994). Epidermal expression of transforming growth factor-alpha in transgenic mice: induction of spontaneous and 12-O-tetradecanoylphorbol-13-acetate-induced papillomas via a mechanism independent of Ha-ras activation or overexpression. *Mol Carcinog* *10*, 15-22.
- Wang, X. J., Greenhalgh, D. A., Lu, X. R., Bickenbach, J. R., and Roop, D. R. (1995). TGF α and v-fos cooperation in transgenic mouse epidermis induces aberrant keratinocyte differentiation and stable, autonomous papillomas. *Oncogene* *10*, 279-289.
- Wang, X. J., Liefer, K. M., Greenhalgh, D. A., and Roop, D. R. (1999). 12-O-tetradecanoylphorbol-13-acetate promotion of transgenic mouse epidermis coexpressing transforming growth factor-alpha and v-fos: acceleration of autonomous papilloma formation and malignant conversion via c-Ha-ras activation. *Mol Carcinog* *26*, 305-311.
- Webster-Cyriaque, J., Middeldorp, J., and Raab-Traub, N. (2000). Hairy leukoplakia: an unusual combination of transforming and permissive Epstein-Barr virus infections. *J Virol* *74*, 7610-7618.
- Wei, M. X., de Turenne-Tessier, M., Decaussin, G., Benet, G., and Ooka, T. (1997). Establishment of a monkey kidney epithelial cell line with the BARF1 open reading frame from Epstein-Barr virus. *Oncogene* *14*, 3073-3081.

- Wiley, H. S., Herbst, J. J., Walsh, B. J., Lauffenburger, D. A., Rosenfeld, M. G., and Gill, G. N. (1991). The role of tyrosine kinase activity in endocytosis, compartmentation, and down-regulation of the epidermal growth factor receptor. *J Biol Chem* *266*, 11083-11094.
- Williams, C. C., Allison, J. G., Vidal, G. A., Burow, M. E., Beckman, B. S., Marrero, L., and Jones, F. E. (2004). The ERBB4/HER4 receptor tyrosine kinase regulates gene expression by functioning as a STAT5A nuclear chaperone. *J Cell Biol* *167*, 469-478.
- Wilson, J. B., Bell, J. L., and Levine, A. J. (1996). Expression of Epstein-Barr virus nuclear antigen-1 induces B cell neoplasia in transgenic mice. *EMBO J* *15*, 3117-3126.
- Wilson, J. B., and Levine, A. J. (1992). The oncogenic potential of Epstein-Barr virus nuclear antigen 1 in transgenic mice. *Curr Topics in Microbiol and Immunol* *182*, 375-384.
- Wilson, J. B., Weinberg, W., Johnson, R., Yuspa, S., and Levine, A. J. (1990). Expression of the BNLF-1 oncogene of Epstein-Barr virus in the skin of transgenic mice induces hyperplasia and aberrant expression of keratin 6. *Cell* *61*, 1315-1327.
- Wong, R. W., Kwan, R. W., Mak, P. H., Mak, K. K., Sham, M. H., and Chan, S. Y. (2000). Overexpression of epidermal growth factor induced hypospermatogenesis in transgenic mice. *J Biol Chem* *275*, 18297-18301.
- Wu, T. C., Mann, R. B., Epstein, J. I., MacMahon, E., Lee, W. A., Charache, P., Hayward, S. D., Kurman, R. J., Hayward, G. S., and Ambinder, R. F. (1991). Abundant expression of EBER1 small nuclear RNA in nasopharyngeal carcinoma. A morphologically distinctive target for detection of Epstein-Barr virus in formalin-fixed paraffin-embedded carcinoma specimens. *Am J Pathol* *138*, 1461-1469.
- Xie, W., Chow, L. T., Paterson, A. J., Chin, E., and Kudlow, J. E. (1999). Conditional expression of the ErbB2 oncogene elicits reversible hyperplasia in stratified epithelia and up-regulation of TGFalpha expression in transgenic mice. *Oncogene* *18*, 3593-3607.
- Yan, Y., Shirakabe, K., and Werb, Z. (2002). The metalloprotease Kuzbanian (ADAM10) mediates the transactivation of EGF receptor by G protein-coupled receptors. *J Cell Biol* *158*, 221-226.
- Yang, X., He, Z., Xin, B., and Cao, L. (2000a). LMP1 of Epstein-Barr virus suppresses cellular senescence associated with the inhibition of p16INK4a expression. *Oncogene* *19*, 2002-2013.
- Yang, X., Sham, J. S., Ng, M. H., Tsao, S. W., Zhang, D., Lowe, S. W., and Cao, L. (2000b). LMP1 of Epstein-Barr virus induces proliferation of primary mouse embryonic fibroblasts and cooperatively transforms the cells with a p16-insensitive CDK4 oncogene. *J Virol* *74*, 883-891.
- Yao, Q. Y., Croom-Carter, D. S., Tierney, R. J., Habeshaw, G., Wilde, J. T., Hill, F. G., Conlon, C., and Rickinson, A. B. (1998). Epidemiology of infection with Epstein-Barr virus

types 1 and 2: lessons from the study of a T-cell-immunocompromised hemophilic cohort. *J Virol* **72**, 4352-4363.

Yarbrough, W. G., Shores, C., Witsell, D. L., Weissler, M. C., Fidler, M. E., and Gilmer, T. M. (1994). ras mutations and expression in head and neck squamous cell carcinomas. *Laryngoscope* **104**, 1337-1347.

Yates, J., Warren, N., Reisman, D., and Sugden, B. (1984). A cis-acting element from the Epstein-Barr viral genome that permits stable replication of recombinant plasmids in latently infected cells. *Proc Natl Acad Sci U S A* **81**, 3806-3810.

Yoshiyama, H., Imai, S., Shimizu, N., and Takada, K. (1997). Epstein-Barr virus infection of human gastric carcinoma cells: implication of the existence of a new virus receptor different from CD21. *J Virol* **71**, 5688-5691.

Yoshizaki, T. (2002). Promotion of metastasis in nasopharyngeal carcinoma by Epstein-Barr virus latent membrane protein-1. *Histol Histopathol* **17**, 845-850.

Yoshizaki, T., Sato, H., Furukawa, M., and Pagano, J. S. (1998). The expression of matrix metalloproteinase 9 is enhanced by Epstein-Barr virus latent membrane protein 1. *Proc Natl Acad Sci U S A* **95**, 3621-3626.

Young, L. S., Dawson, C. W., Clark, D., Rupani, H., Busson, P., Tursz, T., Johnson, A., and Rickinson, A. B. (1988). Epstein-Barr virus gene expression in nasopharyngeal carcinoma. *J Gen Virol* **69**, 1051-1065.

Young, L. S., and Murray, P. G. (2003). Epstein-Barr virus and oncogenesis: from latent genes to tumours. *Oncogene* **22**, 5108-5121.

Yung, W. C., Sham, J. S., Choy, D. T., and Ng, M. H. (1995). ras mutations are uncommon in nasopharyngeal carcinoma. *Eur J Cancer B Oral Oncol* **31B**, 399-400.

Zeuthen, J. (1983). Epstein-Barr virus (EBV), lymphocytes and transformation. *J Cancer Res Clin Oncol* **106**, 1-11.

Zhao, B., Marshall, D. R., and Sample, C. E. (1996). A conserved domain of the Epstein-Barr virus nuclear antigens 3A and 3C binds to a discrete domain of Jk. *J Virol* **70**, 4228-4236.

Zheng, X., Hu, L., Chen, F., and Christensson, B. (1994a). Expression of Ki67 antigen, epidermal growth factor receptor and Epstein-Barr virus-encoded latent membrane protein (LMP1) in nasopharyngeal carcinoma. *Eur J Cancer B Oral Oncol* **30B**, 290-295.

Zheng, X., Yuan, F., Hu, L., Chen, F., Klein, G., and Christensson, B. (1994b). Effect of beta-lymphocyte- and NPC-derived EBV-LMP1 gene expression on in vitro growth and differentiation of human epithelial cells. *Int J Cancer* **57**, 747-753.

Zhu, J., Woods, D., McMahon, M., and Bishop, J. M. (1998). Senescence of human fibroblasts induced by oncogenic Raf. *Genes Dev* 12, 2997-3007.

Zimber-Strobl, U., Kempkes, B., Marschall, G., Zeidler, R., Van Kooten, C., Banchereau, J., Bornkamm, G. W., and Hammerschmidt, W. (1996). Epstein-Barr virus latent membrane protein (LMP1) is not sufficient to maintain proliferation of B cells but both it and activated CD40 can prolong their survival. *EMBO J* 15, 7070-7078.

Zimber-Strobl, U., Kremmer, E., Grasser, F., Marschall, G., Laux, G., and Bornkamm, G. W. (1993). The Epstein-Barr virus nuclear antigen 2 interacts with an EBNA2 responsive cis-element of the terminal protein 1 gene promoter. *EMBO J* 12, 167-175.

Zimber-Strobl, U., Suentzenich, K. O., Laux, G., Eick, D., Cordier, M., Calender, A., Billaud, M., Lenoir, G. M., and Bornkamm, G. W. (1991). Epstein-Barr virus nuclear antigen 2 activates transcription of the terminal protein gene. *J Virol* 65, 415-423.

Zindy, F., Eischen, C. M., Randle, D. H., Kamijo, T., Cleveland, J. L., Sherr, C. J., and Roussel, M. F. (1998). Myc signaling via the ARF tumor suppressor regulates p53-dependent apoptosis and immortalization. *Genes Dev* 12, 2424-2433.

zur Hausen, A., Brink, A. A., Craanen, M. E., Middeldorp, J. M., Meijer, C. J., and van den Brule, A. J. (2000). Unique transcription pattern of Epstein-Barr virus (EBV) in EBV-carrying gastric adenocarcinomas: expression of the transforming BARTF1 gene. *Cancer Res* 60, 2745-2748.

Appendices

Line, ID, Transgenic Status	Tissue	Description
105A.174 LMP1 ^{CAO+} Wasting phenotype	Thymus	Lymphosarcoma. The architecture of the thymus is replaced by dense sheets of large neoplastic lymphocytes that have large round nuclei, a high ratio of nucleus to cytoplasm and 10 to 20 mitoses per high power field. Frequent apoptosis creates a “starry sky” pattern.
	Glandular stomach	Lymphosarcoma. The base of the lamina propria is infiltrated with large neoplastic lymphocytes similar those infiltrating the thymus.
	Tongue	Unremarkable
	Forestomach	Bacteria are adherent to some segments of the surface of the epithelium in the forestomach.
	Trachea Thyroid gland Muscle	Unremarkable
	Junction of forestomach and glandular stomach	Lymphosarcoma. The base of the lamina propria of the glandular stomach is infiltrated with large neoplastic lymphocytes similar those infiltrating the thymus.
	Liver	Lymphosarcoma. Portal areas and sinusoids in all areas of the liver are densely infiltrated with large neoplastic lymphocytes similar those infiltrating the thymus.
	Spleen	Lymphosarcoma. The white pulp and multifocal locally extensive areas of the red pulp of the spleen are infiltrated with large neoplastic lymphocytes similar those infiltrating the thymus.
	Lymph node	Lymphosarcoma. The architecture of the lymph node is effaced by sheets of large neoplastic lymphocytes similar those infiltrating the thymus.

117.44 LMP1 ^{CAO} +	Lymph node	Reactive lymph node. The lymph node has multiple active lymphoid follicles with well-defined mantles and germinal centres. There is hyperplasia of the paracortical zone with frequent apoptosis, producing a “starry sky” pattern. Medullary cords are filled with plasma cells. The lymph node is reactive. There is no evidence of neoplasia.
117.30 LMP1 ^{CAO} +	Ear	Keratoacanthoma and Squamous cell carcinoma. A proliferative epidermal mass consists of an irregular, central crateriform depression lined by stratified squamous epithelium and filled with keratin laminae, degenerate cells and scattered colonies of bacteria. Multiple islands and cords of squamous epithelial cells with 1 to 3 mitoses per high power field and central keratinisation extend into the surrounding dermis. Microabscesses are formed by exudation of neutrophils in the centre of many epidermal islands. There are infiltrates of neutrophils, lymphocytes and plasma cells in the surrounding dermis, along with mild fibrosis. Immunohistochemistry for cytokeratins ¹ reveals staining of spinous and granular layer epithelial cells in proliferating islands and cords. Immunohistochemistry for vimentin ² is uninformative.
117/113.31 LMP1 ^{CAO} + / INK4a -/-	Papilloma size > 4	Squamous cell carcinoma. There is downgrowth of cords and islands of stratified squamous epithelial cells with a prominent granular cell layer and central keratinisation. Intermixed with these moderately well-differentiated cells, there is proliferation of cords and sheets of poorly differentiated squamous epithelial cells that have pleomorphic, ovoid nuclei, open heterochromatic chromatin, eosinophilic nuclei, variable amounts of eosinophilic cytoplasm and 2 to 4 mitoses per high power field. Proliferation of spindle-shaped cells with a fibroblastic appearance is also evident. Hyperkeratosis and serocellular crusting is evident on the surface of the skin. Immunohistochemistry for cytokeratins reveals staining of spinous and granular layer epithelial cells in the epidermis and proliferating islands and cords of cells in the dermis, as well as poorly differentiated sheets of spindle-shaped cells, supporting a diagnosis of poorly differentiated squamous cell carcinoma. Immunohistochemistry for vimentin is uninformative.

<p>117.23986 LMP1^{CAO} +</p>	<p>Skin: Ear A</p>	<p>Keratoacanthoma. Early squamous cell carcinoma. Ulcerative dermatitis. The skin of the ear has segmental acanthosis and marked hyperkeratosis, with localized downgrowth of cords and islands of epidermal cells that have concentric foci of keratinisation. At one margin of this proliferative lesion, there is shallow downgrowth of irregular cords of squamous epithelial cells into the underlying dermis. The squamous epithelial cells have evidence of keratinisation and there are 1 to 2 mitoses per high power field. There is extensive segmental ulceration, with necrosis, exudation of neutrophils, formation of a serocellular crust and proliferation of coccoid bacteria. Locally extensive fibrovascular hyperplasia is evident in the underlying dermis, along with diffuse infiltration by neutrophils and lesser numbers of lymphocytes, plasma cells and other inflammatory cells. This lesion appears to be a shallow keratoacanthoma that has been traumatised, leading to extensive ulceration, formation of granulation tissue and secondary growth of bacteria. There is early transformation to a squamous cell carcinoma.</p>
---	--------------------	---

Appendix 1: Histopathology analysis of tissues from lines 105A, 117 and 117/113 mice

The above table shows the results of histological examination obtained from tissues of several transgenic mice from lines 105A, 117 and 117/113.

Mouse ID	Age in weeks at start of count	Age in weeks of last count	Week of first papilloma	Max number of papillomas
1	6	65	0	0
2	6	65	6	3
3	6	65	6	4
4	6	42	7	3
10	6	15	0	0
11	6	15	0	0
12	6	15	0	0
13	6	39	6	1
14	6	55	29	2
15	6	55	55	1
16	6	17	0	0
30	6	65	21	1
31	6	65	0	0
37	6	65	24	6
38	6	65	27	1
39	6	65	0	0
40	6	60	0	0
41	6	55	0	0
44	6	15	9	2
45	6	46	9	4
46	6	65	9	3

Appendix 2: Spontaneous lesion recording of transgenic mice of line 117

The table above is showing the identification number, the age of the mice, week of first papilloma appearance and the maximum number of papillomas that each mouse developed during the 59 weeks of observation.

Mouse Id	Genotype		Ear phenotypic stage	Age (months)
	LMP1	TGF α		
117.22152 (BK6)	-	+/+	C1	1
117.22151 (BK6)	+	+/+	1	1
117.23549 (BK6)	+	+/+	2	3
117.24882 (BK6)	+	+/+	3	4
117/125.56	+	+/+	3	4
117/125.A404C	-	-/-	C1	1.5
117/125.M23277A	-	-/-	C4	2.5
117/125.A404	+	-/-	1	1
117/125.24789A	+	-/-	2	2
117/125.23995A	+	-/-	4	2.5
117/125.55	+	-/-	3	4
117/125.67	-	+/-	C4	4
117/125.58	+	+/-	4	4

Appendix 3: Details of the mice used for the western blotting experiments in chapter 5.

The table above is showing the mouse identification number or batch number, their genotype, phenotypic ear stage and age at which they were sacrificed. Transgenic positive mice for LMP1^{CAO} are indicated by (+), transgenic negative by (-). Null mice for TGF α are indicated by (-/-), heterozygotes by (+/-) and wild type by (+/+).

